

INFORMATION TO USERS

This was produced from a copy of a document sent to us for microfilming. While the most advanced technological means to photograph and reproduce this document have been used, the quality is heavily dependent upon the quality of the material submitted.

The following explanation of techniques is provided to help you understand markings or notations which may appear on this reproduction.

1. The sign or "target" for pages apparently lacking from the document photographed is "Missing Page(s)". If it was possible to obtain the missing page(s) or section, they are spliced into the film along with adjacent pages. This may have necessitated cutting through an image and duplicating adjacent pages to assure you of complete continuity.
2. When an image on the film is obliterated with a round black mark it is an indication that the film inspector noticed either blurred copy because of movement during exposure, or duplicate copy. Unless we meant to delete copyrighted materials that should not have been filmed, you will find a good image of the page in the adjacent frame. If copyrighted materials were deleted you will find a target note listing the pages in the adjacent frame.
3. When a map, drawing or chart, etc., is part of the material being photographed the photographer has followed a definite method in "sectioning" the material. It is customary to begin filming at the upper left hand corner of a large sheet and to continue from left to right in equal sections with small overlaps. If necessary, sectioning is continued again—beginning below the first row and continuing on until complete.
4. For any illustrations that cannot be reproduced satisfactorily by xerography, photographic prints can be purchased at additional cost and tipped into your xerographic copy. Requests can be made to our Dissertations Customer Services Department.
5. Some pages in any document may have indistinct print. In all cases we have filmed the best available copy.

University
Microfilms
International

300 N. ZEEB RD., ANN ARBOR, MI 48106

8216313

Domack, Eugene Walter

FACIES OF LATE PLEISTOCENE GLACIAL MARINE SEDIMENTS ON
WHIDBEY ISLAND, WASHINGTON

Rice University

PH.D. 1982

University
Microfilms
International 300 N. Zeeb Road, Ann Arbor, MI 48106

PLEASE NOTE:

In all cases this material has been filmed in the best possible way from the available copy.
Problems encountered with this document have been identified here with a check mark ✓.

1. Glossy photographs or pages ✓
2. Colored illustrations, paper or print ✓
3. Photographs with dark background ✓
4. Illustrations are poor copy _____
5. Pages with black marks, not original copy _____
6. Print shows through as there is text on both sides of page _____
7. Indistinct, broken or small print on several pages ✓
8. Print exceeds margin requirements _____
9. Tightly bound copy with print lost in spine _____
10. Computer printout pages with indistinct print _____
11. Page(s) _____ lacking when material received, and not available from school or author.
12. Page(s) _____ seem to be missing in numbering only as text follows.
13. Two pages numbered _____. Text follows.
14. Curling and wrinkled pages _____
15. Other _____

University
Microfilms
International

RICE UNIVERSITY
FACIES OF LATE PLEISTOCENE GLACIAL MARINE
SEDIMENTS ON WHIDBEY ISLAND, WASHINGTON

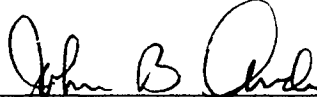
by

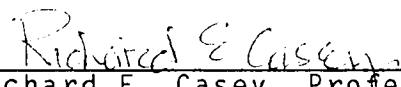
EUGENE W. DOMACK

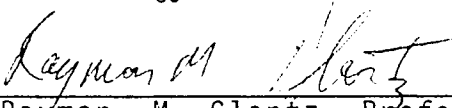
A THESIS SUBMITTED
IN PARTIAL FULFILLMENT OF THE
REQUIREMENTS FOR THE DEGREE

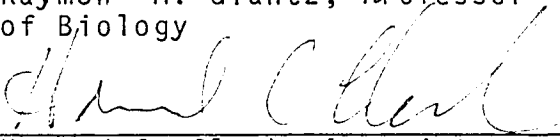
DOCTOR OF PHILOSOPHY

APPROVED, THESIS COMMITTEE:


John B. Anderson, Associate
Professor of Geology, Chairman


Richard E. Casey, Professor
of Geology


Raymon M. Glantz, Professor
of Biology


Howard C. Clark, Associate
Professor of Geology

HOUSTON, TEXAS

APRIL 1982

ABSTRACT

Detailed mapping of over 10 kms of cliff exposure on Whidbey Island, Washington has resulted in the recognition of six major lithofacies within "Everson" age glacial-marine deposits (late-Pleistocene). These lithofacies were deposited in an isostatically depressed basin, comprise up to 25 m of section, and occur in a predictable vertical succession. Proximity to both the ice margin and sources of meltwater input played a key role in the facies distribution. Stratified and convoluted beds of diamicton exhibit sedimentary characteristics indicative of mass flow processes. An ice marginal, submarine environment is assigned to the stratified diamictons since they are interbedded with marine sediments. In most exposures stratified diamictons are directly overlain by pebbly silts, muds, and massive diamictons. Locally, small (300 m wide) delta-like sequences consist of well stratified silty sand which is interbedded with pebbly mud. Turbidity current channel infills consist of normally graded, laminated sands which fine upwards into laminated sand-silt and silt-clay. Both of these facies are overlain by pebbly mud and massive diamicton. Pebbly silt and mud grade up into massive, fossiliferous diamicton. Post depositional mass movement has locally interrupted the normal stratigraphic sequence. With regard to the ice margin, the massive "till-like"

diamictons are interpreted as the most distal of the glacial-marine facies. All exposures are capped by channel lags, beach and eolian sediments which represent emergence of the basin above sea level.

Erosional surfaces at the base of the sequence (glacial and/or meltwater) and above (regressive shoreline) serve to separate the isostatic glacial marine sequence from correlative nearshore, offshore, and terrestrial glacial sequences. Extensive development of meltwater and sediment flow facies suggest that the sequence was deposited in a moderate glacial climatic setting, not unlike the present Gulf of Alaska.

Correlation of the central tendency of pebble fabric and sand content for glacial marine diamictons distinguish them from tills and sediment flow diamictons. Sediment flows are distinguished from tills and glacial marine diamictons by their high and variable clast abundances, textural variability, and variable bedding character.

Deglaciation of central and northern Whidbey Island involved retreat of a highly irregular ice margin which was grounded.

ACKNOWLEDGEMENTS

There are many persons to whom I owe a great deal, the foremost being John Anderson. His encouragement and suggestions, both as advisor and friend, were greatly appreciated during my four years at Rice. I am indebted to Joseph Paterson and Randy Domack who assisted me in the field, all with good humor. The many people I met while working on Whidbey made my stay most memorable, I especially want to thank Margaret Covert and her family. Gerald Thorsen of the Washington State Survey was kind enough to direct me to some key localities on Whidbey Island, a special thanks is given. My appreciation is extended to Fred Pessl, Dave Dethier, and Richard Sylwester of the U.S. Geol. Survey for their advice concerning the many problems on Whidbey Island. I would also like to thank Mary L. Hoerster, Jim Ellis, Richard Casey, Bill Schmidt, Nathan Myers, Robyn Wright, H.C. Clark, and Ray Glantz for their interest and discussion concerning the research.

My research was supported by a Petroleum Research Foundation grant from the American Chemical Society, (PRF-2472-AC2) which was awarded to John Anderson, the Geological Society of America (Grant no. 2814-81), and a grant in aid of research from Sigma Xi. While at Rice I was supported by the Maurice Ewing Fellowship in Marine Geology for which I am truly thankful.

In Memory of my Father

TABLE OF CONTENTS

PAGE

INTRODUCTION	1
Chapter	
1 METHODS.	9
Field Procedures.	10
Laboratory Procedures	11
2 STRATIGRAPHY	15
Regional Quaternary Stratigraphy.	16
Whidbey Island Stratigraphy	25
Pre-Olympia Sediments.	
Olympia Interglacial	
Fraser Glaciation.	
Vashon Drift	
Partridge Gravel.	
Everson Drift	
Stratigraphic Problems	
3 PREVIOUS STUDIES	38
Everson Age Glacial Marine Drift.	39
Late Pleistocene Sea Level.	52
4 GLACIAL MARINE LITHOFACIES ON WHIDBEY ISLAND . 57	
Description	58
Lower Contact.	
Lower Unit	
Stratified Diamicton (Qsd).	
Middle Unit.	
Silty Sand, Sandy Silt (Qsls)	
Silty Clay (Qslc)	
Laminated Sand and Silt (Qls, Qsl).	
Upper Unit	
Pebbly Silt (Qpsl).	
Pebbly Mud (Qpm).	
Massive Diamicton (Qmd)	
Emergence Deposits (Qgl)	
Depositional Process and Interpretation . . 120	
Qsd.	
Qsls, Qslc, Qls, and Qsl	
Qpsl, Qpm, and Qmd	

Chapter		
5	A MODEL173
	The Sedimentary Model174
	The Stratigraphic Model186
	Implications to Other Glacial Marine	
	Deposits.193
6	IMPLICATIONS TO DEGLACIAL HISTORY.200
7	CRITERIA FOR DISTINCTION BETWEEN GLACIAL, FLOW, AND GLACIAL MARINE DIAMICTONS.209
	Pebble Fabric211
	Texture222
	Pebble Shape.229
	Pebble Abundance.232
	Bedding Relationships233
	CONCLUSION239
	REFERENCES CITED242
	APPENDIX A254
	APPENDIX B286

LIST OF FIGURES

<u>FIGURE</u>		<u>PAGE</u>
Figure 1	Map of North America and Greenland showing, in black, the location of late-Pleistocene marine sediments which were deposited in isostatically depressed basins. From Bird (1967), Goldthwait (1949), and other sources.	4
Figure 2	Region of Puget Sound and Strait of Juan de Fuca.	8
Figure 3	Late-Pleistocene stratigraphy of the Puget and Fraser Lowland. From Armstrong and others (1965) and Easterbrook and others (1981).	20
Figure 4	Reconstruction of Vashon Ice Sheet with Juan de Fuca and Puget lobe. From Porter (1964). The Juan de Fuca lobe is shown at two positions, the dashed margin is according to Anderson (1968).	23
Figure 5	Quaternary stratigraphy of Whidbey Island, from Easterbrook (1968, 1981).	27
Figure 6	Whidbey Island with locations mentioned in the text.	29
Figure 7	Stratigraphy of Fraser glacial deposits on Whidbey Island and the Fraser Lowland, from Easterbrook (1968) and Armstrong (1981).	34
Figure 8	Glacial-marine depositional model for late-Pleistocene deposits in the Fraser Lowland according to Armstrong and Brown (1954).	41
Figure 9	Type stratigraphic section of the Everson glacial-marine drift, from Easterbrook (1962).	44
Figure 10	Deglaciation model for the central Puget Lowland (southern Whidbey Island) according to Thorson (1980).	48

LIST OF FIGURES (cont.)

Figure 11	Late-Pleistocene-Holocene sea level fluctuations for the Fraser Lowland; A, according to Thorson (1981), and B, according to Mathews and others (1970). The data are the same for both curves. The eustatic curve is from Curray (1965).	54
Figure 12	Generalized facies diagram of Everson age glacial marine drift on Whidbey Island.	60
Figure 13	Interpretive sketch of exposure north of West Beach. Outcrop is at or close to the marine limit.	64
Figure 14	Photographs of horizontally stratified diamicton exposed near the base of the section at Maylor Point (A,B) and San de Fuca-West (C).	66
Figure 15	Photographs of stratified diamicton facies at Swantown (A), Coupeville-Lovejoy Point (B), and San de Fuca-West (C).	69
Figure 16	Sand, silt, clay ratios for representative samples of Qsd facies.	72
Figure 17	Abundance of greater than 2cm sized stones from Qsd, Qpm, and lodgement till facies. Each bar represents one measurement of the number of stones per square meter.	74
Figure 18	Cumulative grain size distributions for samples SFW-F5, 6, and 7. Photograph shows Qsd unit and sample locations. Distributions for -4.0 to -1.0ø were determined by sieving at .5ø intervals.	76
Figure 19	Photograph of interbedded relationship of sediment flow (Qsd) and pebbly mud (Qpm) at San de Fuca-West.	78

LIST OF FIGURES (cont.)

Figure 20	Sand, silt, clay ratios and grain size frequency distributions for stratified silty sand and sandy silt facies (Qsls). For comparison frequency distributions for similar sediments from Queen Inlet, Alaska, are shown in the upper right, from Hoskin and Burrell (1972).	81
Figure 21	Photographs of sedimentary structures found within Qsls facies at Lovejoy Point. Large scale ripples (A), graded silt rip-ups (B), and convolute bedding (C). Scale in cms.	84
Figure 22	Photographs of channelized silty sands exposed at Lovejoy Point. Digging tool is approximately 30 cm long.	86
Figure 23	Photograph and interpretive sketch of interbedded silty sand (Qsls) and pebbly mud (Qpm).	89
Figure 24	Grain size cumulative distributions for interbedded sequence of silty sands and pebbly muds shown in figure 23.	91
Figure 25	Photographs of silty clay facies exposed at Maylor Point. Soft sediment deformation and wispy laminations (A and B). Lenticular bedding and laminations of current rippled sand and mud (C).	93
Figure 26	Photograph and grain size cumulative distributions for interbedded sandy silts and silty clays found within Qslc facies.	96
Figure 27	Photographs of stratified sands and silts exposed as channel infills at Swantown (A) and West Beach (B).	98
Figure 28	Photographs of horizontal trace fossils found within stratified silts and sands at Swantown (A) and West Beach (B).	100

LIST OF FIGURES (cont.)

Figure 29	Grain size frequency distributions for samples of pebbly silt.	103
Figure 30	Photograph of pebbly mud (A) and massive, fossiliferous diamicton (B).	105
Figure 31	Photographs of laminated pebbly mud (Qpml) exposed at Swantown (A) and Hastie Lake Road-South (B).	107
Figure 32	Sand, silt, clay ratios for pebbly muds and silts (Qpm and Qpsl) and fossiliferous diamictons (Qmd). Shown above are grain size frequency distributions for samples of pebbly mud.	110
Figure 33	Photographs of fossiliferous diamicton (Qmd) exposed at San de Fuca-East (A) and West Beach (B). Fossils appear to be in-situ.	112
Figure 34	Grain size frequency distributions for samples of fossiliferous diamicton.	114
Figure 35	Photographs of deformed sand lenses which can be found within Qmd facies. Forbes Point (A) and Penn Cove-West (B).	116
Figure 36	Classification of sediment flows based upon modern sediments at the terminus of the Matanuska glacier, Alaska, from Lawson (1979).	124
Figure 37	Diagrammatic models for subaqueous flow till deposition based on Pliestocene deposits in Ontario, Canada, A (Evenson et al., 1977) and British Columbia, B (Hickock et al., 1981).	127

LIST OF FIGURES (cont.)

Figure 38	Equal area projections of pebble long axis orientations for stratified diamicton facies (Qsd). Contour intervals are at 1, 3, 5, 7, and greater than 9% of data per 4% of the projection area. Data have not been rotated to horizontal with respect to the dip of the bedding plane. All samples consist of 25 measurements.	130
Figure 39	Location of fabric samples taken from Qsd and Qmd units near Penn Cove. Non-horizontal bedding is indicated by a strike and dip symbol. Paleocurrent directions for deltaic and marine units exposed at Lovejoy Point are also shown.	133
Figure 40	Comparison of grain size frequency distributions of samples from uppermost deltaic sands (C2-26) and overlying, channelized marine sand (C2-12).	136
Figure 41	Underflow and overflow depositional model as described by Bates (1953), figure taken from Reading (1978). Alternate beds of Qsls and Qpm as shown in figure 23 can be explained by this model.	140
Figure 42	Composite of measured sections at Forbes and Maylor Point show increase in thickness of silty clays and sandy silts within depressions. Deposition took place on slopes of up to 5°. Sea level is at 0 meters on vertical scale.	144
Figure 43	Photographs of sedimentary structures within turbidity current channel infill exposed at Swantown. Notice varve-like bedding of upper part of unit (A), normal grading (B), and water escape structures (C).	147
Figure 44	Diagrammatic model to explain turbidity current channel infill and convoluted diamictons exposed at Swantown. Presence of trace fossils within Qsls facies is problematical.	150

LIST OF FIGURES (cont.)

Figure 45	Photographs of highly convolute bedding within diamicton at West Beach (A) and shell rich mud lense exposed just south of measured section HL-1, Hastie Lake Road-North.	154
Figure 46	Grain size frequency distributions of samples of pebbly mud and fossiliferous diamicton taken from section FP-4 at Forbes Point. Notice the fining upward trend in the current derived (silt-clay) component.	160
Figure 47	Grain size frequency distributions for samples of lodgement till from Hastie Lake Road-North, and sand fraction cumulative distributions for samples of pebbly mud and fossiliferous diamicton from section FP-4. Notice the low variability and lack of fine grained sand for the Forbes Point (FP) samples.	162
Figure 48a,b	Equal area projections of pebble long axis orientations from massive, fossiliferous diamictons (Qmd). Contour interval is 1, 3, 5, 7, and greater than 9% of data per 4% of projection area. Sample LB-Qpml-1 was not rotated to horizontal and consists of 20 measurements, all others consist of 25 measurements and were collected from horizontal beds.	165,166
Figure 49	Sphericity and roundness (Krumbein, 1941) plots of clasts from Qmd, lodgement till, and modern beach sediments. Contour intervals are at 5, 10, and 15% of the data per 1% of the graph area. Notice lower roundness for Qmd units versus lodgement till samples and higher roundness for beach sample.	168

LIST OF FIGURES (cont.)

- Figure 50 Diagrammatic model for ice marginal marine deposition based on exposures along Penn Cove. Development of sediment flows (Qsd) occurs along the ice margin and they are progressively buried by meltwater facies (Qsls and Qpm) as the ice margin recedes. Massive ice-rafted diamictons are deposited distal to the ice margin. In this model ablation processes at the ice margin dominate over calving and rates of ice margin retreat are relatively slow. 176
- Figure 51 Diagrammatic model for submarine meltwater fan deposition as based on exposures of Qsls and Qslc facies at Lovejoy Point-Coupeville and Maylor Point. Deposition of silty sands via underflow currents would occur at times of high velocity discharge associated with high suspended sediment concentrations. 179
- Figure 52 Diagrammatic model for glacial-marine deposition along a steep ice margin as based upon exposures on the west coast of Whidbey Island. 181
- Figure 53 Stratigraphic model for late-Pleistocene glacial-marine deposits exposed on Whidbey Island and their relationship to the deep marine section as described by Anderson (1968). 188
- Figure 54 Diagrammatic view of Whidbey Island vicinity as it may have appeared approximately 13,000 years B.P. Deposition of distal glacial-marine facies occurred in seaways between islands, which were slowly emerging as isostatic rebound took place. 206

LIST OF FIGURES (cont.)

Figure 55	Equal area projection of pebble long axis orientations for samples of lodgement till exposed at Hastie Lake Road-North. Contour interval is 1, 3, 5, 7, and greater than 9% of the data per 4% of projection area. Samples consist of 25 measurements. Data are not rotated to horizontal. Beds dip at approximately 18° to the south.	213
Figure 56	Axial ratio diagram for all clasts used in fabric measurements. Diagram from Zingg (1935).	215
Figure 57	Plot of percent sand within matrix and central tendency (percent area of 5% contour interval) of pebble fabric for sediment flow, lodgement till, and ice-rafted diamicton. Least squares regression lines are drawn through the data and values of the correlation coefficient are given. Sample numbers correspond to fabrics in figures 55, 48, and 38.	218
Figure 58	Plot of central tendency (percent area of 5% contour interval) and randomness (percent area of 1% contour interval) for sediment flows, tills, and glacial-marine diamictons.	221
Figure 59	Plot of mean grain size (in PHI units) versus sorting for samples of Qpm, Qpsl, Qsd, Qmd, and till facies.	225
Figure 60	Vertical variation in sand, silt clay percentages for transition from pebbly silt, mud, and massive, fossiliferous diamicton for section FP-4. Note textural homogeneity for massive diamicton (Qmd).	227
Figure 61	Pebble lithology histogram for samples collected from Qmd, lodgement till, and modern beach. Lithologies shown are only the major components for each sample.	231

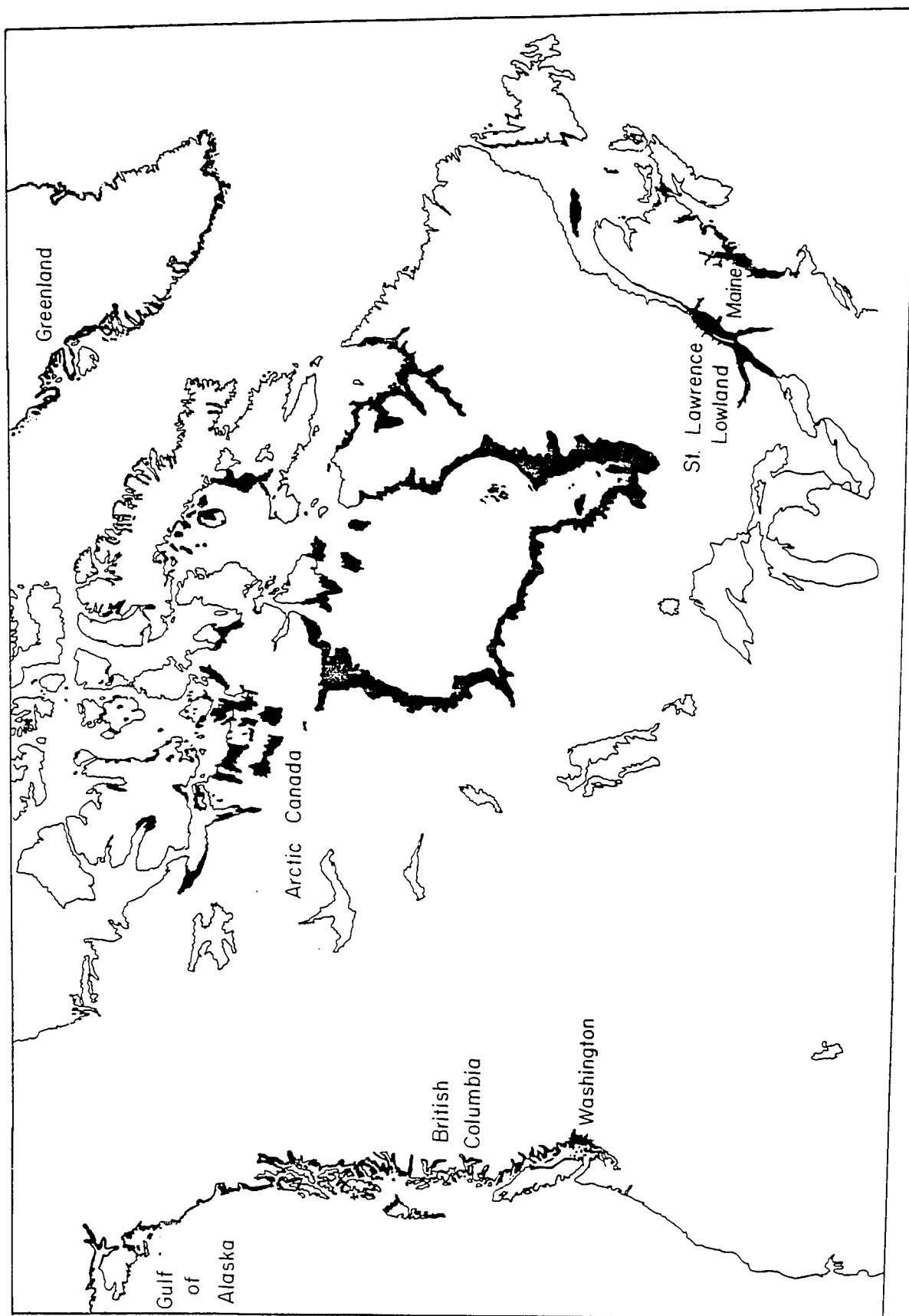
LIST OF FIGURES (cont.)

- Figure 62 Photograph of lodgement till sequence 236
exposed at Hastie Lake Road-North.
Note sheared interbeds of sand and
silt and depositional slopes of up
to 18° to south.

INTRODUCTION

In coastal regions which bordered ice sheets of the late Pleistocene high stands of sea level occurred immediately following deglaciation. These high sea level stands were short lived and the marine regressions which followed opposed the world wide trend of rising eustatic sea level (Curry, 1965). These fluctuations in sea level were the result of crustal depression by ice sheets and the delayed isostatic rebound which followed deglaciation. Our evidence for such events comes from marine sediments which can be found at significant elevations above present sea level. In North America and Greenland such deposits are widespread (Fig. 1) being found along coastal Maine, the Gulf of St. Lawrence, eastern and arctic Canada, coastal Greenland, the Gulf of Alaska, coastal British Columbia and regions bordering Puget Sound, Washington. In order to solve problems of paleo-ice thickness and crustal rheology (for review see Morner, 1980), geologic research to date has focused upon the maximum elevation and age dating of these sediments, the sedimentology largely having been ignored. However, such deposits, although thin, occupy a key position with regard to terrestrial glacial and deep glacial-marine settings. Their recognition in ancient glacial sequences is therefore vital to defining the boundary between subaerial and submarine environments.

Figure 1 Map of North America and Greenland showing, in black, the location of late-Pleistocene marine sediments which were deposited in isostatically depressed basins. From Bird (1967), Goldthwait (1949), and other sources.



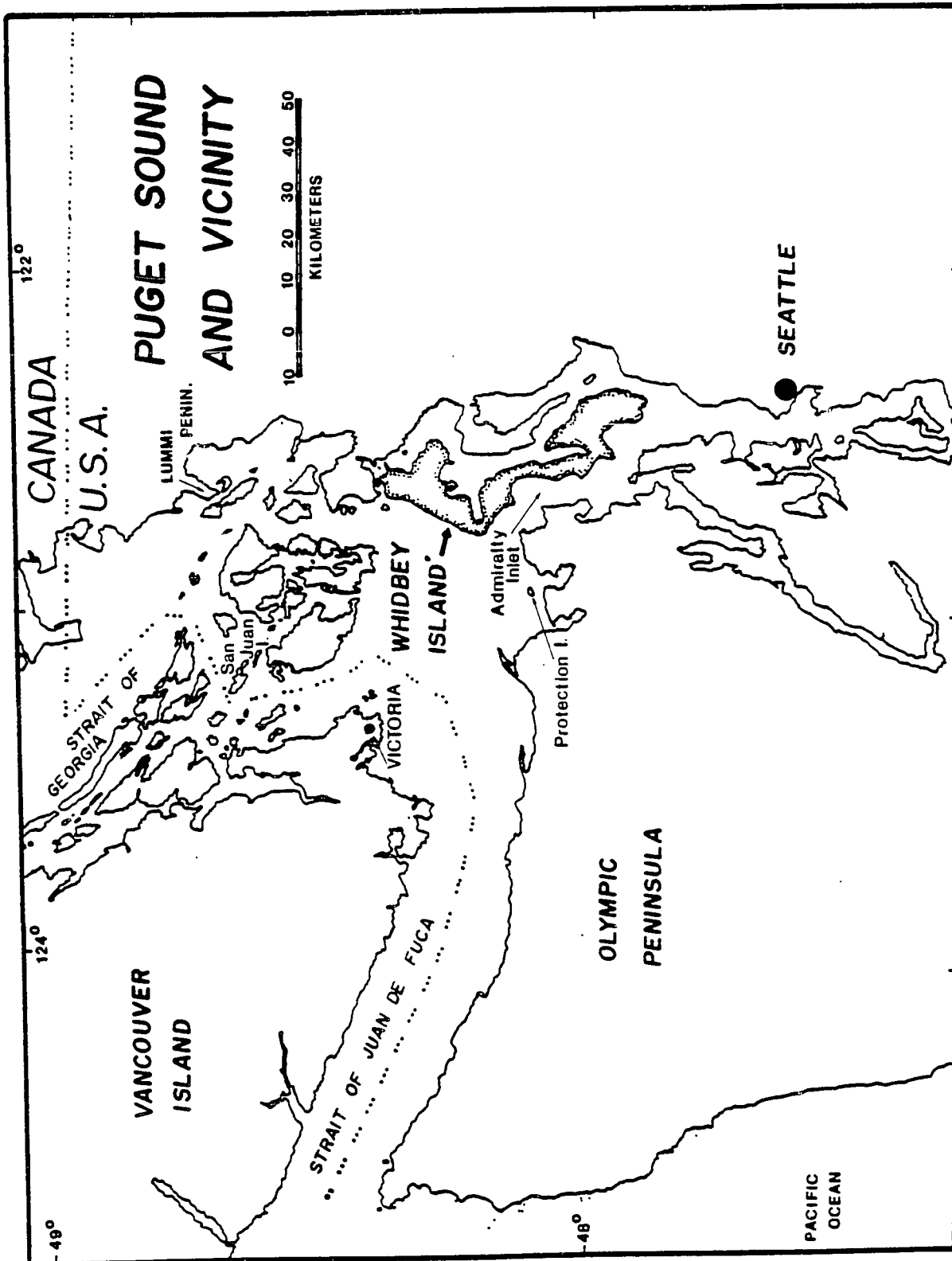
Glacial marine environments today occur under a wide range of physiographic and climatic settings, from the Antarctic where 10 m firn temperatures average -10°C and meltwater is minimal to the coastal areas of the Gulf of Alaska where temperatures average $\sim 15^{\circ}\text{C}$ and meltwater, with its high load of sediment, flows almost continuously into the sea. The influence of climate upon glacial-marine deposition in these two environments is profound. Sedimentation rates in coastal embayments of the Gulf of Alaska exceed 1 m/yr and range up to 3.75 m/yr (Molnia, 1979); on the continental shelf the average rate is 4.5 mm/yr. In the Antarctic rates of terrigenous sedimentation on the continental shelf are on the order of .003 cm/yr (Orheim and Elverhoi, 1981). The facies patterns within these contrasting environments are just now being resolved and are also proving to be distinctive (Anderson et al., 1980; Domack, 1982; Wright and Anderson, 1982; Powell, 1981; Molnia and Bingham, 1980; and Carlson et al., 1977). But can reasonable climatic inferences be made about ancient glacial-marine sequences when, up to now, debate has centered around whether such rocks, particularly diamictites, are in fact glacial (Schermerhorn, 1974 ; Crowell, 1957; Harland et al., 1966). The research presented in the following pages was undertaken with the above problems in mind.

This study centers around the sedimentology of late Pleistocene (13,000-11,000 y.b.p.) glacial-marine deposits

which are exposed above sea level on Whidbey Island, Washington (Fig. 2). The major objective was to provide a detailed depositional model for these sediments and to attempt to place them in a glacial climatic setting consistent with the sedimentology.

A second objective was to establish a reliable set of criteria that can be used to distinguish glacial marine diamictons from associated debris flows and basal tills. In addition, this study has some importance in regards to the deglacial history of Whidbey Island, particularly in regard to the presence or absence of an ice shelf and the position of the ice margin at the time of the marine incursion.

Figure 2 Region of Puget Sound and Strait
 of Juan de Fuca.



CHAPTER 1
METHODS

Field Procedures

Coastal exposures on Whidbey Island were photographed during the summers of 1980 and 1981. Detailed lithofacies maps were constructed from photo mosaics. In total, 10 Kms of section were mapped at an average scale of 1 cm = 4 meters. Appendix B contains a section location map along with the lithofacies maps. In key locations detailed measured sections were described and samples were collected for textural and microfossil analysis. In most cases a systematic sampling pattern was utilized (May and Dreimanis, 1976). Samples were also collected in order to demonstrate textural trends, such as grading, on a small scale. Sample size varied from 10 cm³ to 100 cm³ depending on the overall texture and purpose for which the sample was collected.

Clast abundance data were collected from a number of different diamicton units including Vashon lodgement till. Any clast larger than 2 cm in largest dimension was counted within an area which varied from .09 to 1.48 square meters. Values were then recalculated to clasts per m². Weathered exposures were utilized, hence minor variability may have been introduced due to degree of matrix removal which left clasts exposed and concentrated in outcrop.

Pebble long axis orientations were measured as a bearing and plunge. Only clasts with a long to short axis ratio of greater than 2 were utilized. This is consistent with most published data dealing with clast fabrics of Quaternary

deposits. Sample procedures followed the suggestions of Andrews and Smith (1970) such that at least 2 samples were collected from each locality. Samples consisted of 25 measurements, and data were collected within a $.5 \text{ m}^2$ area for each sample. Measurements were taken from a non-magnetic needle inserted parallel to the long axis orientation of the pebbles.

Clasts were collected for shape analysis by selecting all stones inscribed by a $.5 \text{ m}^2$ area. Areas for collection were chosen at random. At least 3 samples for each site were collected, however, due to improper packing individual samples became mixed during shipping.

Paleocurrent directions were estimated by measuring the bearing of foreset plunge, and trough long axis orientations.

Laboratory Procedures

Textural analysis of selected samples was done following the procedures outlined for the Rice University Automated Sediment Analyzer (RUASA). On the average splits of a 15 gm sample were utilized for grain size distribution. The sand fraction (-1.0 - 4.0ϕ) was analyzed by settling through a 150 cm long column, coarse silt (4.0 - 6.0ϕ) by settling through a 25 cm long column, and fine silt-clay were analyzed using a hydrophotometer (Anderson and Kurtz, 1979). Grain size distributions at $.25\phi$ intervals, were determined using Gibb's formula for -1.0 - 4.0ϕ (Gibbs et al., 1971), and Oden's formula for silt sized particles (Krumbein

and Pettijohn, 1938). Computer output of the system consists of percent gravel, sand, silt, and clay; frequency and cumulative weight percents; mean grain size $M\phi$, standard deviation S_d , skewness S_k , and kurtosis K_t . Graphic displays of frequency and cumulative size distributions are also provided.

As pointed out by May (1981) most investigators utilizing settling tube systems convert settling velocities to Phi size data. Since the RUASA system follows this convention, it should be pointed out that the data produced should not strictly be interpreted as grain size. Rather the assumption is always made that a samples grain distributions have settling velocities equivalent to quartz spheres of the indicated Phi size. However, since settling velocities are being measured hydrodynamic interpretations based on such data are probably more realistic than strict grain size distributions. Data presented within the text can be interpreted with regards to either settling velocity or Phi size equivalent by using table 1 in the Appendix.

Fabric data were collected using a Fortran IV program for construction of Pi diagrams (Warner, 1969). This program was modified by W. Schmidt for use with the Rice University computing facility. Individual samples, consisting of 25 measurements, were contoured at 1, 3, 5, 7 and greater than 9% of data per 4% area. Contour intervals and counting areas for samples not consisting of 25 measurements are indicated alongside the graphs. Composite samples, those

consisting of 4 individual samples or 100 measurements, were also contoured. Fabric data can be found in table 2 Appendix A.

In order to define quantitatively the major differences in fabric between units, a non-standard technique was utilized. An approximation of the randomness for a given fabric can be obtained by measuring the percent area inscribed by the first contour interval (the 1% of data interval). Fabrics which are well developed will have lower areas of the 1% contour interval than samples which have an ill-defined fabric. The degree to which a fabric develops a modal distribution can be approximated by measuring the percent area inscribed by the third contour interval (5% of data). Strongly developed fabrics will have greater areas of the 5% interval than more random fabrics. Areas included by the two contour intervals were measured by planimeter methods and averages of 4 measurements were used as representative. These data along with total circle areas are to be found in the Appendix. Although not a standard method, this technique provides a quantification of graphic data which lends itself, in conjunction with other data, to statistical analysis.

Sphericity and roundness of pebble sized clasts were determined following the method outlined by Krumbein (1941). Barret (1980) discussed in detail measurements used in describing the shape of rock particles. Of the parameters

used in assigning a roundness value, the visual chart of Krumbein's was found the most satisfactory by Barret (1980). Krumbein's sphericity, S , is defined as follows:

$$S = \frac{(I \times S)^{1/3}}{L^2}; (0 < S \leq 1.0)$$

where, I = intermediate axis length, S = short axis length, and L = long axis length. A short program in basic language (SHAPE) was utilized in order to obtain the above values (Appendix). Mean roundness and sphericity values for a given sample are also provided by the program. Graphic displays of sphericity vs. roundness were contoured at 5, 10, and 15% of the data per 1% of graph area.

Sediment samples were also processed for microfossil analysis. Approximately 25 gms were treated with 15% HCl. Upon dissolution of carbonate samples were split, one half being treated with H_2O_2 for siliceous microfossils the other half being treated with HF for palynomorphs. Processing for palynomorphs followed the procedures outlined by Barss and Williams (1973).

CHAPTER 2

- 1) Regional Quaternary Stratigraphy
- 2) Whidbey Island Stratigraphy

Quaternary Stratigraphy

Unlike the Quaternary section of the mid-continent, the glacial sequence of the Puget Lowland is interbedded with marine and volcanogenic deposits. An abundance of datable material has therefore resulted in a stratigraphic sequence of somewhat greater resolution than elsewhere. However, the correlation of late Quaternary deposits between the Fraser lowland, British Columbia, and the Puget Lowland remains as a major problem in regional stratigraphy. In part, correlation problems exist because of the complexity of Pleistocene depositional environments. An accurate regional stratigraphy therefore depends on proper identification of sedimentary units: first with regard to depositional process and second with regard to glacial-climatic interpretations. Unfortunately, detailed sedimentologic studies in the Puget Lowland are lacking. In the following paragraphs, discussion will focus on the development of Quaternary stratigraphic models for the Puget Lowland and on problems of Late Pleistocene stratigraphy of significance to Whidbey Island.

Regional Quaternary Stratigraphy

As early as 1887 multiple glaciations were recognized in areas surrounding Puget Sound (Dawson, 1887). Willis (1898) first used the term "Vashon Drift" for glacial

deposits (tills) exposed on Vashon Island. Willis (1898) and Bretz (1913) recognized older, pre-Vashon, glacial deposits which Willis named Admiralty Drift.

Both drifts were thought to have been associated with a small ice sheet which occupied the Puget Lowland. It flowed from the north, and dominated over local alpine and piedmont glaciers of the Cascade and Olympic mountains (Bretz, 1913). It wasn't until the 1950's that more than two distinct glacial episodes were recognized (Mullineaux et al., 1957). Crandell and others (1958) established a fourfold glacial chronology based upon work in the southern Puget Lowland.

Vashon glaciation

Erosion interval (nonglacial interval)

Salmon Springs glaciation

Puyallup nonglacial interval

Stuck glaciation

Alderton nonglacial interval

Orting glaciation (oldest)

The Vashon, Salmon Springs, Stuck and Orting glacials were separated by nonglacial or erosional intervals (Crandell et al., 1958). Of the four glacials recognized only the Vashon is associated with organic remains that have yielded finite C^{14} ages. Retreat of Vashon ice from the Seattle area occurred just prior to 14,000 radiocarbon years ago (see Crandell et al., 1958). Previous to 1980 the Salmon Springs glacial was generally assumed to be of early

Wisconsin age (Stuiver et al., 1978). Therefore, the Stuck and Orting glacials were considered pre-Wisconsin. Easterbrook and others (1981) have presented convincing evidence that the type Salmon Springs glacial deposits are actually much older, dating to approximately 8×10^5 years B.P. (fission track dating). Resolution of the older glacial units awaits further study, but it now appears they may in fact be quite ancient.

Detailed work in southern British Columbia and the northern Puget Lowland resulted in a subdivision of events in what was previously termed the Vashon glacial (Armstrong et al., 1965). Armstrong and others named the Fraser glaciation for the Fraser Lowland of British Columbia (Fig. 3).

Fraser Glaciation	Sumas Stade
	Everson Interstade
	Vashon Stade
	Evans Creek Stade

The Olympia interglacial separates the Fraser glacial from the next older, Salmon Springs, glacial. The Fraser consists of three separate stadials of which only the Vashon has been recognized throughout the lowland. Prior to the Vashon Stade, minor expansion and retreat of Cascade alpine glaciers took place during the Evans Creek stade (20,000-17,000 years B.P.). A major advance of a small ice sheet took place during the Vashon stade. Ice originating

Figure 3 Late-Pleistocene stratigraphy of
the Puget and Fraser Lowland.
From Armstrong and others (1965)
and Easterbrook and others (1981).

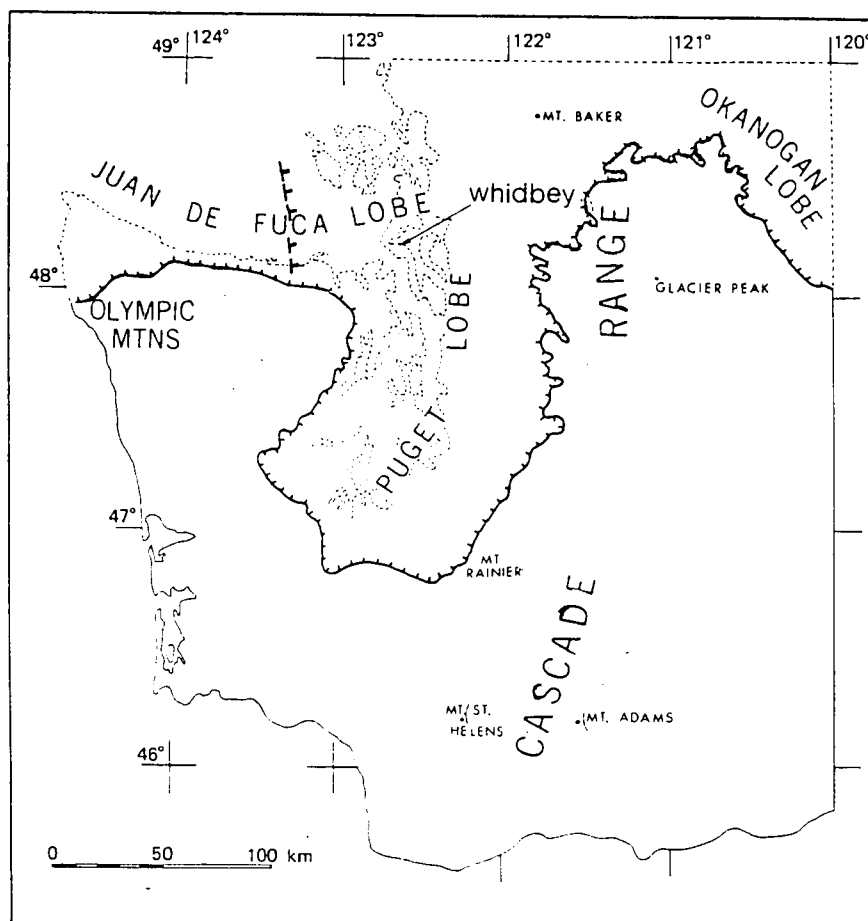
GEOLOGIC - CLIMATE UNITS		ABSOLUTE TIME THOUSANDS of YEARS B.P.	FRASER LOWLAND		EAST COASTAL LOWLANDS VANCOUVER ISLAND Fyles (1963)	SOUTHERN PUGET LOWLAND Crandell (1963) Molenaar & Garling (1963)
			BRITISH COLUMBIA Armstrong (1956 et seq. and unpublished ms.)	WASHINGTON Easterbrook (1963)		
FRASER GLACIATION	SUMAS STADE	10 —	Sumas Drift	Sumas Drift	Capilano sediments	
	EVERSON INTERSTADE	11 —	Whatcom glaciomarine deposits Capilano sediments Newton stony clay Cloverdale sediments	Bellingham glaciomarine drift		
		12 —		Darling sand		
		13 —		Kulshan glaciomarine drift		
	VASHON STADE	14 —	Surrey Drift	Vashon Drift	Vashon Drift	Vashon Drift
	EVANS CREEK STADE	15 —	Surrey Drift	Vashon Drift	Vashon Drift	Vashon Drift
		17 —				
		19 —				
		21 —				
		23 —				
25 —						
OLYMPIA INTERGLACIATION	29 —	Surrey Drift	Vashon Drift	Vashon Drift	Vashon Drift	
	33 —					
	36 —					
	37 —					
	38 —					
	39 —					
SALMON SPRINGS (?) GLACIATION		Semiamu Drift (age unknown)		Dashwood Drift (age unknown)	Salmon Springs Drift	

in the coastal mountains of British Columbia flowed south and reached its maximum extent, 125 km south of Seattle, between 15,000 - 14,000 (C^{14}) years ago (Armstrong et al., 1965; Clague et al., 1980). Granitic material of British Columbian provenance indicates a Canadian source for Vashon deposits. The Vashon ice sheet is generally thought to have consisted of two lobes of ice: the Puget lobe, which flowed south and occupied Puget Lowland proper, and the Juan de Fuca lobe, which flowed west-northwest and occupied the Strait of Juan de Fuca (Bretz 1920, Fig. 4). Anderson (1968) disagrees with the concept of an extensive Juan de Fuca lobe during the Vashon, since glacial marine sediments from the bottom of the strait range in age from 28,700 to 13,150 with no intervening till deposits.

The Everson interstade is named for glacial-marine and non-marine deposits found in the northern part of the lowland (Easterbrook, 1963). Further discussion of the Everson interstade and its associated deposits can be found in the next section.

Armstrong and others (1965) also recognize glacial deposits which post date the Everson at around 11,000 (C^{14}) years ago. To date, glacial deposits of the Sumas stade are limited to regions of the northern Puget Lowland near the U.S.-Canadian border. The Sumas drift is thought to represent a minor readvance of glacial ice at the closing stages of the Fraser glaciation.

Figure 4 Reconstruction of Vashon Ice Sheet
with Juan de Fuca and Puget lobe.
From Porter (1964). The Juan de
Fuca lobe is shown at two positions,
the dashed margin is according to
Anderson (1968).



Additional detailed work in British Columbia has resulted in refinement of the events for the Fraser glaciation (Armstrong, 1981; Hicock and Armstrong, 1981).

Summary

As many as four glaciations are recognized in the Puget Lowland; the Orting, Stuck, Salmon Springs, and Fraser. Of these, finite ages have been obtained for only the Salmon Springs and Fraser.

The Orting and Stuck predate the Salmon Springs which is of early Pleistocene age (~800,000 y.b.p.). The Fraser is late Pleistocene (20 - 10,000 radiocarbon years) and has been divided into three stadials (Evans Creek, Vashon, and Sumas) and one interstadial, the Everson (Armstrong et al., 1965). In the following section the above scheme will be related to Quaternary deposits on Whidbey Island and problems pertaining to the correlation of such units will be discussed.

Whidbey Island Stratigraphy

Since 1913 (Bretz, 1993) at least three glacial sequences have been recognized on Whidbey Island. However, not until 1949 were these deposits recognized as representing three separate glaciations (Hansen and Mackin, 1949). Easterbrook (1968) presented the first relative chronology for Whidbey Island and assigned type sections for four stratigraphic units (Fig. 5).

Pre-Olympia Sediments

The lowermost glacial unit is referred to as the Double Bluff Drift, is named for exposures at Double Bluff (Fig. 6), and consists of till, outwash, and glacial-marine sediment (Easterbrook et al., 1967, 1968). The Whidbey formation overlies the Double Bluff Drift and was deposited during an interglacial climate (Easterbrook 1967; Heusser and Heusser, 1981). At its type section, near Double Bluff (Fig. 6), the Whidbey is comprised of alternating beds of peat, silt, and well stratified sand up to 60 m thick. The Whidbey is thought to have been deposited by meandering streams in a coastal plain environment (Hansen and Mackin, 1949; Easterbrook et al., 1967).

Possession Drift consists of till, outwash and glacial-marine sediment. It overlies the Whidbey formation and is named for exposures at Possession Point (Fig. 6).

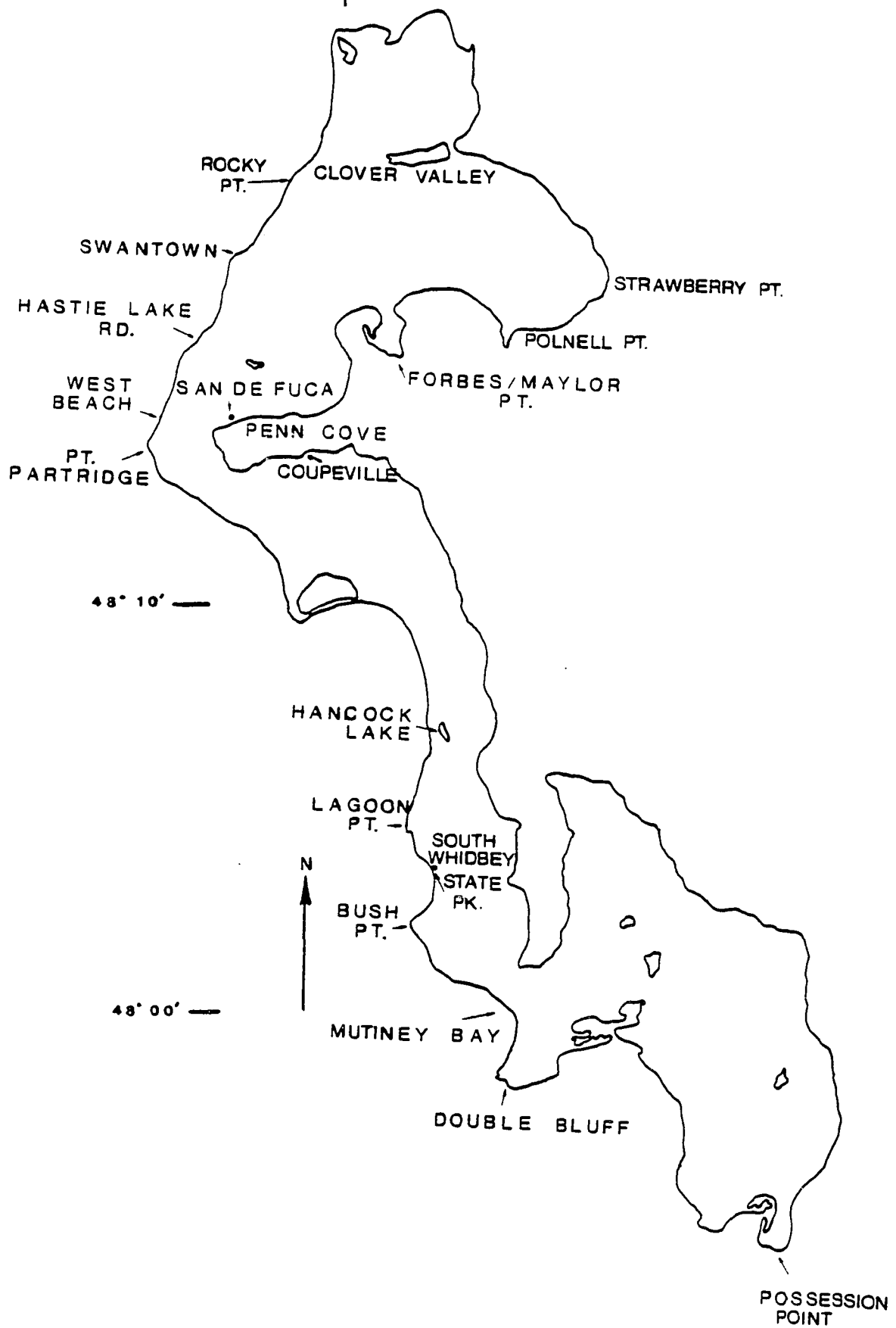
Figure 5 Quaternary stratigraphy of Whidbey
Island, from Easterbrook (1968,
1981).

GEOLOGIC CLIMATE UNITS		STRATIGRAPHIC UNITS	¹⁴ C DATES	Amino Acid Date
FRASER GLACIATION	Everson Interstade	Everson Glacionarine drift	11,850 ± 240 12,535 ± 300 13,010 ± 170	
	Vashon Stade	Partridge Formation		
		Vashon till and associated drift		
		Esperance Sand		
OLYMPIA INTERGLACIATION		Quadra Formation	26,650 ± 1700	
POSSESSION GLACIATION		Possession Drift	>40,000	50 - 80,000
WHIDBEY INTERGLACIATION		Whidbey Formation	>33,200 >35,000 >40,000 >42,000	100 - 150,000
DOUBLE BLUFF GLACIATION		Double Bluff Drift		200 - 300,000

Figure 6 Whidbey Island with locations
mentioned in the text.

122° 40'

6



Problems of correlating the above units with established stratigraphy of the southern Puget Lowland exist because associated organic remains lay outside the resolution capabilities of carbon-14 dating (Easterbrook, 1968). Easterbrook and others (1967, 1968) tentatively assigned the Possession Drift to the Salmon Springs glaciation and suggested that the Double Bluff Drift may correlate with the Stuck glaciation.

Recently, shell and woody material from Double Bluff, Whidbey, and Possession sediments have been dated by amino-acid racemization (Easterbrook and Rutter, 1981). Easterbrook and Rutter assign an age of 50 - 80,000 years B.P. for the Possession glaciation, 100 - 150,000 years B.P. for Whidbey interglacial, and 200 - 300,000 years B.P. for the Double Bluff glaciation. As mentioned earlier, the type Salmon Springs glacial deposits have been recently dated, by fission track, at about 700,000 years B.P. (Easterbrook, et al., 1981). As pointed out by Easterbrook and Rutter (1981), because both the Double Bluff and Possession drifts are younger than the type Salmon Springs, evidence of six major glaciations now exists.

Olympia Interglacial

Except for a peat that overlies Possession Drift at Strawberry Point (Fig. 6, Easterbrook et al. 1967, 1968), deposits of the Olympia Interglacial (37,000 - 18,000;

Armstrong et al., 1965) have not been widely recognized on Whidbey Island. In fact, Hansen and Easterbrook (1974) suggest that the peat at Strawberry Point represents a non-glacial, or interstadial, rather than an interglacial. This was based upon palynological data, indicating a cool unstable depositional environment, and limited C^{14} dates of 27,600 - 22,700 B.P. for the peat (Hansen and Easterbrook, 1974).

Fulton and others (1976) and Alley (1979) disagree with the concept of a non-glacial interval for Olympia sediments. They maintain that similar deposits represent an interglacial in British Columbia, which extended from 51,000 - 21,000 radiocarbon years B.P. The revised age of 50 - 80,000 years for the Possession (Easterbrook and Rutter, 1981) may have resolved the "Possession problem."

An informal stratigraphic unit, the West Beach silt, has recently been recognized in a number of exposures on Whidbey Island (Gerald Thorsen, per com.). It is named for a section north of West Beach (Fig. 6), where it underlies Vashon Drift and overlies Possession deposits. It is a massive silt, probably of eolian origin, and is characterized by a well oxidized gravelly zone at its lower contact with the Possession. Interbedded organic material from the same unit on Protection Island (Fig. 2) has been dated at $33,490 \pm 500$ radiocarbon years B.P. (Gerald Thorsen, per com.) Thus, it appears as though Olympia age deposits may be more widespread on Whidbey Island than previously suggested.

Fraser Glaciation

Deposits of the Fraser glaciation (20,000 - 10,000 years B.P.) are widespread on Whidbey Island and consist of four stratigraphic units (Fig. 7, Easterbrook, 1968).

Esperance Sand

Easterbrook (1968) correlated trough cross-bedded sands and gravels, that underlie Vashon till, with the Esperance sand member of the Vashon Drift (Mullineaux et al., 1965). In places over 60 meters of Esperance sand is exposed. It is thought to consist primarily of proglacial outwash that was deposited with the advance of Vashon ice. No dates as yet are available for this unit on Whidbey Island.

Vashon Drift

Massive diamictons exposed within the upper parts of bluff exposures on Whidbey Island were assigned to the Vashon Drift by Easterbrook (1968). Although Easterbrook mentions the presence of lodgement, ablation, and flow tills, as well as subglacial pro-glacial outwash, within the Vashon Drift, details of distribution and depositional sequence of such units have yet to be worked out. Vashon drift was deposited on Whidbey Island sometime between $26,850 \pm 1700$ and $13,010 \pm 170$ (C^{14}) years B.P. (Easterbrook, 1968).

Partridge Gravel

The Partridge Gravel was named by Easterbrook (1968) for exposures of coarse gravel and sand found near Point

Figure 7 Stratigraphy of Fraser glacial
deposits on Whidbey Island and
the Fraser Lowland, from Easter-
brook (1968) and Armstrong (1981).

LATE PLIESTOCENE

WHIDBEY ISLAND, WA.

EASTERBROOK (1968)

GEOLOGIC-CLIMATE
UNITS

LITHO-
STRATIGRAPHIC
UNITS

FRASER GLACIATION

EVERSON INTERSTADE
11,850 - 13,010 y.B.P.

VASHON STADE

Everson Glacial -
Marine Drift

Partridge Fm.
(gravel)

Vashon Drift
(till and associated
sediments)

Esperance Sand

STRATIGRAPHY

FRASER LOWLAND, B.C.

ARMSTRONG (1981)

GEOLOGIC-CLIMATE
UNITS

LITHO-
STRATIGRAPHIC
UNITS

SUMAS STADE
11,000 - 14,000 y.B.P.

FT. LANGLEY
TIME INTERVAL
11,400 - 13,000

VASHON STADE
13,000 - 18,000 y.B.P.

18,000 - 26,000 y. B.P.

PRE - VASHON
STADE
19,000 - 23,000 y.B.P.

Capilano Sediments
(marine, beach, and
glacial-marine)

Sumas Drift
(till and associated
sediments)

Ft. Langley Fm.
(Intbd. marine, glacial-
marine and glacial
sediments)

Vashon Drift
(tills and associated
sediments)

Quadra Sand

Coquitlam Drift
(till and possible
glacialmarine units)

OLYMPIA INTERGLACIAL

> 26,850 y. B.P.

Partridge and West Beach (Fig. 6). An ice-contact subaqueous origin for the Partridge Gravel was suggested by Easterbrook (1968). Because the unit is associated with well preserved kame and kettle topography and is overlain by Everson glacial-marine deposits, Easterbrook placed it stratigraphically between the Vashon and Everson Drifts.

Everson Drift

Glacial-marine drift deposited during the Everson interstade is exposed in a number of bluffs surrounding Whidbey Island (Easterbrook, 1968, 1969). Radiocarbon dates from shell material range in age from 13,600 to $11,850 \pm 240$ (F. Pessi, per comm.; Easterbrook, 1968; Fig. 7). The origin of Everson age deposits, according to previous workers, is discussed in the next section. However, it will suffice to say that the drift was thought to have been deposited by a combination of ice rafting and marine processes at a time when the basin, in part, was still isostatically depressed (Thorson, 1980).

Summary

In summary, Whidbey Island contains Pliestocene deposits of at least three glaciations; Double Bluff, Possession, and Fraser. Interglacial deposits comprise a significant part of the section and consist of Whidbey and Olympia age materials. A breakdown of Fraser age deposits consists of four stratigraphic units. The Vashon Stade

consists of Esperance Sand and Vashon Drift while the Everson interstade consists of Everson glacial-marine drift and possibly Partridge Gravel.

Stratigraphic Problems

While the Whidbey Island stratigraphy of Easterbrook (1968, 1981) serves as a working model, it should be pointed out that major problems remain. These problems exist because of the reconnaissance nature of Easterbrook's 1968 mapping, a lack of key beds and datable deposits, and the fact that approximately 75% of the total coastal exposure has yet to be related to Easterbrook's stratigraphic model.

Detailed work has shown that several sections need to be reinterpreted. As an example, silts exposed at South Whidbey State Park (Fig. 6) contain abundant foraminiferan assemblages (Cole, 1979) and dropstones structures (pers. observation). Easterbrook's (1968) interpretation of these exposures as belonging to the interglacial Whidbey formation needs to be re-examined. Also, units mapped as Vashon Drift (Easterbrook, 1968), between Lake Hancock and Lagoon Point (Fig. 6), actually lie below a massive silt identical to the West Beach silt (Appendix B, meas. sec. LH-1). Although correlating this silt with the West Beach unit could be questioned, the presence of marine sands and glacial-marine sediment within the unit mapped as "Vashon" (meas. sect. LH-1) necessitates a reinterpretation for this section.

Units of the Sumas Stade, Fraser Glaciation, have not been recognized on Whidbey Island. The type Sumas Drift is limited in distribution to parts of the Fraser Lowland (Armstrong, 1981). However, near Victoria, B.C., (Fig. 2), a lodgement till has recently been recognized that post-dates Everson age glacial-marine deposits (Hicock et al., 1981). The proximity of this locality to Whidbey Island suggests that deposits of Sumas age may be present.

CHAPTER 3

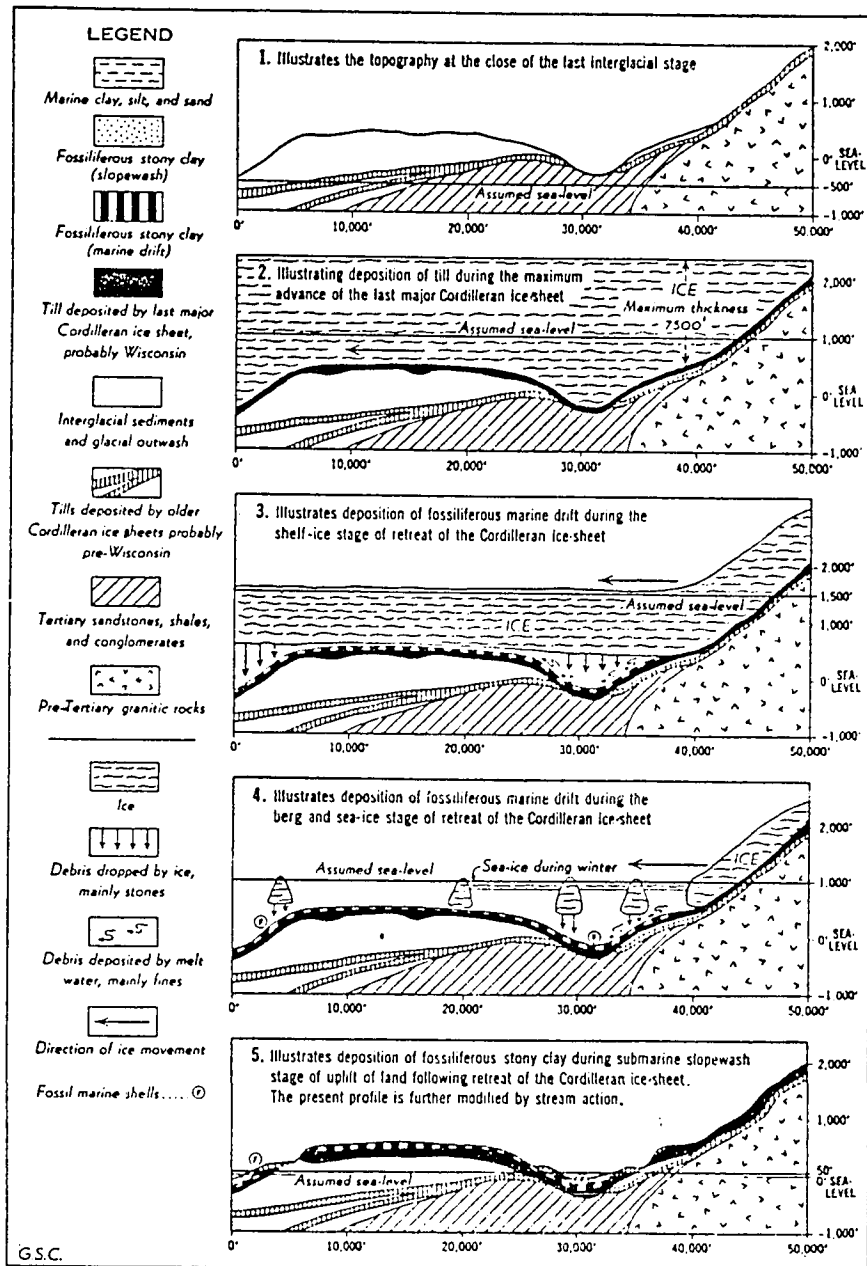
- 1) Previous Studies on Everson Age Glacial-marine Drift
- 2) Late Pleistocene Sea Level

Everson Age Glacial-Marine Drift

Fossiliferous diamictons were first recognized in the Puget and Fraser Lowland by Reagan (1907) and Bretz (1913). These authors attributed the presence of marine shells in "till like" deposits to the incorporation of older marine sediments by grounded glacial ice. Johnston (1923) agreed in part with this idea but also suggested that the fossiliferous diamictons could have been deposited by floating ice. Johnston theorized that the ice-sheet became bouyant in response to thinning and deposited a "till like" sediment which continually buried colonizing marine organisms. This model explained three general observations known at the time. First, shells of marine organisms were extremely well preserved within the sediment and included apparently in-situ baranacles, worm tubes, and Chalmys. Second, fossiliferous diamictons directly overlie tills known to have been deposited by the Cordilleran ice-sheet. Lastly, the fossiliferous units are less compact than underlying tills.

Armstrong and Brown (1954) proposed a two stage model to explain the origin of "fossiliferous till like stony clays" found in the Fraser Lowland. Their model involved both deposition from floating ice and subsequent downslope movement or "slopewash" of marine sediments (Fig. 8). Because the glacial-marine sediments contain a "rather even

Figure 8 Glacial-marine depositional model
for late-Pleistocene deposits in
the Fraser Lowland according to
Armstrong and Brown (1954).



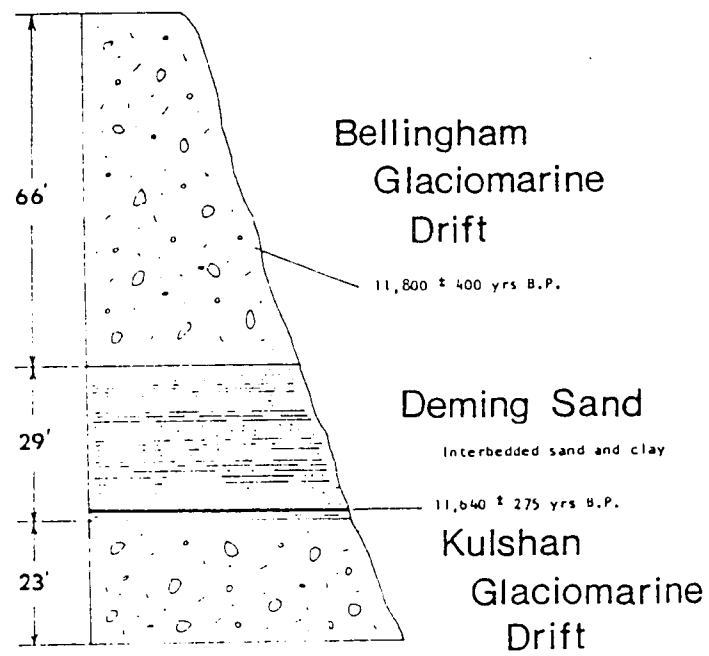
distribution of clasts" Armstrong and Brown (1954) favored an ice shelf rather than an iceberg rafted origin for the deposits.

Armstrong and Brown (1954) also suggested the possibility of sea ice as an active depositional agent and emphasized the importance of sediment input into the marine environment via meltwater processes.

Armstrong and Brown relied on multiple explanations for the deposits because they observed geomorphic associations, different contact relationships, and a variety of marine sediments besides the till-like deposits. Based upon the macro-fossil assemblages collected up to that time, Armstrong and Brown inferred that climatic conditions during deposition of the units were similar to the present day northern Gulf of Alaska (Lat. 60 - 63° N). Details of Armstrong and Brown's model are discussed in relationship to Whidbey Island deposits in a following section.

Easterbrook (1962, 1963) recognized fossiliferous till-like deposits of late Pleistocene age in the northern Puget Lowland, near Bellingham (Fig. 9, Kulshan and Bellingham glacial-marine drift). He attributed their origin to ice shelf and/or iceberg rafting, similar to the model suggested by Armstrong and Brown (1954). Easterbrook recognized the regional extent of such deposits throughout the northern Puget Lowland and calculated an ice shelf thickness of no more than 67 meters based on macro-fossil depth associations

Figure 9 Type stratigraphic section of the
 Everson glacial-marine drift,
 from Easterbrook (1962).



and ice-shelf freeboard calculations. The same deposits were subsequently recognized on Whidbey, Camano, and the San Juan Islands (Easterbrook, 1968 , 1969). Easterbrook mentions that the Everson drift on Whidbey Island contains more silt and clay than elsewhere (Easterbrook, 1968).

Since the initial work of Easterbrook and others, further study has focused on the ice-shelf/iceberg controversy and the interpretation of the Deming sand (Fig. 9).

Paleoecologic conditions for Everson age glacial-marine deposits were inferred for the Fraser Lowland by Wagner (1959), the San Juan Islands by Shaw (1972), and portions of the Fraser and Puget Lowlands by Balzarini (1981).

Based on macrofossil assemblages Wagner suggested late-Pleistocene conditions of the Fraser Lowland approximated those of the Gulf of Alaska, at $60.6 - 61.5^{\circ}$ N latitude. Depths on the order of 20 meters were also indicated by these macrofossil assemblages. Shaw (1972) concluded that Everson drift on the San Juans was deposited in no more than 7 - 10 meters of water and in temperatures close to the present southern Gulf of Alaska.

Balzarini (1981) presented foraminiferal and additional macrofossil evidence that suggests shallow water deposition for the Everson, with water temperatures varying between 0° and 15° C and salinities between 25 and 30‰. The above conditions were inferred for massive glacial-marine diamictos found south of Lummi Peninsula (Fig. 2), on Whidbey Island,

and other regions of the Puget Lowland. Slightly greater paleo-salinities and paleo-depths were inferred for similar deposits north of Lummi Peninsula.

Based on their paleoecologic studies Shaw (1972), Armstrong (1981), and Balzarini (1981) suggest that ice-shelf conditions could never have existed in the lowlands during the deposition of Everson age glacial-marine drift. In support of this view, they cite the lack of ice shelves in the present Gulf of Alaska, which is the climatic analogy they propose for the Everson, and the shallow water in which the units were supposedly deposited (< 50 m). Rather, they support the view that Everson age glacial-marine sediments were deposited in a marine environment bordering the Vashon ice sheet as it retreated northward into Canada. A similar model was proposed by Croll (1980), in part to explain the Deming sand which separates the Kulshan and Bellingham glacial-marine diamictos at the type section (Fig. 9). Croll felt that icebergs played the major role in deposition of the marine diamicton and submarine outwash processes could have produced the intervening "Deming" sand.

Thorson (1980, 1981) outlined a sequence of events involving retreat of the Vashon ice-sheet which called for initiation of marine conditions at a time when ice receded past Admiralty Inlet (Fig. 10, 2). In this scenario, Thorson called for an instantaneous change from a terrestrial or glaciolacustrine environment to a tidewater bounded ice-sheet

Figure 10 Deglaciation model for the central
 Puget Lowland (southern Whidbey
 Island) according to Thorson (1980).

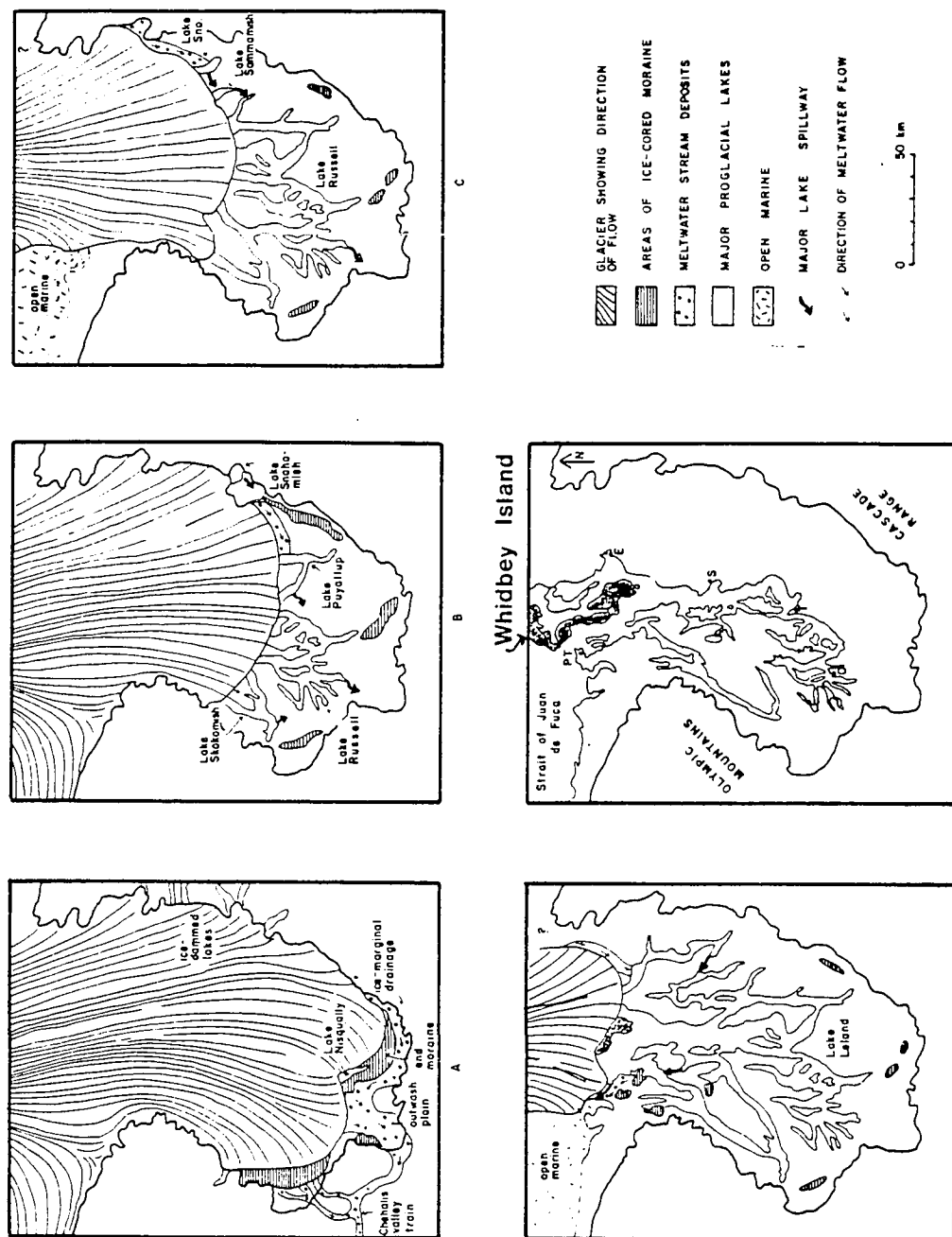


FIG. 9. Generalized paleogeographic maps of the Puget Sound region showing progressive retreat of the Puget lobe. Maximum extents of Glacial Lake Nisqually (A), Puyallup and Skokomish (B), Russell (C), and Leland (D) are shown relative to the present margin of Puget Sound (E). Locations of Port Townsend (PT), Everett (E), Seattle (S), Tacoma (T), and Olympia (O) shown on map E. Area of "open marine" is not patterned on map E.

environment. If significant thinning of the ice sheet did occur prior to the marine event then, according to Thorson (1981), restrained rebound could not have contributed to more than 50% of the total isostatic rebound.

Hicock and others (1981) have found sedimentologic evidence to support an ice sheet/marine environment near Victoria, B.C. In coastal exposures, flow till deposits were found interbedded with marine silts and glacial-marine sediments (Hicock et al., 1981). A supraglacial source, in part, was inferred for the flow tills and therefore a grounded ice-sheet in a shallow marine environment was called for. Similar sedimentary relationships were observed for Fort Langley glacial-marine deposits (Everson age) in the Fraser Lowland (Armstrong, 1981). In addition, Armstrong called upon a variety of marine environments to explain the different facies he recognized within the sequence. These included, ice marginal, submarine outwash, deltaic and ice-berg environments (Armstrong, 1981).

Pessl and others (1981) were the first to recognize a similar complexity for Everson age marine sediments in the Puget Lowland. Besides fossiliferous diamictons, Pessl and others recognized pebbly silt, massive well sorted silt, laminated silt and sand, and massive to crudely stratified sand. Environments of deposition include beach, tidal flat, shallow marine (< 10 m), deep marine (>10 m), glaciofluvial and marine ice contact. In order to explain the diversity

of sediment types, Pessl and others (1981) support the view of an ice-sheet margin that was rapidly retreating and calving in open marine waters.

Powell (1980) briefly studied exposures of Everson glacial-marine drift at three localities including the type section. He recognized a number of distinct lithofacies including diamicton, interbedded sand and mud, and cross-bedded sand. Powell tried to relate these facies to specific environments he had studied in the Gulf of Alaska (see section on glacial-marine models). He suggested a pro-glacial iceberg zone, at a distance from the ice margin, for the origin of the diamicton facies; and tidal flat, braided stream, and beach environments for the interbedded sand-mud and cross bedded sand facies. Powell also recognized a turbidity current channel infill deposit within glacial-marine deposits in the Fraser Lowland.

Summary

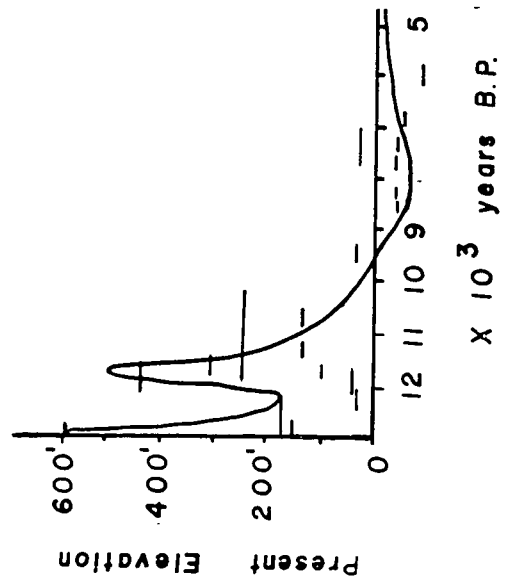
The old view that a thinning Vashon ice-sheet led to an ice-shelf marine environment (Johnson, 1923; Armstrong and Brown, 1954; Armstrong et al., 1965; and Easterbrook, 1962, 1963, 1969) has fallen into disfavor in the light of paleo-ecologic, glaciologic, and isostatic considerations (Shaw, 1972; Balzarini, 1981; Armstrong, 1981; Thorson, 1980). Rather, Everson age glacial-marine deposits most likely represent deposition in a marine environment that bordered

a grounded ice-sheet (Hicock et al., 1981; Croll, 1980; and Pessl et al., 1981). However, hard sedimentologic evidence in support of either view is lacking and a detailed model that accounts for the facies variability both laterally and vertically has yet to be developed in the Puget Lowland.

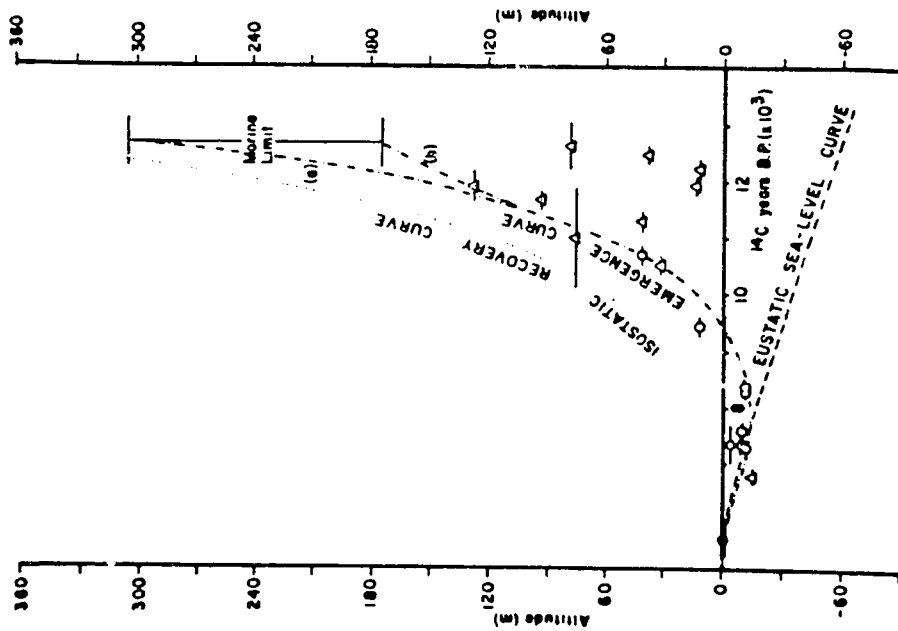
Late Pleistocene Sea Level

Of direct importance to this study is the history of sea level fluctuations in the northern Puget Lowland for the last 13,000 years. However, a lack of reliable dates has precluded the establishment of accurate sea level curves for most regions other than the Fraser Lowland. Easterbrook (1963), Mathews and others (1970), Armstrong (1981) and Thorson (1981) have reviewed the available geologic data and agree that the major cause of post-glacial sea level fluctuation was isostatic rebound. The curve of Mathews and others (1970) is shown in figure 11b and is in general agreement with the results of Easterbrook (1963) and Armstrong (1981). These authors suggest that maximum heights of post-glacial sea level were obtained immediately following deglaciation, at which time isostatic rebound resulted in rapid emergence which continued until about 12,000 (C^{14}) years B.P. This rapid emergence was followed by an even more rapid submergence which Mathews, and others (1970) attributed to the isostatic effects of the Sumas ice advance (Armstrong et al., 1965). This second submergence produced marine limits which were slightly lower than the post Vashon event. Emergence again occurred at around 11,500 (C^{14}) years B.P., following Sumas ice retreat, and resulted in an eventual sea level approximately 30 meters below present.

Figure 11 Late-Pleistocene-Holocene sea level fluctuations for the Fraser Lowland; A, according to Thorson (1981), and B, according to Mathews and others (1970). The data are the same for both curves. The eustatic curve is from Curray (1965).



B.



A.

Sea level then rose steadily to its present level, which was attained roughly 5,000 (C^{14}) years B.P.

Thorson (1981) used the same data and constructed a different curve (Fig. 11a). He suggests that the available data do not disprove the second submergence event but can be explained by a single slightly less rapid emergence. The question concerns whether some C^{14} dates, interpreted by Mathews and others (1970), are from deposits which represent marine limits, such as shoreline sediments, or marine deposits which lay below a marine limit, as proposed by Thorson (1981).

According to Thorson, isostatic rebound occurred at an average rate of 1.7 cm/yr and was essentially complete by 6,000 (C^{14}) years B.P. At this time a constant rate of eustatic rise brought sea level up to its present limit by 5,000 (C^{14}) years B.P. This can be seen in figure 11a where the isostatic sea level curve shows a steady stand and intercepts the eustatic curve of Currey (1965).

The curve in figure 11a is generally applicable to Whidbey Island although the maximum marine limit was about 42.5 m on south Whidbey and 73.2 m on north Whidbey (Thorson, 1981). The regional tilt of the maximum marine limit, at about .92 m/km, to the south reflects the differential isostatic rebound caused by the configuration of the Vashon ice sheet (Thorson, 1980).

The maximum amount of rebound on central Whidbey Island appears to have been about 140 m, thus sea level stood lower than today at around 6,000 (C^{14}) years B.P. The presence of drowned terraces around portions of Whidbey Island, as revealed by seismic profile (Snively et al., 1976), supports the contention of lower sea levels.

Large post-Vashon resubmergences, such as those proposed by Easterbrook (1963), appear to be tectonic in origin as the rates of uplift and relaxation are far too rapid to be accommodated by the isostatic constraints for the Lowland (Thorson, 1981).

The only published dates for late Pleistocene glacial marine sediments on Whidbey Island range from $13,010 \pm 170$ to $11,850 \pm 250$. Since these dates are from the highest stratigraphic lithofacies the implications are that deposition of the entire sequence took place during the maximum height of sea level and was essentially complete prior to substantial emergence.

CHAPTER 4

1) Description of Lithofacies,
Everson Age Glacial Marine Drift

2) Depositional Process and Lithofacies Interpretation

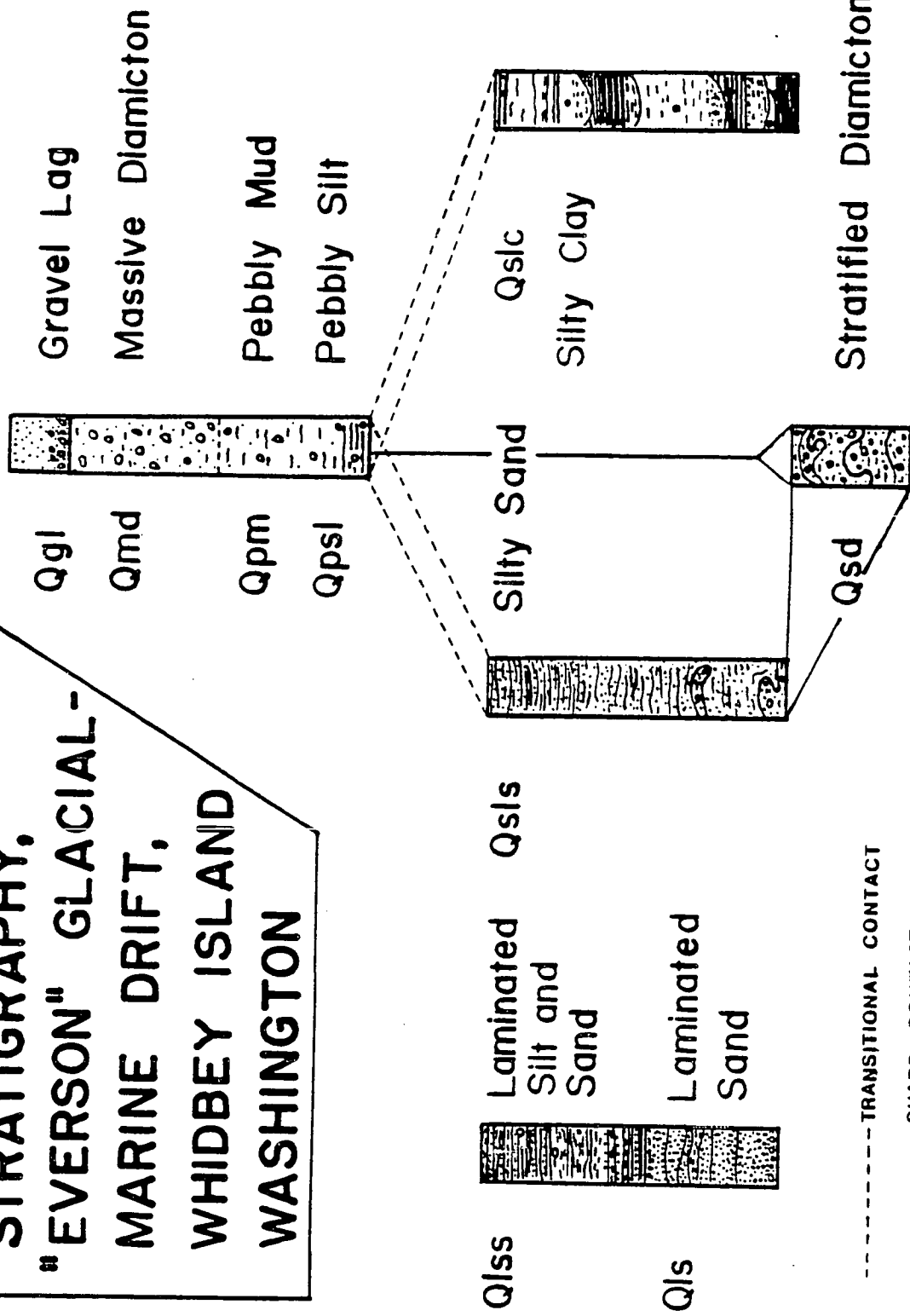
Lithofacies of Everson Glacial Marine Drift

Within the sequence of Everson age glacial-marine deposits on Whidbey Island, three major divisions can be made; (Fig. 12, lower, middle, and upper units). Of these, only the upper unit can be found at every exposure of Everson drift. As can be seen in figure 12, these major divisions can be broken down into six distinct lithofacies. They include: stratified diamicton (Qsd), pebbly silt and mud (Qpsl, Qpm), massive fossiliferous diamicton (Qmd), stratified silty sand and sandy silt (Qsls), massive to stratified silty clay (Qslc), and laminated sand and laminated sand and silt (Qls, Qsl). Sub-facies or variations within these units are also present. The overall texture and stratification of units, as observed in the field, are the major characteristics used to define each of the facies.

Rarely are complete facies transitions present within a single exposure, however, the relationships observed in a number of sections has provided enough information to establish an idealized sequence (Fig. 12). In the following sections individual facies and their subfacies will be described. Individual facies will then be related in a comprehensive glacial-marine model that includes a discussion of depositional process.

Figure 12 Generalized facies diagram of
 Everson age glacial marine drift
 on Whidbey Island.

SEDIMENTARY FACIES AND GENERALIZED STRATIGRAPHY, "EVERSON" GLACIAL- MARINE DRIFT, WHIDBEY ISLAND WASHINGTON



Lower Contact

Of key importance in the interpretation of Everson glacial marine drift is its lower contact with underlying units. This contact varies as much as the drift itself, and therefore necessitates some discussion. As defined by Armstrong and others (1965), the base of the sequence should correspond to the upper contact of Vashon deposits (i.e., till). This relationship is complicated by two factors. First, deposition of Vashon deposits was not uniform and, in fact, non-deposition or erosion was associated with the Vashon ice-sheet in some localities. As a result, Everson glacial marine drift can be found to directly overlies pre-Vashon deposits (San de Fuca-West) and to be unconformable with tills of Vashon or older age (Hastie Lake Road North, Forbes Point). The lower contact in these cases corresponds to a horizon of subglacial erosion.

The second factor involves erosion which occurred in association with the deposition of Everson glacial marine drift. This is best exemplified by channelization, due to turbidity currents, evident in the section near Swantown. Here, subaqueous erosion has produced a contact between Everson glacial marine drift and floodplain deposits of the Whidbey formation.

The two examples given above represent instances where the interpretation of the lower contact is unambiguous. In other cases the lower contact is less well defined either

because it appears to be locally conformable with presumed Vashon deposits (West Beach North, J. Thorsen, per com., Fig. 13) or may represent a transgressive surface over terrestrial outwash sediments (Coupeville-Lovejoy Point, Mutiney Bay). These relationships will be discussed in greater detail in Chapter 6.

In summary, the lower contact of Everson glacial marine drift is, in general, extremely sharp and represents a surface of sub-glacial or sub-aqueous erosion. Locally the contact with assumed Vashon deposits may be conformable or may represent a transgressive surface.

Lower Unit

Stratified Diamicton, Qsd

Units mapped as Qsd are the most variable of all the lithofacies and occur predominantly at the base of the section. In general, the unit is characterized by diamicton textures and pronounced internal stratification. Based on color and nature of stratification, two sub-facies of stratified diamicton can be recognized.

Grey, horizontally stratified diamictos may or may not belong to the Everson depending on their interpretation. Stratification is marked by 3 - 6 cm thick muddy diamicton beds that are separated by laminated silty clay layers. These have dropstone structures (Fig. 14, sections, SFW-1a, MP-1a,1b). Units vary laterally such that laminated mud

Figure 13 Interpretive sketch of exposure
north of West Beach. Outcrop is
at or close to the marine limit.

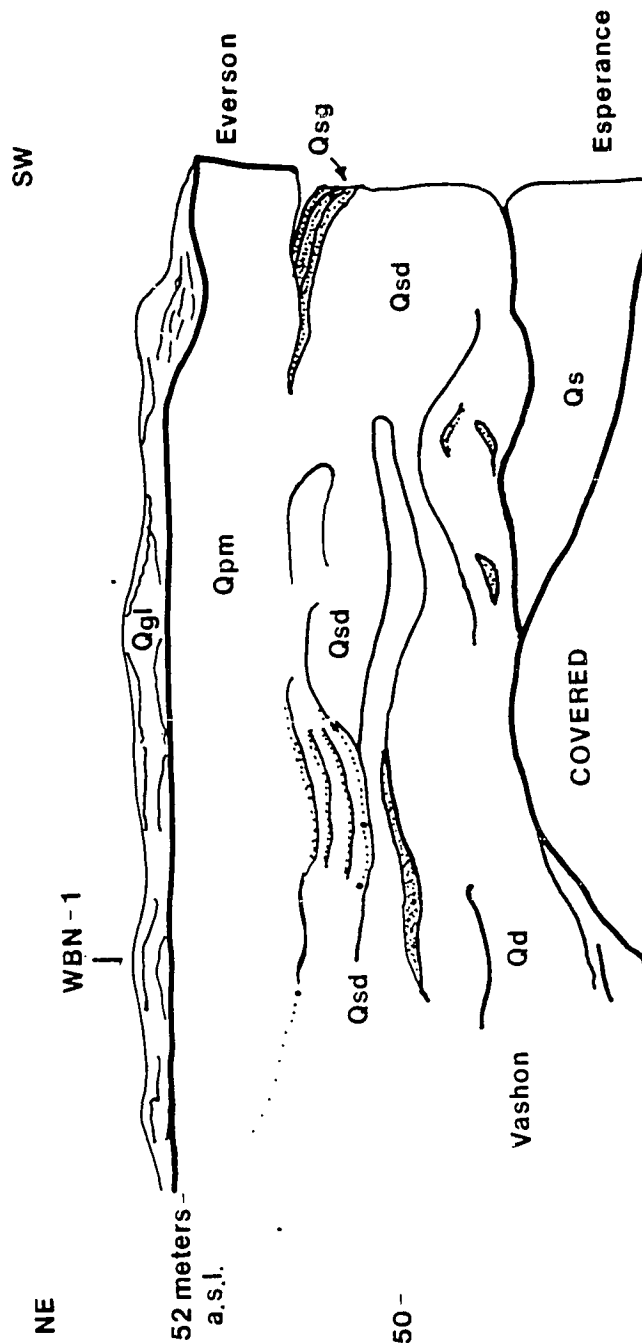


Figure 14 Photographs of horizontally strati-
fied diamicton exposed near the base
of the section at Maylor Point (A,B)
and San de Fuca-West (C).

A

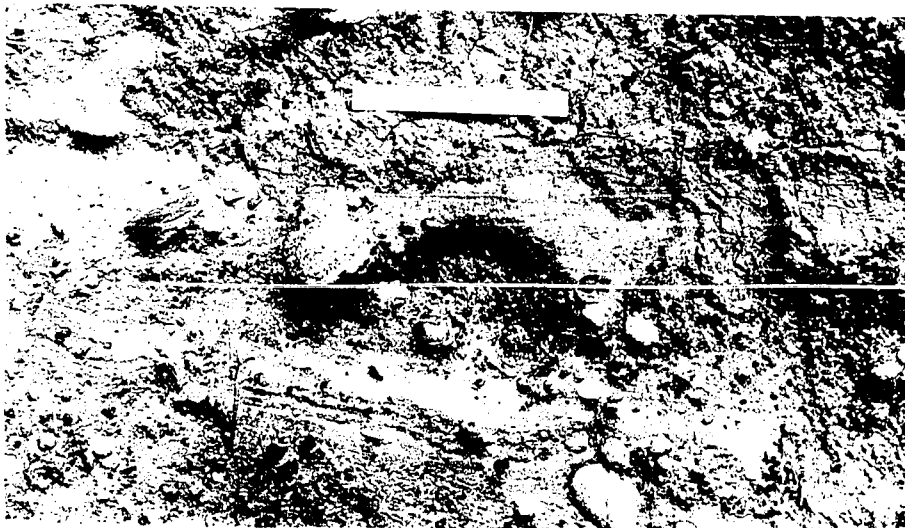
66



B



C



layers increase in thickness and fewer stones are present. Clast size ranges up to boulders (Fig. 14). Such units are restricted in their distribution, occurring as lense like deposits 25 - 30 meters in lateral exposure (San de Fuca-West and Maylor Point). The maximum observed thickness is approximately 2 meters but may actually be greater since most lower contacts have not been observed. Upper contacts are sharp and are marked by thin gravelly sand laminae which are overlain by thin, massive, grey clay beds that are unfossiliferous (section MP-1a).

These units cannot be demonstrated as having been deposited in a marine environment, therefore their assignment to the Everson is questionable. However, they do appear to occupy a transitional stratigraphic level between sub-glacial erosional surfaces and overlying sediments of marine origin.

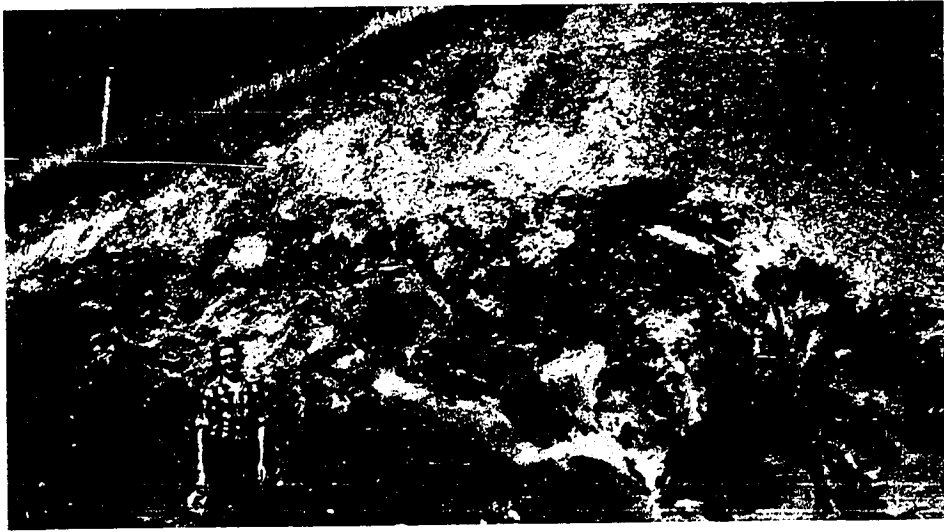
The most abundant sub-facies of stratified diamicton is characterized by deformed bedding and extreme variability of both texture and unit thickness. Deformed bedding is present as internally convoluted stratification (Fig. 15), irregular-lobate contacts with other facies (Fig. 15) and convolute to parallel interbedding of texturally distinct diamictons (Fig. 15). Such units can be traced laterally into massive diamictons which, while mapped as Qsd, exhibit little evidence of internal stratification (San de Fuca-East).

Textural variability of Qsd units within and between

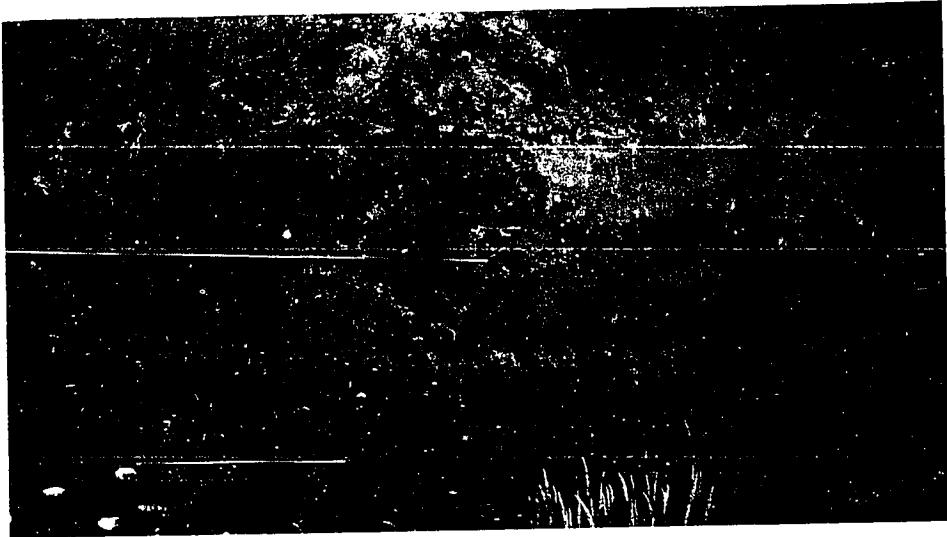
Figure 15 Photographs of stratified diamicton facies at Swantown (A), Coupeville-Lovejoy Point (B), and San de Fuca-West (C).

A

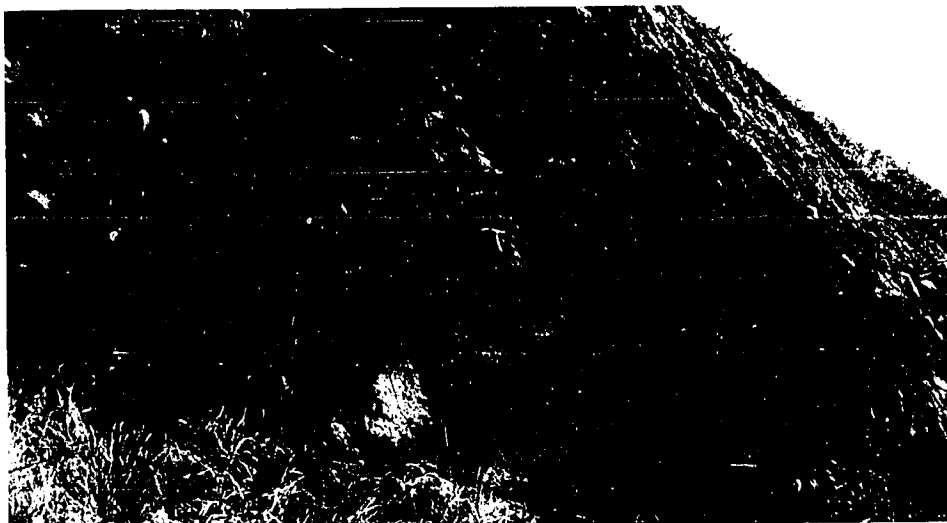
69



B



C



exposures is pronounced as shown by sand:silt:clay ratios (Fig. 16) and pebble abundances (Fig. 17). Within individual units normal grading of the sand-gravel fraction can be observed, but is not common (Fig. 18). Finer grained diamictites may also have concentrations of gravel along their lower contacts (section SFW-1b). Layers and lenses of sand and gravel are commonly found interbedded within Qsd units.

A most distinctive characteristic of this sub-facies of Qsd is the extreme variability of unit thickness within a single exposure (see sections from San de Fuca-East and West). As seen in places along the East San de Fuca section, Qsd units pinch out and swell to thicknesses of up to 5 meters. Units tend to thicken as lower contacts decrease in elevation and thin as such contacts climb in elevation. Maximum thickness of Qsd units is 12 meters, found south of Hastie Lake Road.

Lower contacts of both individual and sequences of multiple Qsd units are almost always sharp and planar, while their upper contacts are sharp but irregular, often with lobate or convex geometries (San de Fuca West, East, Coupeville-Lovejoy Point). The fact that some units are found interbedded with facies of demonstrable marine origin (Figs. 15 and 19) suggests at least partial deposition in marine waters. In such cases this sub-facies of Qsd can be reliably assigned to the Everson glacial marine drift.

In summary, Qsd facies consist of basically two sub-facies.

Figure 16 Sand, silt, clay ratios for representative samples of Qsd facies.

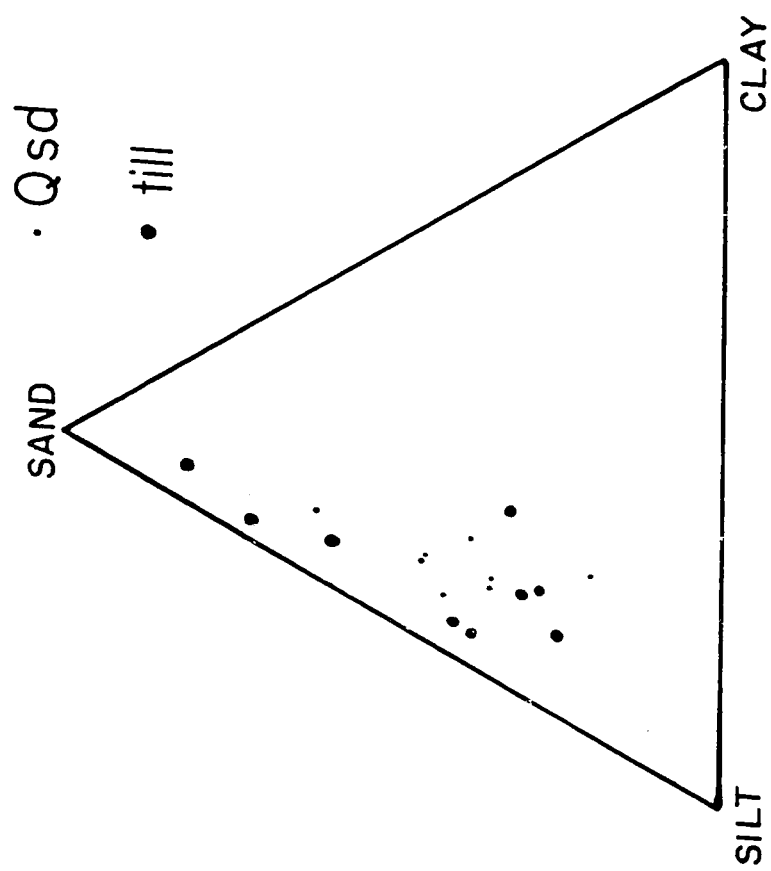


Figure 17 Abundance of greater than 2cm
sized stones from Qsd, Qpm, and
lodgement till facies. Each bar
represents one measurement of the
number of stones per square meter.

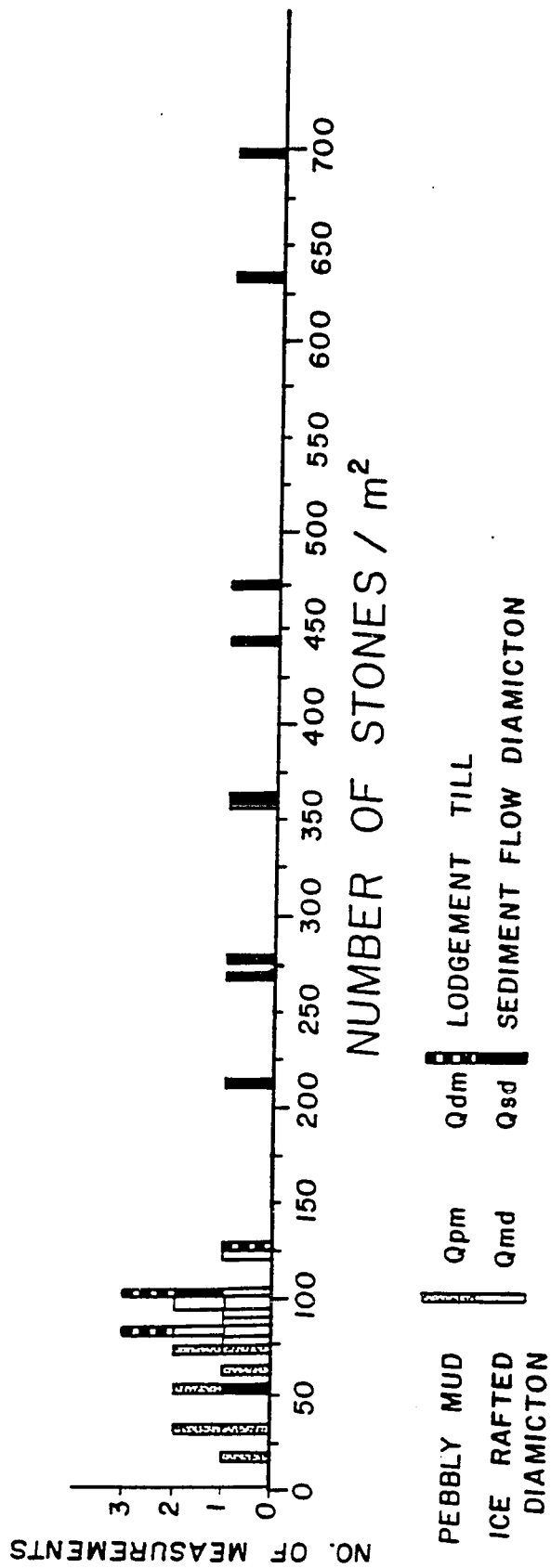


Figure 18 Cumulative grain size distributions for samples SFW-F5, 6, and 7. Photograph shows Qsd unit and sample locations. Distributions for -4.0 to -1.0 ϕ were determined by sieving at .5 ϕ intervals.

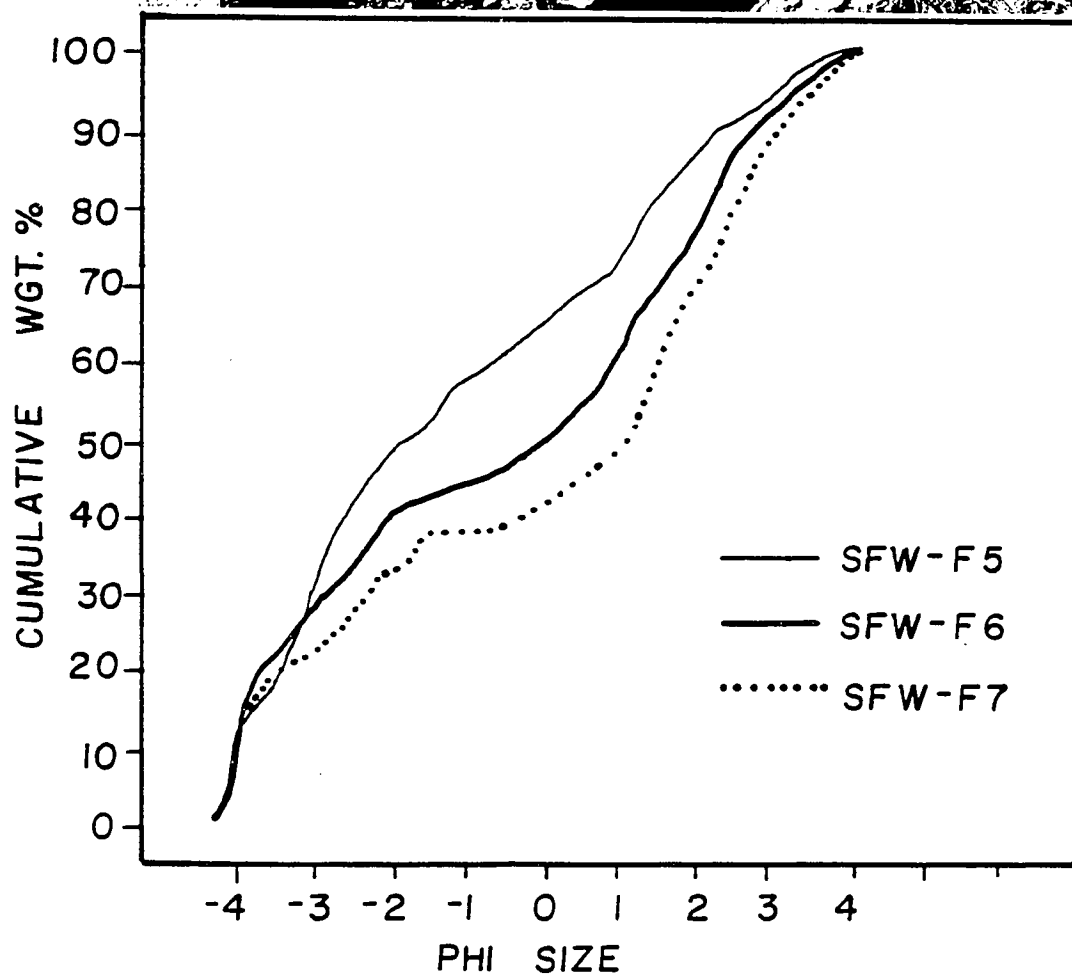
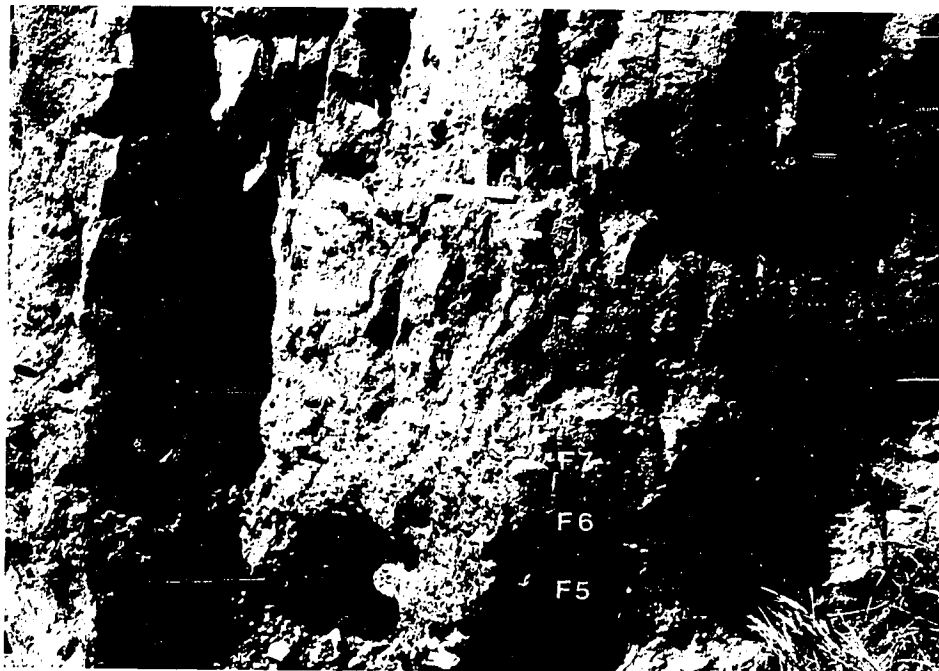


Figure 19 Photograph of interbedded relationship of sediment flow (Qsd) and pebbly mud (Qpm) at San de Fuca-West.



One is limited in exposure, horizontally stratified, and may or may not belong to the Everson "sensu-stricto." The other is well exposed, has deformed bedding, and is interbedded, in part, with facies of known marine origin. Both sub-facies are found predominantly at the base of the section and in the case of the second sub-facies, can be shown to overlies a surface of glacial erosion (San de Fuca-West, East).

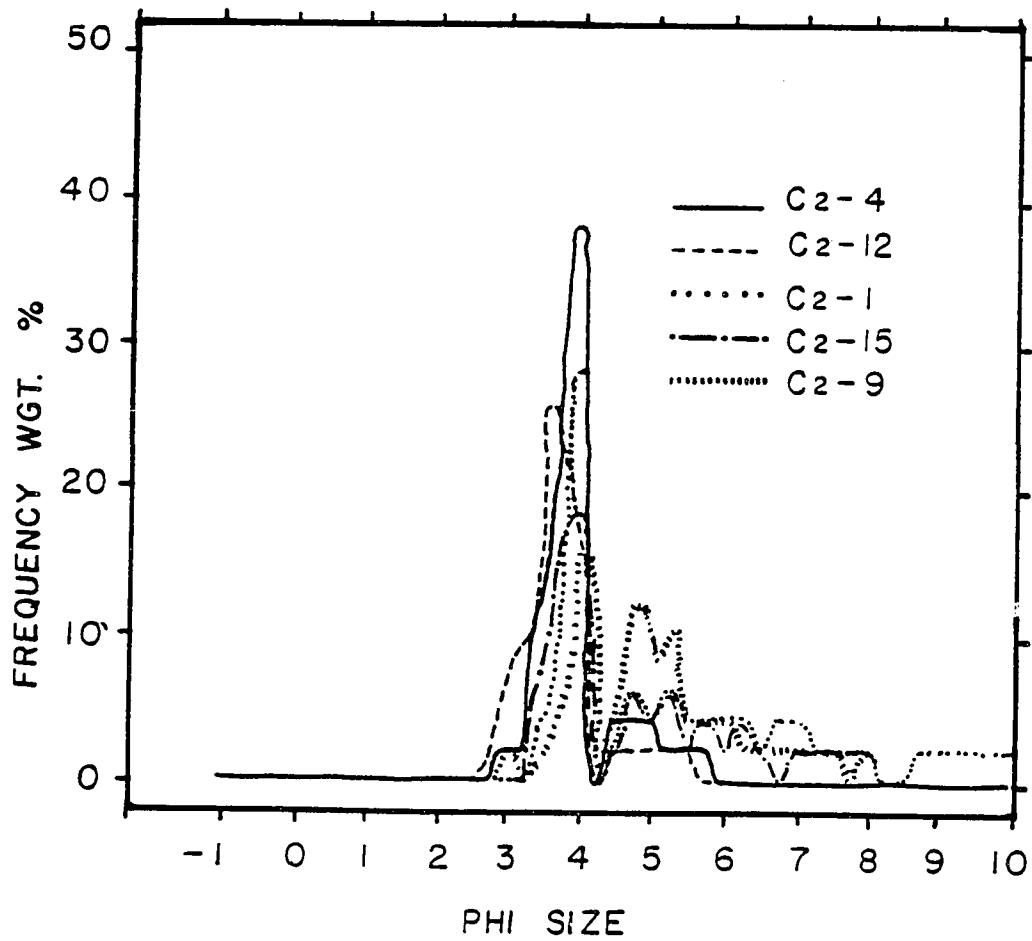
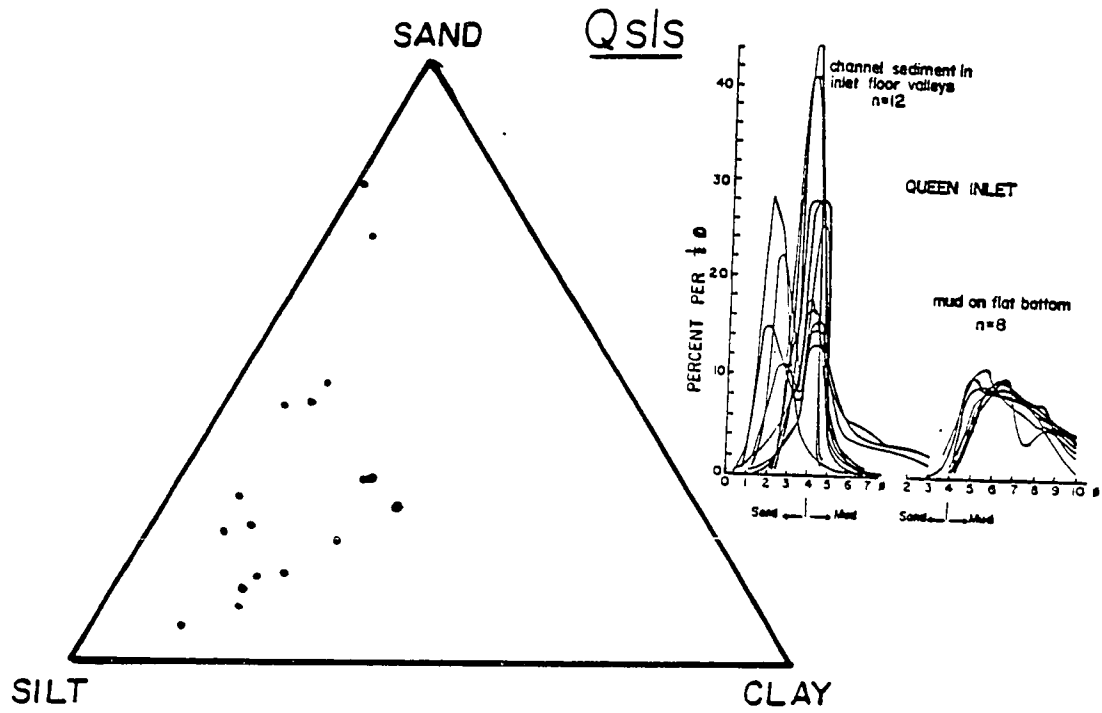
Middle Unit

Facies assigned to the middle unit are similar in that they consist of stratified sands, silts, and clays. Major differences exist however between exposures on the west coast and elsewhere on Whidbey Island. These differences concern the internal arrangement and sorting of stratified sediments within the unit and the nature of the transition into overlying facies.

Stratified Silty Sand and Sandy Silt, Qsls

Locally, stratified silty sand and sandy silt, (Qsls) comprise a significant part of the section and directly overlies Qsd facies. Sand, silt, clay ratios and representative grain size frequency distributions for these sediments can be seen in Fig. 20. Bedding within these units is very discontinuous and this facies tends to grade laterally into overlying (Qpm, Qpsl), often becoming interbedded.

Figure 20 Sand, silt, clay ratios and grain size frequency distributions for stratified silty sand and sandy silt facies (Qs1s). For comparison frequency distributions for similar sediments from Queen Inlet, Alaska, are shown in the upper right, from Hoskin and Burrell (1972).



Stratified silty sands are laminated to very thinly bedded, often with wavy or cross-cutting bed set boundaries. Planer laminations are most abundant but current ripple cross-laminae and large scale ripples can also be found (Fig. 21). Thicker sand beds may exhibit a crude grading of granule sized silt clasts, whereas massive sands contain 2 - 3 cm sized rip-ups of finer grained sediment (Fig. 21). Contorted beds, load style deformation, and water escape structures are also common (Fig. 21). Dropstone structures, while rare, are present as are current lineations.

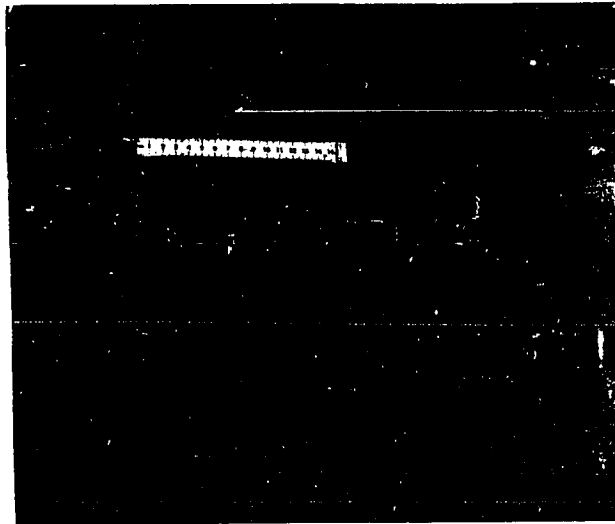
Stratified sandy silts are interbedded with silty sands but in general predominate laterally and above thick silty sand sequences. Sandy silts are very thinly laminated to massive. Very thin laminae are indistinct to discontinuous. Massive units often have very sharp lower contacts which show evidence of loading and deformation.

Sequences of stratified silty sand and sandy silt fine upwards into pebbly silt and mud facies (Qpm, Qps1) and, as mentioned previously, grade laterally into these finer grained sediments as well. This relationship is particularly well exposed at San de Fuca-West and Lovejoy Point. At Lovejoy Point a fairly thick, 6 m, section of stratified silty sand shows evidence of channalization as preserved by multiple sequences of low-angle trough cross-stratification (Fig. 22). Lateral to this exposure, thin beds of laminated silty sand alternate with thin beds of pebbly silt and mud

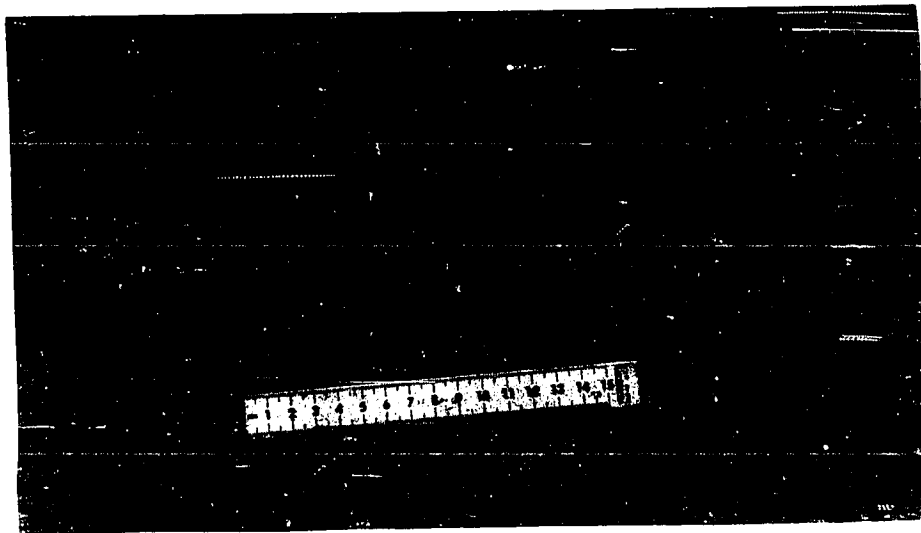
Figure 21 Photographs of sedimentary structures found within Qs1s facies at Lovejoy Point. Large scale ripples (A), graded silt rip-ups (B), and convolute bedding (C). Scale in cms.

A

84



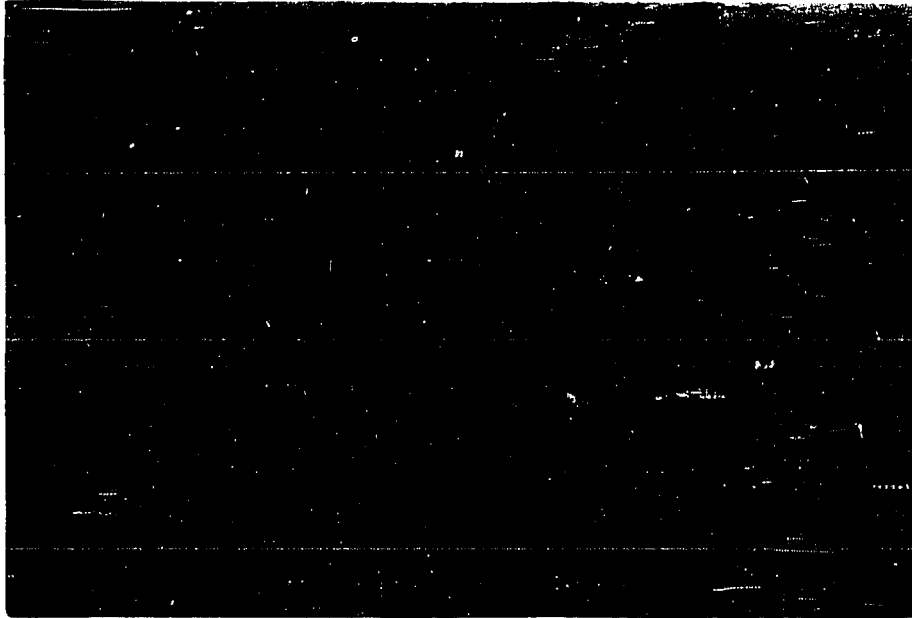
B



C



Figure 22 Photographs of channelized silty
 sands exposed at Lovejoy Point.
 Digging tool is approximately
 30 cm long.



A



B

(Fig. 23) such that silty sands fine upwards into sandy silt and eventually pebbly mud (Fig. 24). Lower contacts of the stratified silty sands are always sharp but their upper contacts with Qpm may be either sharp or gradational (Fig. 23). Qsls facies can comprise the base of the section where Qsd units are missing and in such cases have very sharp basal contacts (Lovejoy Point, Forbes Point). Thickness of Qsls sequences ranges from .2 to 6 meters.

Silty Clay, Qslc

Stratified silty clay facies (Qslc) are exposed at Coupeville and Maylor Point, where they comprise up to 6 meters of section. Massive to wispy laminated clays are interbedded with laminated to thinly laminated silty clays, and clayey silts (Fig. 25). Occasional silty sand laminae, with current rippled surfaces, can also be found. Lenticular bedding and small scale convolutions are also common. Dropstones are more common in this facies than in Qsls units but still are no more frequent than 1 - 2 stones per m². Bedding is difficult to distinguish within this facies but with close examination some interesting relationships can be observed. Lenses of thinly laminated clayey silt, 3 - 2 m in width, grade upwards into massive wispy laminated clay with dropstones. Subsequent laminated lenses never seem to directly overlie the centers of lower units, but are offset by 1 - 2 meters and may cross-cut one another. Such

Figure 23 Photograph and interpretive sketch
 of interbedded silty sand (Qsls)
 and pebbly mud (Qpm).

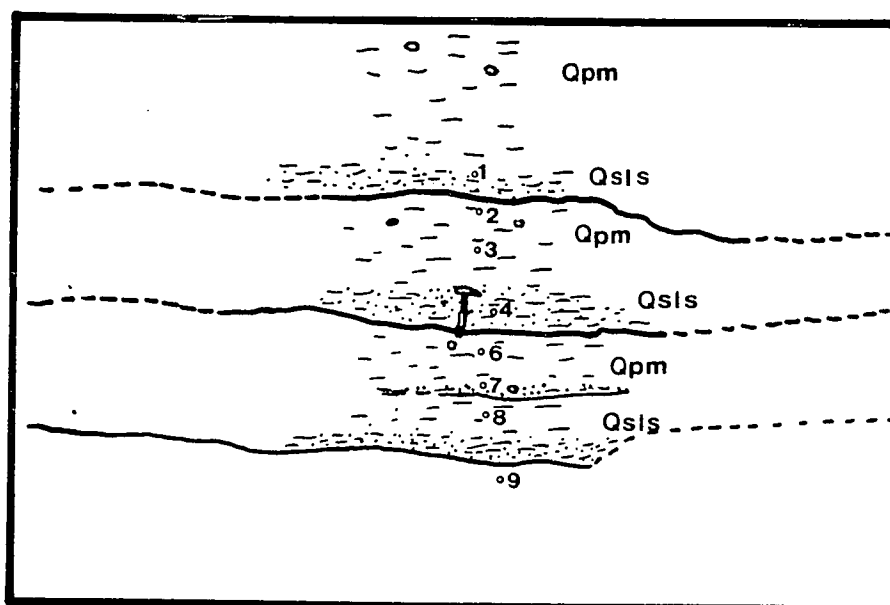


Figure 24 Grain size cumulative distributions
for interbedded sequence of silty
sands and pebbly muds shown in
figure 23.

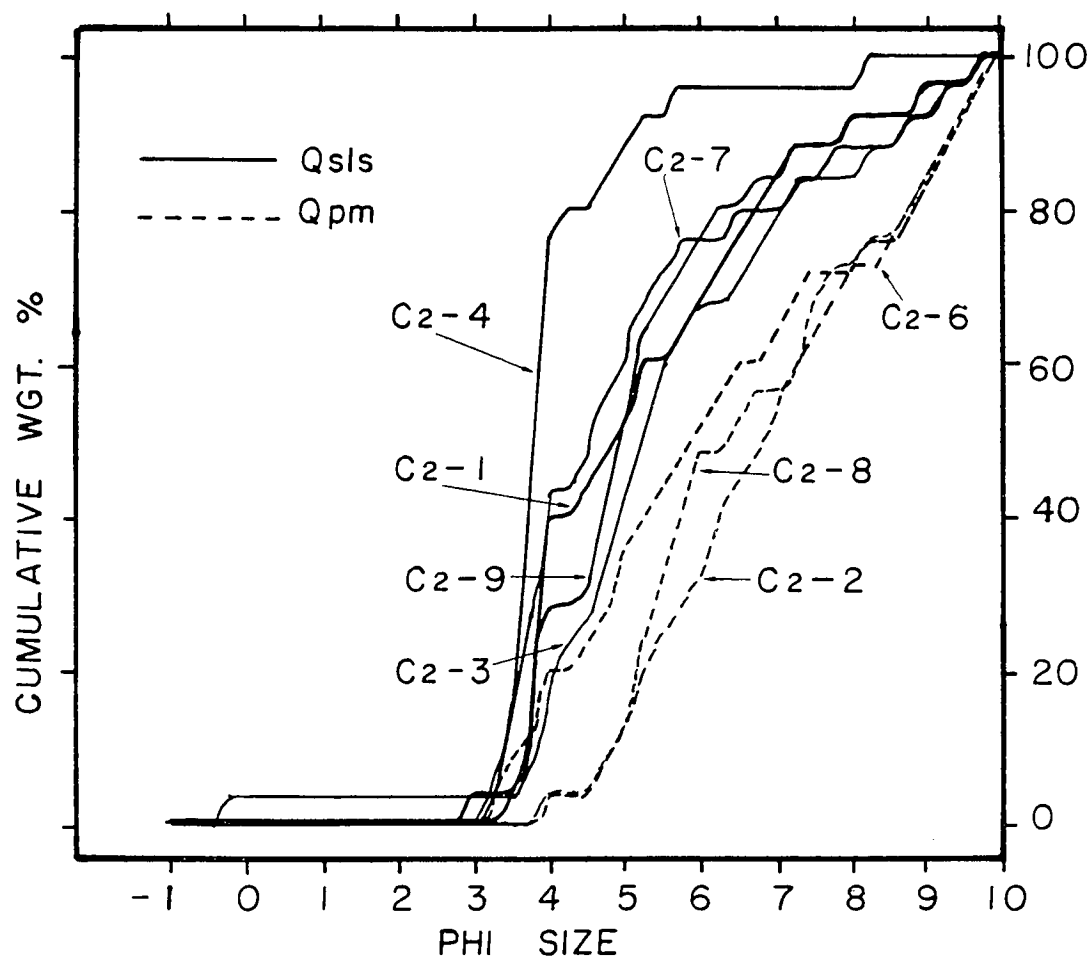
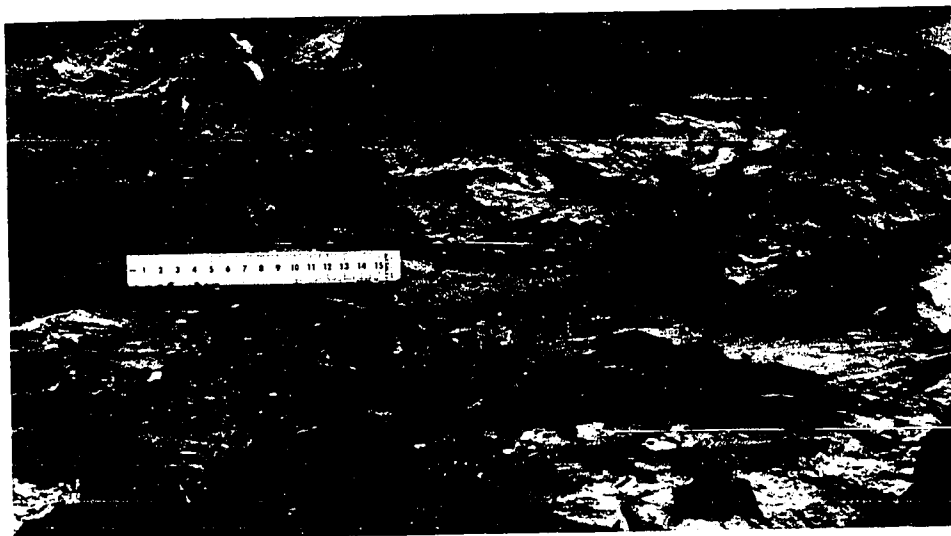


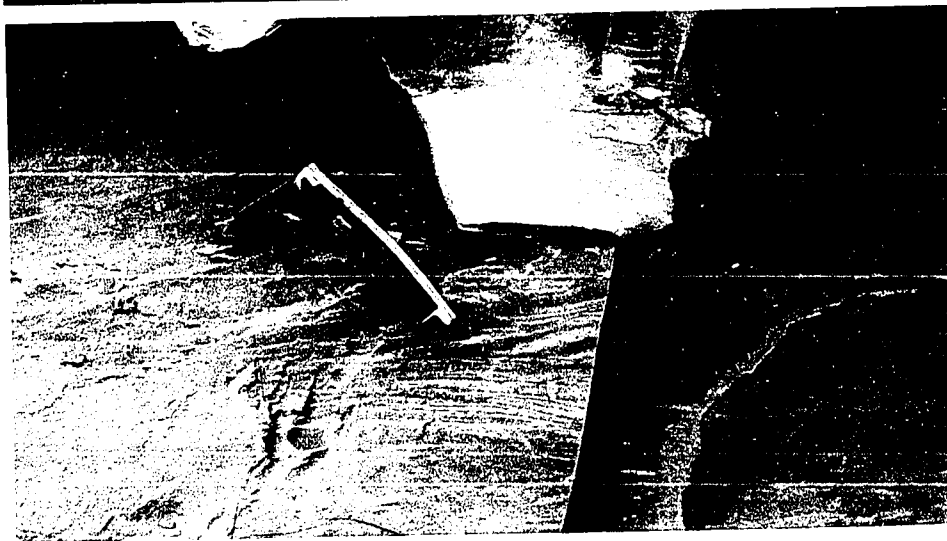
Figure 25 Photographs of silty clay facies exposed at Maylor Point. Soft sediment deformation and wispy laminations (A and B). Lenticular bedding and laminations of current rippled sand and mud (C).

A

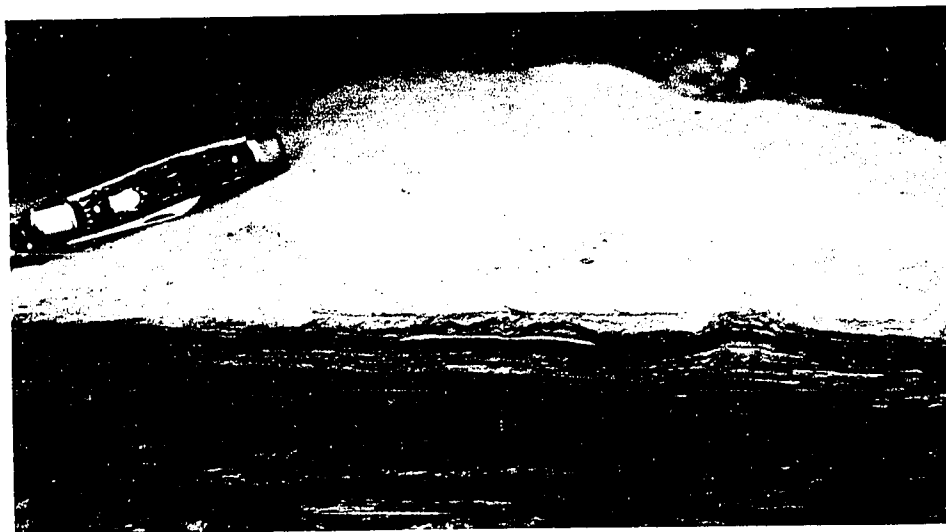
93



B



C



a relationship is shown in Fig. 26, along with grain size frequency distributions for these transitions. As with the Qsls facies, Qslc units grade upwards into overlying pebbly silts or pebbly muds.

Laminated Sand and Laminated Sand and Silt, Qls, Qsl

Along the west coast of Whidbey Island stratified units of sand and (Qls) silt (Qsls, Qsl) are also present (West Beach, Hastie Lake Road-North, Swantown). However, they differ in several ways from the Qsls and Qslc facies found elsewhere. In general, coarser sands are present, sands are better sorted, normal grading is well developed and stratification in the form of parallel composite beds of sand and laminated sand and silt is well defined (Fig. 27, section WB-2, ST-1, HL-1). Dropstones and horizontal trace fossils are common along bedding planes of laminated sand and silt (Fig. 28). Symmetrical ripple surfaces are also present (Fig. 26) .

Overall these units fine upwards from very coarse sand to silt and clay (ST-1) however their upper contacts are very sharp and erosional (WB-1, 2, ST-1). Lower contacts may also be sharp (erosional) and marked by gravel layers, as seen in the section near Swantown (ST-1).

Upper Unit

Facies of the upper unit include pebbly silt (Qpsl), mud (Qpm), and massive diamicton (Qmd). They are the most

Figure 26 Photograph and grain size cumulative distributions for interbedded sandy silts and silty clays found within Qslc facies.

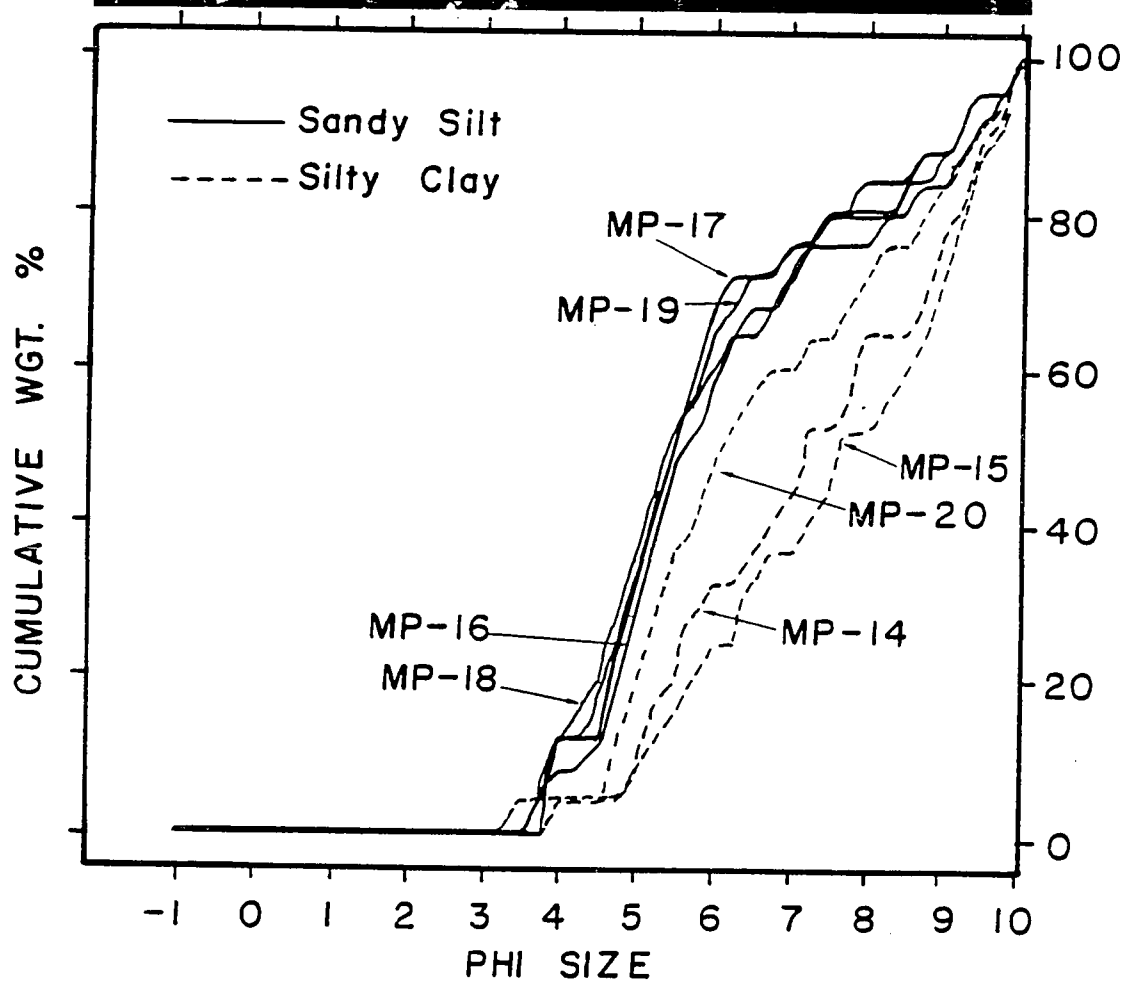
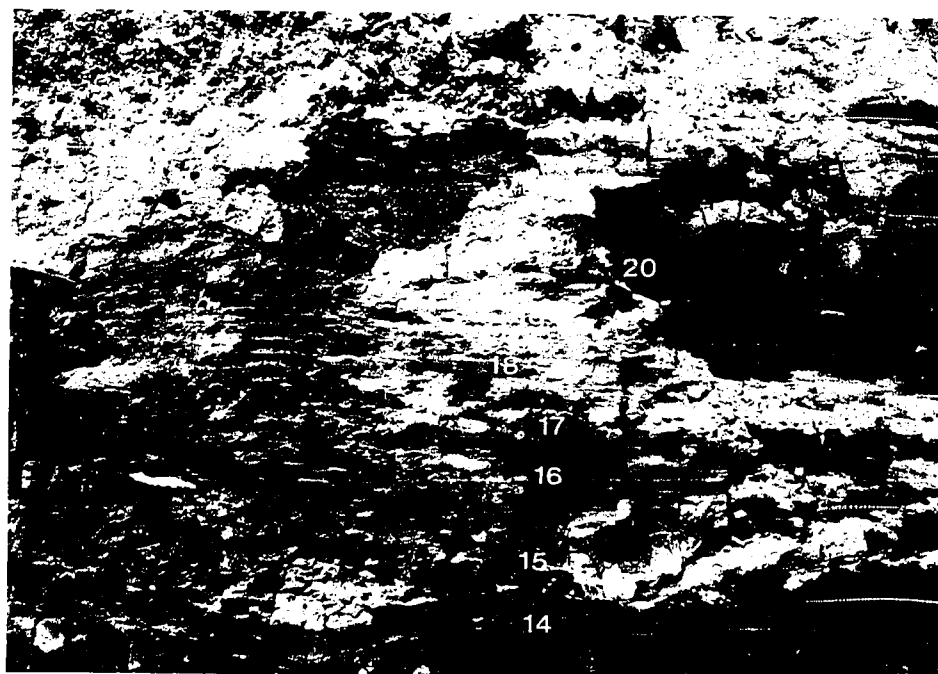
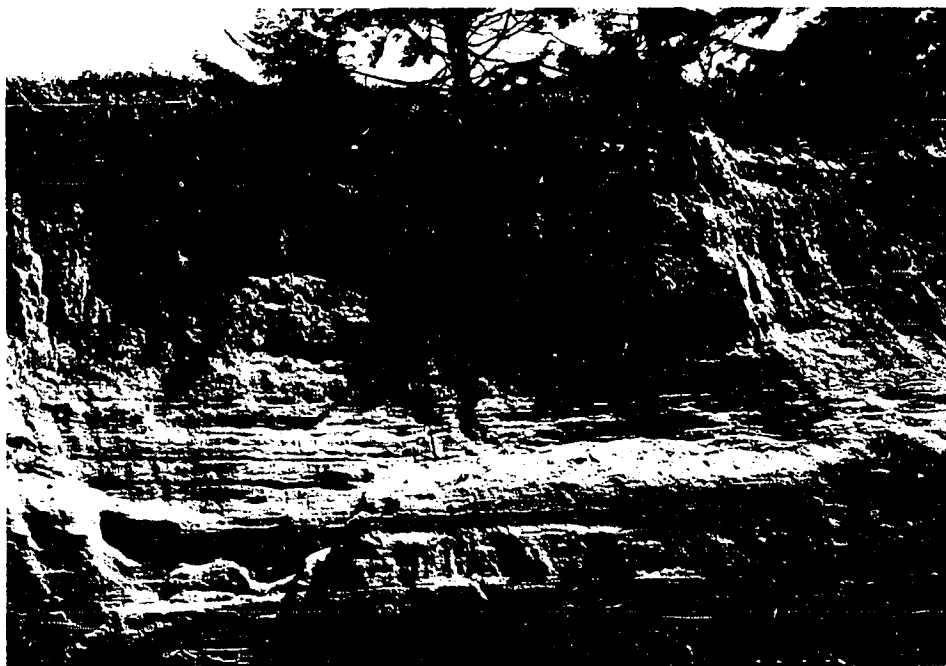
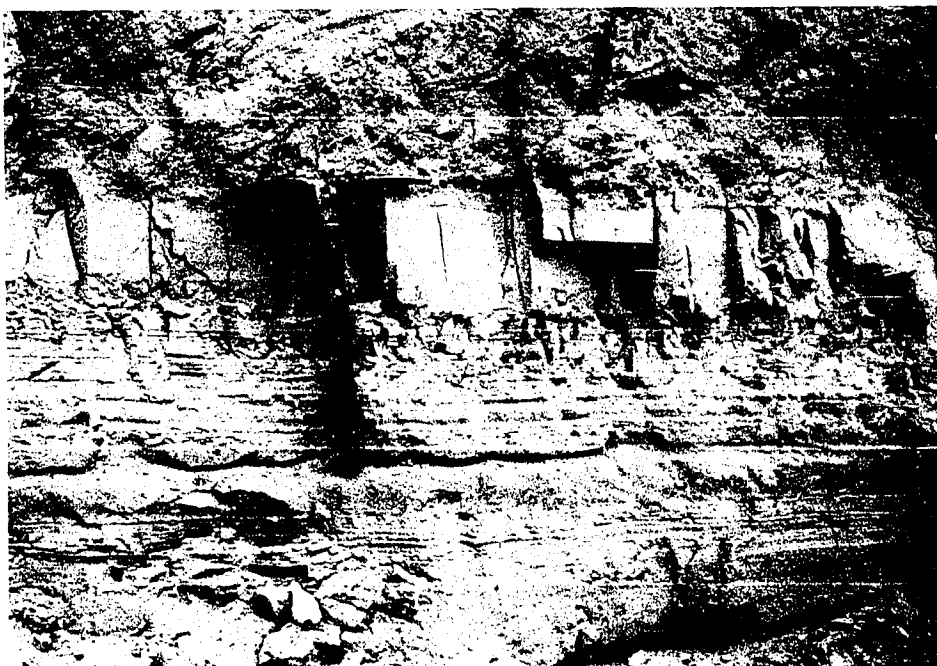


Figure 27 Photographs of stratified sands and
 silts exposed as channel infills
 at Swantown (A) and West Beach (B).



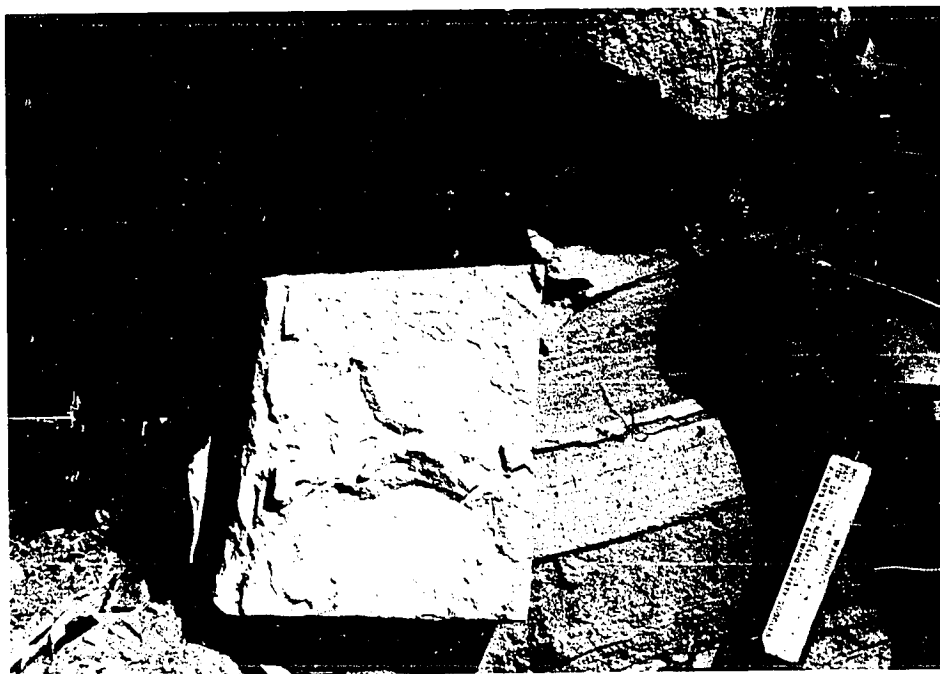
A



B

Figure 28 Photographs of horizontal trace
 fossils found within stratified
 silts and sands at Swantown (A)
 and West Beach (B).

A



B



widespread and only facies found in every exposure of Everson glacial-marine drift on Whidbey Island.

Pebbly Silt, Qpsl

Locally, pebbly silts comprise significant amounts of the upper unit but never attain thicknesses of more than 2 to 3 meters. They usually lie below Qpm and Qmd but frequently grade laterally into pebbly muds. Representative grain size frequency curves for such sediments are shown in figure 29.

Pebbly silts may be massive or consist of 2 - 3 cm thick beds which are bounded by very thin laminae of coarse silt. In general, the greater abundance of >2 cm sized stones separates pebbly silts from underlying stratified sandy silts.

Pebbly Mud, Qpm

Pebbly silts, where present, grade up into pebbly muds (Qpm) which have greater pebble abundances and a finer grained matrix (Figs. 30a, 42). Usually, however, Qpm facies can be found to directly overlie Qsd facies (Swantown, Hastie Lake Road-South) or surfaces of glacial erosion (Mutiney Bay, San de Fuca-West, East, Hancock Lake). Commonly the lower portions of pebbly mud sequences have distinct laminated zones with well preserved dropstone structures (Fig. 31a). These laminated zones grade up into massive to wispy laminated pebbly mud. Characteristic of both pebbly

Figure 29 Grain size frequency distributions
for samples of pebbly silt.

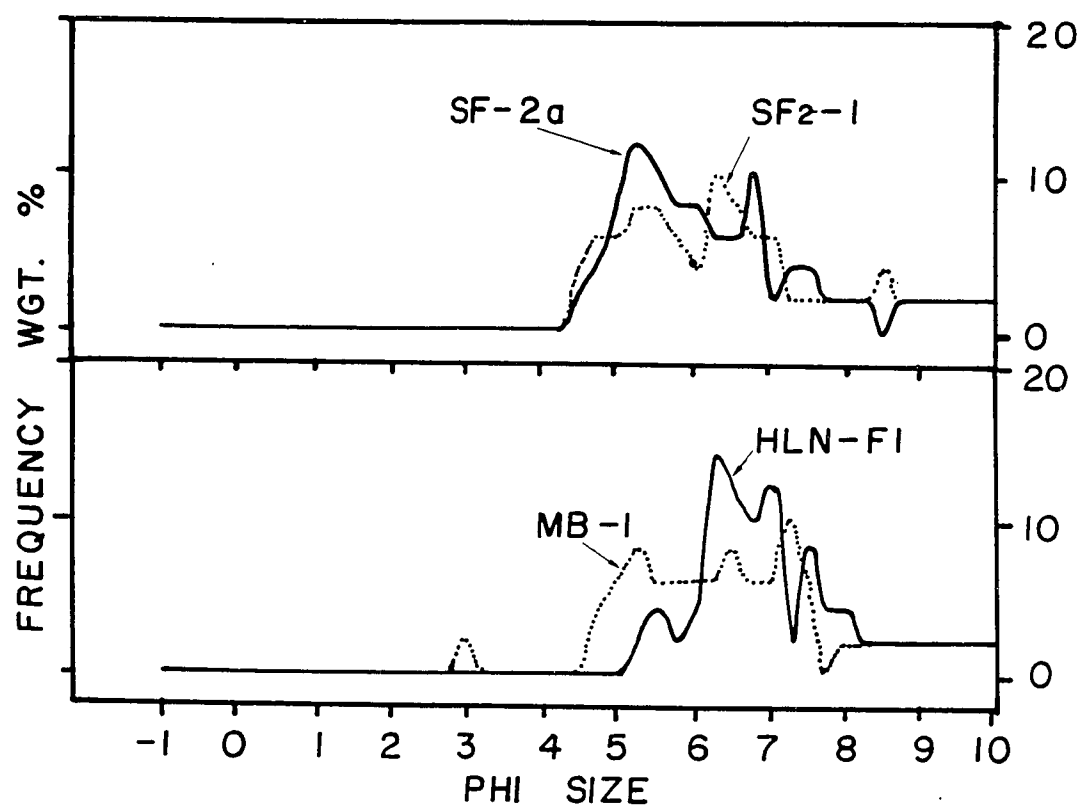


Figure 30 Photograph of pebbly mud (A) and
 massive, fossiliferous diamicton
 (B).

A



B

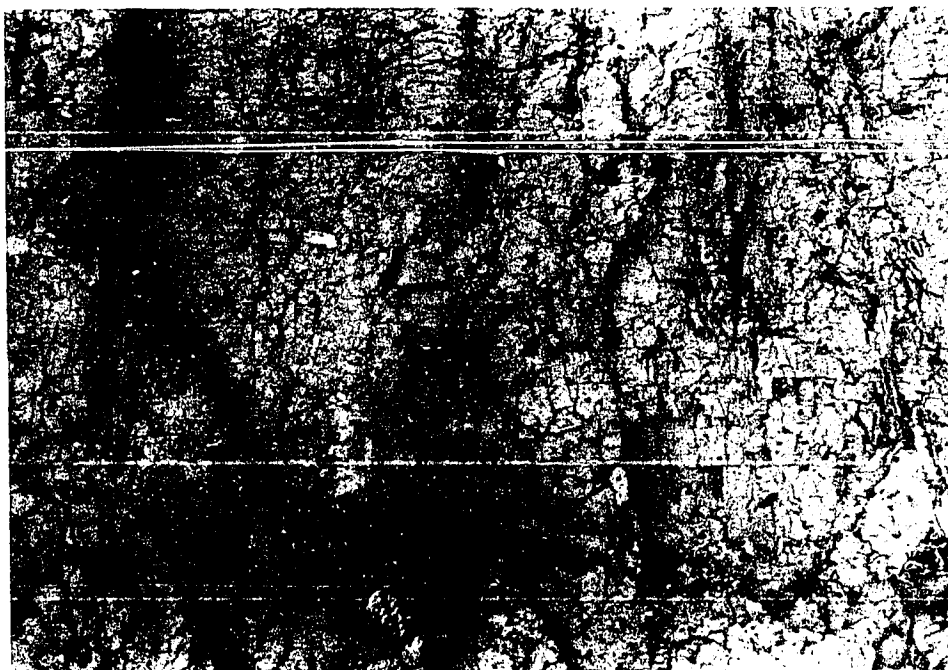
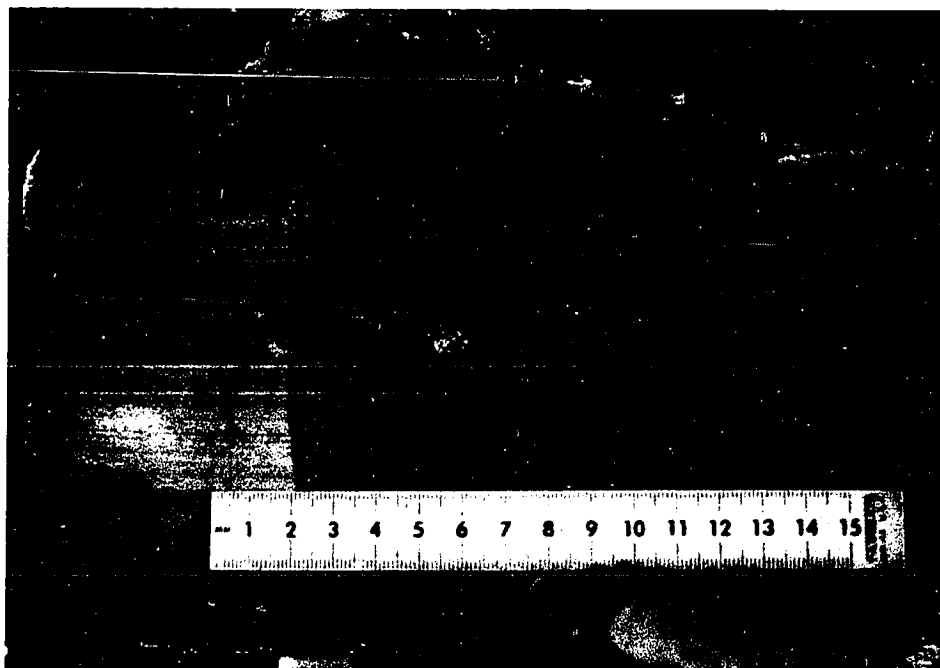
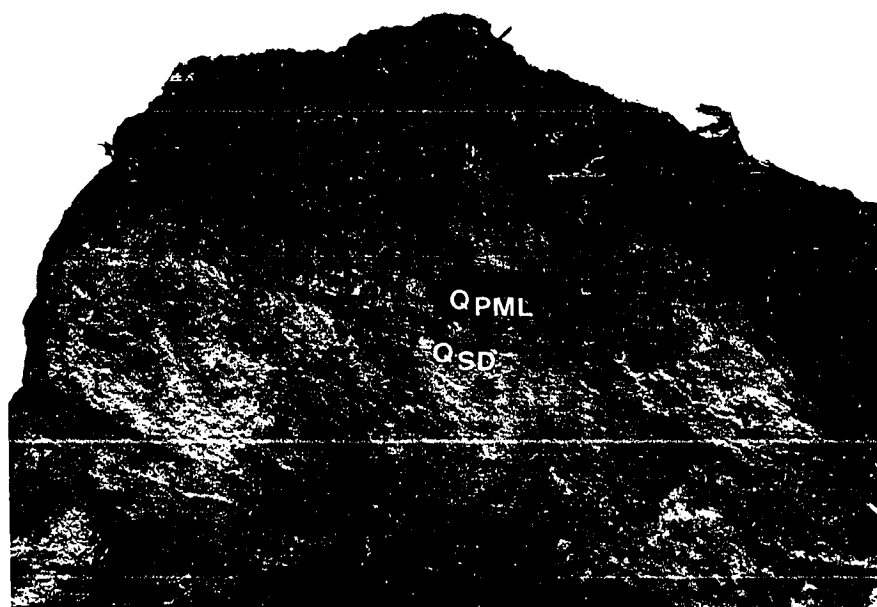


Figure 31 Photographs of laminated pebbly
 mud (Qpml) exposed at Swantown
 (A) and Hastie Lake Road-South
 (B).



A



B

silt and mud is their buff-light brown color and blocky weathering (Figs. 30a, 31b).

Representative grain size frequency distribution curves and sand, silt, clay proportions can be seen in figure 32. It is within these sediments that ice rafted debris (defined as poorly sorted sand sized material, Fig. 32) first becomes an important component of the sediment, comprising up to 14% of the matrix. Diatoms, spicules, and bryozoans, though rare, can be found within both pebbly silts and muds (Appendix A, table 4).

Massive Diamicton, Qmd

The uppermost facies stratigraphically, are massive "till-like" diamictons which are commonly fossiliferous (Figs. 30b, 33). These are the sediments which are most commonly associated with the Everson glacial-marine drift in the literature. They are distinguished from pebbly muds by greater pebble abundances and higher percentages of sand within the matrix (Figs. 30, 32). Representative grain size frequency distributions are shown in figure 34. In general, the matrix of this facies is massive, however, on fresh exposures some stratification can be observed. Deformed lenses or pods of unsorted sand and gravel can also be found (Fig. 35). Dessication jointing is characteristic (Fig. 30b), as is the high degree of weathering of granitic stones. Thickness of these units range from 2 to 6 meters.

Figure 32 Sand, silt, clay ratios for pebbly muds and silts (Qpm and Qpsl) and fossiliferous diamictons (Qmd). Shown above are grain size frequency distributions for samples of pebbly mud.

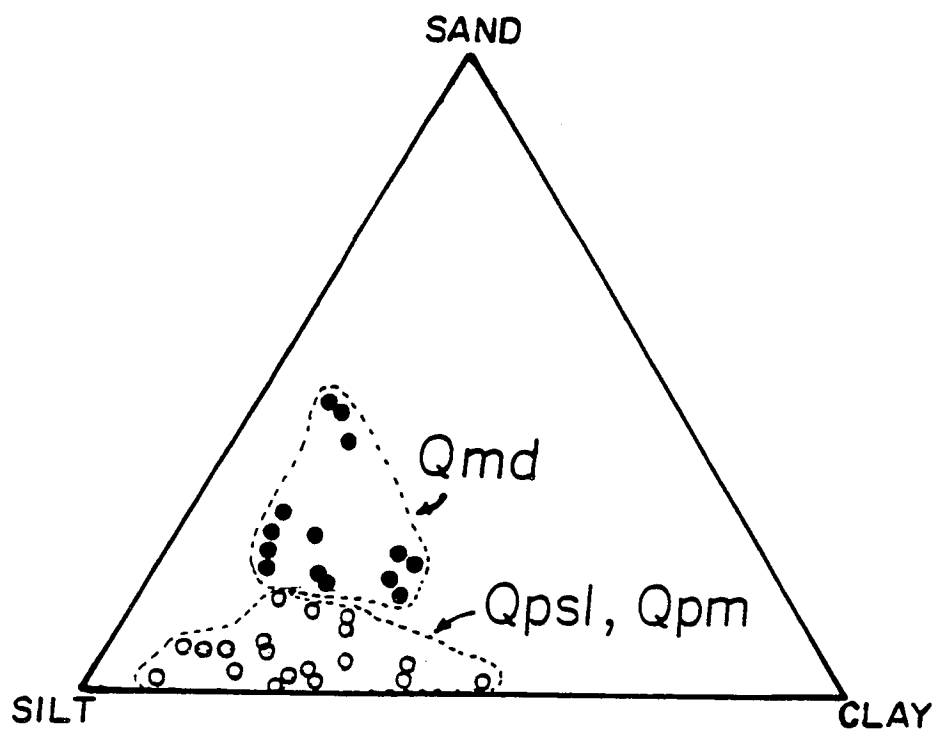
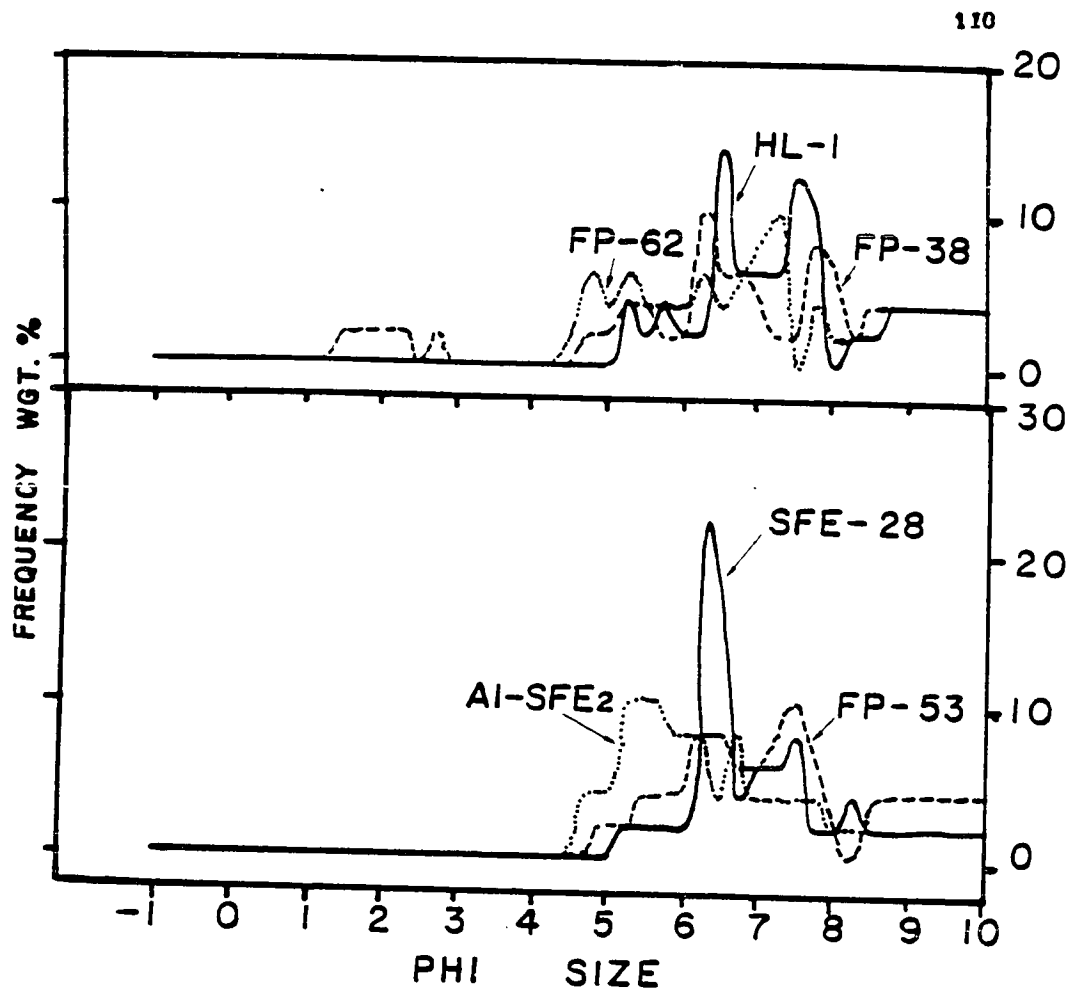


Figure 33 Photographs of fossiliferous
diamicton (Qmd) exposed at San
de Fuca-East (A) and West Beach
(B). Fossils appear to be in-
situ.

A



B

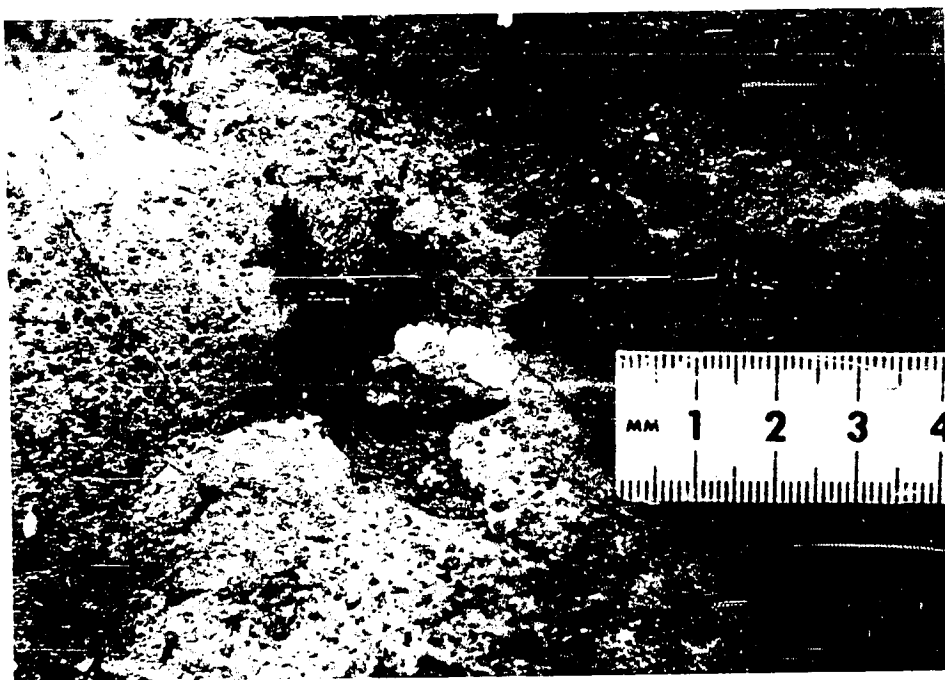


Figure 34 Grain size frequency distributions
for samples of fossiliferous dia-
micton.

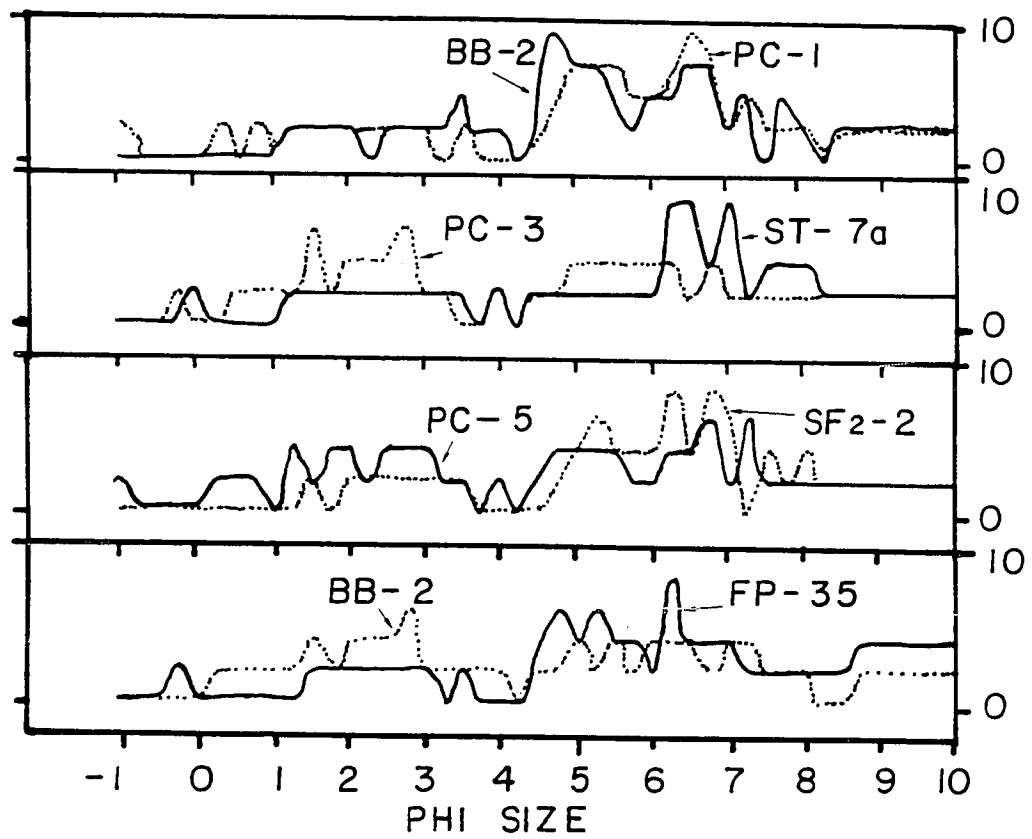
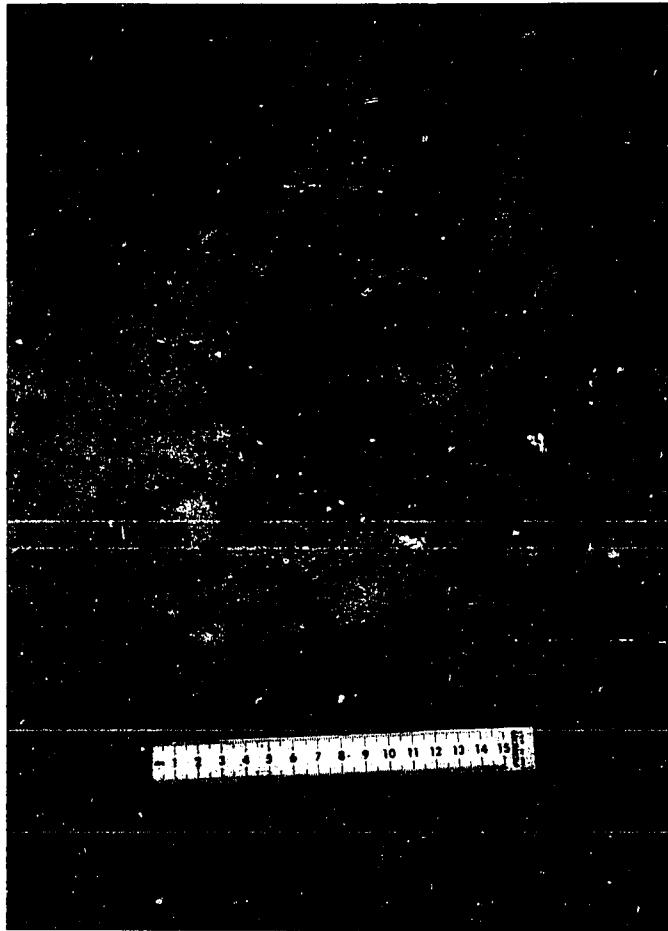


Figure 35 Photographs of deformed sand
 lenses which can be found within
 Qmd facies. Forbes Point (A) and
 Penn Cove-West (B).



A



B

Massive diamictons most often have gradational lower contacts with pebbly muds (FP-1-4, SFW, ST-2). Laterally they also grade into pebbly muds and silts (Maylor Point). Some exposures (Penn Cove, West Beach, Swantown), however, have transitional highly convoluted diamictons and/or very sharp contacts at the base of the massive diamictons.

The most distinguishing characteristic of these units is the presence of pelyceps, barnacles, and worm tubes (Fig. 33), which appear in some cases to be preserved in their living positions. It was noted that sandier diamictons contained the most abundant fossils (SFE, Penn Cove). Foraminifera (Balzarini, 1981) and siliceous microfossils can also be found in a number of localities (table 4 , Appendix). Carbon-14 dates for this unit are available and are listed in table 3 in the Appendix.

In summary, all known exposures of Everson glacial-marine drift on Whidbey Island contain at least one facies of the upper unit. Where all three are present pebbly silts grade up into pebbly muds which grade upward or laterally into massive, fossiliferous diamictons.

Emergence Deposits, Qgl

The above facies sequence is unconformable with an upper surface that is overlain by gravelly sand, sandy gravel or organic rich silty sand (Fig. 15). Usually these sediments are no more than 10 to 30 cm thick but may comprise up to 1 or 2 meters of section (SFW-1b, ST-1). Since these

deposits are unconformable with underlying glacial-marine sediments, they can not be properly assigned to the Everson but must be considered as a separate stratigraphic unit. For simplicity they are included in the generalized facies diagram in figure 12.

Summary

Figure 12 best summarizes the facies breakdown of Everson glacial marine drift as exposed on Whidbey Island. As shown in a number of exposures (see appendix), the Everson consists of a wide variety of sediments besides the "till-like" diamictons which are most commonly cited (Easterbrook, 1968, 1969). These Everson facies can be considered to comprise a sequence of three units bound at the base and top by unconformable surfaces.

A lower unit of stratified diamicton (Qsd) is locally present and overlies the lower unconformity. A middle unit of stratified sands, silts, and clays overlies Qsd facies of the lower unconformity. This middle unit varies greatly in its stratification, texture, and distribution and locally, on the west coast, is not completely conformable with overlying facies.

An upper unit of pebbly mud (Qpm) and massive diamicton (Qmd) is widely distributed and is often the only facies present. The Qmd facies is fossiliferous and has been dated at $13,010 \pm 170$ to $11,850 \pm 240$ (C^{14}) years B.P. (Easterbrook,

1968). This unit has been correlated by Easterbrook (1968) with the type Everson glacial marine drift. The upper sequence boundary is marked by an unconformable surface overlain by coarse sand and gravel. It should be emphasized that correlation of units within the sequence is made on the basis of lithostratigraphic evidence, the only datable horizon being the massive diamicton of the upper unit. The presence of erosional surfaces within the middle of the sequence, on the west coast, suggests hidden complexity.

The following section will discuss the origin of the facies described above and relate them in a comprehensive glacial marine sedimentary model.

Depositional Process

Stratified Diamictons (Qsd)

Stratified diamictons at the base of the Everson glacial-marine drift (Qsd facies) are primarily of mass flow origin. The sub-facies of grey, horizontally stratified diamictons had an ice rafted origin and were probably deposited in sub-glacial depressions proximal to the Vashon ice-sheet margin.

The following observations support a mass flow origin for the stratified diamicton facies:

- 1) Deformed stratification and convolution of several distinct diamicton units within the sequence.

San de Fuca West (see Fig. 15, sect. map)

" " East (sect. map)

Coupeville-Lovejoy Point (sect. map)

Hastie Lake Rd. South (sect. map)

Swantown (Fig.15 , sect. map)

- 2) Discontinuous bedding with convex upper and sharp/planer lower contacts. Distinct lobe shape of individual units.

San de Fuca-West, East (sect. maps)

Coupeville-Lovejoy Point (Fig.15, sect. map)

- 3) Extreme textural variability of multiple units within a single Qsd sequence.

San de Fuca-East (see Figs. 16, 17, sect. map)

"" West (see sect. map)

- 4) Local development of coarse tail grading and concentration of gravel at the base of individual units.

San de Fuca (see Fig. 18).

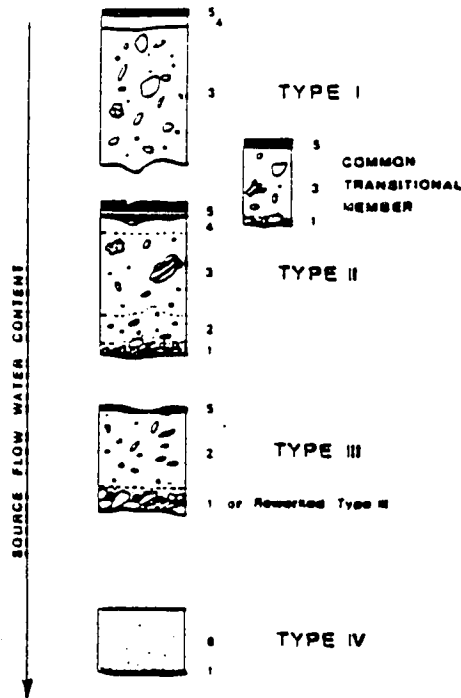
The above observations all point to mass flow processes (Lawson, 1979, and others). However, the source for such deposits remains a problem. Since they are driven under the influence of gravity they must be derived somewhere upslope from the site of deposition. Of particular importance, with regard to environmental reconstructions, is whether the sediment flows were deposited in an ice-marginal sub-aqueous or terrestrial environment.

Mass-flow diamictons are common constituents of some terrestrial ice marginal environments, being referred to as either flow tills (Goldthwait, 1951; Boulton, 1968, 1971; Hartshorn, 1958; and Dremanis, 1981) or, more correctly, sediment flows (Lawson, 1979, 1981). Lawson (1979) recognized a variety of flow types which resulted from the failure of supraglacial debris, due either to saturation or collapse of ice cored slopes. The water content of individual flows was the major variable that controlled mechanisms of grain

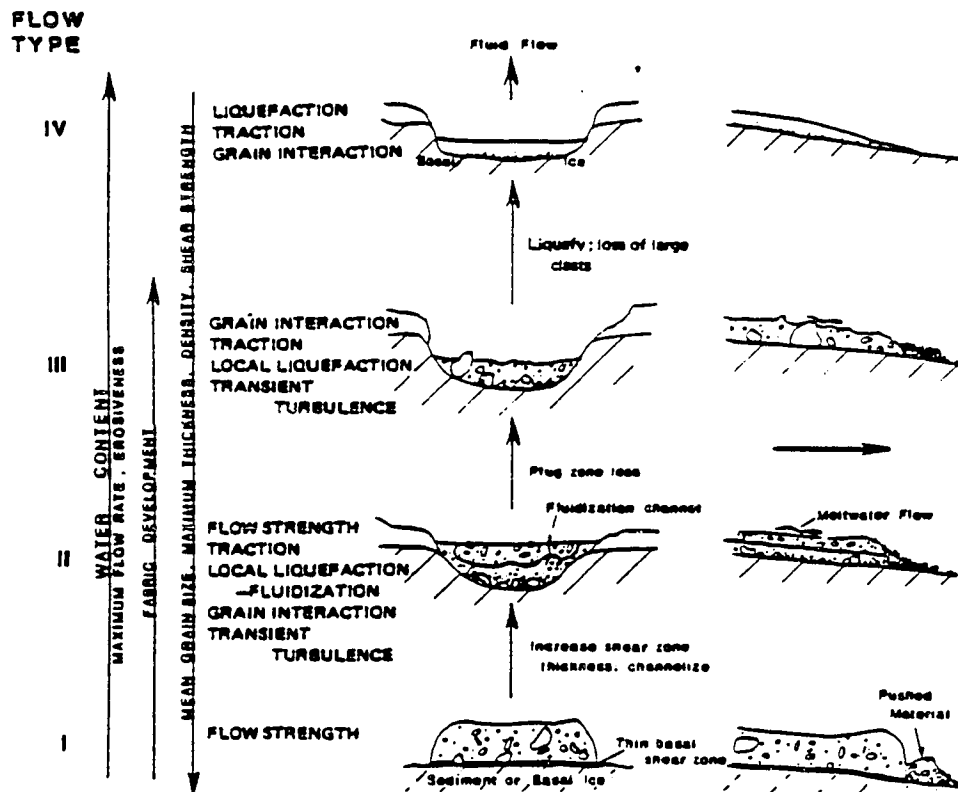
support and transport and therefore in determining the character of resulting deposits. Lawson's classification of sediment flows represents a transitional rather than an end member scheme and is illustrated in figure 36.

In the subaqueous environment diamictos can also be deposited via gravity driven processes and, depending on the mechanism of grain support, are commonly referred to as debris flows (Middleton and Hampton, 1973, 1976). Although direct observations within aquatic environments are lacking, it is thought that such sediments can be derived from previously deposited diamictos, tills (Anderson et al., 1979; Kurtz and Anderson, 1979; Wright, 1980, in press) or from the remobilization of fine grained (silt-clay) and sandy gravel end members of deltaic environments (Cohen, 1981). Like the terrestrial environment, the type of sediment resulting from sub-aqueous downslope movement is largely dependent on the degree of fluidization of the flow (which determines grain support and transport mechanisms). Recent work has shown that debris flows, when in transition to more fluidized flows may produce turbidity currents and associated turbidites (Hampton, 1972; Wright, in press; Broster et al., 1980; Banerjee and McDonald, 1975). This association could then serve to distinguish subaqueous from subaerial environments. Pleistocene diamictos thought to have been deposited via gravity driven processes have been recognized for terrestrial (Marcussen, 1973; Boulton, 1971), as well as glaciolacustrine

Figure 36 Classification of sediment flows
 based upon modern sediments at the
 terminus of the Matanuska glacier,
 Alaska, from Lawson (1979).



Idealized characteristics of sediment flow deposits. Six distinct zones are recognized; any may be missing due to erosion, nondeposition, or absence from source flow. The characteristics of the zones are 1) texturally heterogeneous with increased gravel content of tractional origin, massive to graded, weak to absent pebble fabric; 2) massive, texturally heterogeneous but absence of large grains due to settlement, possible decrease in silt and clay due to elutriation, weak pebble fabric; 3) massive, texturally distinct and sometimes structured sediments may occur, pebble fabric absent, vertical clasts common; 4) massive, fine-grained (sand to clay) similar to matrix of zone 2, lacks coarse clasts due to settlement during and after deposition; 5) stratified to diffusely laminated silts and sands of meltwater flow origin; and 6) massive to partially or fully graded, silty sand, fabric absent. Basal contacts vary from conformable to unconformable, sharp to transitional and deformed to planar. Type III flow sedimentation in fans results in selective deposition of each zone, or of individual particles by size.



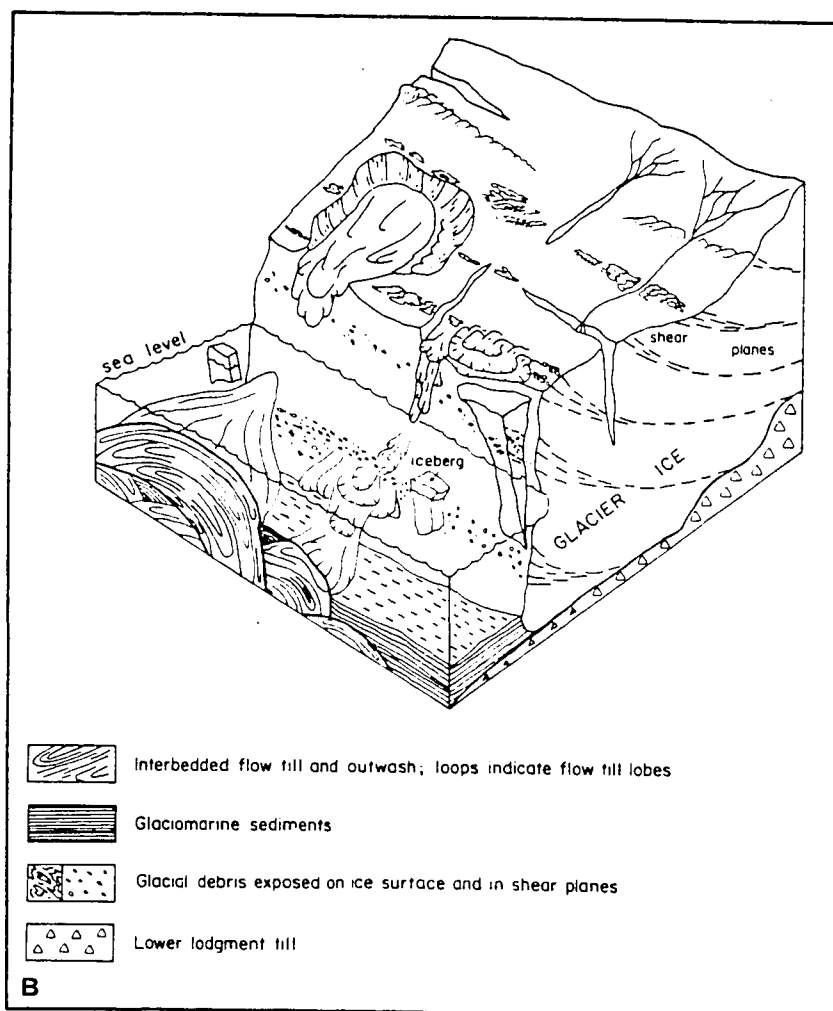
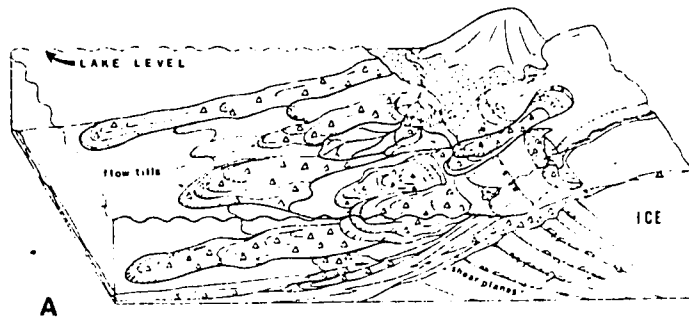
Idealized cross sections, transverse and parallel to direction of flow, of the four sediment flow types. Flow types are transitional to one another. Channels usually are ice-floored with walls of sediment and ice. Grain support and transport mechanisms are indicated. Trends in various parameters are shown; water content increases from bottom to top.

(Evenson et al., 1977; May, 1977) and glaciomarine environments (Hicock et al., 1981). As part of their model for subaqueous deposition the above authors include derivation of sediment from glacial margins and at least partial transport of flows in terrestrial environments (Fig. 37). Final subaqueous deposition for these sediments is suggested by their being interbedded and deformed with glaciolacustrine or glaciomarine facies (Hicock et al., 1981; Evenson, 1977) and their association with turbidity current deposits (Broster et al., 1980).

Sediment flows of the stratified diamicton facies can be demonstrated to have been deposited in a marine environment on the basis of the following criteria.

- 1) Convolute interbedding of stratified diamicton and glacial-marine facies
 - San de Fuca-West (Fig. 19, sect. map)
 - "" East (sect. map)
 - Coupeville Lovejoy Point (Fig. 15, sect. map)
- 2) Preservation of flow geometry and convex upper surfaces. In the terrestrial environment "unaltered flow surfaces are not likely to be preserved unless immediately covered" (Lawson, 1979).
 - San de Fuca-West (Fig. 15, sect. map)
 - San de Fuca-East (sect. map)
 - Coupeville-Lovejoy Point (sect. map, Fig. 15)

Figure 37 Diagrammatic models for subaqueous
 flow till deposition based on
 Pliestocene deposits in Ontario,
 Canada, A (Evenson et al., 1977)
 and British Columbia, B (Hickock
 et al., 1981).



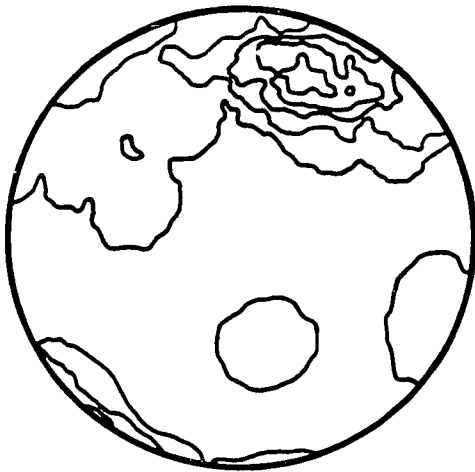
- 3) The fact that they directly overlie surfaces of glacial erosion without any intervening terrestrial deposits.

San de Fuca-East, West (Fig. 15, sect. maps)

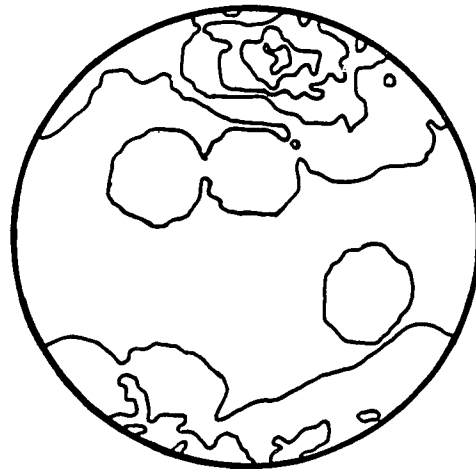
The majority of stratified diamictos were derived from an ice marginal environment. In particular those Qsd sequences which are exposed at the highest local elevation (San de Fuca-West, Swantown) would seem to require an ice-cored slope or glacier margin, simply because they had to have been derived from somewhere upslope. The development of texturally distinct flows, some of which are almost identical to those described by Lawson (1979, types I-III, see Figs. 15, 18, 36). suggest that at least part of the transport path may have been terrestrial. However, extreme convolution of such texturally distinct beds (Fig. 15) suggests that the site of deposition (the edge of a submerged ice margin) was not as stable as a terrestrial environment. Depositional sites for flows in the subaerial environment allow for minor interbedding (Lawson, 1979) but certainly not the kind of extensive deformation shown by these deposits. Minor readvances of the ice front may have also produced such deformation.

Fabric data were obtained from Qsd sequences exposed at East and West San de Fuca (Fig. 38). The fabrics are rather well developed (low dispersion) and, with one exception, show

Figure 38 Equal area projections of pebble long axis orientations for stratified diamicton facies (Qsd). Contour intervals are at 1, 3, 5, 7, and greater than 9% of data per 4% of the projection area. Data have not been rotated to horizontal with respect to the dip of the bedding plane. All samples consist of 25 measurements.



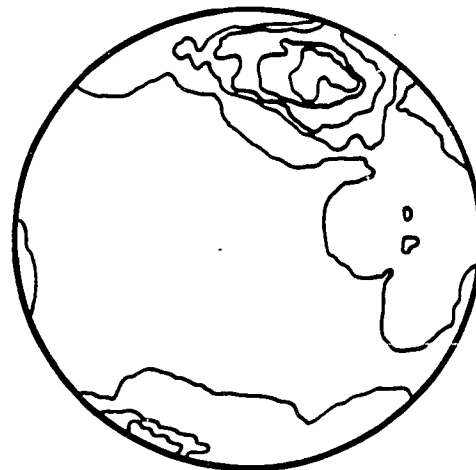
SFW-Qsd-1



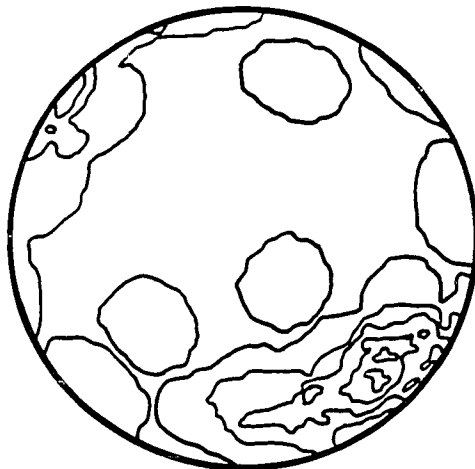
SFW-Qsd-2



SFW-Qsd-4 45% Sand



SFW-Qsd-5 53% Sand



SFE-Qsd-1 38% Sand

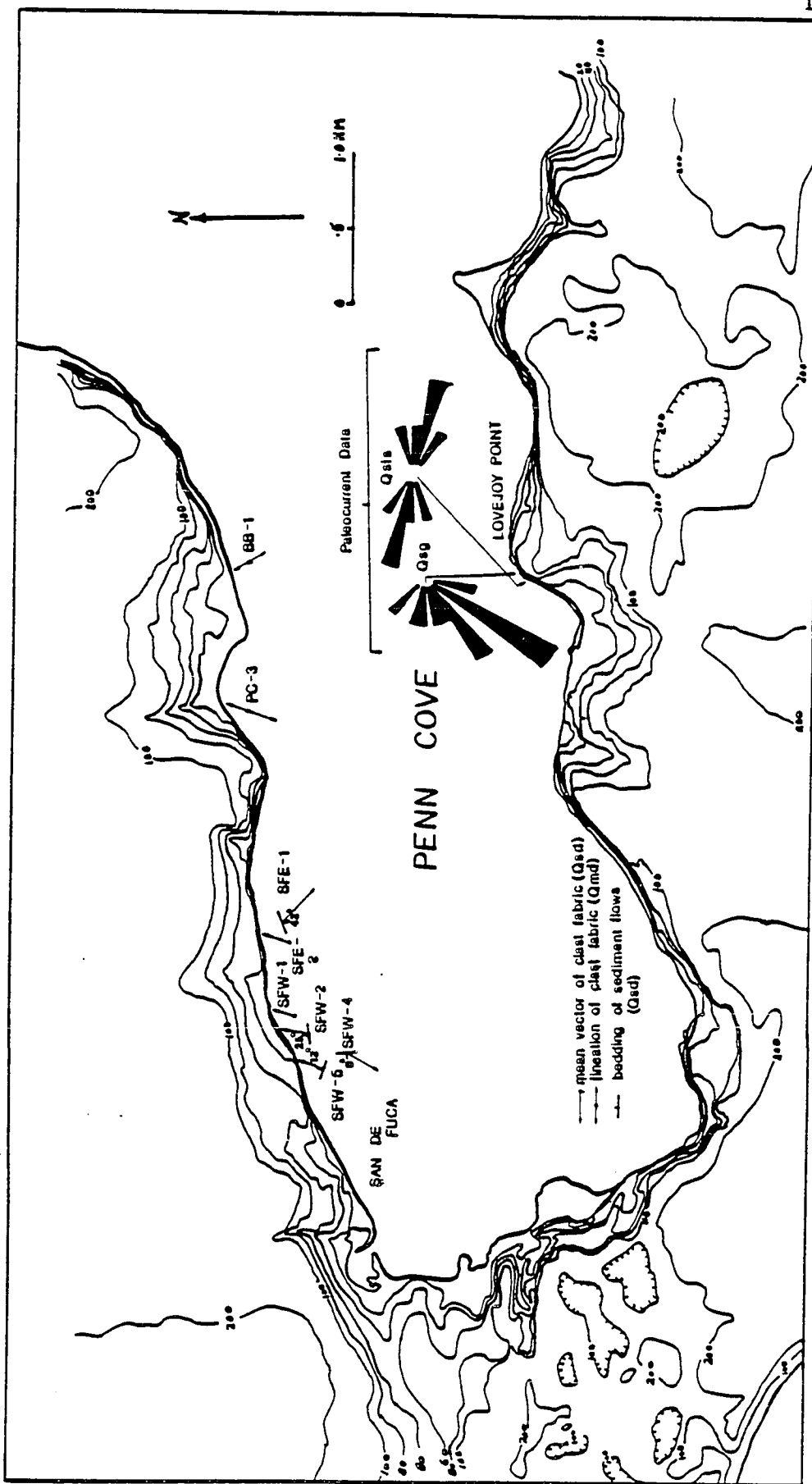


SFE-Qsd-2 42% Sand

a fairly consistent orientation ($9 - 32^{\circ}$), between several distinct units, over a distance of 2 kilometers (Fig. 39). Consistency of mean orientation between sediment flows was not found in the environment studied by Lawson (1979, 1980). As will be discussed later the data in figures 38 and 39 may simply suggest that the local slope (i.e., ice margin) was uniform in comparison to the Matanuska Glacier studied by Lawson (1979). The dispersion of fabric samples from finer grained flows and units which displayed coarse tail grading (Figs. 18, 38) was less than samples from other diamictons (Figs. 15, 38). This observation is consistent with the results of Lawson (1977, 1980), who showed that "as the water content of flows increased the scatter in orientation decreased and preferential orientations parallel to flow developed." Type III flows of Lawson (1979) are similar in texture and structure to Qsd units in figures 15 and 18 and "show relatively strong alignment approximately parallel to the direction of flow." The above observations seem to fit best in the model for submarine "flow till" deposition outlined by Hicock and others (1981). The absence of turbidity current deposits within the Qsd sequences may imply that submarine transport distances were short, thus preventing the development of secondary turbidity currents.

Other Qsd sequences of flow origin may have been derived from remobilization processes which occurred in a deltaic environment. Qsd units exposed at Coupeville-Lovejoy Point

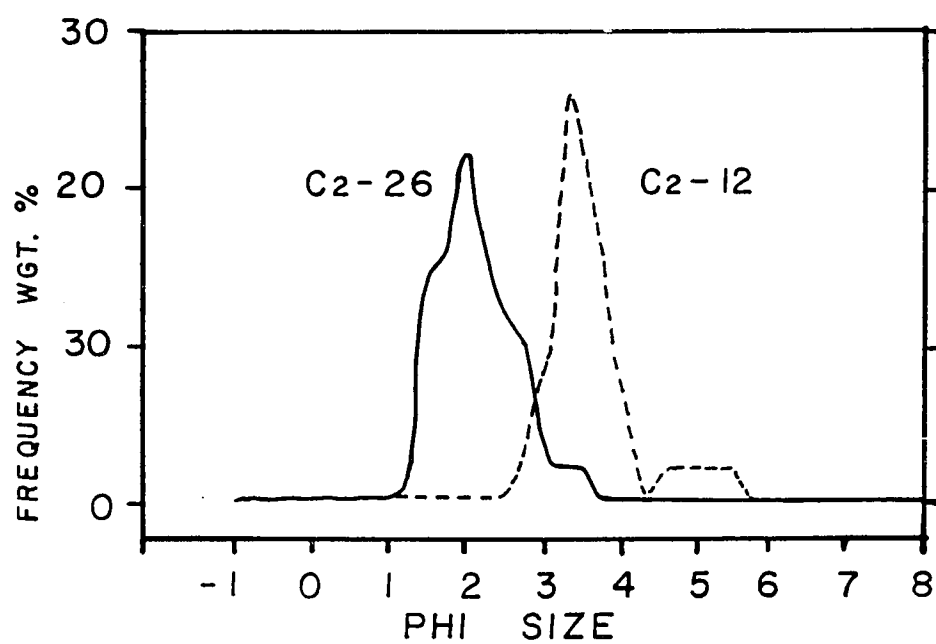
Figure 39 Location of fabric samples taken from Qsd and Qmd units near Penn Cove. Non-horizontal bedding is indicated by a strike and dip symbol. Paleocurrent directions for deltaic and marine units exposed at Lovejoy Point are also shown.



and Maylor Point (Fig. 15) overlie a sequence of stratified gravels, foreset bedded sands and silt-clay rythmites which seem to comprise small deltaic complexes (see section maps in Appendix). Such settings are conducive to the development of debris flows due to gravel avalanches and the failure of fine grained rythmites (Cohen, 1981). However, stratified diamictons of flow origin at Coupeville are restricted above a sharp planer contact and are not interbedded with the underlying deltaic sediments. Since the flows are interbedded with overlying marine sediments (Fig. 15) their emplacement may have been associated with a marine transgression of the deltaic environment. A comparison of paleocurrent directions for the deltaic and overlying marine sediments, in figure 39, shows that they are dissimilar. The coarsest sands of the marine sequence appear to be significantly finer than the uppermost sands of the deltaic deposit (Fig. 40). This data does not support the idea of transgression over a deltaic environment. However, the origin of these Qsd flows, as either ice-contact or deltaic, cannot be concluded until further studies have been done to determine the age of the deltaic sediments and the nature of their upper contact with the marine sequence. Very extensive deformation of the above units within the same exposure, 30 m to the East, may suggest that the Qsd units, if not ice-contact, were at least proximal to the ice margin.

The sub-facies of grey horizontally stratified diamictons

Figure 40 Comparison of grain size frequency distributions of samples from uppermost deltaic sands (C2-26) and overlying, channelized marine sand (C2-12).



most likely had an ice-rafted origin as suggested by the presence of dropstone structures and interbedded laminated silt and clay. They appear to be conformable with overlying marine sediments (Fig. 14) but are themselves unfossiliferous. Their lense like geometry and lateral equivalence to erosional sub-glacial surfaces (San de Fuca-West) suggest that they may have been deposited in small sub-glacial depressions just under the ice margin. The restriction of exposures close to present sea level may imply the absence of subglacial cavities above that elevation.

Gibbard (1980) presented a model whereby stratified diamictons were formed in sub-glacial cavities by the melting of basal debris zones. He found that such deposits, like the unit at Maylor Point (Fig. 14), were finer grained within localized depressions thus implying preferential settling of silt and clay towards lower areas. The grey color of these Qsd units may be due to a high percentage of glacially derived silt and clay in comparison to the overlying marine sediments, which are buff colored.

Silty Sands and Silty Clays, Qsls, Qslc

Stratified silty sands and sandy silts were most likely the product of turbid underflow currents which entered marine waters from supra- or subglacial meltwater channels or terrestrial outwash systems.

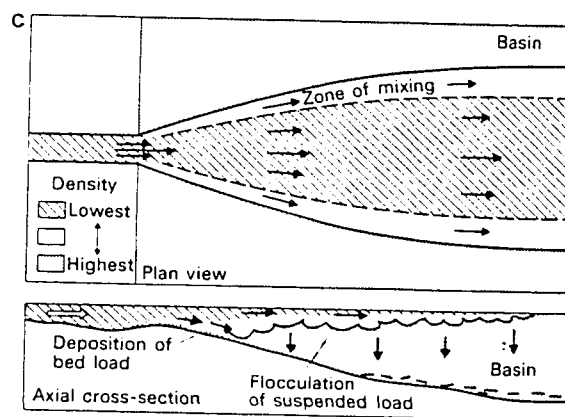
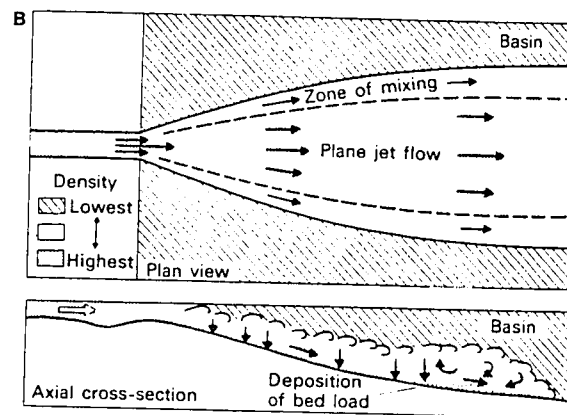
Sedimentary structures (ripple laminations, graded silt rip-ups, current lineations, and erosive lower contacts)

suggest bottom traction processes. The texture and moderate to good sorting ($S_d = .65 - 1.9\phi$) of these sediments (Figs. 20, 24). is also quite similar to channel floor sediment derived from underflow transport in Glacier Bay Alaska (Fig. 20, Hoskin and Burrell, 1972). Water escape structures (Fig. 21a) and the absence of ice rafted material imply rapid rates of deposition. Some Qsls units were deposited on slopes of $> 1^\circ$ as indicated by well developed slump structures (Fig. 21b).

The limited distribution of this facies suggests a localized influence upon sedimentation. Variation of grain size between sites probably reflects the energy and position of meltwater channels into the basin at the time of deposition. Coarse grained silty sands exposed at Coupeville-Lovejoy Point are actually channelized (Fig. 22) and represent a proximal setting in comparison to other finer grained exposures of Qsls facies. The fining upward trend of this facies is an expression of increasing distance, and therefore transport energy, of the underflow current from the meltwater source (ice margin).

Interbedding of Qsls with finer grained pebbly silts (Qpsl) and muds (Qpm) (Figs. 23, 24) probably indicates alternating conditions of bottom traction, underflow, and suspended sediment deposition, inter or overflow, (Fig. 41). Such fluctuations could be in response to variations in meltwater discharge, and thus suspended sediment concentration,

Figure 41 Underflow and overflow depositional model as described by Bates (1953), figure taken from Reading (1978). Alternate beds of Qsls and Qpm as shown in figure 23 can be explained by this model.



into the basin. For marine salinities of 30 - 32‰, fresh water at .50 C would require a suspended sediment concentration of 39 - 40 g/liter in order to sink as an underflow (Gilbert 1979, Hoskin and Burrell, 1972). Although suspended sediment concentrations exceeding 40 g/liter have been recorded (72 and 68 g/liter, Sustina River, Alaska, U.S. Dept. of Interior, 1970) average values for glaciofluvial systems are on the order of 10 - .1 g/l.

Due to dilution from glacier meltwater, near-shore salinities in fiord environments can reach values as low as 16 - 25‰ at depths up to 10 m (Hoskin and Burrell, 1972). Under these conditions average concentrations of suspended sediment in glacial meltwater are sufficient to produce underflow currents where meltwater systems enter the marine environment.

Though exposures are limited, Qsls facies have been traced into coarser grained meltwater deposits only in one locality (Fig. 13), and where present, overlie surfaces of glacial erosion and/or sediment flows of the Qsd facies. This may suggest that channels which introduced sediment laden water into the marine basin were upon or within glacial ice. Later, as the ice margin calved, coarse grained glaciofluvial material could have been removed as ice-rafted debris.

Stratified silty clays (Qslc) were derived through a combination of bottom traction and suspended sediment

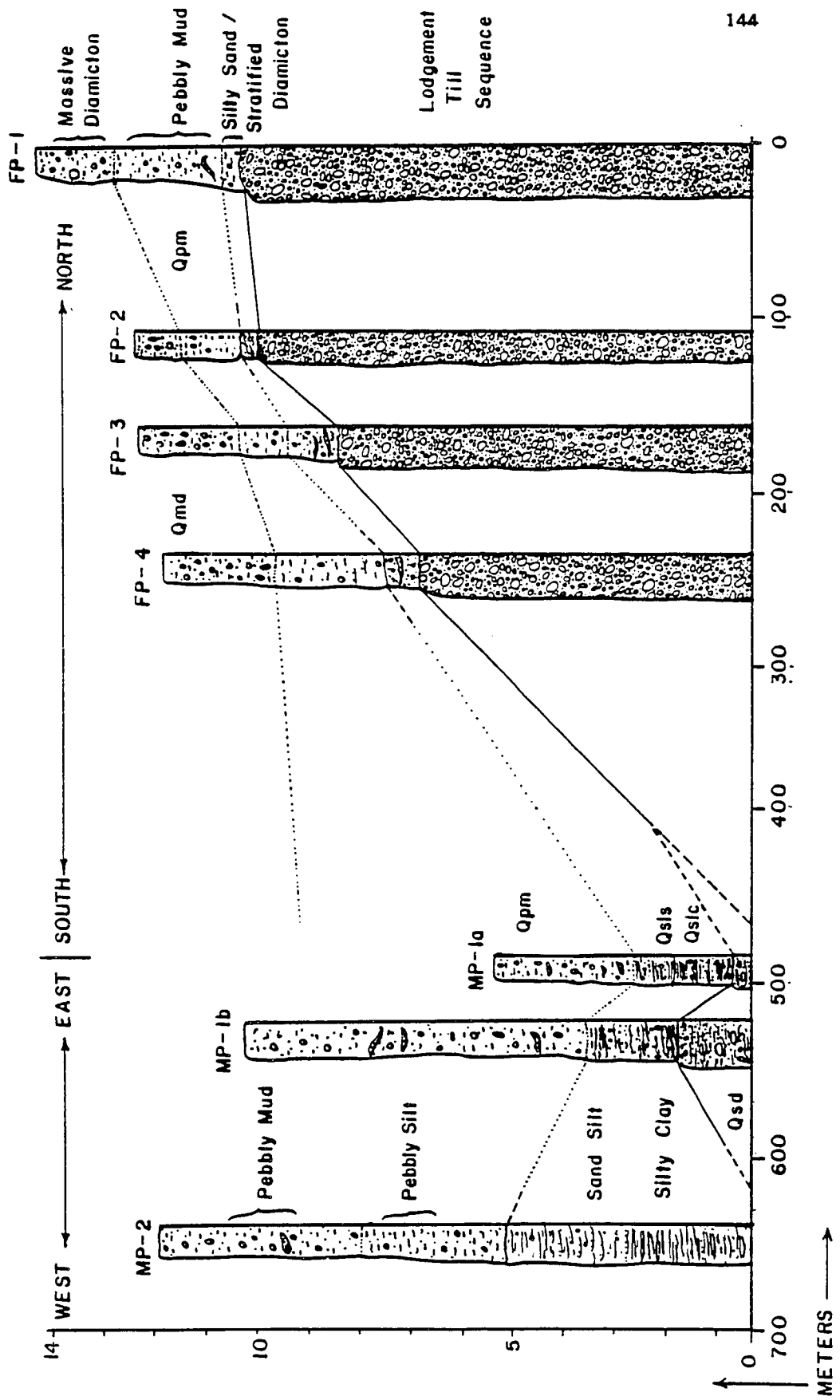
deposition. The facies was deposited in relatively deeper parts of the basin and distal to positions of meltwater influx.

These sediments are much finer grained than Qs1s facies and laminations are on a much finer scale. Lenticular bedding, micro-flaser bedded silts within clays, and current rippled sand laminae (Fig. 25) imply bottom traction processes, while massive to wispy laminated silty clays suggest deposition from suspension. Depositional rates were high, since ice-rafted stones are rare ($<1 - 2/m^2$). Post depositional slumping produced convoluted stratification (Fig. 25). The sequence at Maylor and Forbes Pt. confirms depositional slopes of $.02 - 5^0$, as seen in figure 42.

Alternate bedding of sandy silt and massive silty clay (Fig. 26) suggests fluctuating underflow-interflow, overflow deposition similar to, but distal to like sequences within Qs1s facies (Figs. 22, 23). Finely laminated silt and clay, which is most typical of Qs1c facies, can also be produced by alternating underflow/overflow processes, as suggested for Holocene glacial-marine sediments in Glacier Bay, Alaska (Powell, 1980, 1981).

The proportion of bottom current structures as well as the mean grain size decrease upwards through Qs1c sequences (sect. MP-1b), thus indicating a predominance of interflow or overflow deposition higher within the section. This suggests that sources of sediment input (i.e., ice margin) became

Figure 42 Composite of measured sections at Forbes and Maylor Point show increase in thickness of silty clays and sandy silts within depressions. Deposition took place on slopes of up to 5° . Sea level is at 0 meters on vertical scale.



more distal upwards through the section.

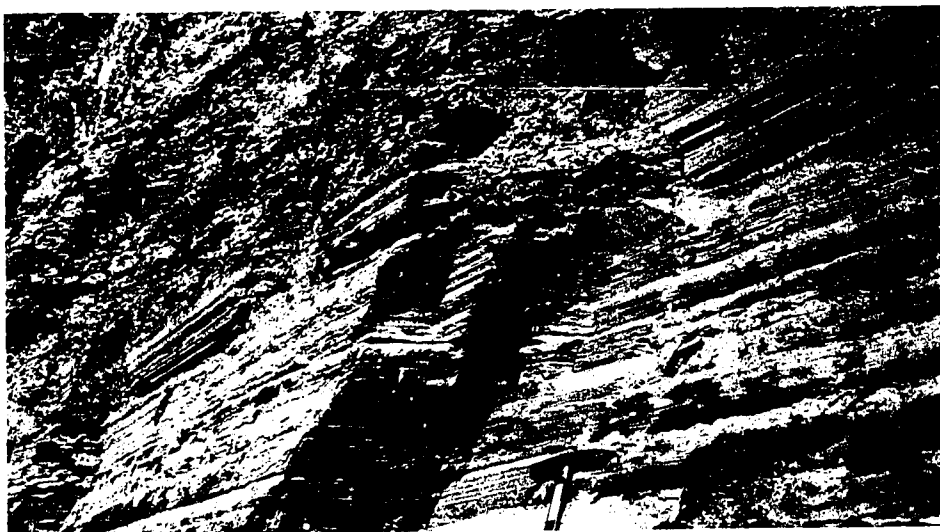
This facies is best developed at low elevations, close to present sea level, and increases in thickness dramatically within depressions (Fig. 42).

Stratified sands and silts (Qs1, Q1s , Qs1s) exposed along the west coast of Whidbey Island appear to represent, at least initially, higher current energy conditions than stratified units found elsewhere. In addition, their transition into overlying facies is abrupt and is marked by partially eroded surfaces.

A channelized sequence of normally graded sands, silts, and clays is well exposed at Swantown and represents a turbidity current channel infill (sect. ST-1, Fig. 27, sect. map). The channel is approximately 24 m wide and 6 m deep and is of erosional type (Nelson and Kulm, 1973). Extensive erosion occurred at the onset of sub-aqueous conditions since diamictos are eroded in the central part of the channel leaving a coarse gravel lag (section ST-1). Turbidity current deposition is implied by the presence of Bouma sequences, water escape structures (Fig. 43), and erosive lower contacts. Sorting of the sands is better than Qs1s facies. Periods of non-deposition, between turbidity flows, are suggested by the preservation of horizontal crawling traces along bedding planes (Fig. 28). Slumping of lower sand units is indicated by their very convolute stratification.

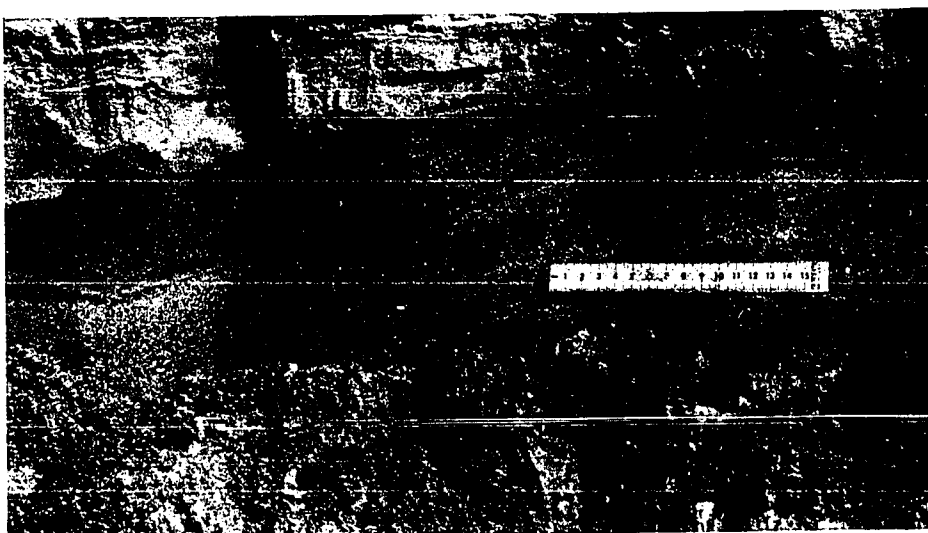
Figure 43 Photographs of sedimentary structures within turbidity current channel infill exposed at Swantown. Notice varve-like bedding of upper part of unit (A), normal grading (B), and water escape structures (C).

A



147

B

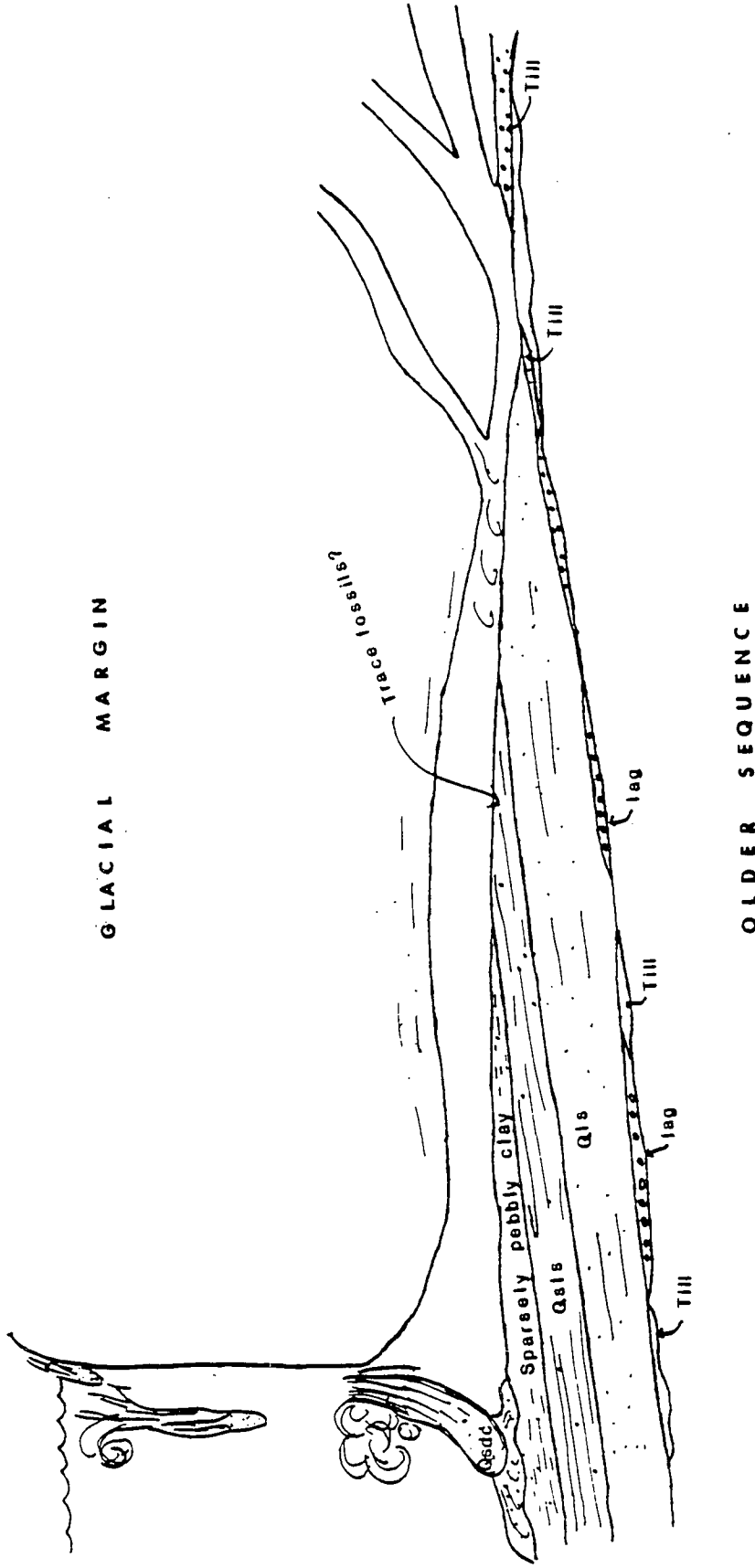


C

Bottom currents appear to have been sufficient to prevent upper Bouma sequences from being deposited in the lower part of the sequence. Finer grained, silts and clays, and more complete Bouma sequences, A-D, do predominate higher up in the section. This fining upward sequence indicates a gradual retreat of the sediment source, possibly subglacial meltwater channels, such that normal currents decreased along with the transport energy of periodic turbidity currents. Slower rates of sedimentation, higher up in the sequence, are indicated by the upward increase in dropstone abundance. Finer grained, upper parts, of the sequence appear almost varvelike (Fig. 43) and suggest seasonal influences upon sedimentation. The sequence finally grades into a 30 cm massive grey clay indicating very sluggish, if non-existent, bottom currents and deposition from suspension.

The contact of this stratified sequence with overlying facies is very abrupt (sect. ST-1). Stratified diamictons directly overlying the contact are extremely convoluted and exhibit chaotic flow structures but eventually grade up into massive diamictons or pebbly muds. Such a transition could represent one of two possibilities. First, the turbidity current channel could have existed sub-glacially such that the complete fining upward sequence was deposited prior to the retreat of a grounded ice margin (Fig. 44). As the margin migrated over the sequence, sediment flows and

Figure 44 Diagrammatic model to explain
 turbidity current channel infill
 and convoluted diamictons exposed
 at Swantown. Presence of trace
 fossils within Qs1s facies is
 problematical.



marine diamicton were deposited on top of the section producing the sharp irregular contact (sect. ST-1, sect. map). Very quiescent bottom conditions could then have existed that resulted in the deposition of the massive grey clays just prior to the initiation of open marine conditions. The presence of trace fossils within the turbidite sequence is problematical although Powell (1981) reports the presence of polychaetes next to the ice margin of tidewater glaciers in Glacier Bay, Alaska. The absence of more abundant ice rafted material may simply mean that the basal ice was depleted of sediment.

In any event very high energy turbulent flow had to have occurred during the erosional stage of the channel, since it eroded down through both Vashon diamicton and peat of the Whidbey formation. In contrast, turbidity current channels in Glacier Bay, Alaska are of the erosional depositional type and have eroded into unconsolidated basin mud, distal to outwash deltas (Powell, 1981, Hoskin and Burrell, 1972).

A second possible explanation for the observed sequence at section ST-1 is that the convoluted diamicton and overlying pebbly mud represents a debris flow. The flow moved downslope as sea level fell, similar to slopewash facies of Armstrong and Brown (1954, Fig. 8). In this case, the turbidite sequence would have been deposited proglacially in an open marine environment.

A 1 to 4 m thick section of horizontally bedded sand and stratified sand and silt is interbedded within stratified diamictons at West Beach (sect. WB-1, 2, sect. map). This section is particularly complex as it exhibits characteristics of wave, glacial-marine, and waning current regime processes.

Symmetrical ripple marks (Fig. 27) indicate partial influence of waves, and the abundance of horizontal trace fossils (Fig. 28) suggest periods of non-deposition. Current regimes varied between high and low energy such that alternate beds of poorly sorted silty sand and md.-fn. grained sand, with heavy mineral stained laminae, were deposited (section WB-2). Some of the sand beds show evidence of mass flow since they are convoluted, contain silt and diamicton clasts and have gravelly zones near their base. Graded bedding, although present, is not common. Overall, the sequence fines upward into laminated sandy silts, with dropstones and wispy-laminated clayey silt.

The upper contact, like the sequence at Swantown, is sharp, erosive, and planar. The stratified sequence is overlain by chaotically stratified diamictons that include convoluted lenses of stratified silt and sand identical to those which comprise the uppermost part of the Qs1s sequence (Fig. 45a, sect. map). This contact was most likely the result of a minor readvance of the ice margin, since it can be traced laterally to a position where the upper and lower

Figure 45 Photographs of highly convolute bedding within diamicton at West Beach (A) and shell rich mud lense exposed just south of measured section HL-1, Hastie Lake Road-North.



A



B

sediment flow facies (Qsds1, Qsdc) merge and the stratified sands are pinched out (see Appendix B).

The degree and style of deformation within the upper diamicton increase towards this position suggesting that a surface of decollement (the Qsdc/Qs1s, Qs contact) developed in the unconsolidated sediment in front of the advancing ice.

Deposition of this stratified sand and silt unit most likely occurred proximal to the ice margin (~ 60 meters distant) under the influence of sediment laden meltwater that discharged into shallow (within wave base) marine waters. Periodic deposition of fluidized mass flows due to very turbid discharges produced massive, clast containing, and crudely graded sands. The composite fining upwards of the sequence reflects waning current energy as the melt-water source became more distal.

A small exposure of horizontally stratified sand and silt just north of Hastie Lake Rd. (sect. HL-1, map section) directly overlies a thick section of basal till but does not appear to have eroded down into it. The lowermost unit is clearly of fluctuating current origin as normally graded cr.-md. , sands rhythmically alternate with laminated fn. grained sand and silt. However, it is sharply overlain by very coarse-md. gr. horizontal to low angle trough cross-bedded sands. Grading is not common within these sands and they appear to be the result of upper flow regime traction currents associated with moderate scale ripple bed forms

(20 - 30 cm λ). Upper contacts with sparsely pebbly mud are extremely sharp indicating rapid changes of depositional environment. The stratified sand sequence constitutes a lense like geometry suggesting channelization of the deposits. The lower rythmically bedded sands and silts may represent turbidity current deposition but are extremely similar to storm generated laminated sands described by Reineck and Singh (1972). Lenses of shell armored mud can be found interbedded with this sequence laterally and suggest deposition within the littoral environment (Fig. 45b). The exposure is extremely inaccessible so more detailed work was unable to be completed.

Pebbly silt (Qpsl), Pebbly mud (Qpm), Massive Diamicton (Qmd)

The origin of pebbly silts and muds found in almost all exposures of the glacial marine section involves both deposition from suspension, due to flocculation of turbid overflow and/or interflows and minor pulses of low density turbidity currents or underflows. This mechanism of fine grained deposition was coupled with an influx of poorly sorted ice-rafted material.

Distinctly laminated pebbly silts and muds, which grade upwards into massive pebbly muds, are characterized by polymodal to unimodal grain size distributions (Fig. 32). Deposition of this material by slow moving, broad underflow currents (low density turbidity currents) could have occurred

at a distance away from channelized Qsls deposition. Alternatively, early settling of the coarser fraction (silts) of turbid inter- or overflows could have resulted in the deposition of this facies over broad regions in the offshore environment. This seems likely since diatoms and spicules can be found within these sediments (table 4 , Appendix A). Massive pebbly muds have somewhat broader, more positively skewed grain sized distributions than the laminated sub-facies (Fig. 32). The lack of well sorted modes and current structures suggest that these sediments were deposited from suspension from the distal parts of either interflow or overflow plumes. Positively skewed grain size distribution of the unflocculated sediment (Fig. 32) would actually represent more unimodal distributions of sediment flocs and individual grains that hydrodynamically had the same settling velocity. This relationship has been demonstrated experimentally for floc sizes less than 8.0ϕ (Kranck, 1973).

Theoretically; as the velocity of the interflow/overflow plume decreased, from a proximal to a distal position, finer individual and flocced grains should settle out of suspension as a unimodal distribution (Kranck, 1975). Eventually a point is reached where individual grains of a given size no longer occur in abundance and only flocs of that size will be deposited. Such a sediment would be represented in the disaggregated condition by a poorly sorted, broad grain size distribution (Kranck, 1973, 1975). In general, current

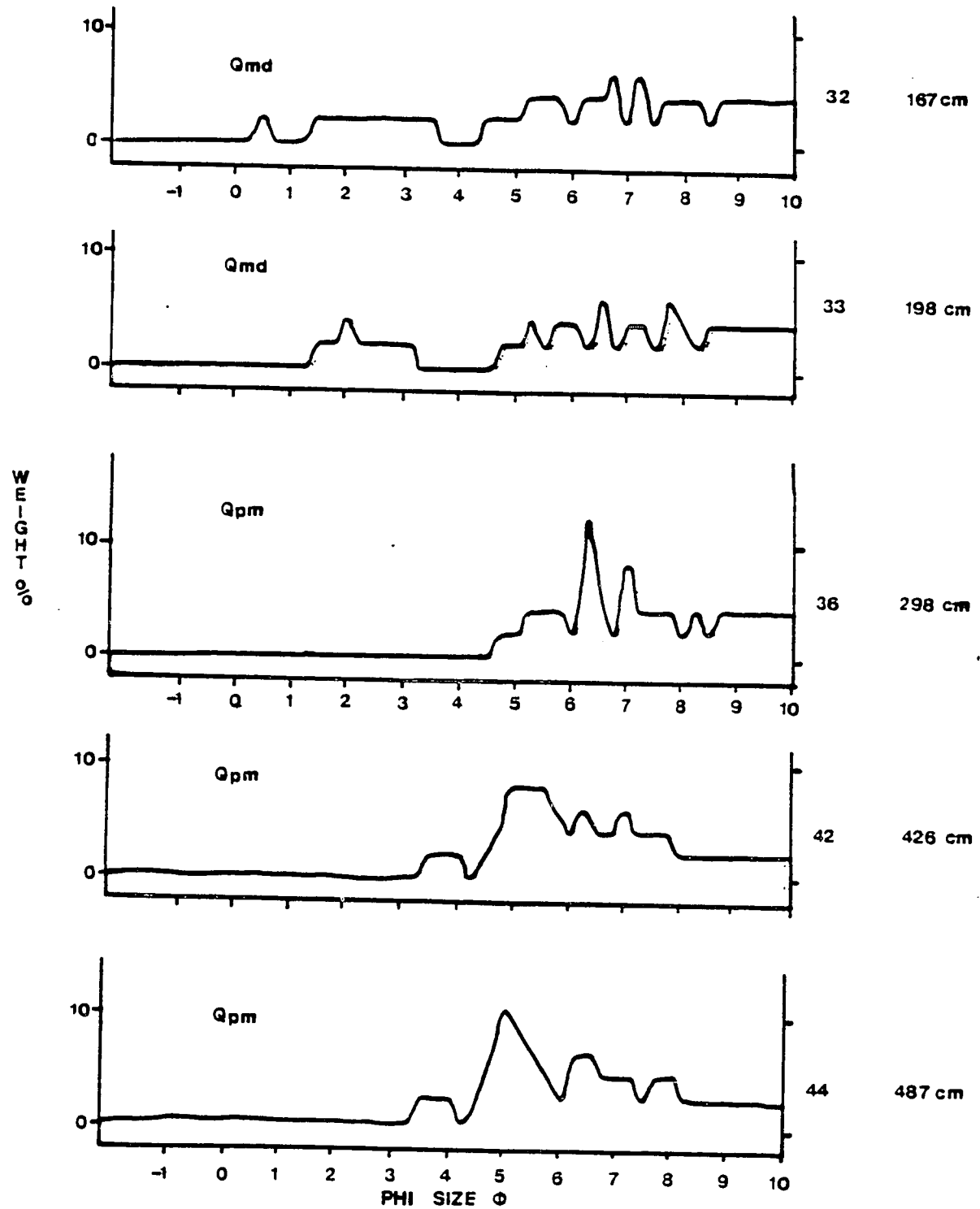
derived modes do fine upwards within pebbly mud sequences (Fig. 46) but only to grain sizes of 7-7.25 ϕ ; beyond this point silt-clay fractions do appear to be non-modal in their grain size distribution.

The broad non-channelized distribution of this facies also supports the interflow/overflow mode of deposition which has been observed for similar sediments in the Gulf of Alaska (Hoskin and Burrell, 1972; Powell, 1981). Poorly sorted ice-rafted material comprises up to 14% by weight of these sediments (Fig. 32) indicating that iceberg rafting was an important process in the environment. Where such sediments were deposited on moderate slopes slumping was an important process as can be seen at West-San de Fuca (see Appendix). Here, post depositional slumping has locally inverted the normal stratigraphic sequence of pebbly silt/pebbly mud to one where pebbly silt overlies pebbly mud. This can be seen just west of measured section SFW-1b. Deformed and sharp contacts of pebbly silts with underlying facies at Maylor Point also indicates post-depositional slumping of the sediment.

An increase in pebble abundance and poorly sorted sand within the matrix results in vertical and lateral transitions of pebbly muds into massive diamictons. These transitions suggest that deposition of ice rafted material increased in proportion to the flux of fine grained silt and clay from suspension.

Figure 46 Grain size frequency distributions of samples of pebbly mud and fossiliferous diamicton taken from section FP-4 at Forbes Point. Notice the fining upward trend in the current derived (silt-clay) component.

Section FP - 4

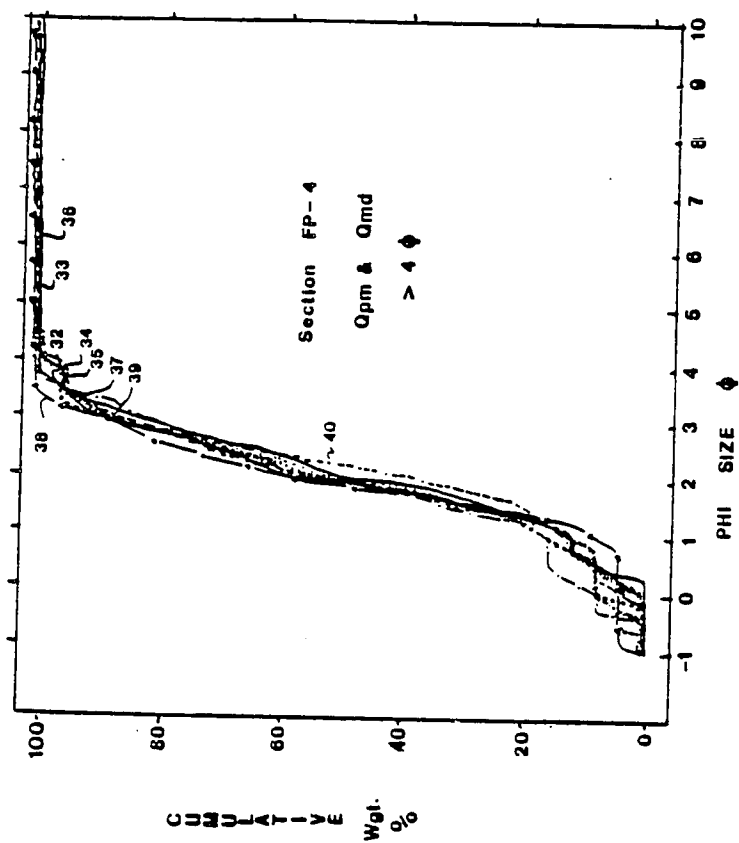
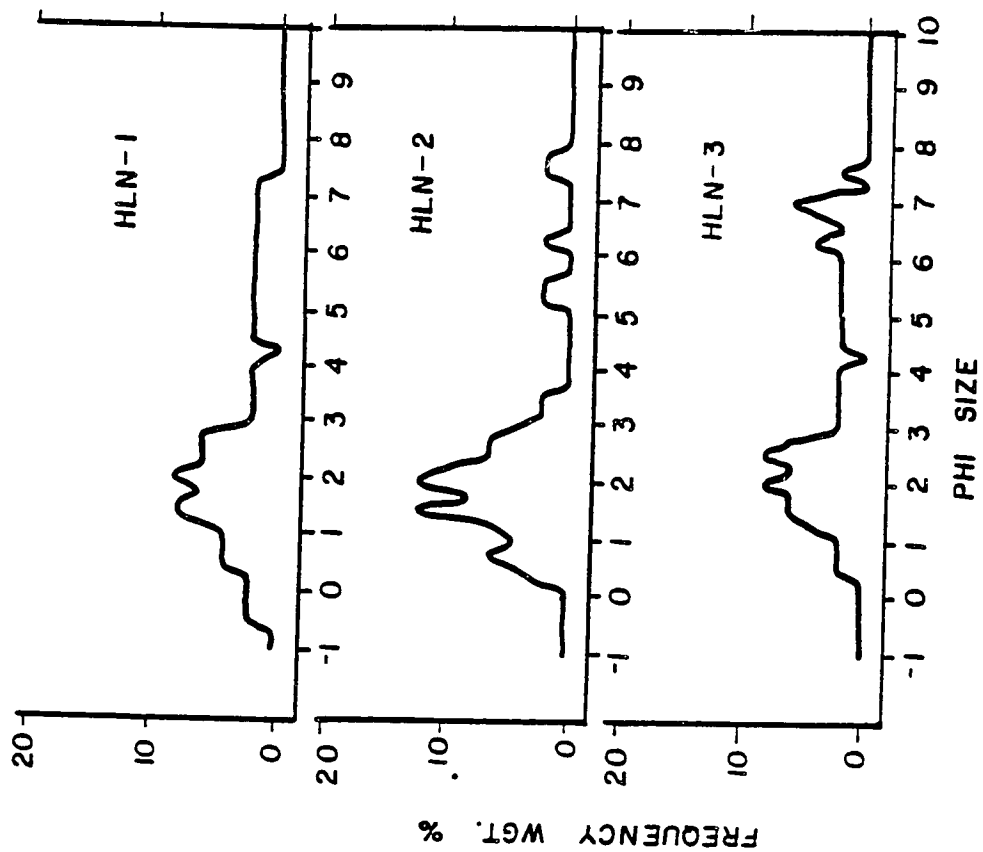


This was caused in most cases by the retreat of turbid overflow plumes in conjunction with a receding ice margin. The fining upward trend of the silt/clay fraction from pebbly mud to diamicton supports this view (Fig. 46). If deposition of suspended sediment decreased due to increased water column turbulence, as would be the case if rebound was bringing the basin into the wave zone, then a coarsening upward trend in the fine grained component would be expected.

The rate of ice-rafting may have been fairly constant, within both the zones of pebbly mud and diamicton deposition, as suggested by the uniform grain size distribution of this component through the facies transition (Fig. 47). In some localities, massive fossiliferous diamictons directly overlie Qsd facies without transitional pebbly mud facies (Penn Cove). In such cases, very high rates of ice-rafting proximal to the ice margin could have diluted the flux of suspended silt and clay.

Isolated sedimentary structures within the Qmd facies point to an ice-rafted origin. Small deformed lenses of sandy gravel and gravelly sand often appear to have been dropped into a soft deformable bottom (Fig. 35a). Lower contacts exhibit load style deformation while upper contacts are convex or non-planar, indicating that the lenses are not channels. In most exposures, however, such structures are missing and the diamictons are truly massive. In such cases pebble fabrics are close to random with a high

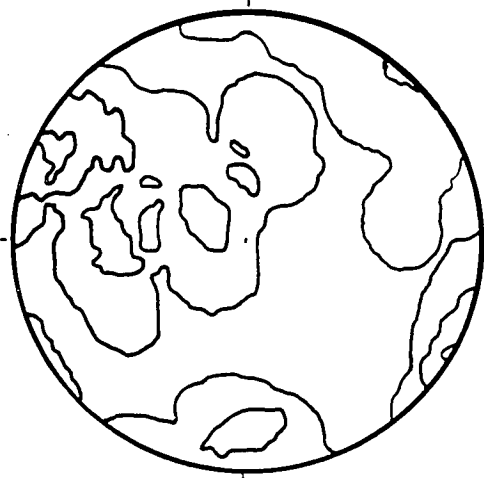
Figure 47 Grain size frequency distributions for samples of lodgement till from Hastie Lake Road-North, and sand fraction cumulative distributions for samples of pebbly mud and fossiliferous diamicton from section FP-4. Notice the low variability and lack of fine grained sand for the Forbes Point (FP) samples.



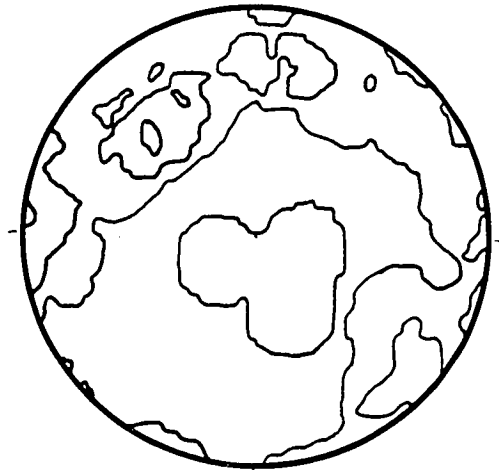
percentage of steeply dipping clasts (Fig. 48). As suggested by Evenson and others (1977), it seems likely that elongate stones, when dropped through the water column, would produce "a random drop fabric" in the ice-rafted deposits. This would be the case only if the bottom was soft enough so that when stones hit they retained their random orientation. On harder substrates it would seem likely that stones would hit and fall parallel to the bottom, as suggested by Gibbard (1979). Such orientations are observed for well laminated pebbly muds (Fig. 48). Coarser grained diamictons, and interestingly those with the most abundant fossils, do have oriented fabrics (Fig. 48). A coarser grained sediment would have had greater matrix strength than finer grained diamictons. These results will be discussed in more detail in chapter 7. In the majority of cases fabric data from massive units does support an ice rafted origin for this facies.

The source of ice-rafted material probably included a number of distinct iceberg rafting mechanisms, including basal debris zones, shear zone, and supraglacial zone transport. The distinct angularity of clasts, when compared to similar lithologies from Vashon lodgement till (Fig. 49) suggests that the majority of material was transported as supraglacial debris. The lack of fine sand is characteristic of the ice-rafted fraction (Fig. 47) and is dissimilar to grain size distributions of local basal tills (Fig. 47).

Figure 48a,b Equal area projections of pebble long axis orientations from massive, fossiliferous diamictons (Qmd). Contour interval is 1, 3, 5, 7, and greater than 9% of data per 4% of projection area. Sample LB-Qpml-1 was not rotated to horizontal and consists of 20 measurements, all others consist of 25 measurements and were collected from horizontal beds.



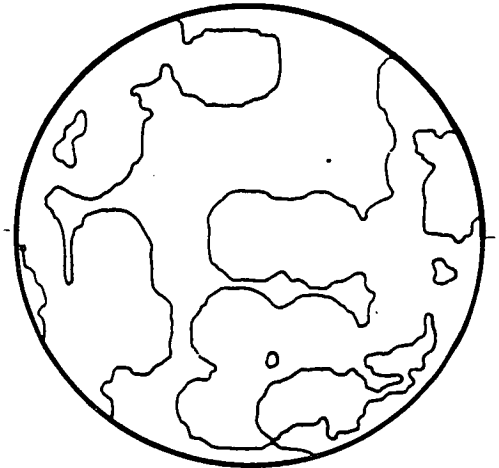
PC-Qmd-1 22% Sand



PC-Qmd-2 5% Sand



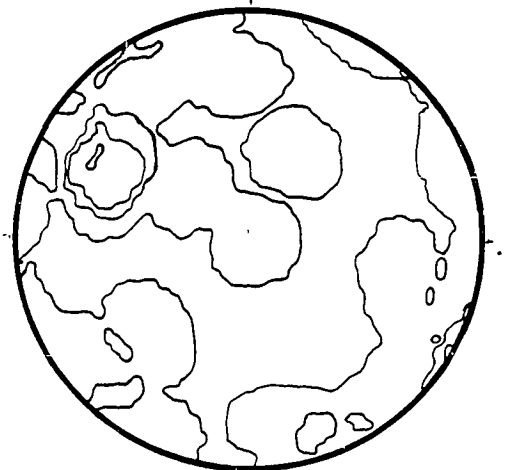
PC-Qmd-3 28% Sand



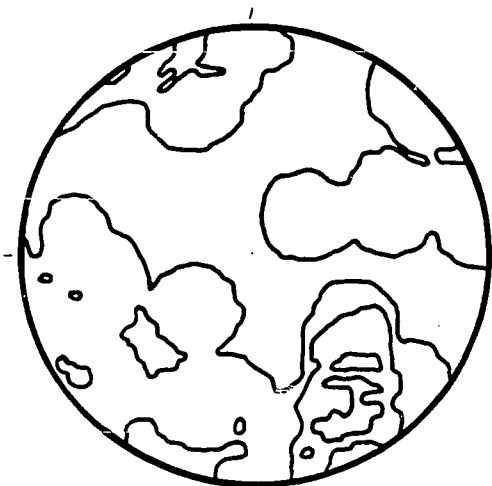
PC-Qmd-4 39% Sand



BB-Qmd-1 45% Sand

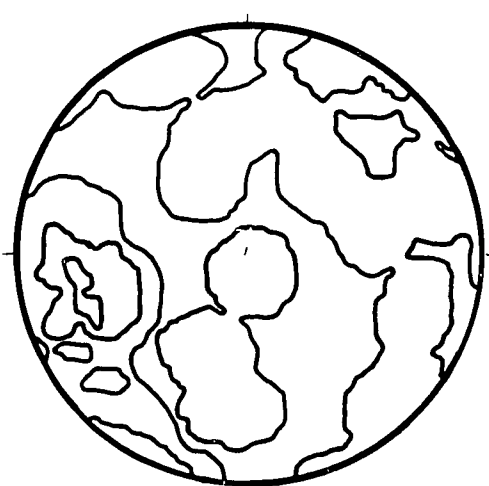


BB-Qmd-2 17% Sand



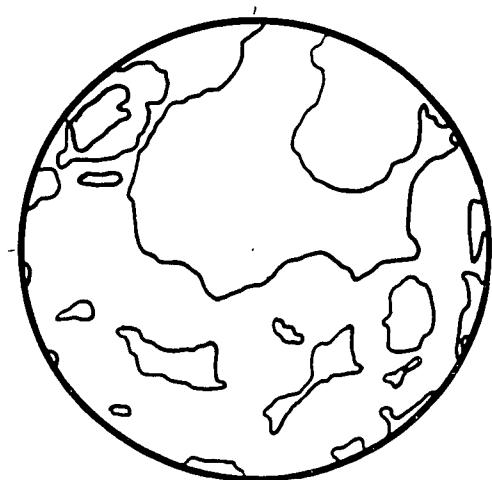
FP-Qmd-1

20% Sand



FP-Qmd-2

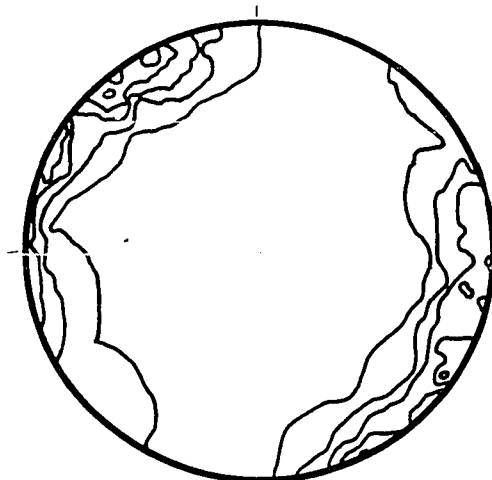
17% Sand



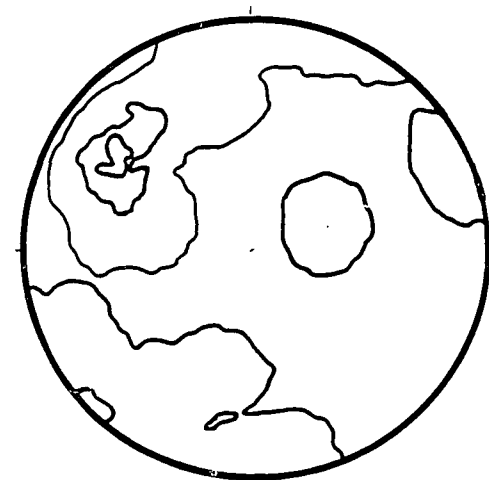
SFW-Qmd-1 17% Sand



SFW-Qmd-2

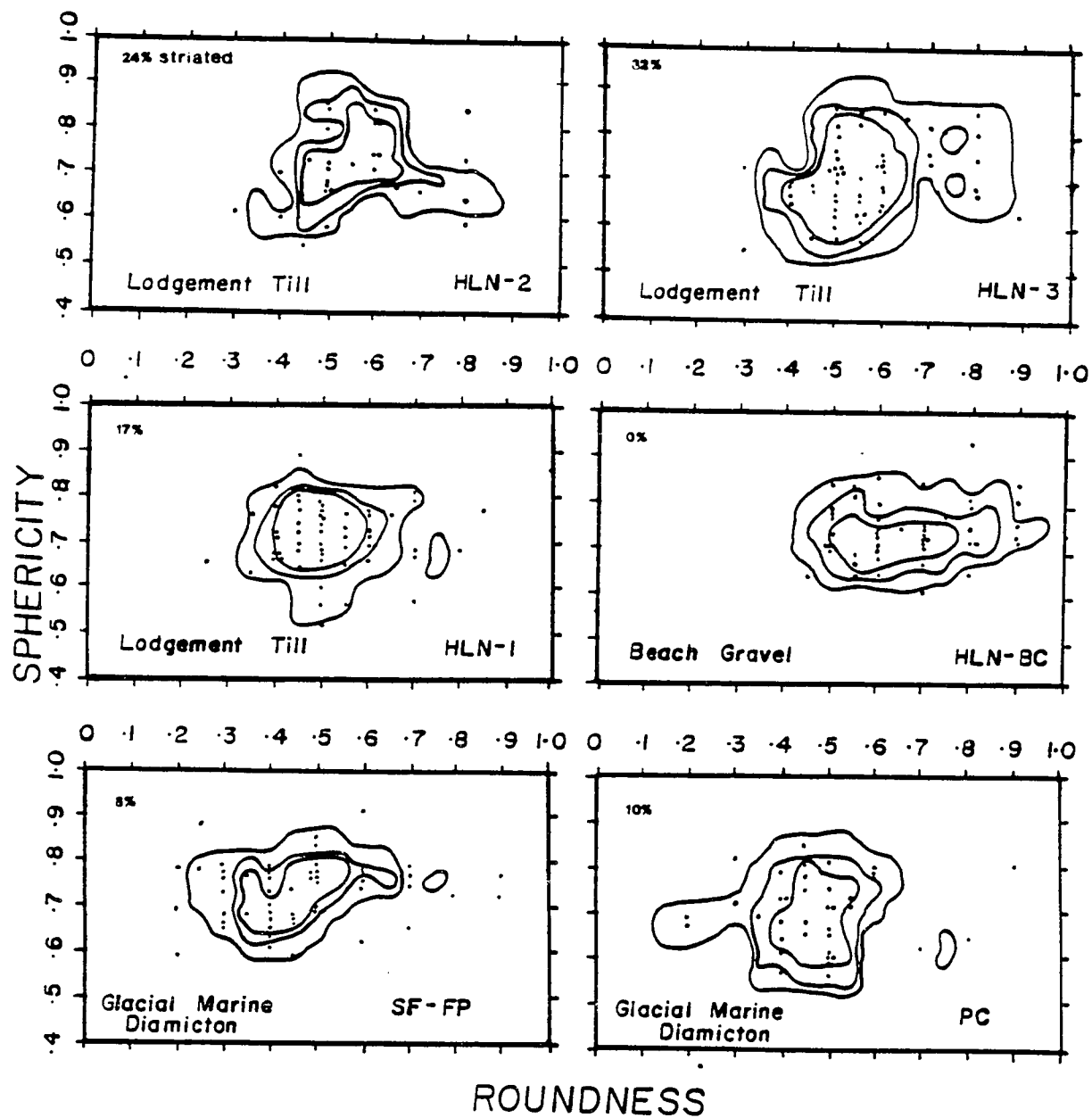


ST-Qpml-1



LB-Qpml-1

Figure 49 Sphericity and roundness (Krumbein, 1941) plots of clasts from Qmd, lodgement till, and modern beach sediments. Contour intervals are at 5, 10, and 15% of the data per 1% of the graph area. Notice lower roundness for Qmd units versus lodgement till samples and higher roundness for beach sample.



Thus, if basal debris zones were a major source of ice-rafted material an additional mechanism would be needed to remove the fine sand fraction from the resulting deposit. Surface precipitation and meltwater commonly remove fine sand and mud from supraglacial debris of modern glacial environments (Ovenshine, 1970, Sharp, 1949). Hence, a supraglacial source for much of the ice rafted debris of the Qmd facies is proposed.

Within a single exposure massive diamictos display extreme textural homogeneity vertically within units, as reflected by both sand:silt:clay proportions and their cumulative sand size distributions (Figs. 32, 34, 47). This suggests rather constant conditions of deposition with a more or less steady rain of ice-rafted debris. Although diamictos can be produced by a combination of iceberg rafting of supraglacial debris coupled with fine grained current deposition (Powell, 1981), iceberg rafting itself has been observed to be rather episodic, involving texturally heterogeneous materials (Ovenshine, 1970). One way to resolve this is to consider the path of icebergs in a nearshore tidal environment. As observed in restricted portions of Puget Sound today, nearshore tidal currents of significant velocity twice daily reverse their direction and flow parallel to the shore. Thus, the residence time of recently calved bergs under similar circulations could be expected to be longer than the time required to deposit the debris load.

The result would be a localized mixing of the sediment source such that textural homogeneity in the ice-rafted deposit is favored.

Unit thickness within a given exposure is quite consistent, indicating uniform rather than localized deposition. Qmd units do, however, thin appreciably as they lap onto upland areas (see sect. maps).

Based on their stratigraphic position and a consideration of depositional process, massive, fossiliferous, diamictos represent the most distal of the glacial-marine facies. The presence of fossils indicating normal marine salinities (Balzarini, 1981) supports the view that such sediments were deposited beyond the influence of turbid and brackish glacial meltwater.

Emergence Deposits (Qgl)

All exposures of glacial-marine sediment on Whidbey Island are capped by .5 - 2 meters of gravelly sand and sandy gravel which represent littoral environments (Fig. 15). Such units can be referred to as emergence deposits and were the result of extremely rapid rebound by the marine basin above sea level. Their lower contacts are extremely sharp, often marked by gravel lag zones which seem to represent erosion of underlying glacial-marine sediments. Gravel zones; however, are not thick suggesting that erosion was not extensive. Therefore, thinning of underlying facies

onto highlands was probably due to their original distribution rather than post-depositional erosion. In some cases, upper contacts of the emergence deposits grade into active surfaces of eolian deposition (West Beach North, Fig. 13). Most sequences are capped by modern soil profiles and vegetation.

CHAPTER 5

- 1) The Sedimentary Model
- 2) The Stratigraphic Model
- 3) Implications to other Glacial Marine Deposits

The Sedimentary Model

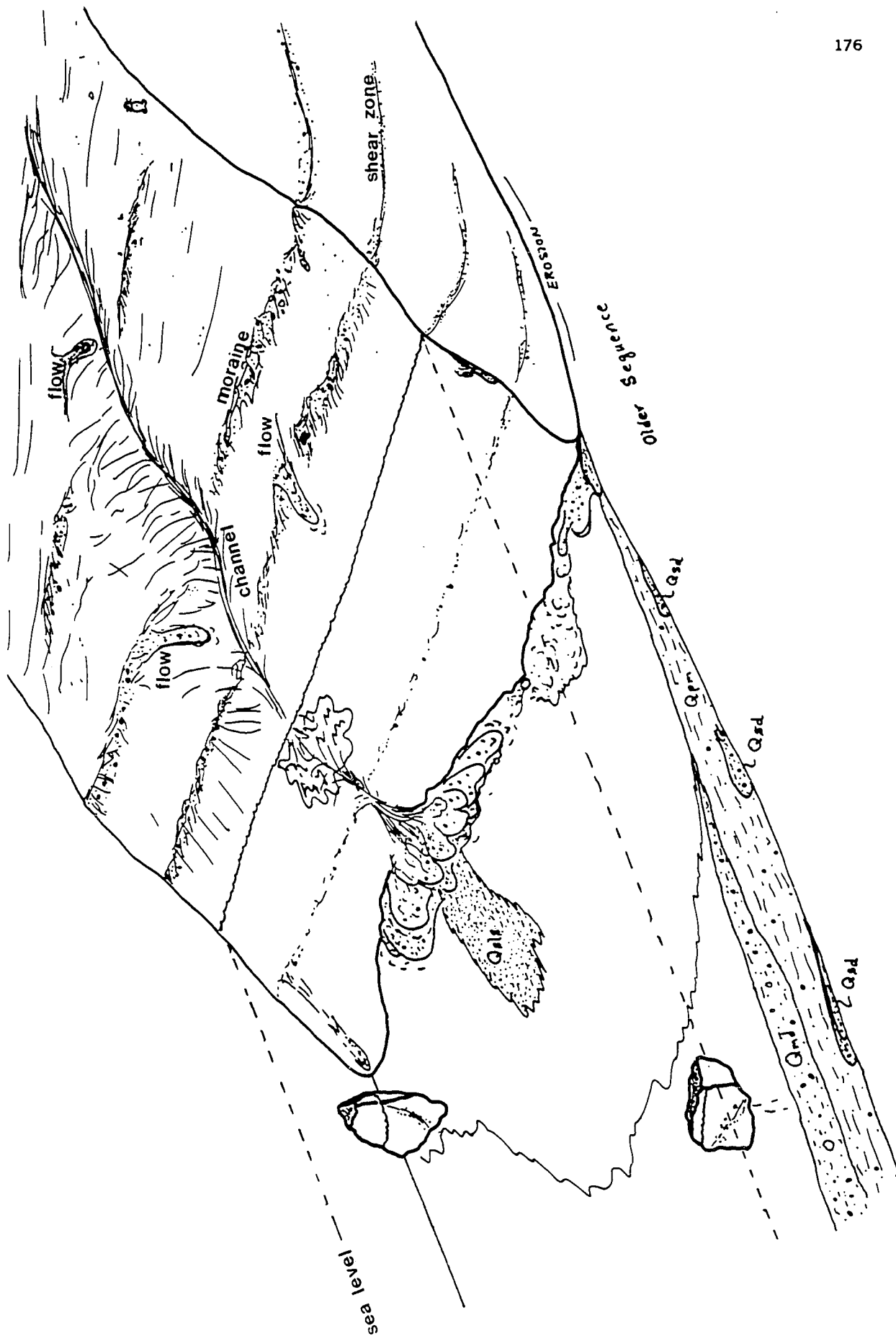
The lithofacies discussed above suggest that complex glacial-marine conditions were in existence at the time when "Vashon" ice retreated from the region. The nature of the ice margin and proximity to meltwater inflow into the basin played a significant role in the facies distribution. Based upon vertical successions and lateral facies relationships, depositional environments ranged from ice-marginal/marine, proximal meltwater, distal meltwater to distal glacial marine (Fig. 50).

The nature of the boundary between glacial ice and marine waters was the major factor in the development of ice marginal deposits. Facies associated with this environment include stratified diamictos (Qsd) and channelized, stratified silts and sands (Qsls, Qls, Qsl). Where the ice margin was partially stable and/or had sufficient supraglacial debris, thick sequences of sediment flows were deposited in the marine basin (Fig. 50).

Channelization of these gravity flows along the ice margin produced thicker deposits in localized depressions and allowed finer grained flows of high water contents to be funneled into the marine environment.

In such an environment, interbedding of flows and meltwater marine sediments occurred. As the ice margin receded rapid burial of individual flows by fine grained meltwater

Figure 50 Diagrammatic model for ice marginal marine deposition based on exposures along Penn Cove. Development of sediment flows (Qsd) occurs along the ice margin and they are progressively buried by meltwater facies (Qsls and Qpm) as the ice margin recedes. Massive ice-rafted diamictons are deposited distal to the ice margin. In this model ablation processes at the ice margin dominate over calving and rates of ice margin retreat are relatively slow.



sediments occurred, thus preserving their depositional geometry.

Near englacial or supraglacial channels, and possibly fluvial systems, stratified silty sands and sandy silts were deposited. Their typical association with underlying sediment flows indicates a continued influence of ice channels upon sedimentation in the basin. As the ice receded broad (10 m) linear trends of such facies were produced. In regions of high discharge, erosional/depositional channels, superimposed upon sediment fans (10 - 30 m wide), were constructed (Fig. 51). Coarser grained silty sands are restricted to channelized portions of the fan. Discharge was highly sporadic resulting in alternating but continuous underflow and overflow/interflow deposition. Depositional rates in such settings were extremely rapid perhaps decimeters/year. Thus, ice marginal marine waters were at the most brackish and extremely turbid, preventing migration of marine organisms both on the bottom and within the water column. Resulting sediments lack fossils of any kind.

Where the ice margin was steep and calving was an active process, sediment flows would be less common and would consist of chaotically stratified units rather than well defined flow lobes (Fig. 52). Subglacial meltwater activity had the greatest influence upon the bottom but deposition associated with these systems was sporadic, allowing for migration of some benthic organisms. Minor readvances of

Figure 51 Diagrammatic model for submarine meltwater fan deposition as based on exposures of Qs1s and Qs1c facies at Lovejoy Point-Coupeville and Maylor Point. Deposition of silty sands via underflow currents would occur at times of high velocity discharge associated with high suspended sediment concentrations.

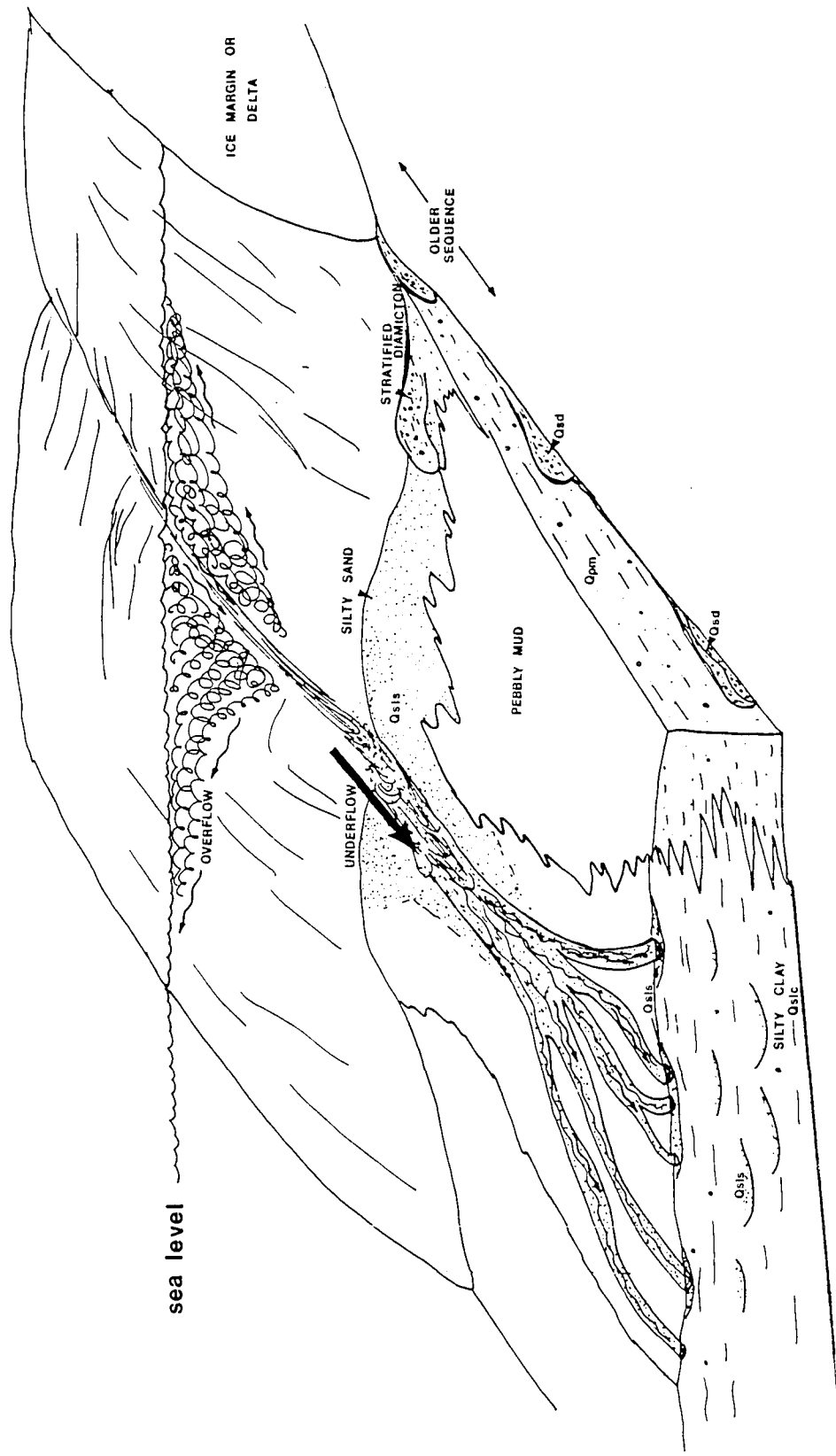
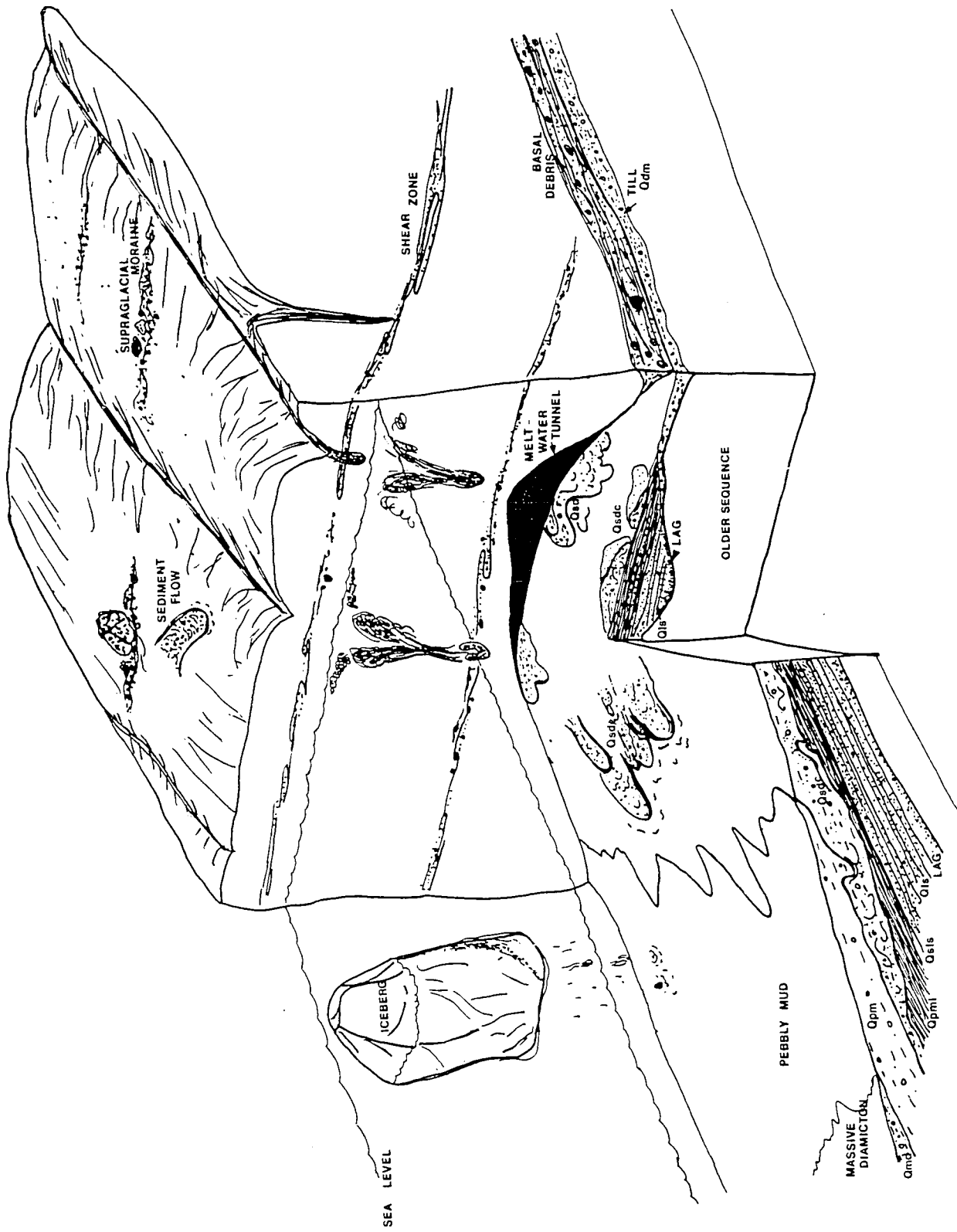


Figure 52 Diagrammatic model for glacial-marine deposition along a steep ice margin as based upon exposures on the west coast of Whidbey Island.



the ice front resulted in localized deformation of proglacial marine sediments.

Removal of the finer grained component of supraglacial debris occurred due to both sediment and meltwater flow processes. This left coarser fractions concentrated upon the ice which later calved, rafting debris seaward.

No sedimentologic evidence exists suggesting that ice-shelf conditions were in existence at the time of Vashon ice retreat. Except for small subglacial cavities which may have had basal debris melted out into, the ice margin appears to have been grounded.

Seaward of the ice margin, proximal meltwater sediments of Qslc, Qpsl, and Qpm facies were deposited. In this zone the boundary between persistent high velocity underflow deposition and low density turbidity current deposition occurred at some distance from meltwater inputs. However, deposition took place primarily as a result of the flocculation of silt and clay within turbid overflow and interflow plumes.

On distal portions of meltwater fans the finest grained, silt-sand, portion of underflow currents deposited sediment in small distributary type channels. Eventually, as the density contrast between these currents and surrounding basin waters became less, the currents either detached from the bed and became interflows or the finest particles (silt-clay) spread out as low density turbidity currents (Fig. 51).

This zone produced the Qslc facies and the laminated Qpsl, Qpml facies.

Extensive flocculation of silt and clay occurred off-shore as soon as mixing between freshwater sediment plumes and marine waters produced salinities of at least 3 - 4‰ (Hoskin and Burrell, 1972, Kranck, 1973). Initially coarse grained silts and silt sized flocs settled out producing pebbly silt facies. Thin laminae were produced due to fluctuations in current strength and sediment input. Seasonal influences may have been important in this regard.

Further seaward, finer individual grains and flocs settled out as mixing with marine waters continued. Microfossils were first becoming incorporated within the sediment but their extremely low numbers reflect continued high sedimentation rates. Continued deposition on slopes produced instability and slumping of the sediments in some areas. Eventually sedimentation rates decreased with increasing distance seaward to the point where steady-rate iceberg rafting contributed up to 14% of the sediment. At this point sediment being deposited from suspension consisted in its non-flocculated state of non-modal poorly sorted fn. gr. silt and clay. This zone of distal meltwater deposition resulted in the pebbly mud facies (Qpm). Where strong wave influence was present winnowed layers of sandy gravel were produced within pebbly muds. Rough volume estimates of this facies suggest that the source of silt

and clay could not have been solely ice margin meltwater channels. These channels did contribute a significant proportion of fines, since Qpm facies thicken in their vicinity, but outwash systems that were in more upland areas probably contributed a major part as well (Pessl et al., 1981).

In positions both distal to meltwater inputs and/or the ice margin, distal glacial marine conditions resulted in the deposition of massive diamicton (Qmd) facies. The facies boundary separating this zone from the distal meltwater zone was a sharp front between a moderately mixed turbid plume and more or less normal marine waters. This boundary fluctuated both seasonally and diurnally such that the eventual vertical successions between facies were more or less gradual. In this zone, constant-rate ice rafting in conjunction with relatively low rates of fine grained sediment deposition produced massive diamictons. Relative proximity to a source of debris laden icebergs is required. Occasional large scale rafting events of very coarse debris produced deformed lenses of sandy gravel.

Well mixed waters and close to normal salinities (Balzarini, 1981) allowed for colonization of the bottom by a variety of marine organisms.

This sedimentologic model has important climatic implications since the development of sediment flows, meltwater facies, and specific mechanisms of ice rafting can be related

to such factors as precipitation, mean annual temperature and glacial regime (Lawson, 1979; Sugden and John 1976; Anderson et al., 1980b). The relationship of this model to other schemes of glacial-marine sedimentation will be discussed in a climatic context in the next section.

So far, discussion has focused upon the sedimentary aspects of the model. However, it must be kept in mind that the sediments studied as part of this investigation represent a very unique setting in relationship to the deep marine and fully terrestrial environments of the region. In the following section, stratigraphic and facies relationships of the glacial-marine sequence on Whidbey Island will be extended to both deeper marine and fully terrestrial sequences.

The Stratigraphic Model

The sequence of late Pleistocene glacial-marine sediments on Whidbey Island represent the most shallow of glacial marine environments. The facies were deposited within an isostatically depressed basin and thus have well defined sequence boundaries which can be used to separate them from deeper marine and fully terrestrial environments. Figure 53 demonstrates the stratigraphic and facies relationships of the Whidbey Island section to the deeper marine section of the Strait of Juan de Fuca and terrestrial environments to the east and south.

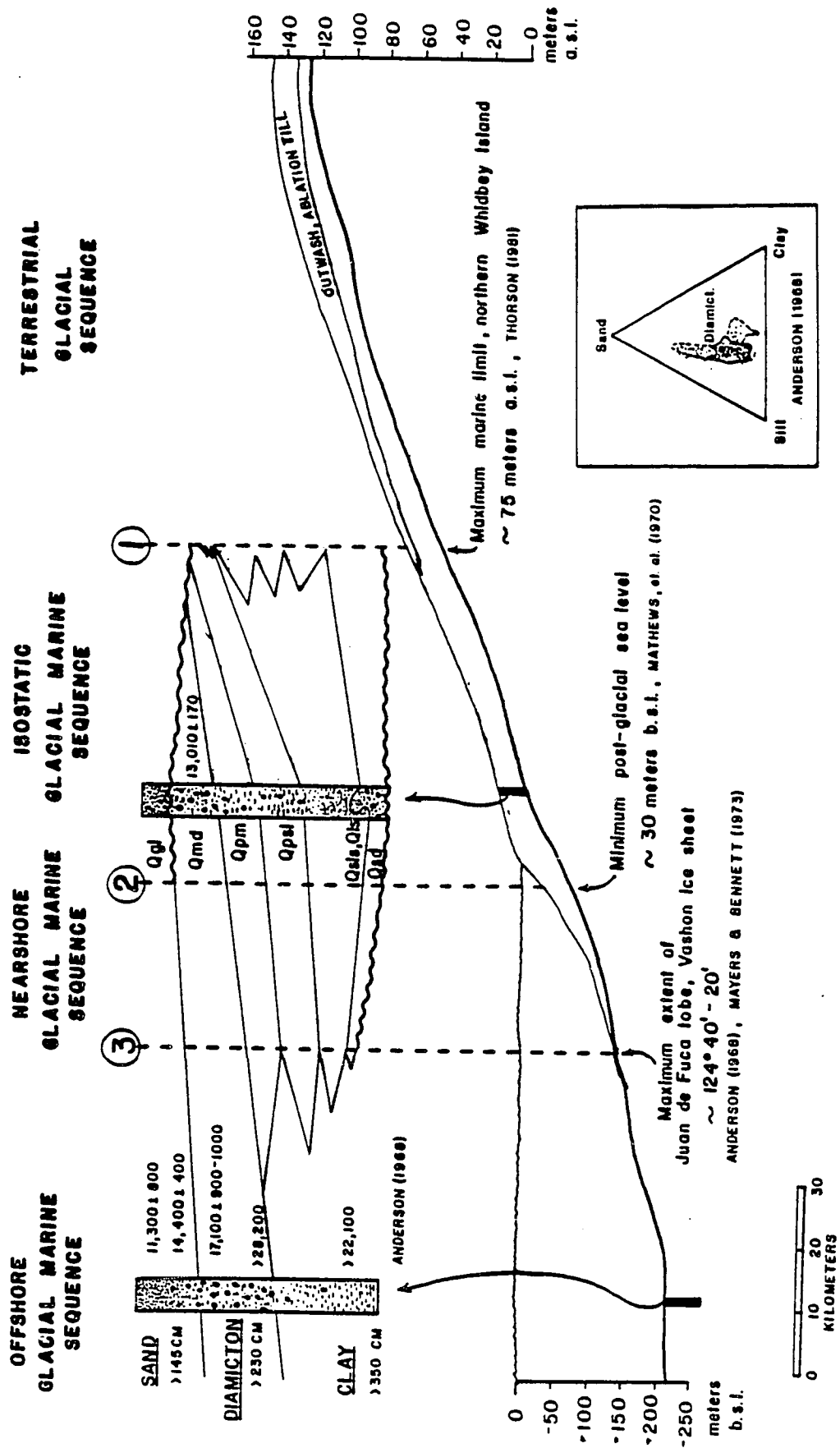
Within this model, three major boundaries can be defined, the first represents the maximum elevation of sea level which was reached prior to complete isostatic rebound. The second boundary is defined by the lowest post-glacial sea level and the third by the maximum seaward extent of grounded ice. The position of a particular section with regard to these limits will determine both the nature of the sequence boundaries and the development of facies within the section.

The composite section of Whidbey Island represents a sequence deposited between boundaries 1 and 2 and is defined as an isostatic glacial marine sequence. Its lower contact is a surface of glacial and/or meltwater erosion, since it lies landward of boundary 3. The upper sequence boundary

Figure 53 Stratigraphic model for late-Pliocene glacial-marine deposits exposed on Whidbey Island and their relationship to the deep marine section as described by Anderson (1968).

WEST

EAST



is a surface of erosion produced as littoral environments migrated over a region in response to falling sea level. The degree of facies preservation within such isostatic glacial-marine sequences depends upon the position of a particular section between boundaries 1 and 2. For instance, it is known that sea level (boundary 1) in the northern Puget Lowland was, at its maximum, at least 73 m (239.5') above present sea level during the retreat of Vashon ice (Thorson, 1981). However, well developed glacial marine facies (Qpm) can only be found up to elevation of approximately 50 meters on northern Whidbey Island. Above this elevation deltaic and littoral sediments (Qgl, facies) can be found, but only up to the maximum high sea level stand (boundary 1). This change in facies is a reflection of the rate of sea level fall, which initially (at high elevations) was extremely rapid (Thorson, 1981). At lower elevations, close to present sea level, sedimentation rates were rapid enough that almost a complete sequence of glacial marine facies were deposited prior to the rapid fall of sea level. Given a constant rate of sea level fall local topographic differences will determine both the degree of erosion at the top of the sequence and the thickness of littoral sediments deposited above the contact.

Landward of boundary 1, glaciofluvial, lacustrine, and ablation till deposits, each with their own complex facies relationships, would comprise the terrestrial glacial

sequence. Minor progradation of these facies past boundary 1 could occur, depending on the relative rates of sea level fall and recession of glacial ice from the region.

It should be pointed out that the model shown in figure 53 represents an idealized east-west cross section approximately along $48^{\circ} 15'N$ latitude. Further south or north the elevation of boundary 1 (the marine limit) is lower and higher respectively. This was due to differential rebound in response to the configuration of the Puget lobe of the Vashon Ice Sheet (Thorson, 1980).

Between boundaries 2 and 3, a nearshore glacial marine sequence would be found. Again, the lower sequence boundary would be defined by a surface of glacial erosion. High resolution seismic data from the Strait of Juan de Fuca shows that the most recent surface of glacial erosion can be traced westward to approximately $123^{\circ} 50'$ (horizon E of Mayers and Bennet, 1973) and thus would define the position of boundary 3 in figure 53. Two older surfaces of glacial erosion were also recognized by Mayers and Bennet (horizons B and C) and were found to extend further west, to $124^{\circ} 40'$. The upper boundary of the nearshore glacial marine sequence would be conformable with overlying normal marine sediments. The type of marine sediments overlying the sequence would depend on modern oceanographic conditions, depth, and proximity to the present shoreline.

The glacial marine sequence itself would consist essentially of the same lithofacies as the isostatic glacial marine sequence, only the upper boundary would be different. One possible exception could be found in the massive diamict-ton facies. Since the nearshore glacial marine sequence represents continual deposition through the glacial-nonglacial boundary, a decrease in ice-rafting within the Qmd facies should be evident. Massive diamictons within the isostatic glacial marine sequence show little evidence of decreasing ice-rafting perhaps because sea level dropped before diminishing iceberg activity had an effect upon deposition. Limiting ages of 13,010 - 11,850 y.b.p. for this facies suggest that erosion may have played a role.

Seaward of the maximum extent of glacial ice (boundary 3), an offshore glacial marine sequence would be found. This sequence would be conformable with both underlying and overlying normal marine sediments. At boundary 3 dramatic facies changes would take place as well.

Sediment flow facies (Qsd) would not be found beyond boundary 3, since they are primarily ice marginal deposits. Proximal meltwater facies (Qsls, Qpsl, Qslc) would also not extend far beyond boundary 3. Decreased fluvial input of silt and clay would inhibit extensive deposition of distal meltwater facies (Qpm). However, if they comprise a significant part of the offshore glacial marine sequence their distribution limits should extend some distance seaward

from boundary 3. The offshore glacial marine sequence should consist primarily of distal glacial-marine facies (massive diamicton, Qmd). The late Pleistocene stratigraphy for the Strait of Juan de Fuca (Anderson, 1968) supports this model. As shown in figure 53, massive glacial-marine diamictons are conformable with both underlying and overlying marine clays, silty clays, and sands. Sand, silt, clay percentages for the diamicton unit are identical to samples of Qmd facies from Whidbey Island (Fig. 53). Anderson (1968) reports that deposition of the diamicton occurred in waters which were initially estuarine but became increasingly more marine. Carbon-14 dates of $21 - 17 \times 10^3$ years B.P. for the diamicton unit point to its deposition during the Vashon Stade maximum, which Anderson associated with an ice margin located at $123^{\circ} 20'$ in the Strait of Juan de Fuca. This is approximately 20 km east of the boundary suggested by the data of Mayers and Bennett (1973).

Thus the offshore glacial marine sequence reported by Anderson (1968) was deposited at least 16 km from the inferred ice front. The apparent absence of other glacial marine lithofacies (Qpm) at this locality, and further seaward, suggests that limits of their distribution were within 16 km as shown in figure 53.

The sequence of late Pleistocene glacial-marine sediments on Whidbey Island are the result of a unique combination of isostatic, eustatic and sedimentary processes.

These sediments are part of a continuum of glacial and glacial-marine sequences which differ both in their type of lithofacies and in the nature of their stratigraphic boundaries.

Implications to other Glacial Marine Deposits

Facies associations of the Whidbey Island sequence reflect specific paleoclimatic conditions and the observed stratigraphic relationships can be related to the isostatically depressed setting of the basin at the time of deposition. Therefore, the model used to explain late-Pleistocene sediments on Whidbey Island has great potential in the interpretation of pre-Pleistocene glacial sequences, which now appear to be more common than previously thought (Hambrey and Harland, 1981).

Carey and Ahmad's (1961) classic paper on glacial marine sedimentation was the first work which emphasized glacial regime as an important sedimentologic factor. They recognized two glacial regimes, a cold based (basal ice temperatures below pressure melting), and warm based (basal ice temperatures at pressure melting). Their conceptual model was based on the physiographic differences between ice shelves, ice sheets, and outlet glaciers, as observed in the Antarctic. Although the model was widely applied during the 1960's and 1970's (i.e., Reading and Walker, 1966;

Lindsey, 1970) it was based on depositional settings and glaciologic variables which were, at that time, poorly known.

We now know, or at least have a better understanding, that the variability of glacial morphology in the Antarctic, as described by Carey and Ahmad (1961), is the result of complex glacial flow dynamics rather than strictly basal thermal regime (Jour. of Glaciology, 1979, v. 24, no. 90, and Hughes, 1981). The influence of an ice shelf setting, versus and ice sheet margin, upon glacial marine sedimentation in Antarctica is primarily upon the supply of ice-rafted debris (Drewry and Cooper, 1981).

Our knowledge of Antarctic glacial marine sediments has greatly expanded over the last few years (Anderson et al., 1979, 1980a; Webb et al., 1979; Kellogg, et al., 1979; Orheim and Elverhoi, 1981; Domack, 1982). These studies show that diamictons are the most common sediment recovered by piston cores from the Antarctic continental shelf, exclusive of the Antarctic Peninsula. They are found at depths which range from 100 to 1000 meters and originated as either basal till, deposited during glacial expansion onto the continental shelf (Kellogg et al., 1979; Anderson et al., 1980a), or as ice-rafted sediments, deposited beneath ice-shelves which were only locally grounded on the continental shelf (Domack, 1982; Orheim and Elverhoi, 1981, and Drewry, 1979). Post depositional slumping of these

diamictons is also an active process (Kurtz and Anderson, 1979; Wright, 1980). Stratified meltwater deposits (silts or sands), which were thought to be present by Carey and Ahmad (1961), are conspicuously absent on the continental shelf (Domack, 1982). The transition from grounded ice to ice-shelf, or open marine, conditions is sometimes recorded by very thin sandy intervals (Kellogg et al., 1979; Domack, 1982) which are overlain by biogenic deposits (silicious oozes). Domack (1982) suggests that these sharp transitions reflect the absence of significant meltwater processes at the grounding line of receding glaciers.

Again, the Antarctic has an extreme polar climate, with average summer temperatures along the coast of about -10.00°C , and has apparently remained in this setting for at least the last 30,000 years (Paterson, 1969; Lorius et al., 1979). Precipitation occurs exclusively as snowfall in amounts which range from 5 to 70 cms, water equivalent (Paterson, 1969). These climatic constraints control the thermal regime of Antarctic glaciers such that basal meltwater is present only under the thickest portions of the interior ice sheet, or where extremely rapid velocities, associated with outlet glaciers, contribute to frictional heat (Hughes, 1981). Firn depths are on the order of 100 meters (Gow, 1971) and projected equilibrium lines lie well out to sea. These conditions influence glacial-marine sedimentation such that ice-rafted debris is

predominantly of basal debris origin (Anderson et al., 1980b, Domack et al., 1980). Supraglacial debris is rare and supraglacial ablation moraines do not form (Shaw, 1977). Most importantly, meltwater processes at the glacial margin are insignificant (Rains et al., 1980). These observations hold for most of the Antarctic but further north, along the Peninsula under slightly warmer conditions, supraglacial moraine formation and meltwater processes become more important (Sugden and Clapperton, 1981).

In the Gulf of Alaska, a strikingly different glacial-marine environment can be found. Recent studies by the U.S. Geological Survey and a number of other groups have shown that meltwater sediments comprise a significant part of the late Pleistocene-Holocene glacial marine section.

Powell (1980, 1981) presented a detailed model for glacial marine sedimentation in Glacier Bay, Alaska, where valley glaciers terminate in narrow fiords. Meltwater input into the fiord occurs either at the ice margin, from subglacial or englacial outlets, or along outwash fan deltas, where glaciers have receded beyond the marine limit. As a result, "iceberg zone mud" and "marine outwash mud" accumulate at rates exceeding 4 meters/year (Powell, 1981). Underflow currents produce stratified "sand and mud" lithofacies and turbidity current activity results in erosional depositional channel infills. Diamictos are

produced both at the ice margin, as part of a "morainal bank lithofacies," and through a combination of ice rafting and fine grained suspended load sedimentation. A similar suite of lithofacies can be found in the Gulf of Alaska, both in the Holocene (Molinia and Carlson, 1975) and in the Plio-Pleistocene/Yakataga Formation (Miller, 1953, and Plafker and Addicott, 1976). As described by Powell, the association of specific facies within a single fiord depends upon the depth of water and rate of ice margin retreat. However, the variables controlling the sedimentary processes are climatic.

As a reflection of the moderate maritime climate, glaciers along the coast of the Gulf of Alaska have extremely high accumulation rates coupled with high rates of ablation. Precipitation is also high along the coast, averaging 250 cm/year (Péwé, 1975). As a result, ablation zones characterized by supraglacial moraines and sediment flows develop in marginal zones of the glaciers (Lawson, 1979, and others). Glaciofluvial activity is pronounced and results in discharge of highly sediment laden meltwater into the marine environment (Hoskin and Burrell, 1972; Molnia, 1979). Iceberg rafting consists primarily of supraglacial debris (Ovenshine, 1970; Powell, 1980).

The late-Pleistocene glacial marine sequence on Whidbey Island was deposited under climatic conditions similar to

the present day Gulf of Alaska. The sediments reflect this in several ways. The abundance of stratified silty sands, pebbly silts and muds all indicate pronounced meltwater influence upon marine deposition. These deposits are identical to lithofacies described by Powell (1980); ice-berg zone mud, marine outwash mud, and interbedded sand and mud. Indications of underflow deposition, as preserved in alternate bedding of silty sand and pebbly mud (Fig. 23), imply abnormally high suspended sediment concentrations and/or dilution of marginal marine waters. Sediment flow facies (Qsd) are common and were deposited, for the majority of cases, in an ice marginal marine environment. Ice-rafted diamictos (Qmd) have a large component of supra-glacial material.

The sequence on Whidbey Island is not unlike other late-Pleistocene glacial marine sequences which were influenced by isostatic processes (Fig. 1). Although some of these deposits are lithologically similar, the important analogy is in the sequence boundaries (Fig. 53). Deposits from coastal Maine (Goldthwait, 1949; Stuiver and Borns, 1975; and Smith, 1981), the St. Lawrence Lowland (Gadd, 1971; Rust and Romanelli, 1975), and East Baffin Island, Arctic Canada (Mode, 1980) are described as having erosional upper surfaces that are overlain by gravel lags. The lags are interpreted by Gadd, Rust and Romanelli as wave washed horizons and by Mode as regressive beach and backshore

deposits. The lower contacts of the sequences are not described in detail but range from erosional, due to subaqueous meltwater, to conformable, with glaciolacustrine deposits. In all cases, however the marine sequence is underlain by the most recent till deposit or erosional horizon.

If the stratigraphic relationships shown in figure 53 can be recognized in other isostatically influenced sequences, of late Pleistocene age, then the application of the model to much older sequences can provide important constraints on paleoglacial reconstructions. Recent models of glacial marine sedimentation have emphasized facies relationships (Powell, 1981; Nelson, 1981) and are primarily conceptual (Edwards, 1978; Drewry and Cooper, 1981). The strength of the model presented in this thesis is that it is based on detailed field evidence and not only accounts for facies variability but also the observed stratigraphic relationships.

CHAPTER 6

Implications to Deglacial History

Although the major goal of this investigation was to provide a model for glacial-marine sedimentation, the results do have some implications to the deglacial history of this part of the Puget Lowland. In particular the deglacial model proposed by Thorson (1980) can be tested by data generated in this study. Thorson's model, although similar to previous workers (Bretz, 1912), called for a catastrophic marine transgression at a time when the Vashon ice sheet retreated past the entrance to the Strait of Juan de Fuca (Admiralty Inlet, Fig. 10). Marine waters entered an isostatically depressed Puget Lowland and the southern edge of Vashon Ice Sheet had a marine margin. According to the model, glacial marine sediments were then deposited as the ice sheet retreated northward. The position of the ice margin at the time of this transgression should be reflected in the sediments as follows. South of the ice margin distal glacial-marine facies should directly overlie terrestrial outwash or glaciolacustrine sediments which were deposited in front of the retreating Vashon ice sheet, more proximal glacial marine facies should overlie such deposits as one approaches the paleo-ice margin. Ice contact or marginal ice deposits should be interbedded with glacial-marine sediment at a position approximating the paleo-ice margin. Regions which were subglacial at the time of the marine

event should be evident by subglacial deposits, or erosional surfaces, which are directly overlain by ice marginal and proximal glacial-marine facies. Normal glacial-fluvial and subaerial deposits would be absent below the marine limit since such regions would be exposed directly to marine conditions as the ice receded.

Although exposures are limited and often times inaccessible, an examination of the facies distribution on Whidbey Island suggests that the southern ice margin may have been in the vicinity of Penn Cove at the time of the marine incursion (Fig. 5). Exposures of Everson age glacial-marine sediment approximately 30 - 35 kms south of Penn Cove, at Lake Hancock and Mutiney Bay-East, consist of pebbly silts and muds (Qps1, Qpm). These distal meltwater facies overlie terrestrial ablation till and meltwater sediments at East-Mutiney Bay (sect. map). Although no dates are available for the underlying sediments they have been interpreted as Vashon (Easterbrook, 1968). Just south of Lake Hancock pebbly silts and muds overlie outwash sands of pre-Vashon age. The exposure is inaccessible but large float blocks revealed that the lower contact of the distal glacial-marine sediments is marked by gravel lags and thin lenses of sandy diamicton. At Coupeville-Lovejoy Point a deltaic sequence of unknown age underlies marine sediments of proximal meltwater origin.

It is only at Penn Cove, and further north, that ice marginal and proximal glacial-marine facies can be found within the section. Their continued presence in exposures further north suggests that the ice margin lay somewhere between Lake Hancock and Penn Cove during the marine incursion. This would have allowed for the deposition of distal glacial-marine sediments to the south and explains the absence of ice marginal marine facies at Lake Hancock and Mutiney Bay. Thorson (1980) however, proposes that the ice margin was a bit farther south at the time of the marine incursion. If the ice margin was at Penn Cove then a major re-entrant in the southern boundary of the ice sheet would have existed in order to block Admiralty Inlet.

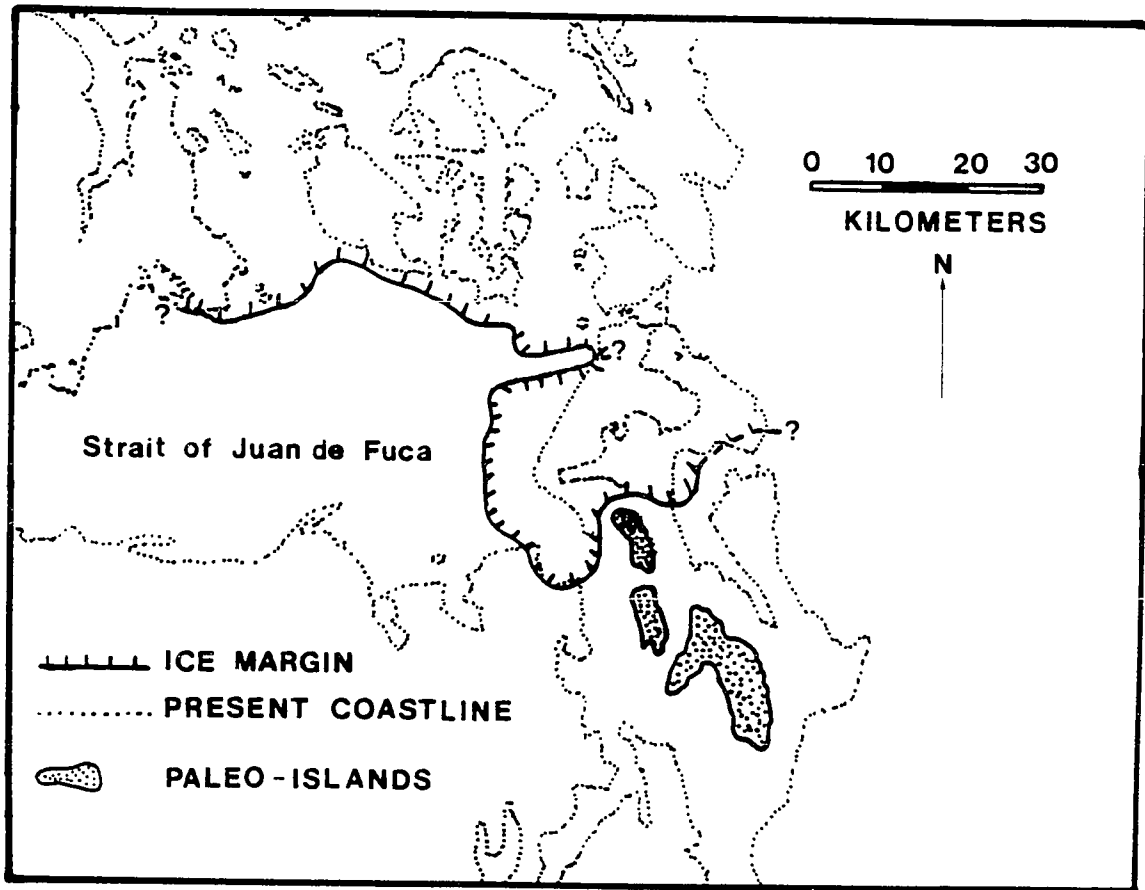
It is interesting to note the difference in topography on Whidbey Island between regions south and north of Lake Hancock (Appendix B). South of Lake Hancock prominent channels have incised into the topography above approximately 76 m (250'). Below this, wave cut terraces interrupt the drainage on the west coast. The terraces are more subdued along the eastern side of the island. To the north, such channels are conspicuously absent even at elevations above 122 m (400'). Although such channels have been reported from Camano Island, Thorson (1980) suggests that the marine limit was much higher to the north than it was on south Whidbey Island. The presence of subaerial channels on

portions of south Whidbey Island suggests that at the time of the marine incursion a series of emergent islands were produced south of the ice margin (Fig. 54). Distal glacial-marine sediments were then deposited in seaways between the islands, namely at East Mutiney Bay and near Lake Hancock. The absence of deeply incised subaerial channels to the north was the result of higher marine limits and the continued presence of glacial ice bordered by marine waters. The deglacial history of the rest of Whidbey Island can be evaluated in terms of both facies relationships and C^{14} dates.

In general, two groups of ages are apparent for glacial marine deposits on Whidbey Island (table 3, Appendix A). Shells from massive diamictons (Qmd facies) in the vicinity of Penn Cove range in age from $11,850 \pm 240$ to $13,010 \pm 170$ (Easterbrook, 1968), with an average date of $12,640 \pm 150$ (Dave Dethier, per. comm.). These ages are significantly younger than shells found in gravel and sand deposits to the north, near Clover Valley (Fig. 6). The dates obtained from these shells range from 13,600 to 13,595 (F. Pessl and D. Dethier, per. comm.). The discrepancy in ages between Penn Cove and Clover Valley suggests one of two possibilities.

First, ice may have receded from Clover Valley earlier, by some 800 years or so. This implies that

Figure 54 Diagrammatic view of Whidbey Island vicinity as it may have appeared approximately 13,000 years B.P. Deposition of distal glacial-marine facies occurred in seaways between islands, which were slowly emerging as isostatic rebound took place.



regional ice flow patterns may not have been strictly north to south; if they were, then recession of ice in Clover Valley would necessitate earlier recession from Penn Cove, which is not supported by the C^{14} dates. Alternatively, recession of ice from Clover Valley may have been related to a calving bay retreat of a westerly flowing ice stream. Bedrock striations and grooves at the western end of Clover Valley, at Rocky Point (Fig. 6), trend to the west (G. Thorsen, per comm.). The presence of westerly flowing ice on northern Whidbey Island is likely since separation of the west flowing Juan de Fuca lobe and the south flowing Puget lobe, of the Vashon ice sheet, is thought to have occurred in this general area (Bretz, 1920). The persistence of ice near Penn Cove until after approximately 12,500 may have been related to partial stagnation or a slower recession of an ice stream which occupied Penn Cove. The glacial marine facies exposed at San de Fuca support a model of slow ice recession from the region. In addition, sediment flow facies (Qsd) appear to have been deposited by flowage to the north, as indicated by beds which dip predominantly to the north and pebble fabric mean orientations to the north-northeast (Fig. 39). But why would ice have receded at Clover Valley sooner than it did at Penn Cove? Perhaps deeper water to the north enhanced the recession of ice streams via calving bay retreat. Calving of the ice streams may have begun to the west, in deep waters of the

Strait of Juan de Fuca. Calving continued towards the east into Clover Valley, which was isostatically depressed to a greater degree than regions to the south. Thorson (1980) called for recession of the Juan de Fuca lobe prior to deglaciation of the central Puget Lowland. It seems likely that ice feeding the Juan de Fuca lobe may have been affected by an early recession of ice within the Strait.

It should be kept in mind that dates obtained from shells at Penn Cove are from facies which are relatively distal. Exposures at San de Fuca-West (see Appendix B) contain 3 to 6 meters of ice marginal sediment flows (Qsd) and meltwater facies (Qpsl, Qpm, and Qsls) below fossiliferous diamictos (Qmd facies) which have yielded C^{14} dates of 13,010 to 11,850 (Easterbrook, 1968). However, a date of $12,640 \pm 150$ was obtained from a diamicton at Coupeville (section C-1, Appendix B) which is overlain by stratified silty sands and clays (Qslc). The silty clays appear to be distal equivalents to submarine outwash facies exposed to the east at Lovejoy Point (see Appendix B). Therefore, melting ice seems to have been in the vicinity of Penn Cove at the time indicated by the C^{14} dates.

It is apparent that additional field work needs to be done in order to test the hypothesis of a Clover Valley ice stream.

CHAPTER 7

Criteria for Distinction between Glacial, Flow and Glacial Marine Diamictos

During this study it was important to make a distinction between glacial-marine diamictos, sediment flows, and tills of the Vashon. This was often relatively easy because the glacial-marine diamictos were fossiliferous, had characteristic weathering, and were less dense than the associated glacial deposits (Easterbrook, 1964). Occasionally, the configuration of deformed lenses of sandy gravel or muddy layers within the Qmd would leave little doubt as to their combined ice-rafted and marine current origin (Fig. 35). For the most part, however, the unit remained quite massive. In the ancient record the distinction of such units within a similar sequence would be much more difficult since lithification, absence of fauna, and limited exposure would eliminate those characteristics which are most useful.

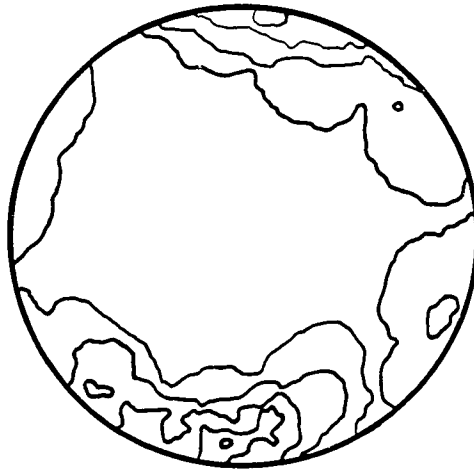
A number of different data was collected with the goal of establishing reliable sedimentologic criteria which can be used to distinguish ice-rafted diamictos from tills or debris flows. The most useful parameter seems to be pebble fabric, which in combination with matrix texture, clast shape, pebble abundance, and bedding character, results in a clear distinction between the various diamictos.

Fabric

Over 20 individual fabric samples consisting of 25 measurements were obtained from Qmd, Qsd and Vashon lodgement till facies. Graphic displays of the data are shown in figures 38, 48, and 55. From the graphic comparison it can be seen that there tends to be greater dispersion of pebble long axis orientations in the Qmd units than in either Qsd or lodgement till facies. These differences are not due to shape influences since all measured stones cluster tightly on the Zingg (axial ratio) diagram in figure 56.

As discussed previously, the random orientation of stones in Qmd units is a reflection of their ice-rafted origin. Several authors have suggested that ice-rafted diamictons may be distinguished by random azimuthal pebble orientations (Edwards, 1978; Evenson et al., 1977; Lavarushin, 1968). Others have noted a preference for near vertical orientations particularly for clasts with centers of gravity near one end (Gibbard, 1980; Griggs and Kulm, 1969; Dalland, 1976). In reality, almost no data have been published, only one sample consisting of 52 measurements was illustrated by Lavarushin (1968). The data collected from ice-rafted marine deposits from Whidbey Island suggest that several factors may influence the orientation of ice rafted stones. The most important factor appears to be the nature of the substrate upon which the stone falls. For massive ice-rafted diamictons (Qmd facies) there appears to

Figure 55 Equal area projection of pebble long axis orientations for samples of lodgement till exposed at Hastie Lake Road-North. Contour interval is 1, 3, 5, 7, and greater than 9% of the data per 4% of projection area. Samples consist of 25 measurements. Data are not rotated to horizontal. Beds dip at approximately 18° to the south.



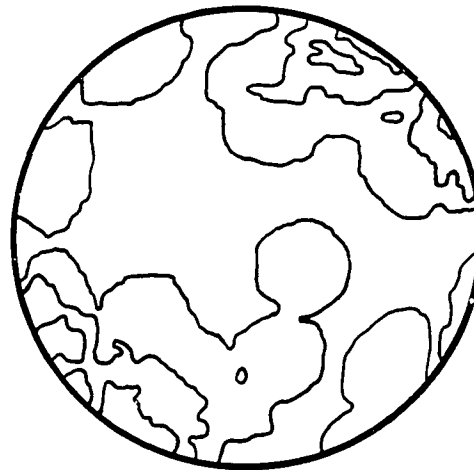
HLN-1

71% Sand



HLN-2

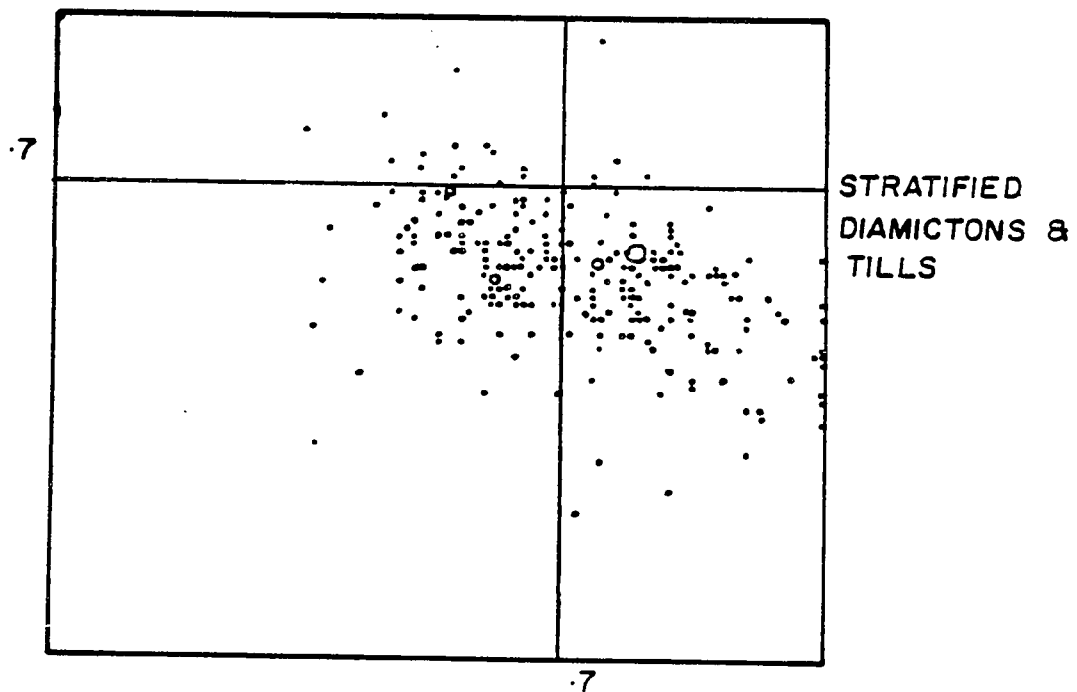
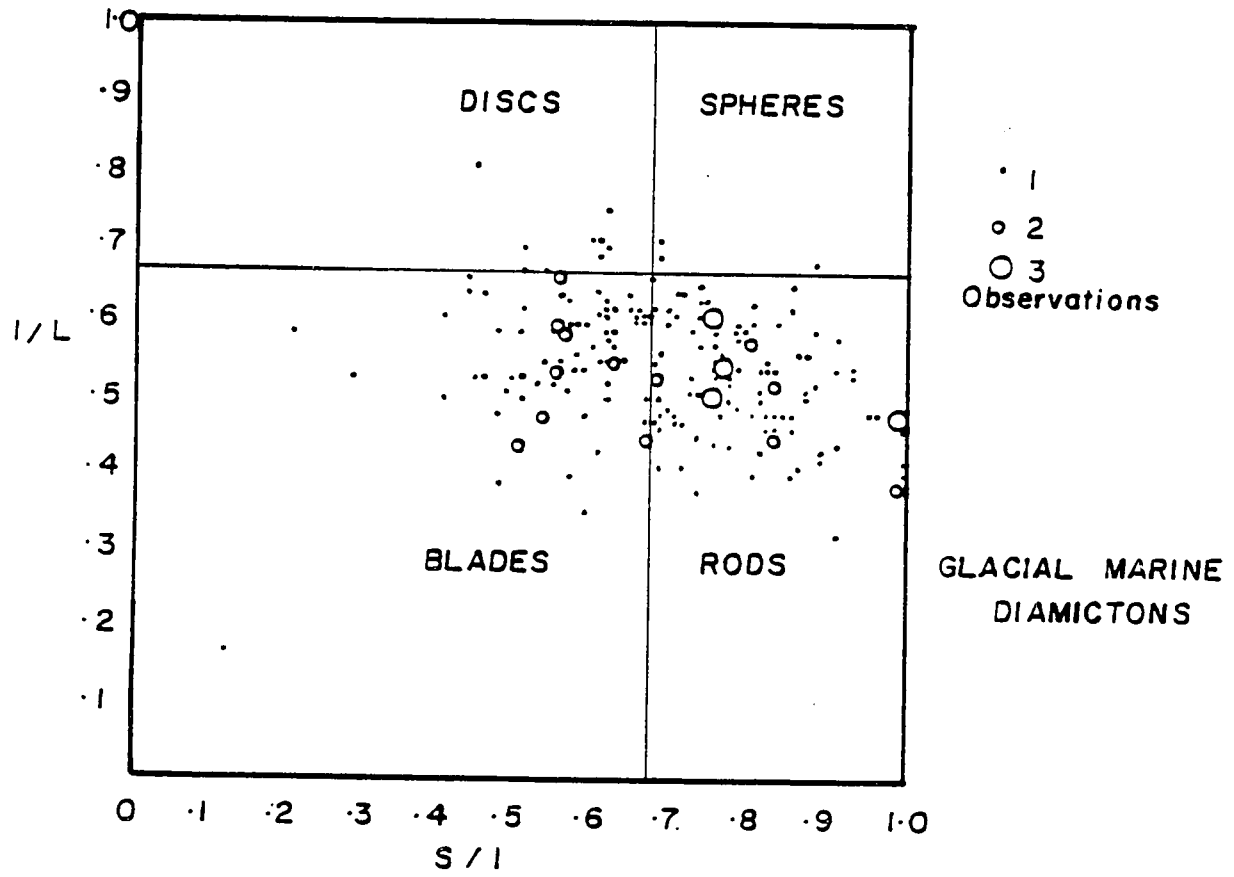
81% Sand



HLN-3

59% Sand

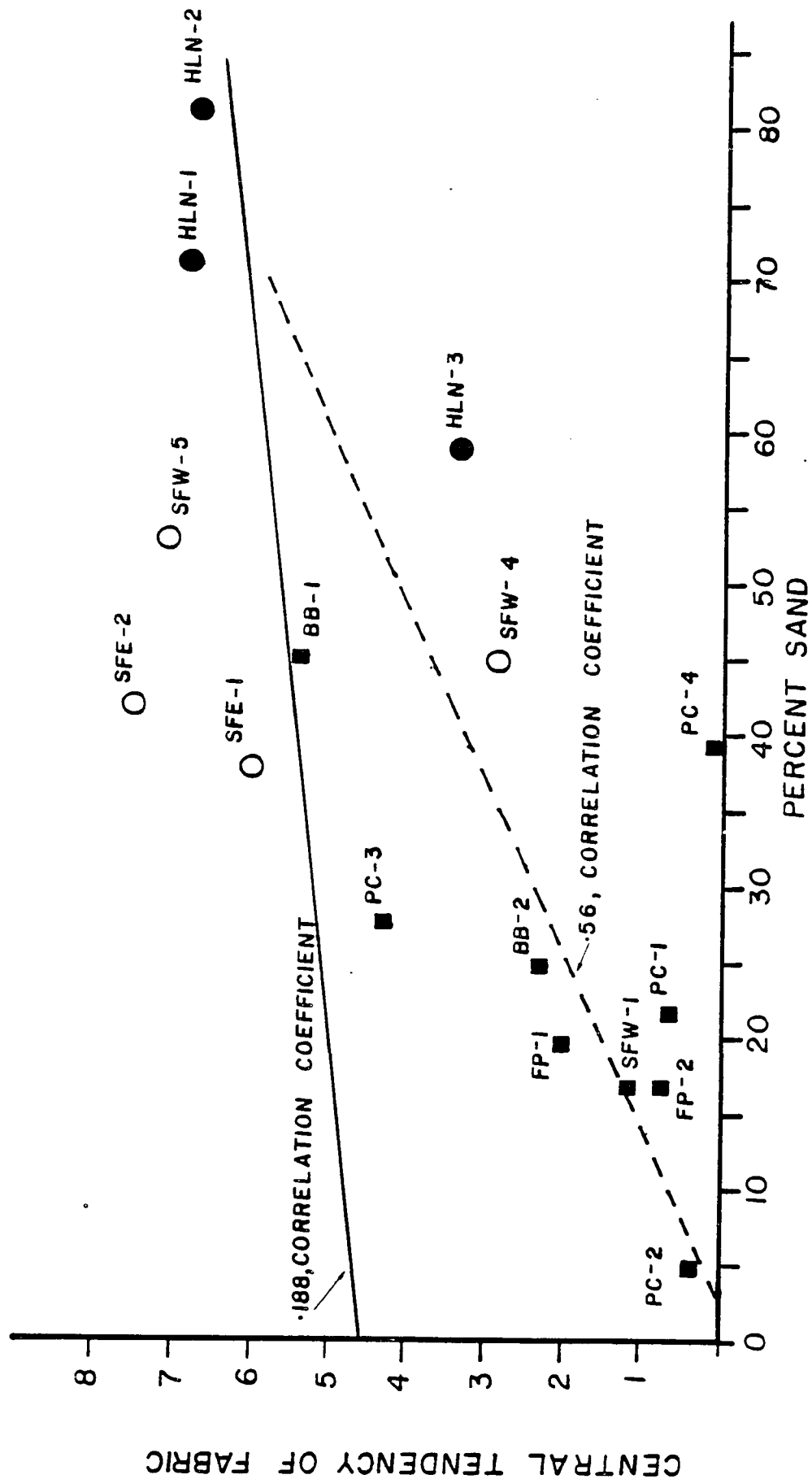
Figure 56 Axial ratio diagram for all clasts
 used in fabric measurements.
 Diagram from Zingg (1935).



be a positive correlation between the degree of central tendency of individual fabrics and percent sand within the matrix (Fig. 57). Highly dispersed fabrics are in association with finer grained diamictos. As was suggested in an earlier section and by Dalland (1976), the strength of the bottom, which is strongly controlled by sediment texture, would control the orientation such that stones hitting a resistant substrate, i.e., sandier bottom, would lay flat and stones hitting a soft substrate, i.e., muddy bottom, would tend to penetrate and become fixed in a random orientation. If this is the case, then a strong horizontal foliation should develop in the coarser grained diamictos. However, coarser grained diamictos are observed to have a strong azimuthal orientation developed upon a weak horizontal foliation (Fig. 48). A transverse maxima is developed in sample BB-Qmd-1. This is difficult to explain with the limited data. There is no evidence of current activity since the grain size distributions are very poorly sorted (Fig. 34). It is interesting to note, however, that the lineations developed in samples BB-Qmd-1 and PC-Qmd-3 parallel, exactly, the local contours (Fig. 39) which would reflect the direction of nearshore tidal currents.

The development of lamination also appears to have influenced the strength of the substrate, as laminated pebbly muds have well developed foliations parallel to bedding (Fig. 48). The partial development of lineations in

Figure 57 Plot of percent sand within matrix and central tendency (percent area of 5% contour interval) of pebble fabric for sediment flow, lodgement till, and ice-rafted diamicton. Least squares regression lines are drawn through the data and values of the correlation coefficient are given. Sample numbers correspond to fabrics in figures 55, 48, and 38.



- ICE RAFTED DIAMICTON
- SEDIMENT FLOW DIAMICTON
- LODGEMENT TILL

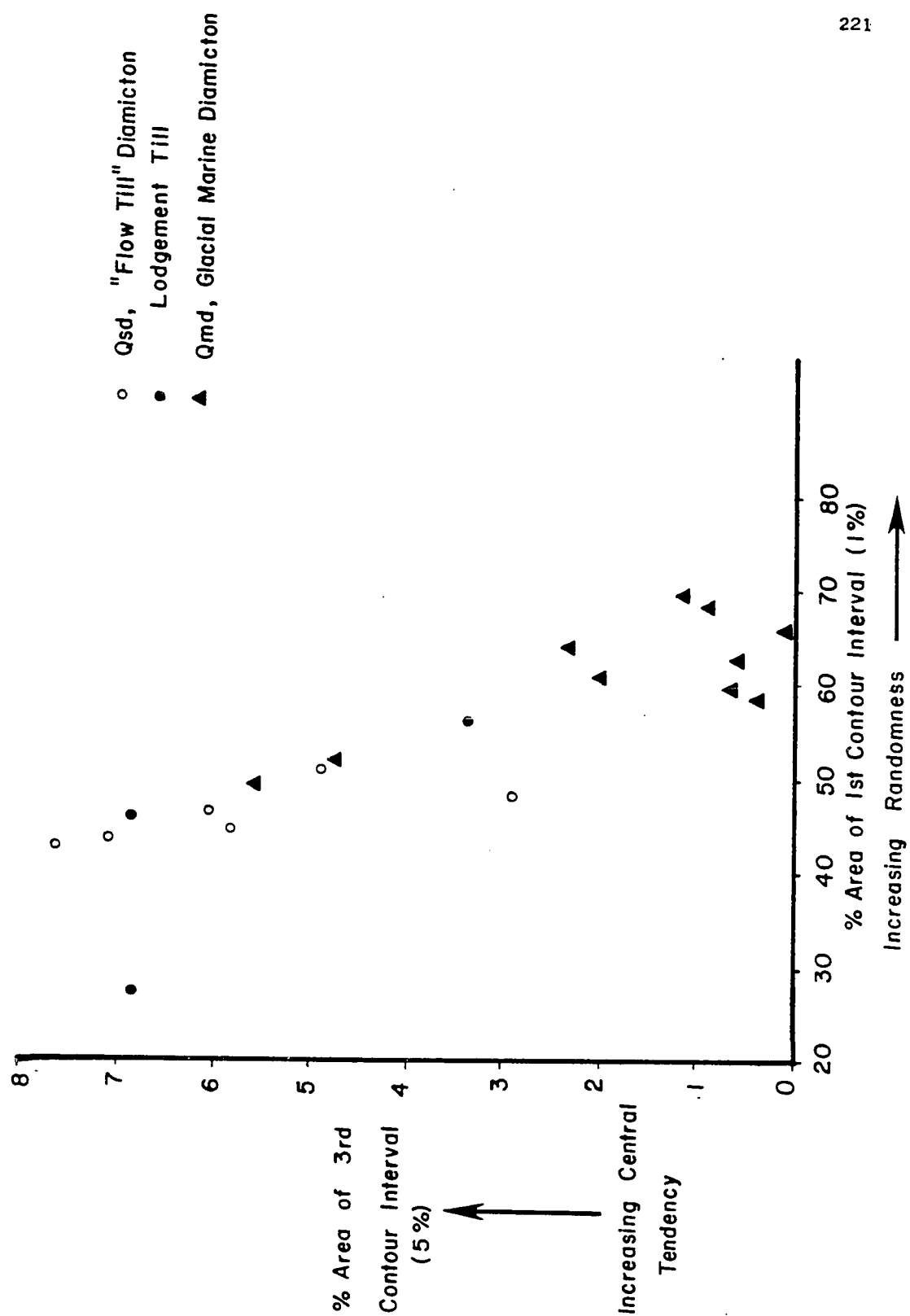
samples ST-Qpml-1 and LB-Qpml-1 is, however, also difficult to explain without additional data.

Observed fabrics for the sediment flow facies (Qsd) and lodgement tills (Figs. 38, 55) are all consistent with previous studies (Lawson, 1979; Lindsay, 1968; Boulton, 1971; and others). In order to compare these fabrics quantitatively, it was decided that the area enclosed by the first and third contour intervals could be used as measures of the randomness and central tendency of individual fabrics. Since the area within a contour reflects both the strength of a mode and foliation development (Lindsey, 1968), it was felt that such measurements would best distinguish glacial-marine diamictos from debris flows and tills. Other measurements, such as two and three dimensional vector strengths will be applied to the data in the future.

Based on the available fabric data (Fig. 58) glacial marine diamictos can be distinguished from sediment flows and tills, with which they superficially resemble, by their higher degrees of randomness and lower central tendencies. However, the variables plotted in figure 58 are not independent measures (correlation coefficient $(r) = -.86$) and, therefore, only serve to demonstrate differences between the diamictos.

A more useful pair of variables, percent sand and central tendency of fabric, are plotted in Figure 57. Although the data are less numerous, they demonstrate that

Figure 58 Plot of central tendency (percent area of 5% contour interval) and randomness (percent area of 1% contour interval) for sediment flows, tills, and glacial-marine diamictons.



the correlation of percent sand with central tendency of the fabric is greater for ice-rafted diamictons ($r = .56$) than it is for flow and till facies ($r = .188$). At the 90% confidence interval the hypothesis that percent sand is related to central tendency of fabric is accepted for glacial-marine diamictons, while it is rejected for flows and tills. This suggests that percent sand is more related to the development of preferred fabrics in ice-rafted deposits than it is for flows or basal tills. These observations should not be interpreted as implying that random fabrics cannot develop in basal tills and sediment flows. In fact, under the right conditions, fabrics similar to those in figure 48 can develop (Lawson, 1979; Shaw, 1979; Boulton, 1976). If a number of data sets are collected for a given diamicton facies that represent a range of textures, then fabrics can distinguish between sediment flow, till, and ice-rafted diamicton.

Texture

A number of authors have relied upon textural data to distinguish diamictons of debris flow, glacial, and glacial marine origin (Landim and Frakes, 1968; Kurtz and Anderson, 1979; Anderson et al., 1980a, and others). Textural criteria alone cannot be used to distinguish the various massive diamictons on Whidbey Island. Graphic displays of mean grain size versus sorting demonstrate some

overlap between the different diamicton facies as do sand, silt, clay ratios (Fig. 59). On the average, glacial marine diamictons appear to be finer grained than either associated sediment flows or basal tills. This is consistent with the results of Lavarushin (1968). However, as can be seen from figure 59, there are some exceptions.

Kurtz and Anderson (1979) and Anderson and others (1980) cite textural homogeneity as one means of distinguishing glacial-marine diamictons from debris flows and basal tills collected in piston cores from the Antarctic continental margin. However, individual units of glacial-marine diamicton from Whidbey Island are just as homogeneous vertically as tills and sediment flows (Fig. 60). The greatest difference seems to be that between sites, variability of texture is greater for flows and tills than it is for the glacial-marine diamictons. This is understandable as glacial-marine diamictons, of the Qmd facies, were deposited under approximately the same conditions (water depth, currents, etc.) over a widespread area. Individual sediment flows, although comprising a facies that is equally widespread, reflect localized conditions such as source, water content, and transport distance. Samples of basal till are few, but the textural variability, even within a single sequence of multiple lodgement till, is great (Fig. 59). The distribution of Vashon basal till facies on Whidbey Island is very

Figure 59 Plot of mean grain size (in PHI units) versus sorting for samples of Qpm, Qpsl, Qsd, Qmd, and till facies.

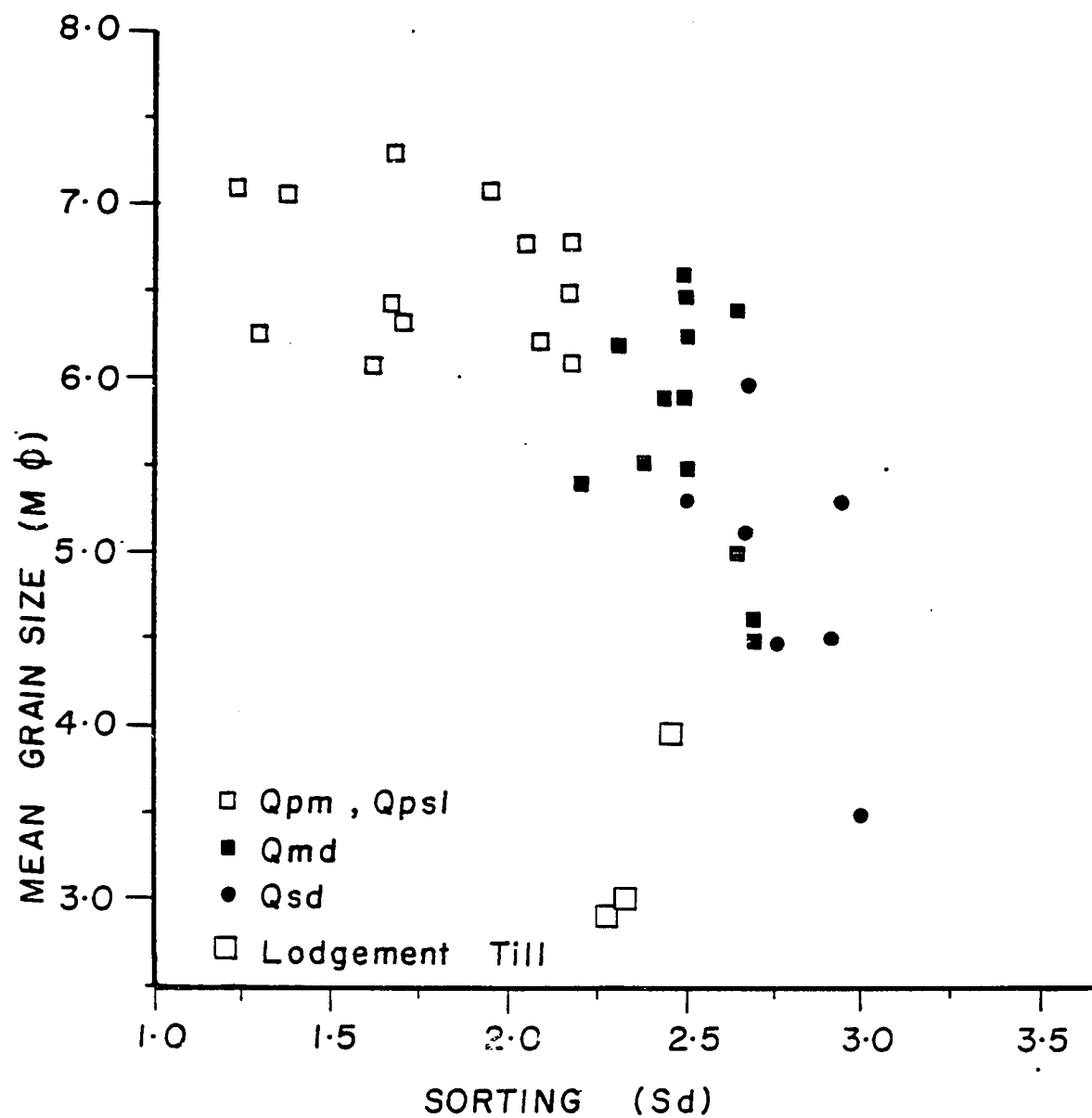
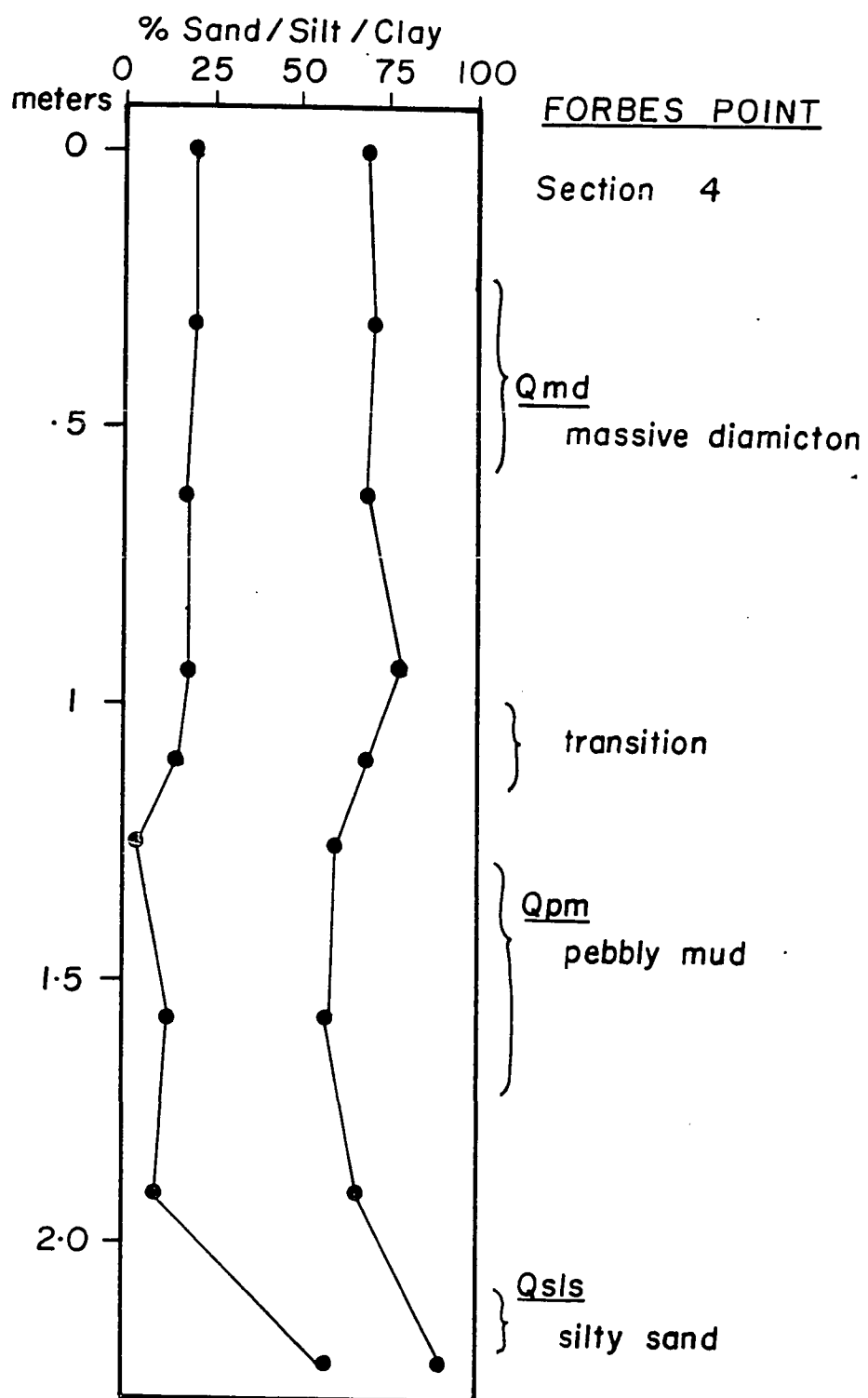


Figure 60 Vertical variation in sand, silt
 clay percentages for transition
 from pebbly silt, mud, and
 massive, fossiliferous diamicton
 for section FP-4. Note textural
 homogeneity for massive diamicton
 (Qmd).



limited, unlike other glacial-marine settings (Anderson et al., 1980a). Therefore, it may also reflect a strong control of local factors (substrate, basal ice regime, etc.) upon deposition.

Anderson and others (1980a) also distinguish between glacial-marine sediments and basal tills using individual grain size frequency distributions, most importantly the complete lack of sorting in basal tills as opposed to subtle sorting in glacial marine sediments. In their studies, the presence of a current derived mode (fine silt or clay) in an otherwise poorly sorted grain size distribution was evidence for a glacial-marine origin. Massive glacial-marine diamictos from Whidbey Island show little evidence of such current derived modes (Fig. 34). Anderson and others (1980) do recognize certain transitional diamictos that lack the stratification and grain size characteristics of their glacial-marine sediments, but which are similar in structure and texture to basal tills. They believe such units represent glacial-marine sediments deposited near the grounding line of ice shelves, where ice rafting is locally intense.

In summary, grain size of an individual unit cannot be used to distinguish glacial-marine diamictos from diamictos of either sediment flow or basal till origin. However, textural variability of diamictos of the same facies but at different exposures is greater for sediment flows (Qsd) than

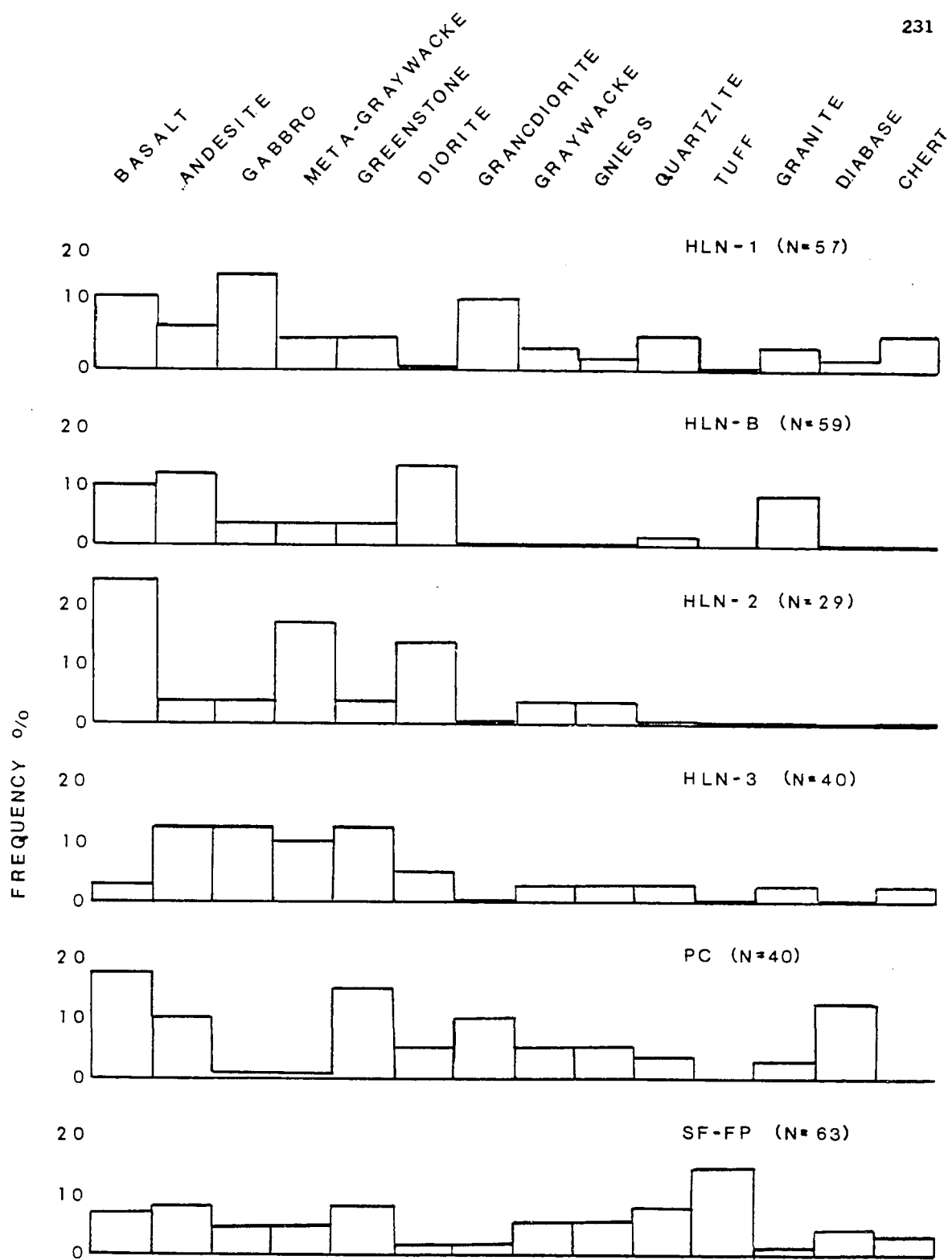
it is for glacial-marine sediments.

Pebble Shape

A total of 271 pebble sized clasts were sampled from glacial-marine diamictons and basal tills. Measurements of sphericity and roundness (Krumbein, 1941) are graphically displayed in figure 49. Samples from glacial-marine diamictons have a greater proportion of clasts with lower roundness values than samples from lodgement till. The lithology of these samples is displayed in figure 61. From this data it appears as though there is no relationship between shape indices and lithology. As a comparison, cobbles collected along the beach in front of till exposures, where samples HLN-1,2,3 were collected, are plotted in figure 49. Again, the lithologies are not substantially different but the beach cobbles have significantly more clasts of higher roundness and sphericity. These data demonstrate the effectiveness with which shape is acquired by clasts in dynamic environments, in this case swash zone abrasion has altered the shapes of stones derived from the till.

As discussed by Drake (1972), Boulton (1978), and Domack and others (1980), the roundness of stones in a glacial environment can, if other variables are equal, be related to transport modes within a glacier system. Lower roundness values suggest passive, supraglacial or englacial, transport

Figure 61 Pebble lithology histogram for
samples collected from Qmd,
lodgement till, and modern beach.
Lithologies shown are only the major
components for each sample.



while medial to high roundness suggest active, basal, transport. Glacial abrasion along the ice-sediment interface is the active force in producing the higher roundness values. The data in figure 49, along with the lower abundance of striations, support the model of supraglacial debris as a major source of ice-rafted material for the Qmd facies. Therefore, clast shape may be useful in discriminating between till and glacial-marine diamicton within the late Pleistocene sequence on Whidbey Island. However, this is possible only because mechanisms of ice rafting appear to have involved significant proportions of supraglacial debris. In other settings, such as the Antarctic, glacial-marine sediments may have more limited ice-rafted sources and the distinction between basal till and glacial-marine diamicton, based on clast shape, may not hold (Domack et al., 1980).

Pebble Abundance

The abundance of greater than 2 cm sized stones within exposures of basal till, sediment flow, and glacial-marine sediment are displayed in figure 17. These data represent measurements taken along a single exposure of a particular facies at intervals which ranged from 15 - 20 meters. A very pronounced trend in the data is the great variability in pebble abundance for the sediment flow (Qsd) facies. Some samples of Qsd do, however, have equivalent pebble

abundances to pebbly muds (Qpm) and ice-rafted diamictos (Qsd). Pebbly muds, in general, have fewer stones/m² than tills or glacial marine diamictos. Glacial marine diamictos exhibit identical pebble abundances to those lodgement tills sampled.

The data suggest that, if a number of measurements are collected from within a facies, it should be possible to distinguish sediment flow diamictos from basal till or ice-rafted diamictos. The sediment flows will exhibit higher standard deviations from a mean value and individual flows may contain a greater number of stones/m².

Bedding Relationships

If exposures are adequate, on the order of .5 km, it should be possible to distinguish lodgement till facies from ice-rafted and sediment flow diamictos using contact and bedding relationships. In addition, observations of small scale (1 - 2 m) interbedded relationships can provide some insight.

In a single exposure, sediment flow facies (Qsd) can be seen to consist of many distinct units which along strike usually overlap, cut-out, or merge into one another (see maps in Appendix). In some instances actual flow lobes can be preserved (Fig. 15). Lodgement till sequences also consist of individual units, however, the units themselves are generally continuous and other units are stacked vertically

upon one another (Fig. 62). Upper and lower contacts are always sharp and planer in lodgement tills while sediment flows often exhibit irregular or convex upper contacts (Fig. 15).

Small lenses of stratified gravel, sand, or silt can be found in all three diamicton facies. The bounding contacts of these stratified lenses are unique for two of the facies. In lodgement till sequences well stratified gravels, sands, and silts are commonly interbedded between individual lodgement units (Fig. 62). Their lower contacts vary from sharp and planer to irregular, but upper contacts are always sharp and planer. Sheared structures consisting of fine silt and clay are also common.

Lenses of sorted material in ice-rafted diamictons are common but are distinctly different from lenses found within lodgement tills. Lower contacts may be planer but most often are irregular, exhibiting load style deformation (Fig. 35). Upper contacts are always irregular or convex. A similar structural arrangement of individual lenses can be found within Qsd facies, and thus are not as useful in distinguishing flows from ice-rafted diamictons. Lodgement tills, being a product of the subglacial environment exhibit bedding characteristics unique from either ice-rafted or sediment flow diamictons. The planer nature of bounding contacts can be used to distinguish them from both ice-rafted and flow diamictons. Deposition of sediment flow facies

Figure 62 Photograph of lodgement till sequence
exposed at Hastie Lake Road-North.
Note sheared interbeds of sand and
silt and depositional slopes of up
to 18° to south.



occurred as many separate flows and resulted in lateral interbedding of units and preservation of flow fold geometries. These characteristics serve to distinguish them from ice-rafted and lodgement till facies.

No single criterion can serve to distinguish ice-rafted diamictons from either lodgement tills or sediment flows 100% of the time. The positive correlation between sand content and central tendency of pebble fabric (for Qmd) may provide more discriminating value than any other combination of measurements and thus are the most valuable data to collect where exposures are limited. Regional tectonics, however, should be taken into consideration as structural deformation may overprint depositional fabrics (Lindsay et al., 1970; Robertson, 1971).

If exposures are fairly continuous, measurements of pebble abundance and sand, silt, clay ratios should provide useful data. Units which exhibit great variability with regard to the above are most likely of sediment flow origin. Pebble shape may not always provide adequate information, particularly where sources of ice-rafted material are dominated by basal debris.

If detailed mapping of units is possible, variable bedding and contact relationships may provide definitive proof as to the origin of a sediment flow facies. Important

characteristics to note would be the nature of interbedded sand or gravel lenses. Sharp planer upper contacts are most characteristic of lodgement till facies. Table 5 in the Appendix summarizes these criteria.

CONCLUSIONS

Late Pleistocene glacial-marine sediments on Whidbey Island consist of six major lithofacies which were deposited in contact with, proximal to, and distal to a grounded ice sheet. The major controls upon sedimentation included proximity to both the ice front and sources of meltwater input, as well as the nature of the ice margin with regard to calving versus ablation. Sedimentation rates were extremely rapid, particularly for submarine meltwater facies, and most of the sequence was deposited prior to significant rebound, in water depths which ranged from 75 to 15 meters. Striking similarities of lithology and facies development strongly suggest that this sequence has a climatic analogy with the present day Gulf of Alaska.

The sequence is bounded by unconformities consisting of a lower surface of glacial or meltwater erosion and an upper surface of wave erosion associated with the late Pleistocene-early Holocene regression. These unconformable stratigraphic boundaries and the facies relationships serve to separate the isostatic glacial-marine sequence from correlative nearshore and offshore glacial-marine sequences and the terrestrial glacial section.

Ice marginal glacial-marine facies are just encountered at, and north of, Penn Cove while only distal facies are exposed to the south. This suggests that a highly irregular ice margin was in existence at the time marine waters first

flowed into the basin.

A combination of pebble fabric and grain size analysis can distinguish between massive ice-rafted diamictons, sediment flows, and basal tills. For glacial-marine diamictons a reliable, positive correlation exists between the central tendency of a fabric and % sand within the matrix. No such relationship has been found for the other diamicton facies. Measurements of pebble abundance, matrix grain size, and bedding thickness indicate extreme lateral variability is characteristic of sediment flow facies when compared to basal till or glacial-marine diamicton. Pebble shapes for basal tills and ice-rafted diamictons are significantly different and reflect contrasting modes of debris transport. It is felt that, with the application of the quantitative criteria listed above, a reliable distinction can be made between diamictons or diamictites of ice rafted, mass flow, or glacial origin.

No other rocks can tell us as much about the earth's paleoclimatic history as can glacial and glacial marine deposits. In order to gain the most from the study of such sequences, we must thoroughly apply our knowledge of recent analogs. This research has hopefully added some understanding of a truly unique sedimentary environment.

BIBLIOGRAPHY

- Alley, N.F., 1979, Middle Wisconsin Stratigraphy and Climatic Reconstruction, Southern Vancouver Island, British Columbia: Quaternary Research 11, 213-239.
- Anderson, F.E., 1968, Seaward Terminus of the Vashon Continental Glacier in the Strait of Juan de Fuca: Marine Geology, v. 6, pp. 419-438.
- Anderson, J.B. and Kurtz, D.D., 1979, RUASA: An automated sediment analysis system: Jour. Sed. Petrology, vol. 49, No. 2, pp. 625-627.
- Anderson, J.B., Kurtz, D.D., and Weaver, F.M., 1979, Sedimentation on the Antarctic continental slope: in Doyle, L. and Pilkey, O. (eds.), Geology of continental slopes. SEPM Spec. Pub. No. 27, pp. 265-283.
- Anderson, J.B., Kurtz, D.D., Domack, E.W., and Balshaw, K.M., 1980a, Glacial and glacial marine sediments of the Antarctic continental shelf: Journal of Geology, vol. 88, pp. 399-414.
- Anderson, J.B., Domack, E.W., and Kurtz, D.D., 1980b, Observations of sediment-laden icebergs in Antarctic waters; implications to glacial erosion and transport: Jour. of Glaciology 25(93):387-396.
- Andrews, J.T., and Smith, D.I., 1970, Till fabric analysis; methodology and local and regional variability (with particular reference to the North Yorkshire cliffs): Quart. Jour. Geol. Soc. London, v. 125, pp. 503-542.
- Armstrong, J.E., 1981, Post-Vashon Wisconsin Glaciation, Fraser Lowland, British Columbia, Geol. Survey Canada Bulletin 322, 33 p.
- Armstrong, J.E., and Brown, W.L., 1954, Late Wisconsin marine drift and associated sediments of the lower Fraser Valley, British Columbia, Canada: Bull. Geol. Soc. Am., v. 65, pp. 349-364.

- Armstrong, J.E., Crandell, D.R., Easterbrook, D.J., and Noble, J.B., 1965, Late Pleistocene stratigraphy and chronology in southwestern British Columbia and northwestern Washington: *Geol. Soc. America Bull.*, v. 76, pp. 321-330.
- Balzarini, M.A., 1981. Paleoeecology of Everson-age glacialmarine drifts in Northwestern Washington and Southwestern British Columbia: unpubl. M.S. thesis, Univ. of Washington, March, 1981, pp. 110.
- Banerjee, I., and McDonald, B.C., 1975, Nature of esker sedimentation: In *Glaciofluvial and glaciolucustrine sedimentation* (A.V. Jopling and B.C. McDonald, Eds.) Society of Economic Paleontologists and Mineralogist, Spec. Publ. n. 23, pp. 132-154.
- Barret, P.J., 1980, The shape of rock particles, a critical review: *Sedimentology*, v. 27, pp. 291-303.
- Barrs, M.S. and Williams, G.L., 1973, Palynology and nannofossil processing techniques: *Geol. Surv. Can. Pap.*, pp. 73-26.
- Bates, C.C., 1953, Rational theory of delta formation: *Bull. Am. Ass. Petrol. Geol.*, v. 37, pp. 2119-2162.
- Bird, J.B., 1967, The physiography of Arctic Canada, with special reference to the area south of Parry Channel: Johns Hopkins Press, 336 pp.
- Boulton, G.S., 1968, Flow tills and related deposits on some Vestspitsbergen glaciers: *Jour. of Glaciol.*, v. 7(51), pp. 391-412.
- _____. 1971, Till genesis and fabric in Svalbard, Spitsbergen. In, *Till: A symposium* (R.P. Goldthwait, ed.): Columbus: Ohio State Univ. Press, pp. 41-72.
- _____. 1976, The origin of Glacially Fluted Surfaces-Observations and Theory: *Jour. of Glaciology*, vol. 17, No. 76
- _____. 1978, Boulder shapes and gram-size distributions of debris as indicators of transport paths through a glacier and till genesis: *Sedimentology* (1978), 25, 773-799.

- Bretz, J.H., 1913, Glaciation of the Puget Sound Region: Washington Geological Survey Bulletin 8, 1-244.
- _____. 1920, The Juan de Fuca lobe of the Cordilleran ice sheet: *Journal of Geology*, v. 28, pp. 333-339.
- Broster, B.E., Dreimanis, A., and Hicock, S.R., 1980, Multiple flow and support mechanisms in subaquatic debris flows: *Geol. Soc. Amer. Abstracts with program*, Annual Meeting, Atlanta, pp. 392-393.
- Carey, S.W., and Ahmad, N., 1961, Glacial marine sedimentation: In Raasch, G. (ed.), *First Int. Symp. on Arctic Geology*, Proceedings, v. 2, Univ. Toronto, pp. 865-894.
- Carlson, P.R., Molnia, B.F., Kittelson, S.C., and Hampson, J.C., Jr., 1977, Distribution of bottom sediments on the continental shelf, northern Gulf of Alaska: U.S.G.S. map MF-876.
- Clague, J.J., Armstrong, J.E. and Mathews, W.H., 1980, Advance of late Wisconsin Cordilleran ice sheet in southern British Columbia since 22,000 years B.P.: *Quaternary Research*, v. 13, no. 3, pp. 322-326.
- Cohen, J.M., 1981, Mechanisms for the production of subaquatic mass flows in a high energy ice marginal deltaic environment and problems with the identification of flow tills: INQUA comm. on genesis and lithology of Quaternary deposits. Abstracts of meeting Wyoming and Idaho, Aug. 20-30, 1981.
- Cole, M.L., 1979, Nearshore glacialmarine sedimentation, based on late Pleistocene deposits of the Puget Lowlands, Washington and British Columbia: Unpublished M.A. thesis, Rice University, Houston, Texas.
- Crandell, D.R., Mullineaux, D.R., and Waldron, H.H., 1958, Pleistocene sequence in southeastern part of the Puget Sound Lowland, Washington: *Amer. Jour. of Science*, vol. 256, pp. 384-397.
- Croll, T.C., 1980, Stratigraphy and depositional history of the Deming sand in northwestern Washington: unpubl. M.S. thesis, Univ. of Washington, 59 pp.
- Crowell, J.C., 1957, Origin of pebbly mudstones: *Geol. Soc. Am. Bull.*, v. 72, pp. 1289-1306.

- Curry, J.R., 1965, Late Quaternary History, Continental shelves of the United States: in The Quaternary of the United States, pp. 723-736, ed. H.E. Wright Jr. and D.G. Frey, Princeton, New Jersey: Princeton University Press.
- Dalland, A., 1976, Erratic clasts in the Lower Tertiary deposits of Svalbard-evidence of transport by winter ice: Norsk Polarinstitutt Arbök, pub. 1977, pp. 151-165.
- Dawson, G.M., 1887, Report on a geological examination of the northern part of Vancouver Island and adjacent coasts: Canada Geol. Survey Ann. Rept. 1886, v. 2, pt. B, 107 pp.
- Domack, E.W., Anderson, J.B., and Kurtz, D.D., 1980, Clast shape as an indicator of transport and depositional mechanisms in glacial marine sediments: George V continental shelf, Antarctic: Jour. Sed. Petrol., v. 50, no. 3, pp. 813-820.
- Domack, E.W., 1982, Sedimentology of glacial and glacial marine deposits on the George V-Adelie continental shelf, East Antarctica: Boreas, No. 1, pp. 79-97.
- Drake, L.D., 1972, Mechanisms of clast attrition in basal till: Geol. Soc. Amer., Bull., v. 83, pp. 2159-2165.
- Dreimanis, A., 1981, Quaternary glaciations: implications for the interpretation of Proterozoic glacial deposits: International Proterozoic Symposium, Abstracts, Univ. Wisconsin-Madison, May 18-21, unpubl.
- Drewry, D.J., 1979, Late Wisconsin reconstruction for the Ross Sea region, Antarctica: Jour. of Glaciol., v. 24, n. 90, Symposium on Dynamics of large ice masses.
- Drewry, D.J., and Cooper, A.P.R., 1981, Processes and models of Antarctic glaciomarine sedimentation: Annals of Glaciology, v. 2, pp. 117-122.
- Easterbrook, D.J., 1962, Pleistocene geology of the northern part of the Puget Lowland, Washington: unpubl. Ph.D. dissert., Univ. of Washington, 106 pp.
- _____. 1963, Late Pleistocene glacial events and relative sea level changes in the northern Puget Lowland: Geol. Soc. Amer. Bull., v. 7, pp. 1465-1484.

- Easterbrook, D.J., 1968, Pleistocene Stratigraphy of Island County, Washington: Wash. State Div. of Water Resources Bull., 25, pp. 1-34.
- . 1969, Pleistocene chronology of the Puget Lowland and San Juan Islands, Washington. Geol. Soc. Amer. Bull., 80, 2273-2286.
- Easterbrook, D.J., Crandell, D.R., and Leopold, E.B., 1967, Pre-Olympia Pleistocene Stratigraphy and chronology in the central Puget Lowland, Washington: Geol. Soc. Amer. Bull., v. 78, pp. 13-20.
- Easterbrook, D.J., and Rutter, N.W., 1981, Amino acid ages of Pleistocene glacial and interglacial sediments in Western Washington: Geol. Soc. of America, Abstracts with programs, vol. 13, no. 7, Cincinnati.
- Easterbrook, D.J., Biggs, N.D., and Westgate, J.A., and Gorton, M.P., 1981, Age of the Salmon Springs Glaciation in Washington, Geology, v. 9, pp. 87-93.
- Edwards, M., 1978, Glacial environments. In, Sedimentary environments and facies (H.G. Reading, ed.): Oxford, Blackwells, pp. 416-438.
- Evenson, E.B., Dreimanis, A., and Newsome J.W., 1977, Sub-aquatic flow tills: a new interpretation for the genesis of some laminated till deposits. Boreas, vol. 6, 1977, pp. 115-133.
- Fulton, R.J., Armstrong, J.E., and Fyles, J., 1976, Discussion: Stratigraphy and palynology of late Quaternary sediments in the Puget Lowland, Washington: Discussion and reply. Geol. Soc. Amer. Bull., v. 87, pp. 153-155.
- Gadd, N.R., 1971, Pleistocene geology of the St. Lawrence Lowland, pp. 153, Mem. geol. surv. Brch. Can., 359.
- Gibbard, P., 1980, The origin of stratified Catfish Creek till by basal melting, Boreas, vol. 9, pp. 71-85.
- Gibbs, R.J., Matthews, M.D., and Link, D.A., 1971, The relationship between sphere size and settling velocity: Jour. Sed. Petrology, v. 41, pp. 7-18.
- Gilbert, R., 1979, Observations of the sedimentary environments of fjords on Cumberland Peninsula, Baffin Island: In Fjord Oceanography (H.J. Freeland, D.M. Farmer, and C.D. Levings, eds.) Plenum, New York, pp. 633-338.

- Goldthwait, L., 1949, Clay survey, 1948: Maine Development Commission Report of State Geologist 1947-1948, pp. 63-69.
- Goldthwait, R.P., 1951, Development of end moraines in east-central Baffin Island: Jour. of Geology, v. 59, pp. 567-577.
- Gow., A.J., 1971, Depth-time temperature relationships of ice crystal growth in polar glaciers: US Army Cold Reg. Res. Engng. Lab. Res. Rept. 300, 18 pp.
- Griggs, G.B., and Kulm, L.D., 1969, Glacial marine sediments from the Northeast Pacific: Jour. Sed. Petrol., v. 39, no. 3, pp. 1142-1148.
- Hambrey, M.J. and Harland, W.B., 1981, The Earth's Pre-Pleistocene glacial record. Cambridge Univ. Press, 1024 pp.
- Hampton, M.A., 1972, The role of subaqueous debris flow in generating turbidity currents. Jour. Sed. Petrol., v. 42, pp. 775-793.
- Hansen, H.P. and Mackin, J.H., 1949, A pre-Wisconsin forest succession in the Puget Lowland, Washington: Am. Jour. Sci., v. 247, pp. 833-855.
- Hansen, B.S. and Easterbrook, D.J., 1974, Stratigraphy and Palynology of Late Quaternary Sediments in the Puget Lowland, Washington: Geol. Soc. Amer. Bull., v. 85, pp. 587-602.
- Harland, W.B., Herod, K., and Krinsley, D.H., 1966, The definition of tills and tillites: Earth Sci. Rev., v. 2, pp. 225-256.
- Hartshorn, J.H., 1958, Flow till in southeastern Massachusetts: Geol. Soc. Amer. Bull., v. 69, pp. 477-482.
- Heusser, C.J., and Heusser, L.E., 1981, Palynology and paleotemperature analysis of the Whidbey Formation, Puget Lowland, Washington, Can. Jour. of Earth Sci., v. 18, pp. 136-149.
- Hicock, S.R., and Armstrong, J.E., 1981, Coquitlam Drift: a pre-vashon Fraser glacial formation in the Fraser Lowland, British Columbia: Can. Jour. of Earth Science, v. 18, no. 9, pp. 1443-1451.

- Hicock, S.R., Dreimanis, A., and Broster, B.E., 1981, Submarine flow tills at Victoria, British Columbia, v. 18, no. 1, pp. 71-80, *Can. Jour. Earth Sci.*
- Hoskin, C.M., and Burrell, D.C., 1972, Sediment transport and accumulation in a fjord basin, Glacier Bay, Alaska: *Jour. of Geology*, v. 80, pp. 539-551.
- Hughes, T.J., 1981, Numerical reconstruction of Paleo-Ice sheets: in Denton, G.H. and Hughes, T.J., eds., *The Last Great Ice Sheets*, Wiley, New York, pp. 222-260.
- Johnston, W.A., 1923, Geology of Fraser river delta map-area: *Geol. Surv. Canada*, memoir 135, 87 pp.
- Kellogg, T.B., Truesdale, R.S., and Osterman, L.E., 1979, Late Quaternary extent of the West Antarctic ice sheet: New evidence from Ross Sea cores: *Geology*, v. 7, pp. 249-253.
- Kranck, K., 1973, Flocculation of suspended sediment in the sea: *Nature, Lond.*, v. 246, pp. 348-350.
- _____. 1975, Sediment deposition from flocculated suspensions: *Sedimentology*, v. 22, pp. 111-123.
- Krumbein, W.C. (1941) Measurement and Geological Significance of shape and roundness of sedimentary particles: *Jour. Sed. Petrol.*, 11, 64-72.
- Krumbein, W.C., and Pettijohn, F.J., 1938, *Manual of sedimentary petrology*, 549 pp., New York: Appleton-Century-Crofts, Inc.
- Kurtz, D.D., and Anderson, J.B., 1979, Recognition and sedimentologic description of recent debris flow deposits from the Ross and Weddell Seas, Antarctica: *Jour. Sed. Petrology*, v. 49, pp. 1159-1170.
- Landim, P.M.B., and Frakes, L.A., 1968, Distinction between tills and other diamictos based on textural characteristics: *Jour. Sed. Petrol.*, v. 38, pp. 1213-1223.
- Lawson, D.E., 1979, Sedimentologic analysis of the western terminus region of the Matanuska Glacier, Alaska, CREEL report no. 79-9, Hanover, N.H., 112 pp.
- _____. 1981, Distinguishing characteristics of diamictos at the margin of the Matanuska glacier, Alaska: *Annals of Glaciology*, v. 2, pp. 78-84.

- Lavrushin, Y.A., 1968, Features of deposition and structure of the glacial marine deposits under conditions of a fjord coast (based on the example of Spitsbergen) *Litologiya i Poleznye Iskopaemye* 3, 63-79.
- Lindsay, J.F., 1968, The development of clast fabric in mudflows: *Jour. Sed. Petrol.*, v. 39, n. 4, pp. 1242-1253.
- Lindsey, D.A., 1970, Glacial marine sediments in the Precambrian Gowganda formation at Whitefish Falls, Ontario (Canada): *Paleo.*, *Paleo.*, *Paleo.*, v. 9, pp. 7-25.
- Lindsay, J.F., Summerson, C.H., and Barrett, P.J., 1970, A long-axis clast fabric comparison of the Squantum "Tillite" Massachusetts and the Gowganda Formation, Ontario: *Jour. Sed. Petrology*, v. 40, pp. 475-479.
- Lorius, C., Merlivat, L., Jouzel, J., and Pourchet, M., 1979, A 30,000 year isotope climatic record from Antarctic ice, *Nature*, v. 280, pp. 644-648.
- Marcussen, I., 1973, Studies on flow till in Denmark: *Boreas*, v. 2, pp. 213-231.
- Mathews, W.H., Fyles, J.G., and Nasmith, H.W., 1970, Post-glacial crustal movements in southwestern British Columbia and adjacent Washington State: *Canadian Jour. of Earth Sciences*, v. 7, pp. 690-702.
- May, J.P., 1981, $CHI(x)$: A proposed standard parameter for settling tube analysis of sediments: *Jour. of Sed. Petrol.*, v. 51, n. 2, pp. 607-610.
- May, R.W., 1977, Facies model for sedimentation in the glaciolacustrine environment: *Boreas*, v. 6, pp. 175-180.
- May, R.W., and Dreimanis, R., 1976, Compositional variability in tills: In *Glacial Till* (R.F. Legget, ed.) pp. 99-121.
- Mayers, I.R., and Bennett, L.C., Jr., 1973, Geology of the Strait of Juan de Fuca: *Marine Geology*, v. 15, pp. 89-117.
- Middleton, G.V., and Hampton, M.A., 1973, Sediment gravity flows: Mechanics of flow and deposition: Society of Economic Paleontologists and Mineralogists, short course notes, Anaheim, Pacific section, pp. 1-38.

- Middleton, G.V., and Hampton, M.A., 1976, Subaqueous sediment transport and deposition by sediment gravity flows: In Marine sediment transport and environmental management (D.J. Stanley and D.J.P. Swift, Eds.) New York: John Wiley and Sons, pp. 197-220.
- Miller, D.J., 1953, Late Cenozoic marine glacial sediments and marine terraces of Middleton Island, Alaska: Jour. Geology, v. 61, no. 1, pp. 17-40.
- Mode, W.N., 1980, Quaternary Stratigraphy and palynology of the Clyde Foreland, Baffin Island, N.W.T., Canada: unpubl. Ph.D. dissertation, Univ. Colorado, 219 pp.
- Molnia, B.F., 1979, Sedimentation in coastal embayments, northeastern Gulf of Alaska: Proceedings of the 1979 Offshore Technology Conference, 665-670.
- Molnia, B.F. and Bingham, 1980, Glacial marine sedimentation: does the definition fit the deposits? Geol. Soc. Am. Abstr. with Programs, Ann. Meeting, Atlanta, p. 486.
- Molnia, B.F., and Carlson, P.R., 1975, Surface sediment distribution, northern Gulf of Alaska: U.S. Geol. Surv. open file report 75-505, 1 map.
- Morner, N.A., 1980, Earth Rheology-Isostasy and Eustasy: Wiley, New York, 599 pp.
- Mullineaux, D.R., Crandell, D.R., and Waldron, H.H., 1957, Multiple glaciation in the Puget Sound basin, Washington: Geol. Soc. Amer. Bull. (Abstracts), v. 68, no. 12, p. 1772.
- Mullineaux, D.R., Waldren, H.H. and Rubin, Meger, 1965, Stratigraphy and chronology of late interglacial and early Vashon glacial time in the Seattle area, Washington, U.S. Geol. Survey Bull. 1194-0, p. 01-010.
- Nelson, A.R., 1981, Quaternary glacial and marine stratigraphy of the Qivitu Peninsula, northern Cumberland Peninsula, Baffin Island, Canada: Summary: Geol. Surv. Amer. Bull., v. 92, pp. 512-518, part 1.
- Nelson, C.H., and Kulm, L.D., 1973, Submarine fans and channels. In: Turbidites and Deep Water sedimentation, p. 39-78, Soc. Econ. Paleont. Miner., Pacific Section, Short Course, Anaheim.

- Orheim, O. and Elverhøi, A., 1981, Model for Submarine Glacial Deposition: *Annals of Glaciology*, v. 2, pp. 123-128.
- Ovenshine, A.T., 1970, Observations of iceberg rafting in Glacier Bay, Alaska, and the identification of ancient ice rafted deposits: *Geol. Soc. Amer. Bull.*, v. 81, pp. 891-894.
- Paterson, W.S.B., 1969, *The Physics of glaciers*: London, Pergamon, 249 p.
- Pessl, F., Jr., Dethier, D.P., Keuler, R.F., Minard, J.P., and Balzarini, M.A., 1981, Sedimentary facies and depositional environments of late Wisconsin glacial-marine deposits in the central Puget Lowland, Washington: *Amer. Assoc. Petr. Geol., Abstracts Annu. Meeting*, San Francisco, 1981.
- Péwé, T.L., 1975, Quaternary geology of Alaska: U.S. Geol. Surv. prof. paper, 835, 145 pp.
- Plafker, G., and Addicott, W.O., 1976, Glaciomarine deposits of Miocene through Holocene age in the Yakataga Formation along the Gulf of Alaska margin, Alaska: U.S. Geol. Surv. open file report, 76-84, 36 pp.
- Powell, R.D., 1980, Holocene glacimarine deposition by tidewater glaciers in Glacier Bay, Alaska: unpubl. Ph.D. thesis, Ohio State Univ.
- _____. 1981, A model for sedimentation by tidewater glaciers: *Annals of Glaciology*, v. 2, pp. 129-134.
- Rains, R.B., Selby, M.J., and Smith, C.J.R., 1980, Polar desert Sandar, Antarctica: *New Zeal. Jour. Geol. Geophy.*, v. 23, pp. 595-604.
- Reading, H.G., 1978, (ed.) *Sedimentary Environments and Facies*: Elsevier, New York, 557 pp.
- Reading, H.G., and Walker, R.G., 1966, Sedimentation of Eocambrian tillites and associated sediments in Finmark, Northern Norway: *Palegeo., Paleclim., Paleoecol.*, v. 2, pp. 177-212.
- Reagan, A.B., 1907, Some geological studies on northwestern Washington and adjacent British territory: *Kans. Acad. Sci. Trans.*, v. 255, pp. 95-121.

- Reineck, H.E., and Singh, I.B., 1972, Genesis of laminated sand and graded rhythmites in storm-sand layers of shelf mud: *Sedimentology*, v. 18, pp. 123-128.
- Robertson, J.A., 1971, A long-axis clast fabric comparison of the Squantum "Tillite," Massachusetts and the Gowganda Formation, Ontario-Discussion: *Jour. Sed. Petrology*, v. 41, n. 2, pp. 606-608.
- Rust, B.R., and Romanelli, R., 1975, Late Quaternary sub-aqueous outwash deposits near Ottawa, Canada: in *Glacial and Glaciolacustrine Sedimentation* (Jopling and McDonald, eds.), pp. 177-192.
- Schermerhorn, L.J.G., 1974, Late Precambrian mixtites: glacial and/or nonglacial?: *Amer. Jour. of Science*, v. 274(7), pp. 673-824.
- Sharp, R.P., 1949, Studies of superglacial debris on valley glaciers: *Amer. Jour. Sci.*, v. 247, pp. 289-315.
- Shaw, J.D., 1972, Late Pleistocene, Paleontology of Orcas, Shaw, Lopez and San Juan Islands of the San Juan Archipelago: unpubl. M.S. thesis, Univ. Washington, 60 pp.
- Shaw, J., 1977, Tillis deposited in arid polar environments: *Can. Jour. Earth Sci.*, v. 14, pp. 1239-1245.
- . 1979, Genesis of the Sveg tillis and Rogen moraines of central Sweden: a model of basal melt out: *Boreas*, v. 8, pp. 409-426.
- Smith, G.W., 1981, Kennebunk glacial advance: a reappraisal: *Geology*, v. 9, pp. 250-253.
- Snively, P.D., Jr., Gower, H.P., Yount, J.C., Pearl, J.E., Tagg, A.R., and Lee, J.W., 1976, High resolution seismic profiles adjacent to Whidbey and Fidalgo Islands, Washington: U.S. Geol. Surv. open file report 76-187.
- Stuiver, M., Heusser, C.J., and Yang, I.C. 1978, North American glacial history back to 75,000 years B.P.: *Science*, v. 200, pp. 16-21.
- Stuiver, M., and Borns, H.W., Jr., 1975, Late Quaternary marine invasion in Maine: Its chronology and associated crustal movement: *Geol. Soc. Amer. Bull.*, v. 86, pp. 99-104.

- Sugden, D.E., and Clapperton, C.M., 1981, An ice-shelf moraine, George VI Sound, Antarctica: *Annals of Glaciol.*, v. 2, pp. 135-141.
- Sugden, D.E., B.S. John, 1976, *Glaciers and Landscapes*: Halsted Press, London, 376 pp.
- Thorson, R.M., 1980, Ice-sheet glaciation of the Puget Lowland, Washington, during the Vashon Stade (Late Pleistocene): *Quaternary Research* 13, 303-321.
- _____. 1981, Isostatic effects of the last glaciation in the Puget Lowland, Washington: U.S. Geol. Survey, open file report 81-370, p. 100.
- Wagner, F.J.E., 1959, Paleoeecology of the marine Pleistocene faunas of southwestern British Columbia: *Geol. Surv. Canada, Bull.*, 52, 67 pp.
- Warner, J., 1969, Fortran IV program for the construction of Pi diagrams with the Univac 1108 computer: *Kansas Geol. Survey Computer Contr.* 3, 38 pp.
- Webb, P.N., Ronan, T.E., Lipps, J.H., DeLaca, T.E., 1979, Miocene glaciomarine sediments from beneath the southern Ross Ice shelf, Antarctica: *Science*, v. 203 (4379), pp. 534-537.
- Willis, B., 1898, Drift phenomenon of Puget Sound, *Geol. Soc. Amer. Bull.* 9, 111-162.
- Wright, R., 1980, Sediment gravity transport on the Weddell Sea continental margin: unpubl. M.A. thesis, Rice University, 96 pp.
- Wright, R., and Anderson, J.B., 1982, The importance of sediment gravity flow to sediment transport and sorting in a glacial marine environment: Eastern Weddell Sea, Antarctica: in press, *Geol. Soc. Amer. Bull.*
- Zingg, Th., 1935, Beitrag zur Schotteranalyse: *Schweizer. Mineral. u. Petrog. Mitt.*, v. 15, pp. 38-140.

TABLE 1	Phi size versus settling velocity in cms/sec.
TABLE 2	Pebble fabric data.
TABLE 3	C ¹⁴ dates for Everson age deposits on Whidbey Island.
TABLE 4	Textural and fossil data.
TABLE 5	Criteria for distinguishing Qmd, Qsd, and till (Qd) lithofacies.
TABLE 6	SHAPE program and pebble shape data.

<u>SYMBOLS</u>	<u>LOCATION</u>
ST	Swantown
HLN	Hastie Lake Road-North
HLS	Hastie Lake Road-South
WBN	West Beach North
WB	West Beach
LB	Libbey Beach, West Beach
LH,HLK	Lake Hancock
CH	Crescent Harbor
FP	Forbes Point
MP	Maylor Point
PC	Penn Cove-West
BB	Penn Cove-East, Blowers Bluff
SFE	San de Fuca-East
SFW	San de Fuca-West
C	Coupeville, Lovejoy Point
MB	Mutiney Bay

TABLE 1

255

<u>PHI SIZE</u>	<u>SETTLING VELOCITY CM/SEC (CHI)</u>
-1.0	27.0
0.0	15.0
1.0	7.6
2.0	3.2
3.0	1.1
4.0	.32
5.0	.08
6.0	.02
7.0	.00054
8.0	.00014
9.0	.000035
10.0	.000001

TABLE 2
FABRIC DATA

<u>Site/Sample</u>	<u>Area of 1% contour</u>	<u>Area of 5% contour</u>	<u>Total Area</u>
San de Fuca East (SFE)			
Qsd-1	2017.1/46.5%	264/6.09%	4334
Qsd-2	1807/43.6%	315/7.6%	4139
San de Fuca West (SFW)			
Qsd-1	1854/45.3%	240/5.8%	4089
Qsd-2	2108/51.4%	204/4.98%	4098
Qsd-4	1984/48.6%	122/2.99%	4076
Qsd-5	1788/44%	292/7%	4064
Qmd-1	2849/70%	49.5/1.2%	4054
Qmd-2(3)	2633/64%	25.25/.6%	4097
Hastie Lake Road North (HLN)			
Qd-1	1891.75/46%	284.75/6.99%	4070
Qd-2	1127/27%	279/6.84%	4078
Qd-3	2341/57%	142/3.5%	4070
Penn Cove West (PC)			
Qmd-1	2462/60%	28/.68%	4079
Qmd-2	2374/58%	15/.37%	4083
Qmd-3	2144/52%	177/4.3%	4104
Qmd-4	2699/66%	0	4084
Penn Cove East (BB)			
Qmd-1	2025/47%	228/5.6%	4083
Qmd-2	2639.7/64%	96/2.3%	4118
Forbes Point (FP)			
Qmd-1	2501/61%	85/2.07%	4100
Qmd-2	2773/68%	33/.8%	4074

Site/Sample

Mutiney Bay MB
Hancock Lake HLK
West Beach North WBN
Libbey Beach LB
Swantown ST

LB QPML

ST QPML-1

20 OBSERVATIONS

25 OBSERVATIONS

DATA ARE LINEATIONS

DATA ARE LINEATIONS

STRIKE PLUNGE

STRIKE PLUNGE

203.	5.
350.	8.
65.	7.
346.	31.
321.	32.
313.	20.
287.	51.
337.	20.
242.	16.
294.	29.
216.	22.
68.	63.
175.	12.
210.	31.
308.	28.
194.	0.
195.	43.
283.	34.
297.	20.
307.	36.

304.	10.-
108.	4.
112.	9.
75.	4.
129.	17.
344.	10.
145.	2.
158.	10.
259.	11.
87.	10.
145.	9.
138.	1.
329.	0.
110.	4.
115.	13.
125.	0.
85.	9.
260.	3.
103.	11.
329.	11.
338.	8.
305.	7.
328.	14.
228.	7.
75.	16.

SFW QSD-2

SFW QSD-1

25 OBSERVATIONS

25 OBSERVATIONS

DATA ARE LINEATIONS

DATA ARE LINEATIONS

STRIKE PLUNGE

STRIKE PLUNGE

24.	29.
338.	4.
15.	18.
15.	0.
115.	41.
305.	50.
155.	14.
48.	20.
172.	10.
2.	0.
205.	26.
211.	6.
20.	26.
355.	22.
18.	8.
131.	8.
2.	65.
0.	30.
355.	19.
40.	39.
8.	29.
223.	6.
20.	0.
8.	17.
351.	21.

35.	37.
5.	24.
52.	20.
28.	17.
20.	10.
355.	15.
47.	0.
225.	2.
50.	11.
110.	12.
26.	21.
300.	21.
16.	22.
14.	32.
165.	50.
291.	49.
28.	32.
13.	25.
22.	17.
330.	22.
32.	10.
115.	0.
29.	3.
333.	38.
355.	12.

SEW QSD-4

SEW QSD-5

25 OBSERVATIONS

25 OBSERVATIONS

DATA ARE LINEATIONS

DATA ARE LINEATIONS

STRIKE PLUNGE

STRIKE PLUNGE

145.	25.
144.	30.
124.	35.
186.	15.
240.	24.
240.	39.
175.	16.
218.	29.
24.	14.
18.	15.
204.	25.
346.	21.
208.	7.
319.	11.
336.	15.
116.	34.
211.	17.
20.	25.
23.	9.
231.	27.
44.	9.
210.	14.
210.	55.
213.	32.
143.	13.

6.	20.
0.	21.
83.	46.
34.	29.
62.	21.
25.	6.
203.	16.
180.	15.
5.	20.
20.	26.
108.	21.
19.	16.
29.	10.
150.	0.
31.	20.
34.	30.
22.	41.
24.	4.
9.	37.
353.	19.
25.	27.
83.	11.
13.	19.
345.	3.
30.	6.

SFE QSD-2

25 OBSERVATIONS

DATA ARE LINEATIONS

STRIKE PLUNGE

10.	27.
340.	51.
36.	5.
223.	18.
4.	3.
244.	6.
15.	4.
350.	30.
26.	9.
53.	30.
28.	15.
168.	0.
20.	14.
35.	3.
190.	19.
40.	10.
5.	10.
304.	23.
4.	11.
310.	17.
35.	21.
30.	11.
60.	38.
15.	30.
192.	2.

SFE QSD-1

25 OBSERVATIONS

DATA ARE LINEATIONS

STRIKE PLUNGE

125.	9.
175.	33.
138.	26.
115.	25.
228.	42.
18.	26.
145.	20.
152.	13.
130.	11.
288.	11.
138.	68.
145.	34.
174.	26.
171.	25.
192.	21.
130.	20.
172.	9.
144.	20.
225.	7.
132.	8.
161.	12.
312.	15.
303.	3.
125.	20.
81.	8.

MB QD-D

48 OBSERVATIONS

DATA ARE LINEATIONS

STRIKE PLUNGE

5.	10.
44.	4.
22.	12.
165.	6.
34.	36.
114.	17.
65.	20.
288.	26.
15.	2.
11.	5.
16.	5.
350.	10.
86.	5.
11.	32.
216.	7.
7.	17.
115.	14.
256.	47.
170.	14.
7.	2.
195.	2.
182.	7.
192.	7.
200.	6.
5.	19.
170.	16.
355.	11.
270.	10.
170.	5.
10.	7.
11.	5.
14.	3.
11.	10.
35.	2.
135.	11.
328.	19.
50.	19.
28.	5.
166.	0.
45.	25.
60.	22.
202.	27.
194.	19.
25.	6.
148.	15.
98.	4.
141.	5.
48.	7.

261

MB QD-D,

18 OBSERVATIONS

DATA ARE LINEATIONS

STRIKE PLUNGE

118.	48.
197.	34.
150.	16.
359.	22.
9.	10.
342.	6.
121.	31.
112.	0.
30.	21.
95.	9.
235.	30.
346.	6.
84.	0.
81.	15.
344.	6.
155.	12.
330.	13.
150.	72.

ME QFT-A2

18 OBSERVATIONS

DATA ARE LINEATIONS

STRIKE PLUNGE

315.	0.
220.	20.
251.	18.
324.	0.
295.	26.
202.	31.
138.	27.
155.	15.
90.	47.
354.	16.
359.	2.
349.	12.
54.	24.
285.	25.
10.	64.
351.	0.
349.	4.
335.	10.

ME QFT-A

28 OBSERVATIONS

DATA ARE LINEATIONS

STRIKE PLUNGE

348.	20.
164.	26.
350.	16.
340.	12.
211.	14.
340.	0.
343.	0.
350.	20.
168.	0.
10.	19.
340.	19.
350.	4.
164.	19.
342.	25.
340.	19.
10.	9.
350.	20.
5.	20.
343.	21.
345.	12.
347.	36.
355.	15.
317.	15.
346.	11.
11.	26.
326.	8.
215.	29.
152.	6.

SFW QSD-1A

MB QFT-1

10 OBSERVATIONS

30 OBSERVATIONS

DATA ARE LINEATIONS

DATA ARE LINEATIONS

STRIKE PLUNGE

STRIKE PLUNGE

212.	13.
28.	0.
86.	1.
200.	21.
26.	0.
263.	23.
212.	6.
131.	28.
226.	4.
125.	4.

179.	20.
161.	13.
169.	20.
322.	6.
185.	30.
184.	19.
245.	29.
2.	10.
172.	17.
91.	11.
174.	2.
174.	17.
150.	38.
174.	25.
343.	6.
350.	18.
354.	2.
22.	6.
289.	7.
170.	4.
188.	9.
182.	17.
206.	5.
146.	3.
173.	24.
334.	2.
156.	43.
4.	2.
142.	47.
119.	4.

HLK QDT

HLK QDM

25 OBSERVATIONS

25 OBSERVATIONS

DATA ARE LINEATIONS

DATA ARE LINEATIONS

STRIKE PLUNGE

STRIKE PLUNGE

185.	19.
202.	4.
236.	5.
200.	19.
90.	89.
248.	12.
66.	15.
252.	9.
340.	46.
233.	25.
190.	25.
212.	9.
346.	29.
190.	2.
332.	21.
236.	29.
333.	28.
80.	10.
334.	6.
236.	17.
490.	30.
174.	4.
193.	9.
152.	1.
205.	8.

190.	22.
65.	9.
143.	0.
200.	10.
85.	39.
101.	10.
245.	11.
59.	25.
102.	25.
245.	40.
35.	7.
19.	11.
160.	27.
70.	30.
63.	62.
75.	29.
112.	38.
155.	26.
184.	44.
262.	7.
58.	30.
249.	13.
266.	2.
215.	5.
232.	13.

WBN QMD-1

HLK QDS

25 OBSERVATIONS

25 OBSERVATIONS

DATA ARE LINEATIONS

DATA ARE LINEATIONS

STRIKE PLUNGE

STRIKE PLUNGE

124.	15.
290.	27.
310.	14.
305.	24.
145.	55.
152.	20.
348.	0.
138.	0.
10.	4.
346.	9.
310.	40.
5.	0.
288.	21.
258.	27.
258.	30.
109.	9.
238.	31.
214.	31.
283.	8.
234.	7.
165.	9.
118.	5.
104.	16.
28.	11.
81.	25.

97.	12.
190.	18.
100.	29.
163.	30.
155.	34.
168.	6.
42.	24.
357.	18.
41.	26.
56.	10.
266.	28.
84.	24.
11.	36.
8.	33.
334.	30.
21.	22.
51.	10.
182.	6.
20.	36.
325.	28.
9.	18.
4.	7.
258.	57.
230.	5.
314.	7.

FC QMD-4

SFN QPM-2

25 OBSERVATIONS

17 OBSERVATIONS

DATA ARE LINEATIONS

DATA ARE LINEATIONS

STRIKE PLUNGE

294.	0.
259.	38.
185.	54.
265.	4.
184.	21.
240.	11.
130.	21.
142.	11.
325.	4.
74.	11.
166.	30.
120.	22.
305.	22.
90.	89.
83.	8.
160.	18.
300.	24.
353.	24.
95.	35.
72.	18.
150.	45.
93.	65.
160.	20.
53.	5.
232.	34.

STRIKE PLUNGE

330.	9.
190.	60.
345.	18.
68.	30.
338.	5.
206.	45.
238.	15.
90.	15.
182.	12.
90.	89.
16.	7.
272.	16.
266.	13.
181.	42.
1.	14.
178.	3.
10.	0.

PC QMD-2

PC QMD-3

25 OBSERVATIONS

25 OBSERVATIONS

DATA ARE LINEATIONS

DATA ARE LINEATIONS

STRIKE PLUNGE

STRIKE PLUNGE

142.	1.
290.	14.
155.	60.
120.	9.
51.	16.
30.	30.
120.	32.
135.	5.
22.	11.
8.	21.
266.	15.
318.	38.
330.	38.
135.	16.
346.	12.
281.	5.
314.	35.
320.	32.
236.	74.
80.	10.
270.	4.
6.	24.
105.	73.
297.	33.
348.	25.

20.	22.
195.	2.
125.	20.
325.	12.
20.	9.
147.	2.
238.	46.
190.	3.
256.	10.
8.	41.
325.	59.
200.	9.
198.	8.
175.	67.
170.	67.
215.	49.
190.	41.
342.	32.
200.	75.
21.	25.
20.	18.
5.	0.
11.	52.
12.	4.
200.	77.

HLN QD-3

PC QMD-1

25 OBSERVATIONS

25 OBSERVATIONS

DATA ARE LINEATIONS

DATA ARE LINEATIONS

STRIKE PLUNGE

STRIKE PLUNGE

208.	0.
228.	41.
200.	0.
225.	18.
130.	18.
165.	43.
187.	24.
230.	10.
286.	9.
24.	11.
65.	5.
118.	68.
208.	14.
0.	28.
248.	10.
62.	26.
27.	25.
10.	21.
246.	2.
30.	11.
200.	34.
325.	5.
8.	46.
54.	2.
210.	14.

82.	30.
294.	24.
58.	13.
42.	20.
262.	32.
242.	37.
20.	5.
279.	67.
328.	75.
308.	10.
105.	3.
328.	65.
112.	2.
275.	42.
297.	9.
300.	16.
231.	74.
174.	8.
316.	35.
184.	21.
274.	49.
18.	59.
321.	39.
175.	15.
8.	44.

HLN QD-1

HLN QD-2

25 OBSERVATIONS

25 OBSERVATIONS

DATA ARE LINEATIONS

DATA ARE LINEATIONS

STRIKE PLUNGE

STRIKE PLUNGE

166.	12.
60.	17.
66.	11.
125.	2.
160.	15.
8.	3.
36.	5.
195.	6.
221.	14.
183.	20.
215.	7.
200.	8.
177.	8.
186.	23.
25.	25.
109.	17.
224.	18.
104.	1.
235.	16.
359.	10.
183.	11.
153.	32.
165.	21.
5.	3.
200.	0.

59.	38.
137.	4.
354.	7.
180.	1.
355.	9.
57.	17.
7.	10.
36.	11.
178.	0.
10.	19.
343.	30.
200.	25.
155.	0.
185.	12.
213.	4.
60.	5.
7.	10.
6.	35.
166.	10.
188.	17.
189.	11.
10.	22.
342.	42.
10.	16.
38.	13.

BB QMD-1

25 OBSERVATIONS

DATA ARE LINEATIONS

STRIKE PLUNGE

112.	11.
215.	11.
327.	11.
215.	15.
315.	14.
126.	14.
315.	29.
146.	0.
305.	6.
290.	16.
321.	0.
340.	22.
40.	0.
346.	41.
322.	2.
660.	50.
311.	8.
335.	10.
261.	12.
22.	12.
275.	42.
330.	28.
255.	42.
295.	25.
350.	29.

BB QMD-2

25 CBSEERVATIONS

DATA ARE LINEATIONS

STRIKE PLUNGE

230.	12.
289.	33.
300.	9.
296.	10.
170.	18.
300.	30.
228.	39.
108.	26.
324.	18.
310.	60.
208.	7.
208.	5.
292.	30.
223.	35.
298.	30.
298.	39.
90.	89.
162.	2.
25.	54.
101.	4.
150.	7.
100.	33.
66.	5.
135.	10.
354.	27.

FP QMD-1

FP QMD-2

25 OBSERVATIONS

25 OBSERVATIONS

DATA ARE LINEATIONS

DATA ARE LINEATIONS

STRIKE PLUNGE

STRIKE PLUNGE

272.	22.
127.	45.
339.	29.
248.	8.
346.	19.
70.	38.
147.	25.
193.	36.
260.	34.
68.	33.
230.	17.
147.	24.
168.	21.
154.	6.
48.	4.
200.	27.
77.	6.
135.	12.
135.	36.
333.	0.
355.	4.
55.	66.
226.	60.
156.	21.
133.	42.

135.	11.
185.	31.
70.	16.
253.	17.
337.	11.
240.	20.
330.	57.
20.	4.
262.	12.
162.	83.
76.	43.
227.	8.
15.	34.
250.	38.
216.	11.
42.	50.
257.	34.
254.	41.
348.	44.
28.	9.
108.	23.
201.	51.
18.	9.
276.	29.
277.	16.

SFW QMD-3

25 OBSERVATIONS

DATA ARE LINEATIONS

STRIKE	PLUNGE
--------	--------

51.	70.
2.	53.
30.	28.
306.	40.
282.	0.
202.	49.
65.	8.
218.	2.
329.	29.
2.	10.
10.	3.
7.	6.
215.	30.
231.	30.
190.	77.
8.	24.
293.	21.
49.	6.
311.	40.
8.	26.
132.	41.
318.	27.
338.	82.
356.	50.
324.	65.

SFW QMD-1

27 OBSERVATIONS

DATA ARE LINEATIONS

STRIKE	PLUNGE
--------	--------

168.	6.
40.	20.
233.	15.
109.	21.
258.	38.
315.	14.
300.	22.
268.	10.
33.	5.
340.	11.
208.	16.
120.	31.
131.	62.
317.	15.
190.	20.
40.	39.
308.	18.
175.	48.
280.	30.
320.	3.
309.	1.
176.	60.
153.	18.
113.	33.
237.	53.
80.	2.
80.	15.

TABLE 3
C14 DATES

<u>AGE (years B.P.)</u>	<u>Reference</u>	<u>Sample No.</u>	<u>Locality</u>	<u>Unit</u>	<u>Elevation</u>
13,600 \pm ?	Pessl, et al. (1981), per. com.	?	Clover Valley 48°19'40" 122°39'	Foreset Gravels (shells)	-30m
13,595 \pm ?	Pessl, et al. (1981), per. com.	?	Clover Valley 48°20'30" 122°41'30"	Sandy Gravels (shells)	<10m
13,010 \pm 170	Easterbrook (1968)	UW-32	Penn Cove 48°14' 122°42'30"	Qmd (shells)	<4m
12,640 \pm 150	D. Dethier per. com.	USGS-1304	Penn Cove 48°13'15" 122°41'	Qmd	<1m
12,535 \pm 300	Easterbrook (1968)	I-1079	West Beach 48°13'30" 122°46'	Qmd	-1.5m
12,300 \pm 180	Easterbrook (1968)	I-2154	Polnell Point 48°17' 122°33'	Qmd	?
11,850 \pm 240	Easterbrook (1968)	I-1448	Penn Cove 48°14'30" 122°40'	Qmd	?

TABLE 4

274

<u>Sample</u>	<u>Facies</u>	<u>G;S,Sl,C</u>	<u>MØ</u>	<u>Sd</u>
HLN-L1	Qd	10;71,26,3	3.07	2.34
HLN-L2	Qd	5.5;81,14,5	2.83	2.23
HLN-L3	Qd	3.7;59,35,6	3.93	2.49
SFW-F1	Qsd	2.3;35,53,12	5.17	2.54
SFW-F2	Qsd	13.8;45,44,11	4.53	2.91
SFW-F3	Qsd	8;35,52,13	5.12	2.69
SFW-F4	Qsd	44.5;61,30,9	3.56	3.00
SFW-F5*	Qsd		1.45	1.16
SFW-F6*	Qsd		1.81	1.17
SFW-F7*	Qsd		1.99	1.03
SFW-F9	Qsls	0.0;6,31,13	6.20	1.49
SFE-25	Qsd	10.8;38,45,17	5.14	2.90
C2-23	Qsd	9.5;20,59,21	6.01	2.60
PC-1	Qmd	8.1;22,65,13	5.52	2.44
PC-2	Qpm	1.7;5,82,13	6.27	1.65
PC-3	Qmd	12.7;43,45,12	4.67	2.75
PC-5	Qmd	6.5;39,46,15	5.04	2.79
BB-1	Qmd	37.5;45,46,9	4.55	2.70
BB-2	Qmd	1.3;25,63,12	5.45	2.21
ST-7a	Qmd	1.6;24,58,18	5.95	2.52
SF2-2	Qmd	1;17,60,23	6.26	2.28
HL-1	Qpm(1)	.3;3,69,23	7.37	1.61
A1 SFE-2	Qpm	0.0;1,81,18	6.62	1.43
SF2-1	Qpsl	.7;6,78,16	6.28	1.69
SFE-28	Qpm	.2;0,76,24	7.13	1.27
MB-1	Qpsl	.14;6,81,13	6.42	1.62
HLN-F1	Qpsl	.11;2,79,19	7.09	1.34
SF-1a	Qpm	1.1;19,67,14	5.41	2.84
PC-4	Qmd	7.6;28,58,14	5.49	2.57
SF-2a	Qpsl	4.8;1,89,10	6.31	1.33
C2-1	Qsls	0.0;42,49,9	5.39	1.71
C2-2	Qpm	0.0;3,67,30	7.03	1.76
C2-3	Qsls	0.0;22,64,14	5.68	1.92
C2-4	Qsls	0.0;78,20,2	4.20	1.07
C2-5	Qsls	0.0;21,68,11	5.67	1.66
C2-6	Qpm	0.0;20,53,27	6.36	2.12
C2-7	Qsls	0.0;46,41,13	5.23	1.96
C2-8	Qpsl	0.0;3,70,27	6.85	1.76
C2-9	Qsls	0.0;27,63,10	5.39	1.71
C2-12	Qsls	0.0;82,15,3	4.02	1.37
C2-15	Qsls	0.0;43,45,12	5.35	1.87
C2-16	Qpm	16;2,36,62	8.19	1.66
C2-17	Qsls	0.0;70,23,7	4.35	1.70
C2-18	Qpm	0.0;1,53,46	7.82	1.39
C2-19	Qsd	12;30,44,26	5.72	3.02
C2-20	Qpm	4.1;25,42,33	6.41	2.81

* Analysis of -1.0 0 to 4.0 0 only.

TABLE 4 (cont.)

275

<u>Sample</u>	<u>Facies</u>	<u>G;S,Sl,C</u>	<u>M Ø</u>	<u>Sd</u>
C2-21	Qpm	37;30,43,27	5.39	3.21
C2-26	Qs	0.0;98,1,1	2.20	.63
FP-32	Qmd	3.2;21,48,31	6.39	2.59
FP-33	Qmd	2.1;20,48,32	6.46	2.64
FP-34	Qmd	2.3;17,51,32	6.55	2.53
FP-35	Qmd	3.4;18,60,22	5.96	2.47
FP-36	Qpm	.17;4,63,33	7.2	1.84
FP-37	Qpm	1.3;15,51,34	6.34	2.51
FP-38	Qpm	.81;11,59,30	6.84	2.21
FP-39	Qpm	1.2;10,60,30	6.83	2.17
FP-40	Qsls	41;59,30,11	4.15	2.67
FP-42	Qpm	.24;7,73,20	6.50	1.71
FP-43	Qpm	3.5;12,64,24	6.42	2.13
FP-44	Qpm	1.5;6,73,21	6.51	1.82
FP-45	Qpm	.05;14,67,19	6.21	1.86
FP-49a	Qpm	0.0;4,66,30	6.96	1.72
FP-49b	Qmd	1.1;14,68,18	6.15	2.17
FP-50	Qpm	0.0;8,67,25	6.94	1.86
FP-51	Qpm	0.0;1,72,27	7.24	1.50
FP-52	Qpm	0.0;2,72,26	7.03	1.55
FP-53	Qpm	0.0;1,70,29	7.42	1.45
FP-54	Qpm	0.0;1,62,37	7.42	1.54
FP-56	Qpm	.98;14,58,28	6.59	2.28
FP-57	Qpm	.64;13,65,22	6.24	2.15
FP-58	Qpm	.54;15,62,23	6.18	2.28
FP-59	Qpm	.83;16,64,20	6.04	2.25
FP-60	Qpm	0.0;6,70,24	6.53	1.87
FP-61	Qpm(1)	3.0;16,68,16	5.37	2.19
FP-62	Qpm(1)	0.0;6,67,27	6.83	1.92
FP-63	Qslc	0.0;1,54,45	7.48	1.73
FP-64	Qsls	0.0;5,78,17	6.44	1.64
FP-65	Qslc	0.0;0,46,54	8.01	1.61
FP-66	Qsls	0.0;0.0,81,19	6.87	1.41
FP-67	Qslc	0.0;1,68,31	7.14	1.56
FP-68	Qsls	0.0;15,80,5	5.53	1.32
FP-69	Qsls	0.0;32,66,2	4.84	1.38
MP-14	Qslc	0.0;2,61,37	7.39	1.83
MP-15	Qslc	0.0;3,50,47	7.67	1.83
MP-16	Qsls	0.0;9,72,19	6.25	1.74
MP-17	Qsls	0.0;12,70,18	6.09	1.75
MP-18	Qsls	0.0;14,63,23	6.23	1.91
MP-19	Qsls	0.0;13,67,20	6.14	1.80
MP-20	Qslc	0.0;5,67,28	6.76	1.79

TABLE 4 (cont.)

276

<u>Sample</u>	<u>Facies</u>	<u>Microfossils</u> (siliceous)	<u>Other</u>
WB-10a	Qsls	spicules	
WB-1	Qpsl	barren	
HLN-L1	Qd	barren	
SFW-F9	Qsls	barren	
PC-3	Qmd	barren	
SFW-F8	Qsd	barren	
HL-1a	Qpm	spicules	
FP-43	Qpsl	spicules	
FP-51	Qpm	spicules	
FP-58	Qpm	spicules	
FP-63	Qpm	spicules, holith. spine	
HL-1	Qpm(1)	barren	
HL-2	Qsd	barren	
HL-3	Qpm	barren	
SFE-7	Qpm	barren	
SFE-9	Qsd	barren	
SFE-10	Qsls	barren	
SFE-17	Qpsl	spicules	
SFE-28	Qpm		bryozoan fragm.
SFE-20	Qpm	barren	
ST-17	Qpm(1)	spicules, diatoms	
FP-34	Qmd	barren	
FP-37	Qmd	spicules	
MP-4	Qslc	barren	
FP-39	Qpm	barren	
MP-11	Qslc	barren	
C2-1	Qsls	barren	
C2-23	Qsd	barren	
MP-16	Qsls	spicules	
SF2-1	Qpm	barren	
SF2-2	Qmd	barren	

TABLE 5
CRITERIA FOR DISTINGUISHING
GLACIAL-MARINE, SEDIMENT FLOW AND
GLACIAL DIAMICTONS

<u>FACIES</u>	<u>PEBBLE FABRIC</u>	<u>PEBBLE SHAPE/% STRIATED</u>	<u>PEBBLE ABUNDANCE</u> no./m ²	<u>M Ø</u>	<u>CONTACT RELATIONS</u>
Qmd	Central tendency <3, randomness >55. Correlation between central tendency and % sand in matrix correlation coef. = .56	Mean roundness = .46- .47/ 8 - 10% striated	Range 75 - 110. Mean = 93	4.55- 6.55	Lwr. contact gradational or sharp, upr. contact sharp.
Qsd	Central tendency >3, Randomness <55. No correlation between central tendency and % sand in matrix, correlation coef. = .18.	No data available	Range 50- 690. Mean = 350	3.56- 6.01	Lwr. contact sharp and planer, upr. contact sharp and irregular or convex.
Qd (till)	Central tendency >3, randomness <55.	Mean roundness = .50- .56/ 17-32% striated	Range 80- 130. Mean = 105	2.83- 3.93	Lwr. contact sharp and planer, upr. contact sharp and planer.

TABLE 6
SHAPE DATA

279

Shape Program

A=long axis, B=intermediate, C=short

```

100 REM*THIS PROGRAM DISPLAYS SPHERICITY AND ROUNDNESS
105 OPEN #1, "TRM:PRINTR",OUTPUT
110 PRINT "SPHERICITY"
115 PRINT "ENTER NO. OF SAMPLES": INPUT N
116 DIM A(N),B(N),C(N),R(N),S(N)
120 PRINT
130 PRINT #1, "X","Y"
135 PRINT "#";
137 FOR I=1 TO N
140 INPUT A(I),B(I),C(I),R(I)
150 LET X=B(I)/A(I)
160 LET Y=C(I)/B(I)
170 PRINT #1,X, Y

179 S(I)=((X^2)*(Y))^.333333
180 PRINT #1,S(I)
181 NEXT I
183 FOR I=1 TO N
184 SUMS=S(I)+SUMS
185 SUMR=R(I)+SUMR
186 Z=SUMS
187 Q=SUMR
188 NEXT I
189 R'=Q/N
190 S'=Z/N
194 PRINT #1,"MEAN SPHERICITY"
195 PRINT #1,S'
196 PRINT #1,"MEAN ROUNDNESS"
197 PRINT #1,R'
200 CLOSE #1
210 END

```


Hastie Lake Road HLN-1

N=56

X	Y	X	Y	X	Y
.75	.722222	.721125	.375	.666667	.6
.740624	.722222	.75	.833333	.64366	
.75		.776806		.814815	.681818
.740624		.863636	.421053	.767825	
.723404	.970588	.679724		.571429	.95
.797871		.727273	.625	.676939	
.714286	.933333	.691446		.666667	.75
.780897		.733333	.681818	.693362	
.895833	.465116	.715743		.666667	.714286
.72001		.890909	.571429	.682176	
.666667	.566667	.768322		.75	.944444
.631512		.452381	.868421	.809903	
.758621	.863636	.562229		.722222	.769231
.792125		.567376	.583333	.737564	
.958333	.5	.572646		.913043	.47619
.771497		.763636	.547619	.734945	
.526316	1	.683519		.833333	.7
.651875		.702703	.615385	.786283	
.742857	.807692	.672301		.866667	.5
.763869		.611111	.772727	.721481	
.659341	.666667	.660829	.5	.75	.888889
.661774		.590909		.793701	
.866667	.615385	.558904	.55	.758621	.727273
.773186		.740741		.748024	
.888889	.708333	.670757		.684211	.692308
.824096		.676471	.608696	.686899	
.470588	.625	.65308		.714286	.7
.517274		.709677	.818182	.709492	
.885714	.419355	.744145		.695652	.625
.69033		.882353	.9	.671256	
.857143	.4	.888197		.555556	.7
.664848		.814815	.727273	.600046	
.666667	.65	.784522		1	.466667
.661064		.689655	.9	.775656	
.909091	.5	.753649			
.744838		.866667	.423077	MEAN SPHERICITY S'	
.714286	.8	.682404		.712626	
.741785		.766667	.73913	MEAN ROUNDNESS R'	
		.757376		.502679	

HLN - BC

A
N=30

X	Y	X	Y	X	Y	X	Y
.677966	.85	.702703	.730769	.809524	.852941	.677966	.85
.731047	.857143	.711937	.560976	.823745	.809524	.731047	.857143
1	.692308	.732143	.571429	.65625	.809524	1	.692308
.949914	.692308	.76087	.540541	.703811	.833333	.949914	.692308
.742857	.692308	.69161	.75	.681818	.689655	.742857	.692308
.72561	.905091	.822222	.928571	.728985	.714286	.72561	.905091
.709677	.7	.714939	.645161	.805556	.583333	.709677	.7
.770744	.714286	.9	.806452	.764905	.772727	.770744	.714286
.645161	.69697	.846933	.806452	.65625	.913043	.645161	.69697
.662946	.744186	.636364	.766667	.675052	.962963	.662946	.744186
.813953	.555556	.721787	.7	.666667	1	.813953	.555556
.779275	.740741	.911765	.806452	.637644	.92	.779275	.740741
.942857	.923077	.812478	.806452	.6875	.954545	.942857	.923077
.852515	1	.911765	.766667	.71481	.888889	.852515	1
.716667	.758621	.875215	.766667	.676471	.541667	.716667	.758621
.725725	.636364	.688889	.7	.74759		.725725	.636364
.818182	.8125	.726037	.809091	.710526		.818182	.8125
.719133	.9	.75	.8	.786303		.719133	.9
.72973	.789474	.755515	.73913	.758621		.72973	.789474
.733382	.6	.652174	.952381	.831795		.733382	.6
.684211	.611885	.667742	.869565	.735294		.684211	.611885
.75603	.8	MEAN SPHERICITY S'		.792325		.75603	.8
.526316	.804145	[.744493]		.785714		.526316	.804145
.651875	.625	MEAN ROUNDNESS R'		.838382		.651875	.625
.74359	.705777	[.693333]		.5625		.74359	.705777
.748567	.745098	X		.655186		.748567	.745098
.6	.759606	Y		.705882		.6	.759606
.611885	.8	Y		.646248		.611885	.8
.8	.726848	Y				.8	.726848
.804145		Y				.804145	
.625		Y				.625	
.705777		Y				.705777	
.745098		Y				.745098	
.759606		Y				.759606	
.8		Y				.8	
.726848		Y				.726848	

MEAN SPHERICITY S'
[.744373]
MEAN ROUNDNESS R'
[.613153]

HLN - 2
N = 28

X .815365
.855999
.769231
.745425
.791667
.690946
.591837
.601302
.914894
.854032
.833333
.734852
.633333
.649658
.804878
.755886
.842105
.821311
.8
.611422
.711111
.733762
.882353
.854001
.65
.709728
.7
.667568
.8
.861774
.592593
.674798
.733333
.682404
.741935
.741
.75
685007

Y .943396
.7
.526316
.62069
.744186
.571429
.684211
.666667
.78125
.357143
.76125
.8
.846154
.607143
1
.875
.590909
.73913
.571429

X

.6
.669433
.807692
.7197
.485871
.555802
.692308
.597226
.863636
.755847
.68
.625562
.75
.721125
.722222
.804972
1.06667
.828595
NEAN SPHERICITY
C.721762
MEAN ROUNDNESS
L.553571

S'

R'

1

.5

Y

.833333
.571429
.733333
.444444
.578947
.529412
.666667

HLN - 3
N = 38

X .636364
.661344
.732394
.705216
.8
.770343
.857143
.801189
.75
.74299
.580645
.599445
.527273
.58609
.947368
.842653
.777778
.724473
.675676
.748696
.88
.842682
.535714
.644616
.625
.598928
.807692
.699126
.666667
.701818
.714286
.57537
.6
.630723
.673077
.637329
.418182
.550988

Y

.714286
.653846
.714286
.7
.729167
.638889
.724138
.666667
.628571
.92
.772727
.933333
.55
.52381
.777778
.373333
.69697
.571429
.956522

Penn Cove

PC
N=38

HLN-3
(cont.)

X

Y

.685185
.663306
.644444
.571004
.717391
.689296
.8
.829627
.75
.721125
.641026
.627048
.9
.748887
.878788
.810588
.625
.649062
.806452
.730751
.64
.674746
.851852
.857716
.6875
.766974
.740741
.690496
.625
.731005
.566667
.641867
.653846
.631201
.85
.820561
.73913
.747559

MEAN SPHERICITY S'
[.701769]
MEAN ROUNDNESS R'
[.559211]

X

Y

.962264
.807493
.571429
.625646
.758621
.715459
.863636
.79913
.486372
.610151
.5
.560907
.96875
.801377
.626866
.654747
.73913
.717624
.833333
.822071
.666667
.64366
.8125
.797813
.584906
.614247
.783784
.809055
.823529
.818834
.545455
.641882
.6
.711379
.827586
.656373
.882353
.746039

X

Y

.708333
.726647
.76087
.69161
.789474
.746211
.675
.684436
.85
.725901
.722222
.684694
.628571
.599546
.627907
.674345
.612903
.69528
.84
.777719
.826087
.733776
.969697
.851361
.625
.602536
.75
.655186
.6
.6
.96
.726848
.571429
.568437
.642857
.591198
.8
.782974

MEAN SPHERICITY S'
[.701563]
MEAN ROUNDNESS R'
[.473684]

SEP 1 1963

$$N=61$$
[illegible]

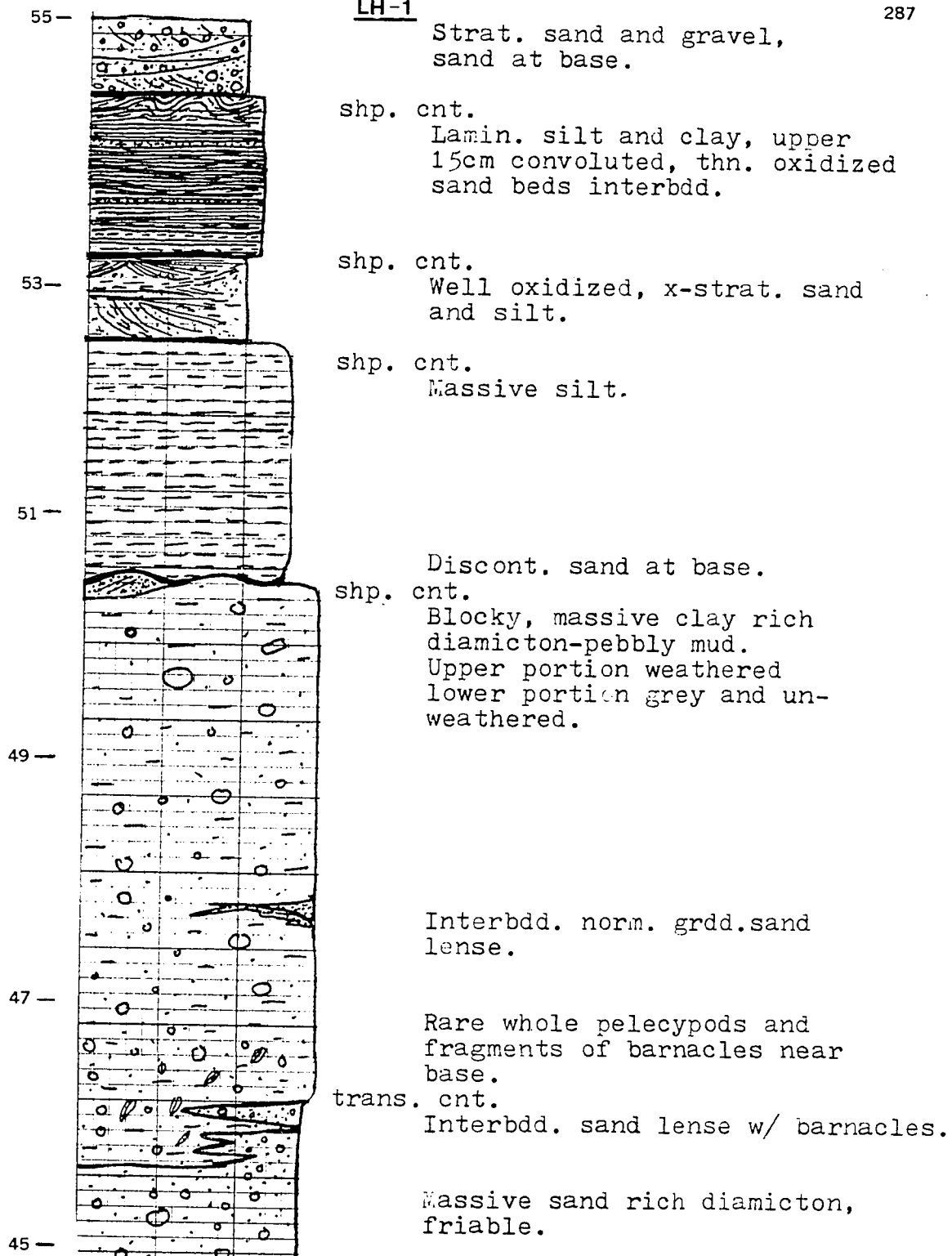
Measured sections.

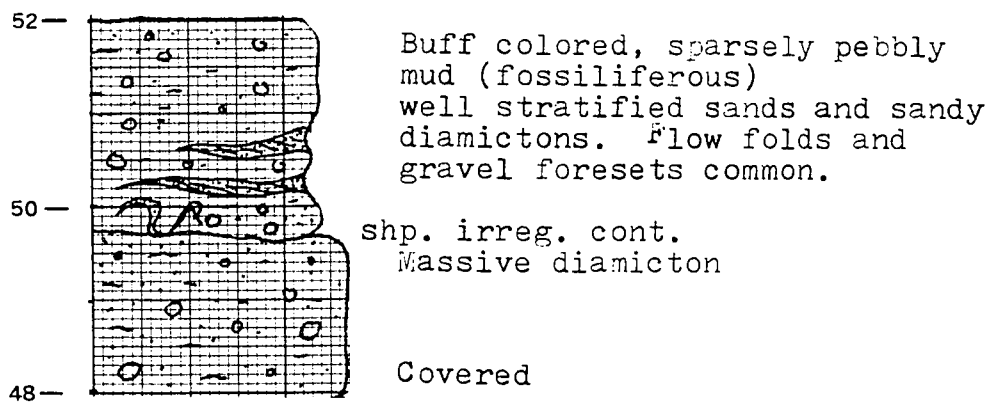
Lithofacies Maps.

Topographic and section location maps (in envelope).

The location of lithofacies maps within this Appendix can be found on the two detailed topographic maps of central and southern Whidbey Island which are in the map envelope. It should be noted that symbols used to map lithofacies are explained for each individual section. The significance of a particular symbol (i.e. Qsd) often times will vary between sections. Older sequences which lie below the Vashon-Everson contact, including some Vashon deposits, are mapped in some cases with the same symbols. This is true for stratified diamictons at Hastie Lake Road-South, Mutiney Bay-East, and Maylor Point. The base of each lithofacies section is high tide and the horizontal scale is approximately equal to the vertical scale, which is in meters.

The location of detailed measured sections can be found either on the lithofacies maps or on one of the two topographic maps.





Esperance Sand Fm.

Whidbey Fm.

0—
meters

— Sea Level

3-



Whispy lamin. silty clay,
sparsely pebbly.

2-

grad. cnt.

Ripple bdd. sandy silt and clay.
Wavey bdd. clayey silt, lamin.
silty sand.

1-

V. thn. lamin. clay, massive clay.

shp. cnt.

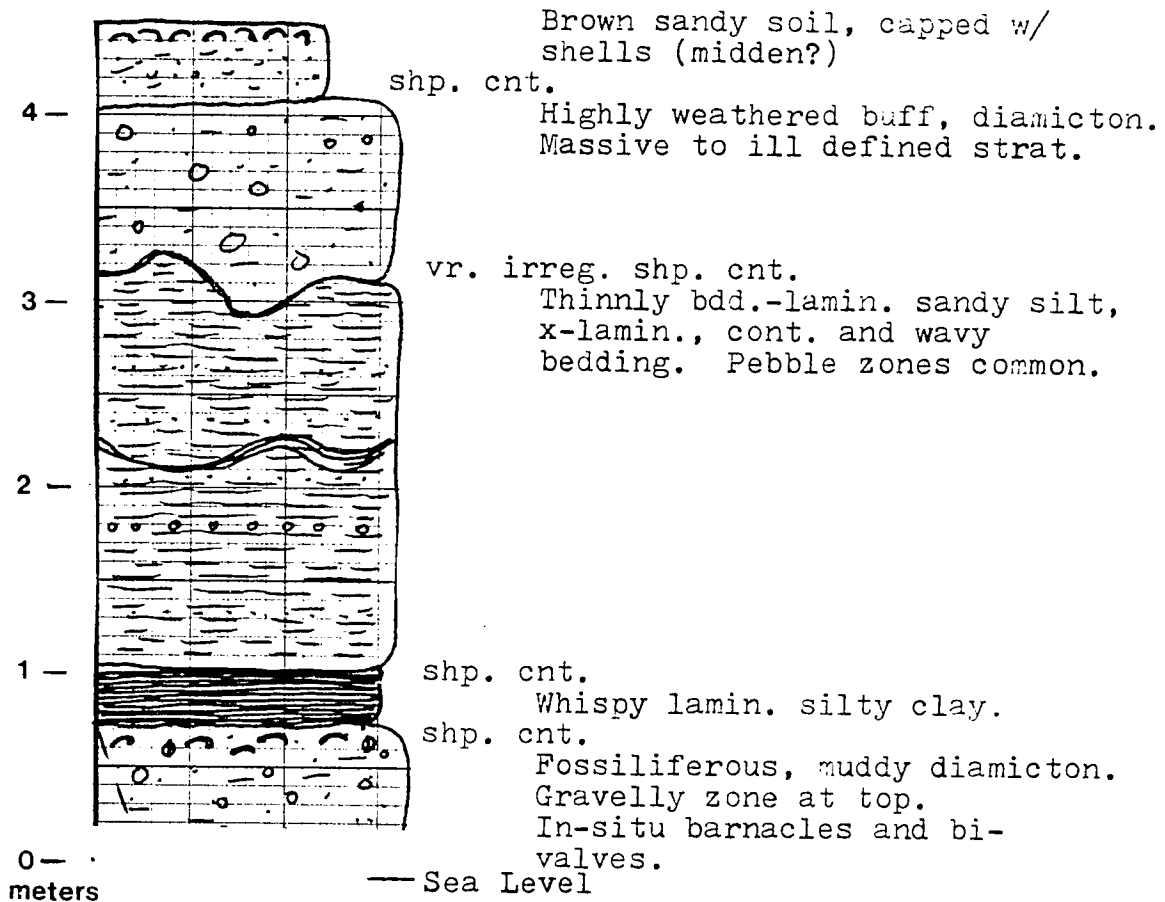
Mottled muddy diamicton.
In-situ bivalves and barnacles
common in upper part of
diamicton.

0-

meters

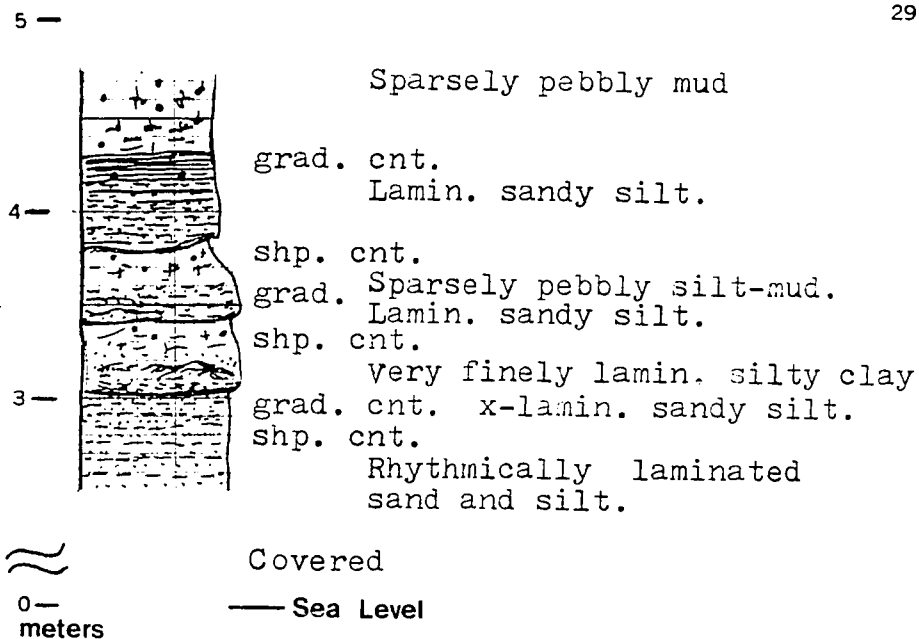
— Sea Level

C¹⁴ sample USGS 1304
12,640 ± 150

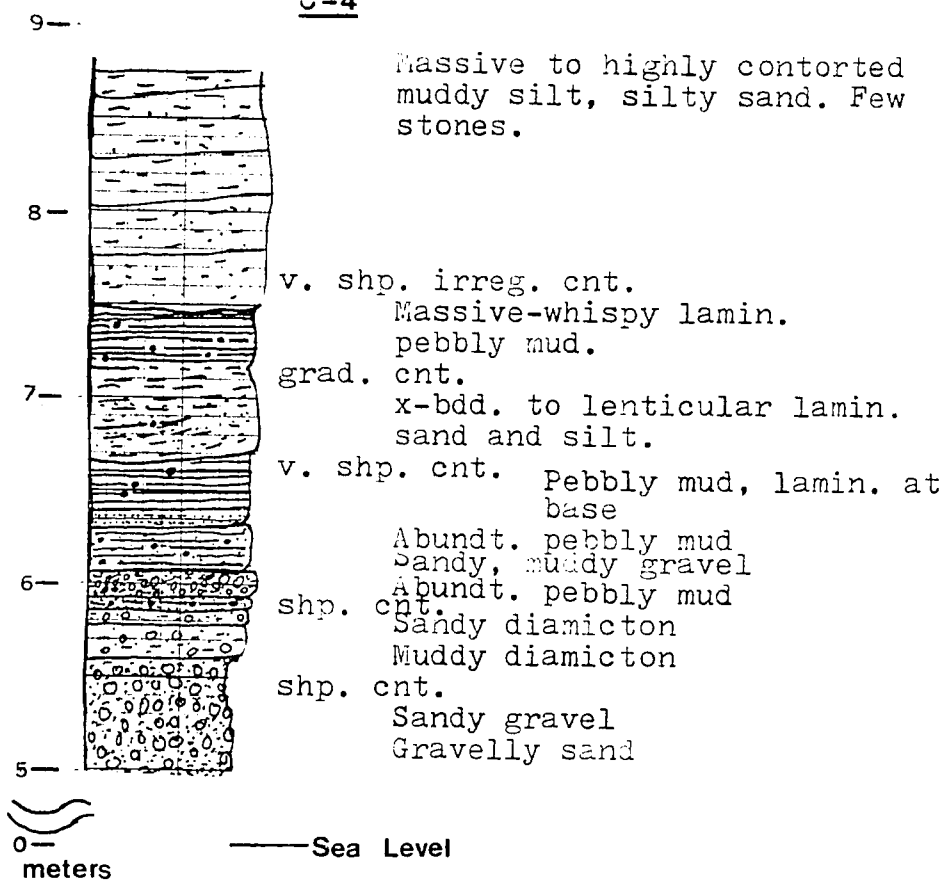


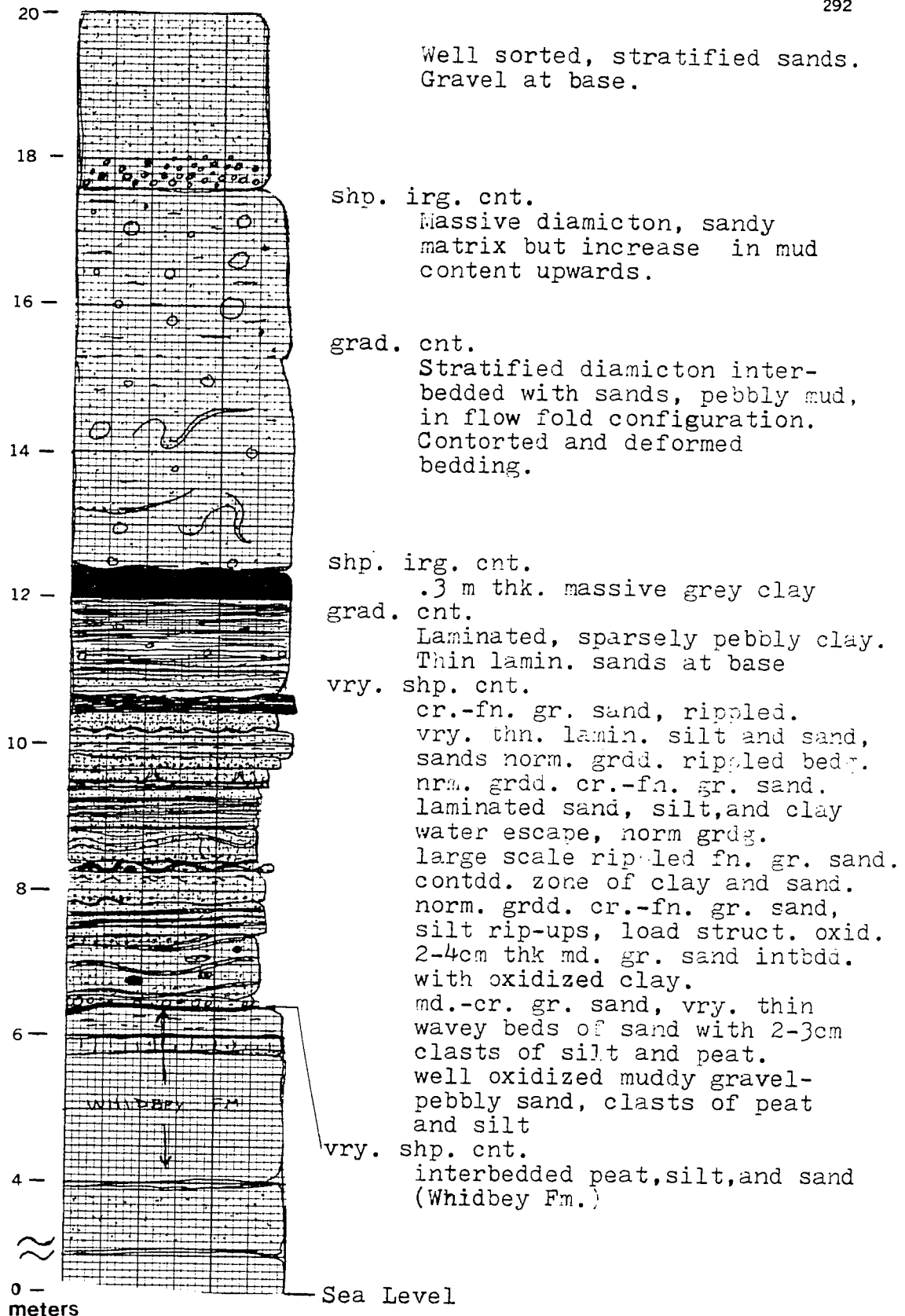
C-3

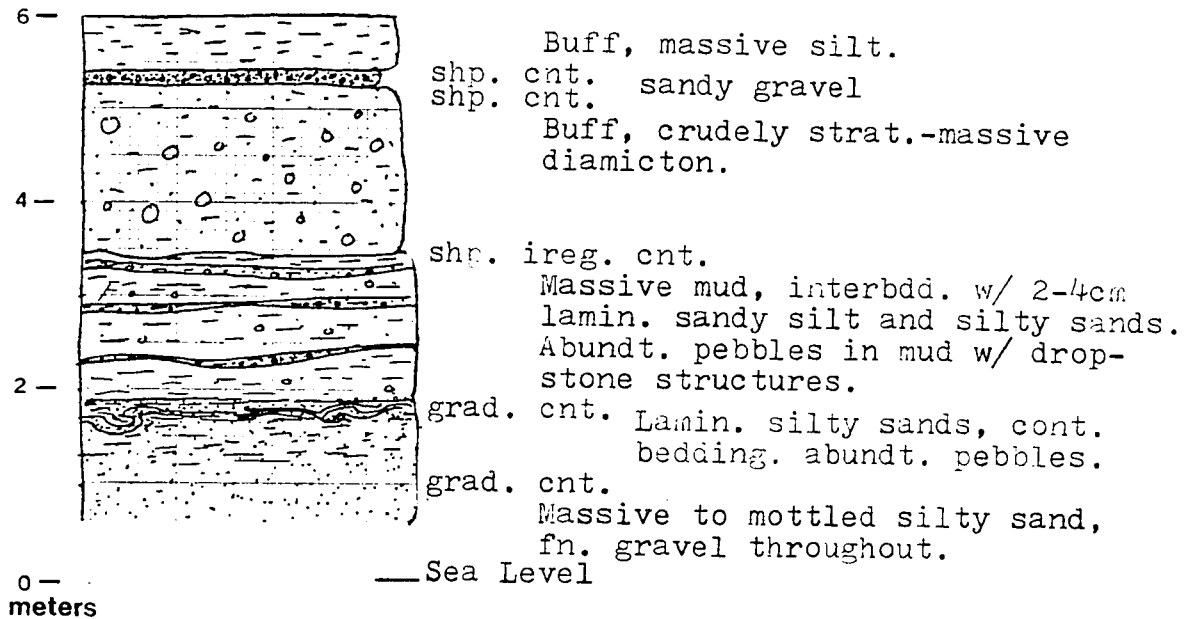
291

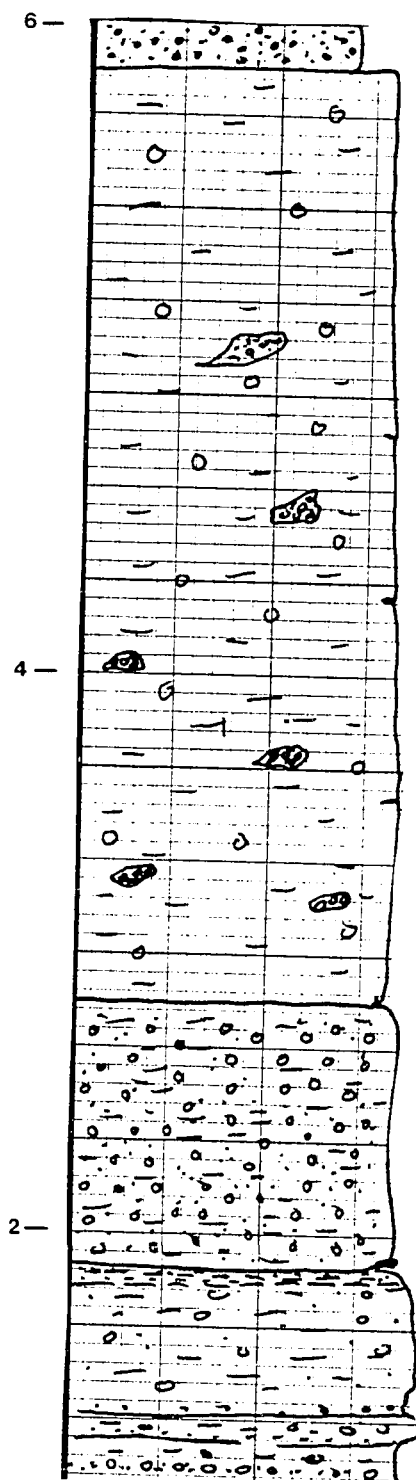


C-4









Dk. brown sandy soil, sandy gravel.

shp. cnt.

Massive buff colored pebbly silt. Isolated pods and lenses of gravel are common.

shp. cnt.

Stratified sandy-silty gravel.

shp. cnt.

Lamin., buff, sandy silt, discontinuous.

grad. cnt.

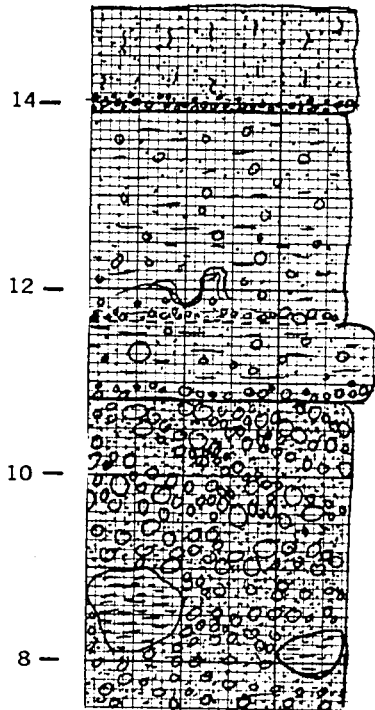
Well strat. horizontally bdd. grey diamicton. Drop-stones and pebble layers common. Silt and clay lamin. common.

0—
meters

Covered

— Sea Level

16 -



Black, sandy soil, gravel
at base.
shp. cnt.
Pebbly mud to sparsely
pebbly silt. Siltier near
base.

Very sparsely pebbly.
Concen. of gravel at base.
grad. cnt.
Stratified, sandy diamicton,
concent. of well rounded stones
at base.

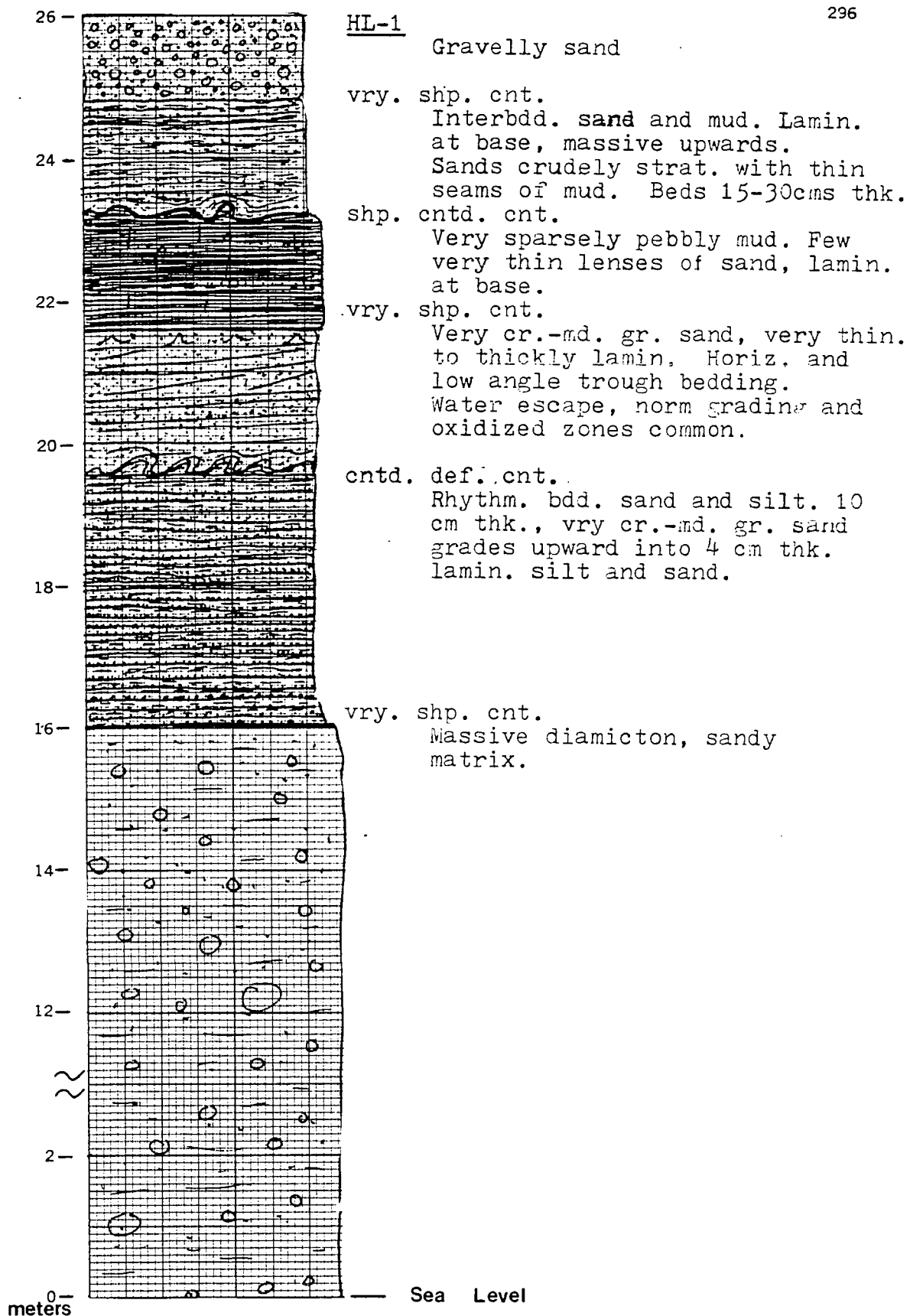
vry. shp. cnt.
Coarse gravel and gravelly
sand. Large silt blocks
abundant.

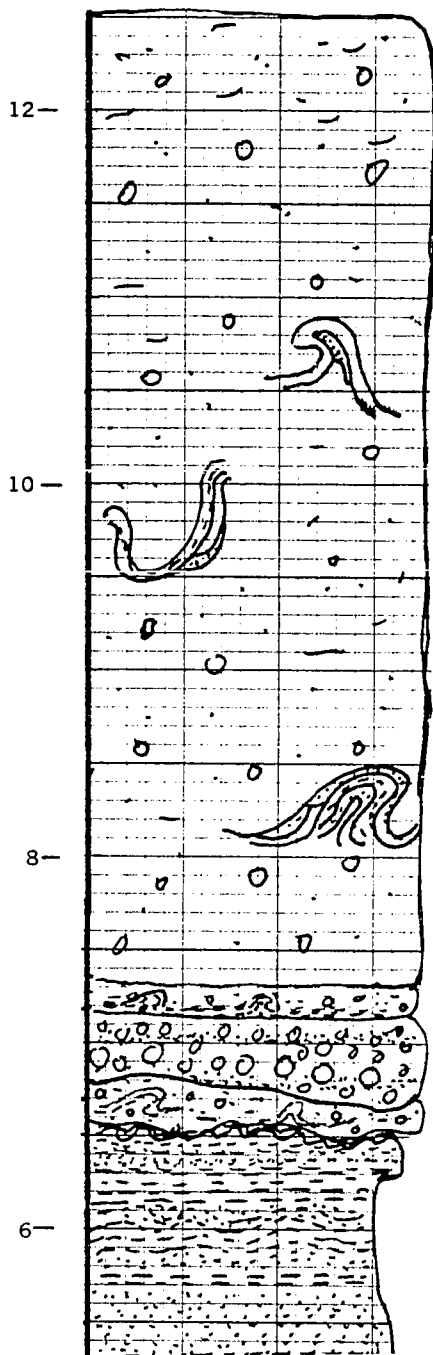
6 -

4 -

0 -
meters

— Sea Level





Buff colored, contorted, stratified diamicton. Small discont. deformed lenses of sand and silty sand.

grad. cnt.

Crudely strat. silty diamicton, contorted lamin. of silt. Stratified sandy gravel w/ abundt. clasts and discont. silt lenses. Crudely strat., contdd. diamict.

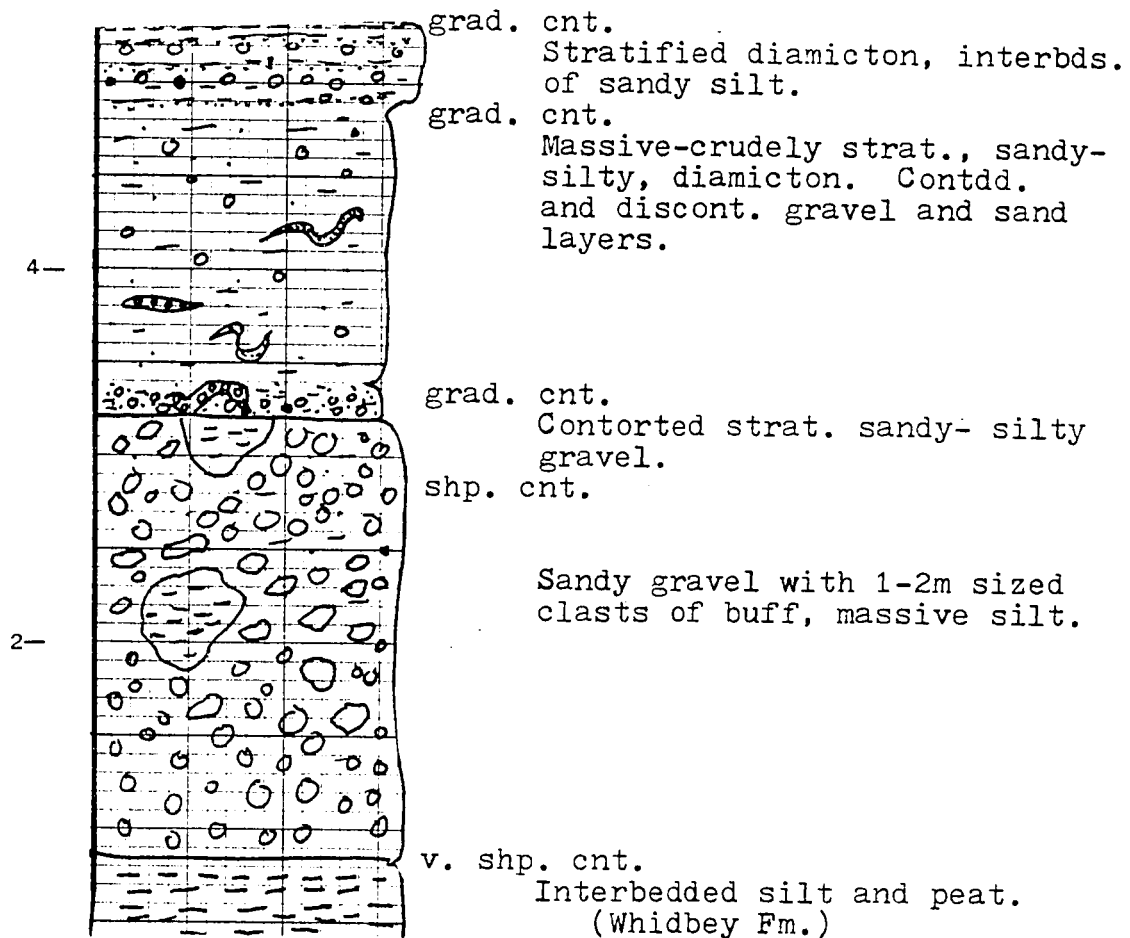
Buff colored, finely lamin.- very thinn. bdd. silt and sandy silt. Horiz. trace fossils, drop-stones.

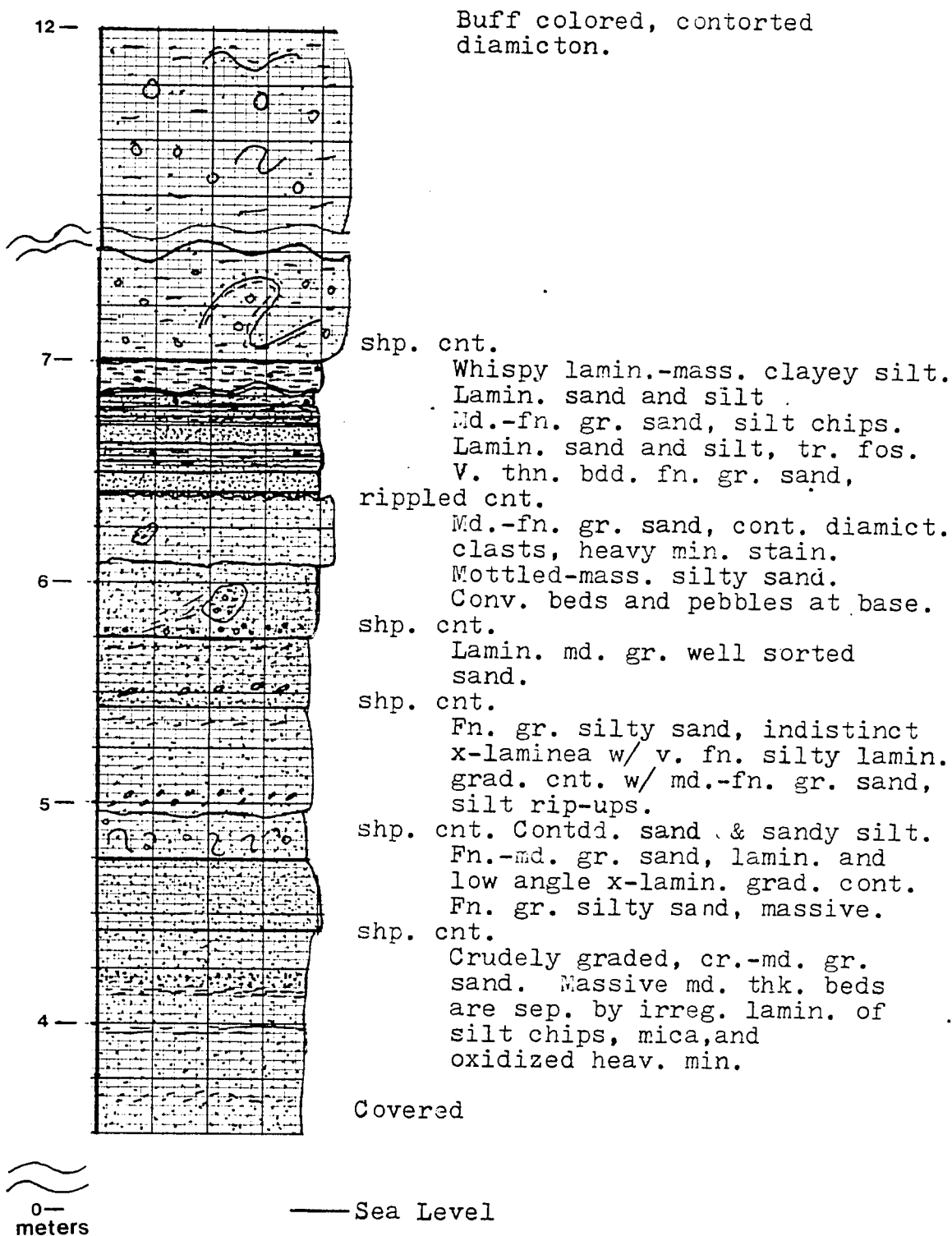
grad. cnt.

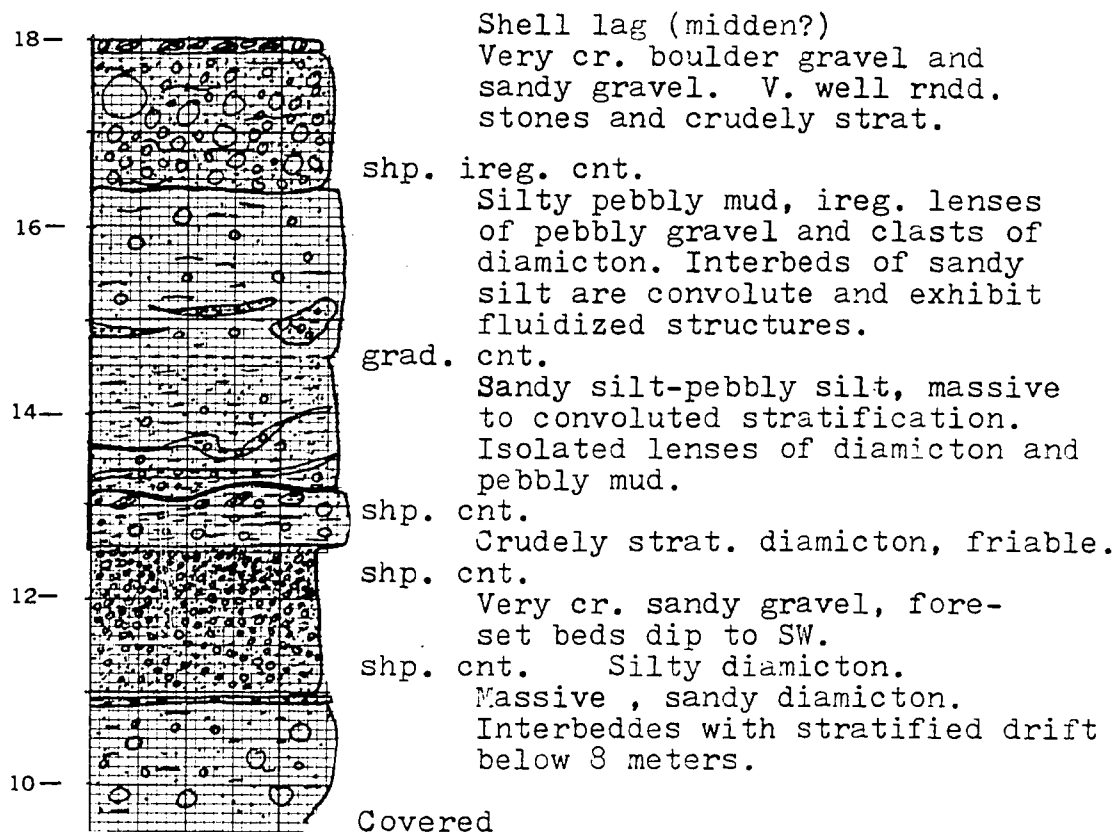
Lamin. silt and sand grades to lamin sand. Highly contdd. sand-silt lamin.

grad. cnt.

(continued next page)

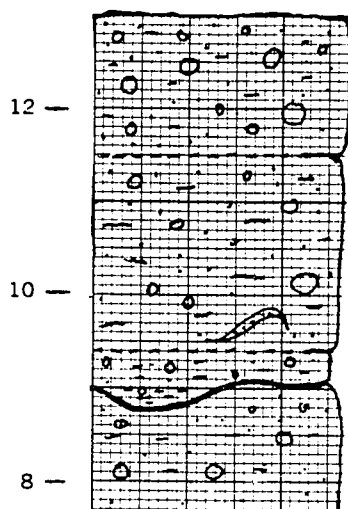






0—
meters

— Sea Level



Muddy, massive diamicton.

grad. cnt.

Abundantly pebbly mud.

grad. cnt.

Sparsely pebbly mud.

shp. irreg. cnt.

Crudely stratified to massive
diamicton.

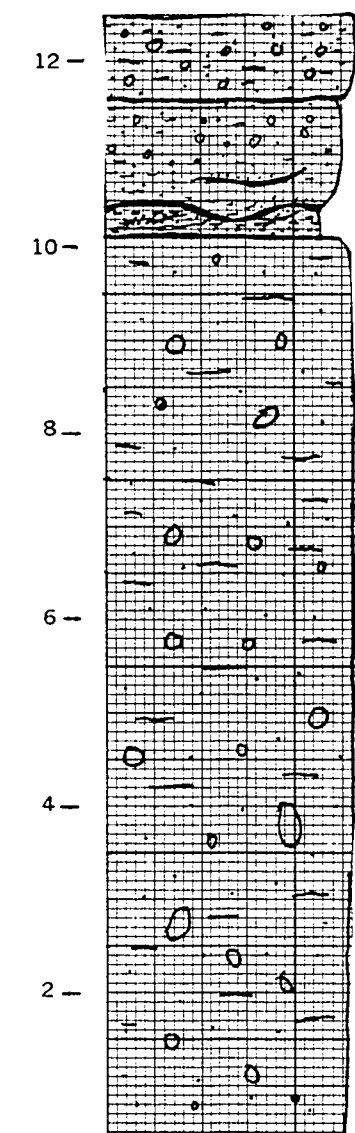
6 —



0 —

meters

— Sea Level



Weathered, massive diamicton.

shp. wavy cont.

Sparsely pebbly mud, wispy
laminations of clay

irreg. cnt.

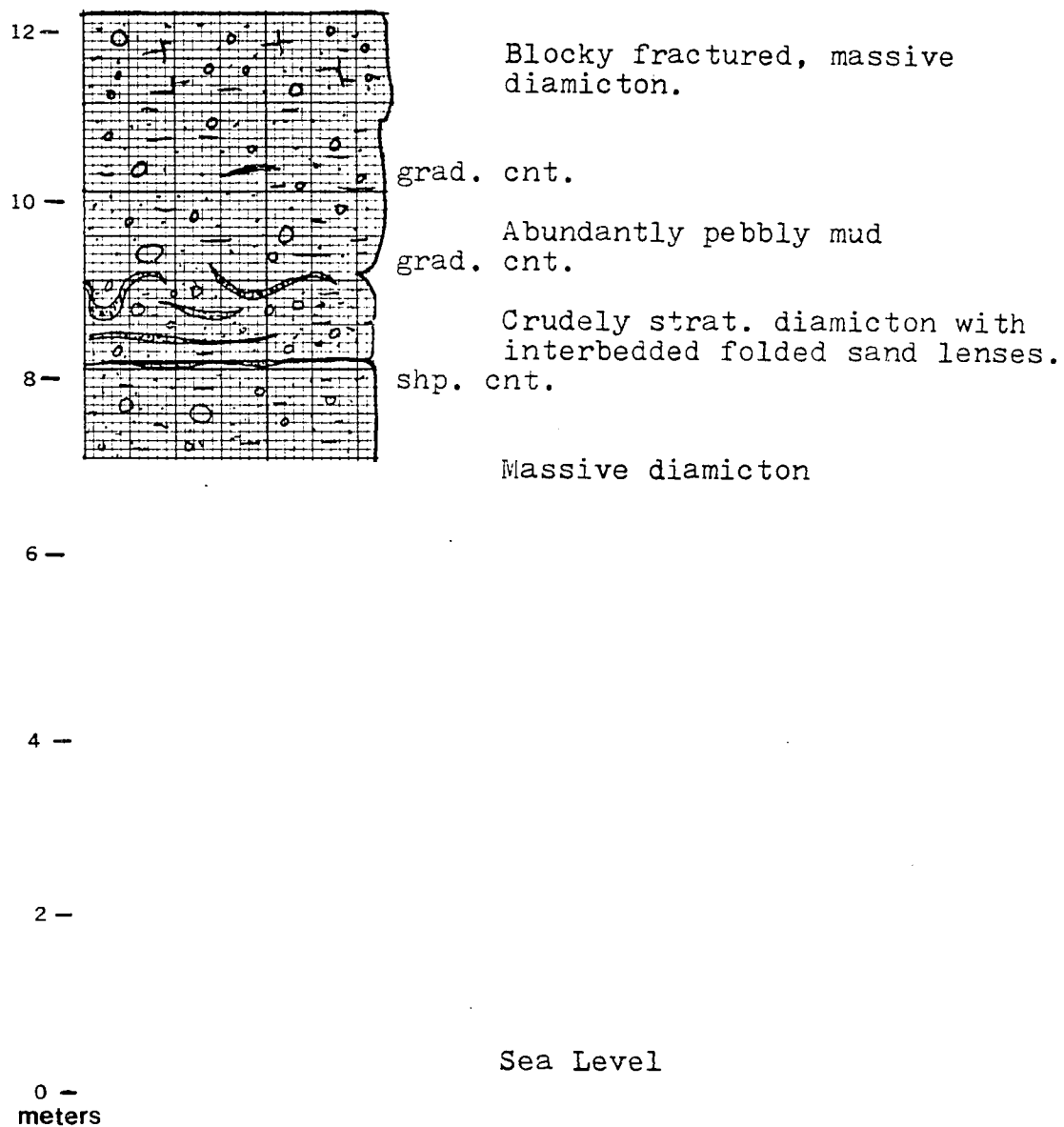
Strat. sand and silty sand,
gravel layers present.

shp. cnt.

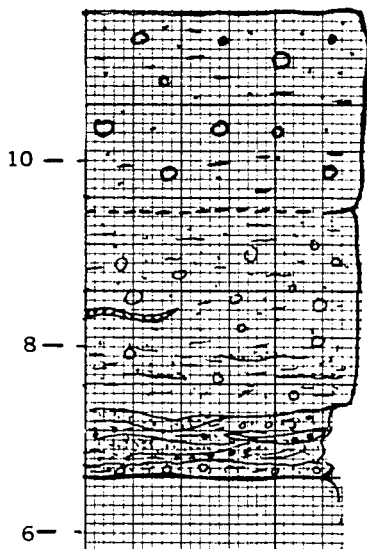
Massive diamicton.

0-
meters

— Sea Level



12- .



Blocky, massive diamicton.

grad. trans. cnt.
Pebbly mud, decrease in silt
upwards.
Discontinuous prly. srtd. sand
lenses.
Thin discont. sand laminae.

Discont. sand and diamicton
lenses. Vry. thn. strat. diam.
shp. cnt.
Stratified sand, gravel, and
silt.

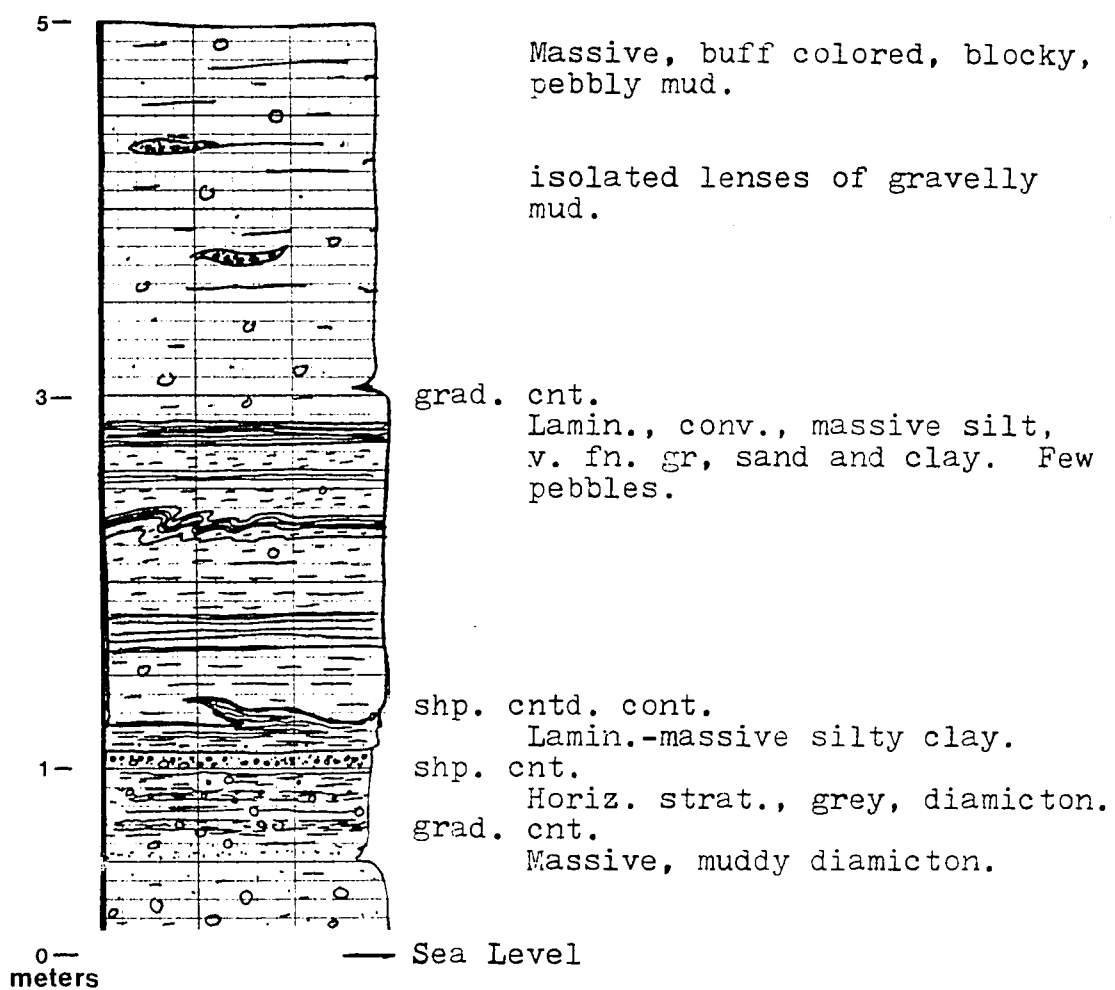
shp. cnt.
Massive diamicton.

4-

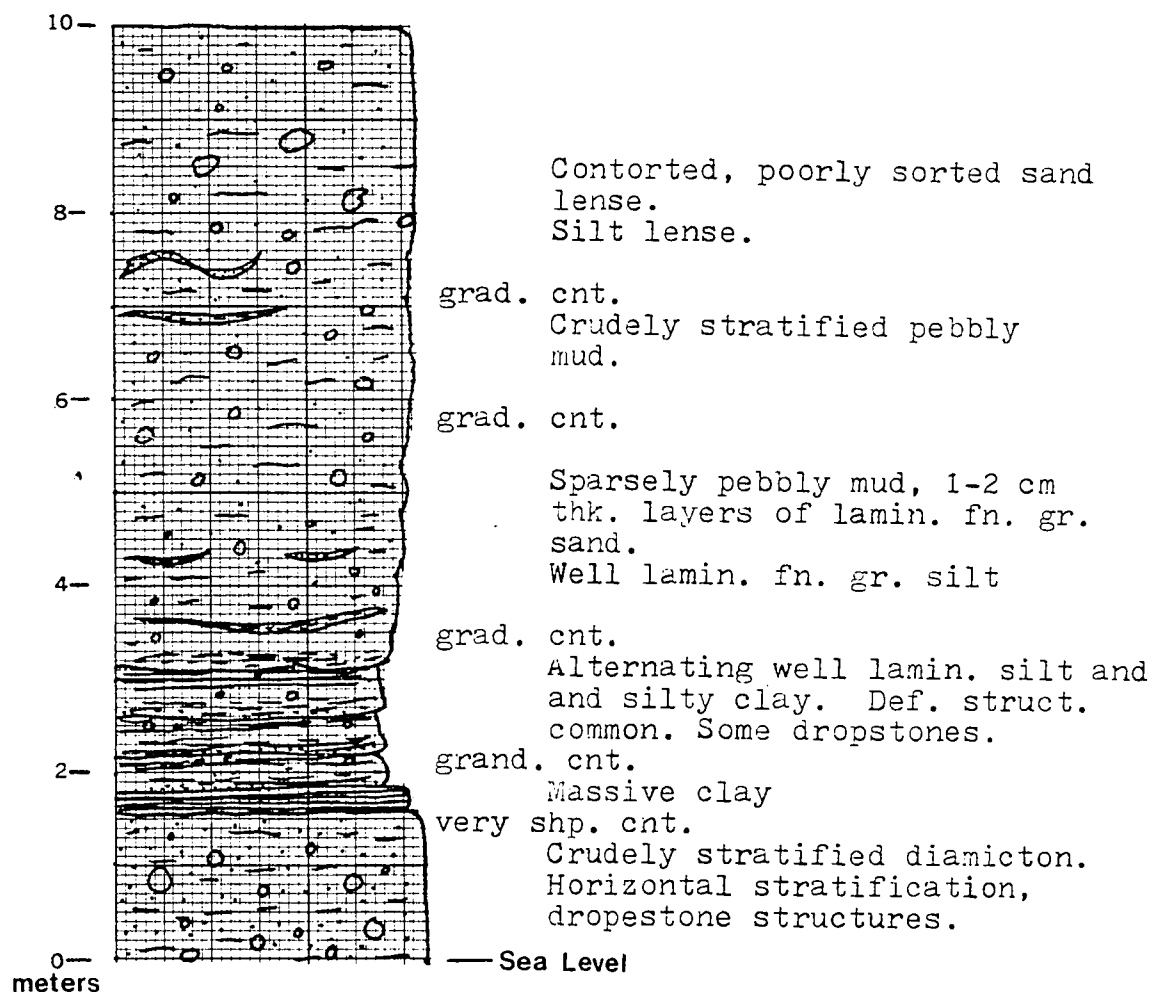
2-

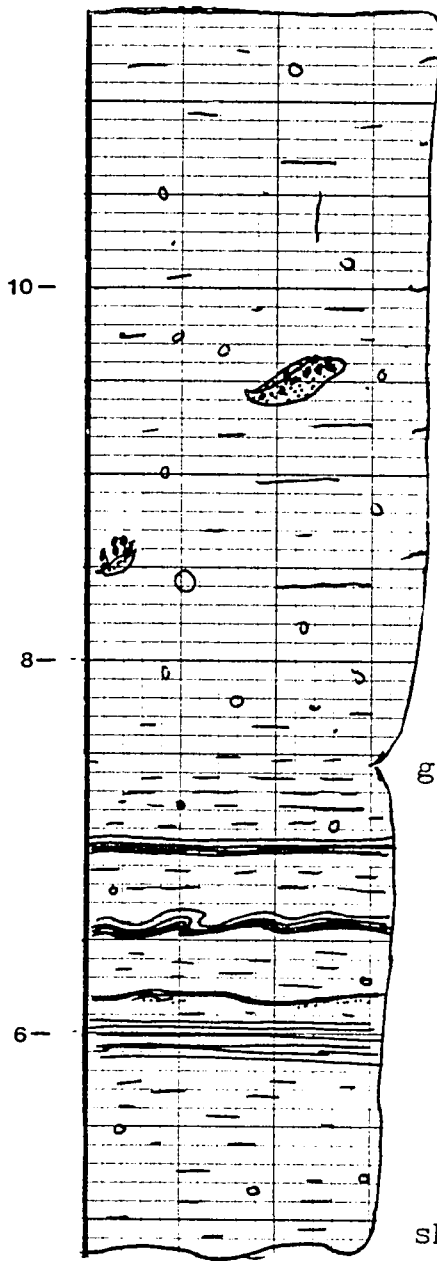
Sea Level

0-
meters



Pebbly mud, highly weathered
and mottled in places.





Massive, blocky weathering
pebbly mud.

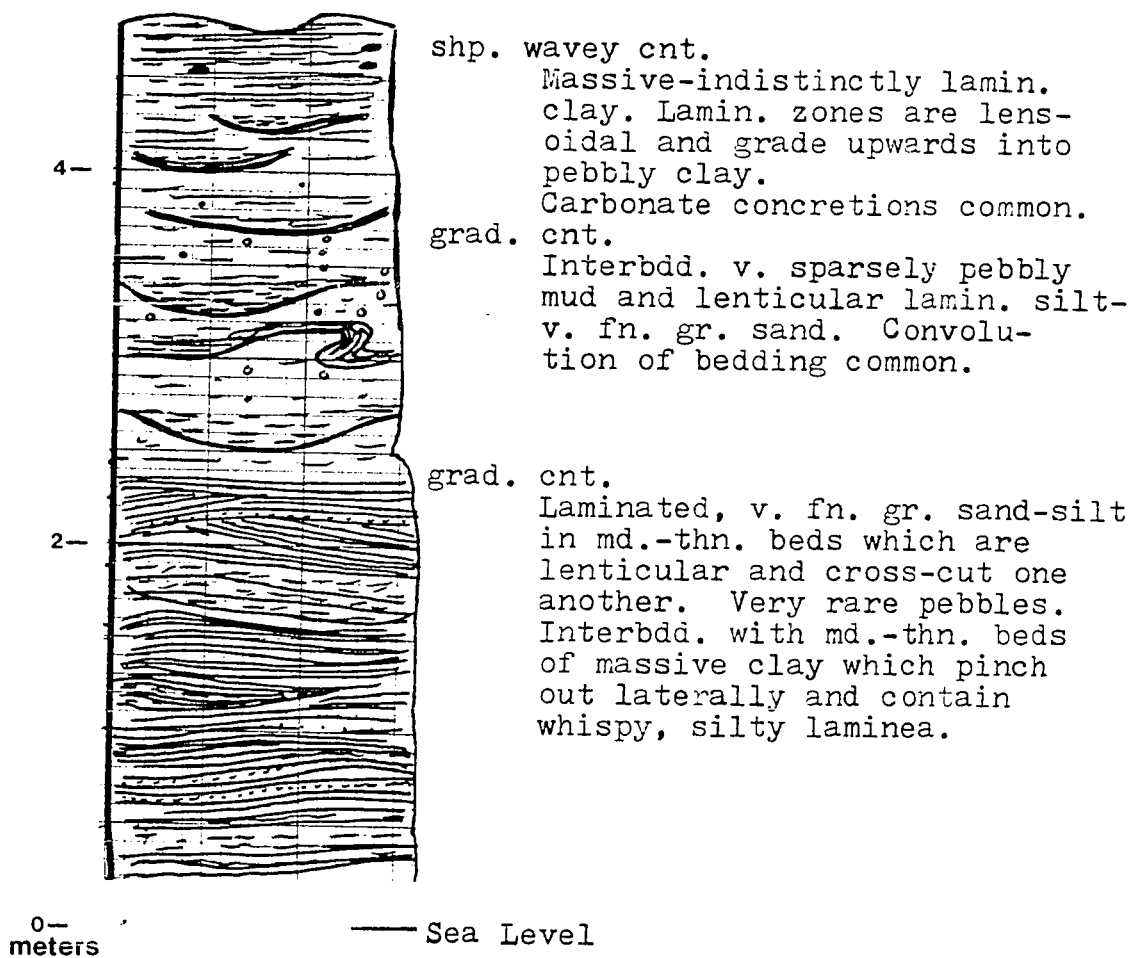
Isolated pods of cr. sand
and gravel.

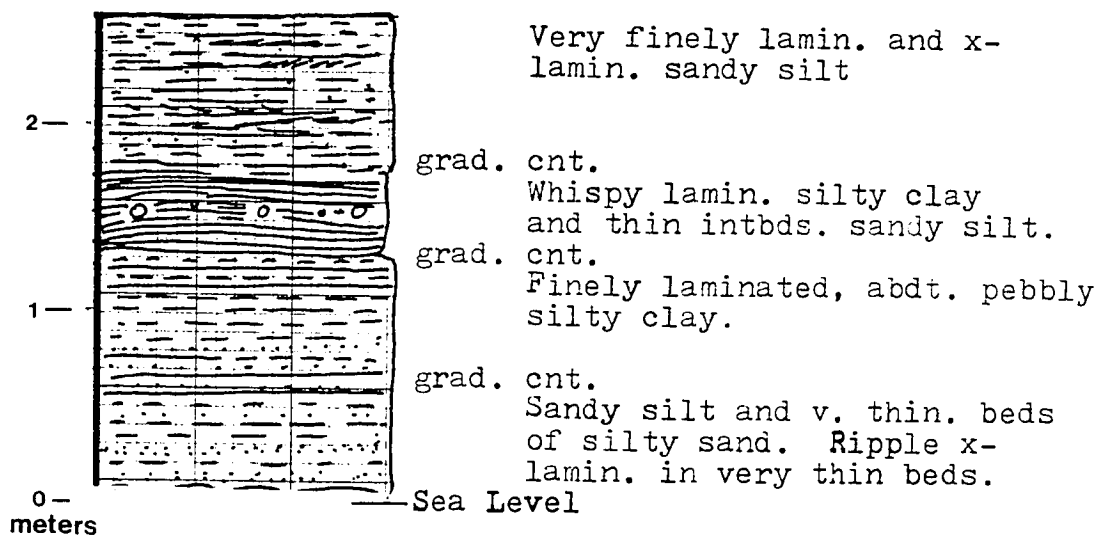
grad. cnt.

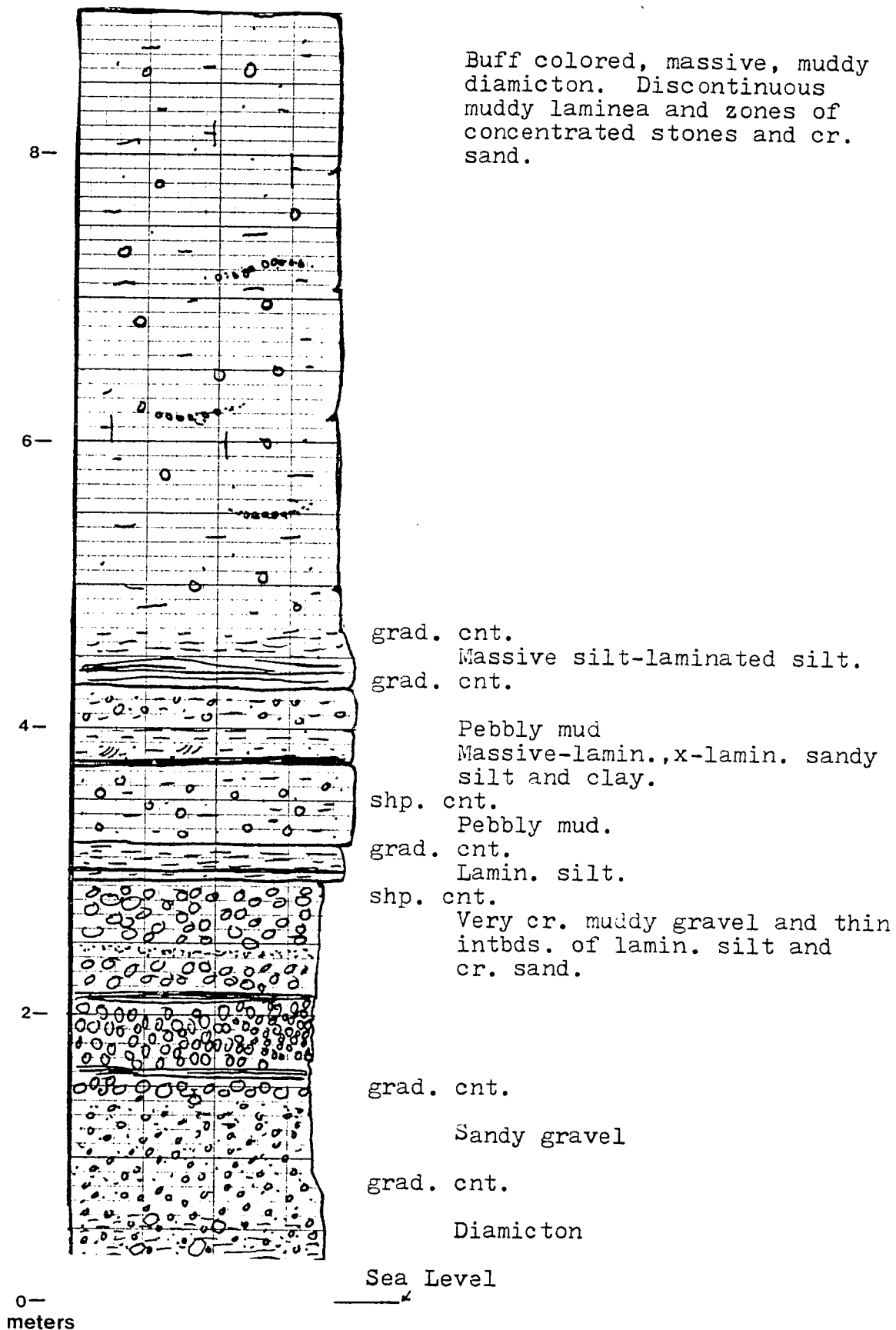
Massive to convoluted, thinlly
bdd. sandy silt, clay.
Sparsely pebbly, v. thin beds
of lensoidal sand-silt-clay.

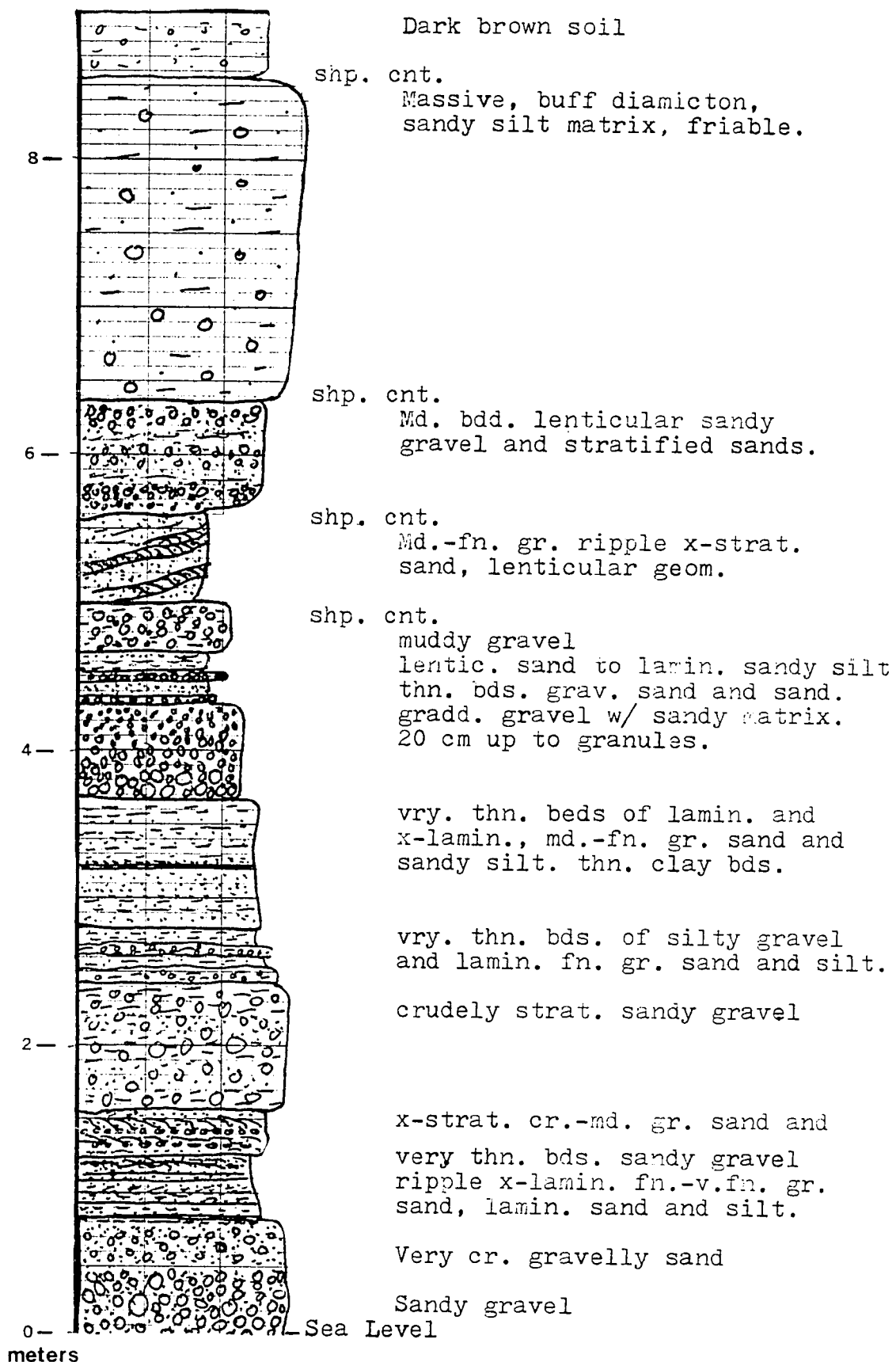
shp. wavey cnt.

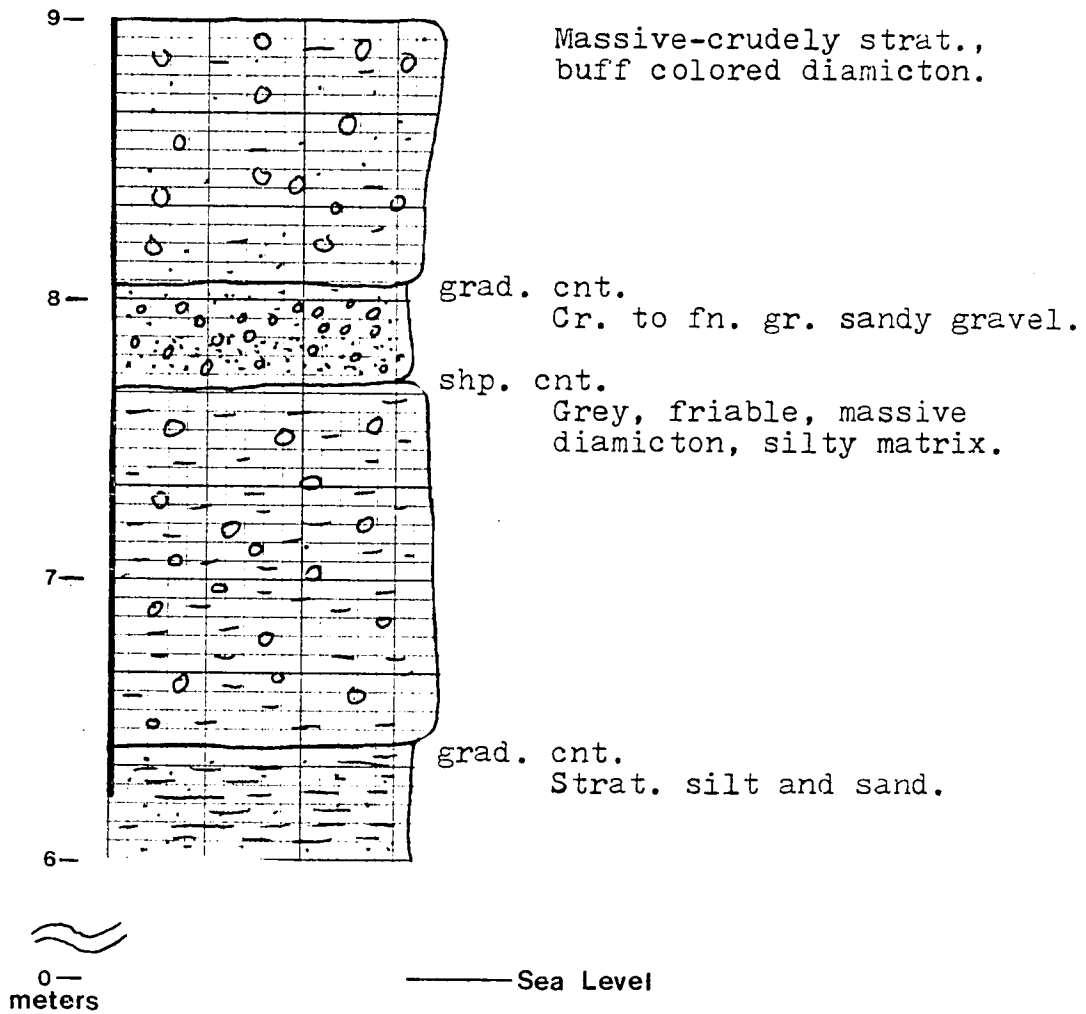
(continued on next page)

MP-2 (contin.)









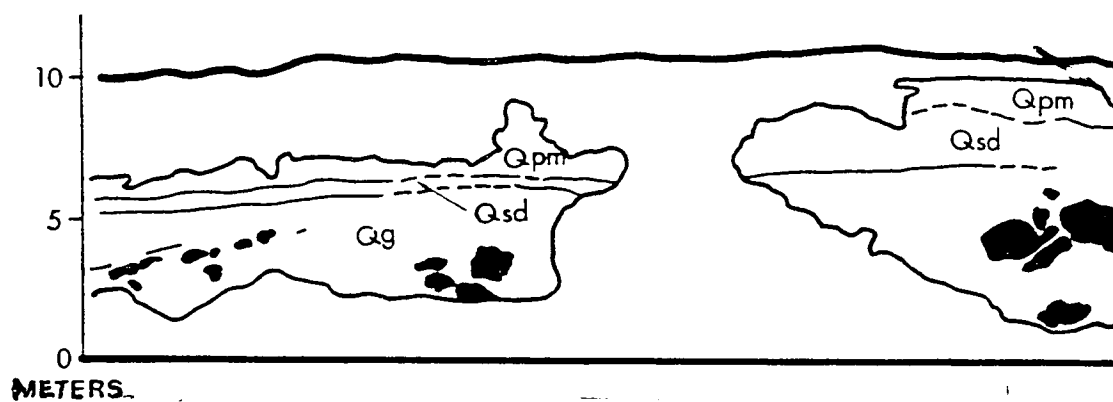
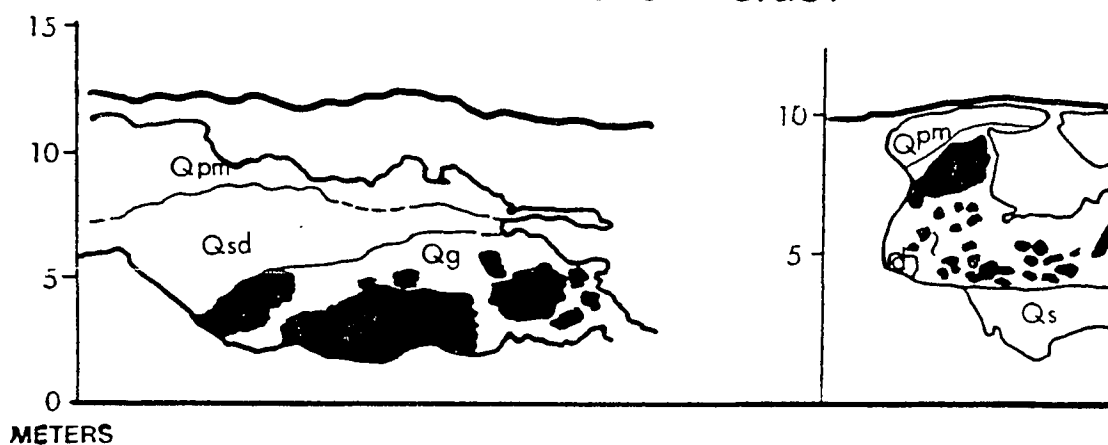






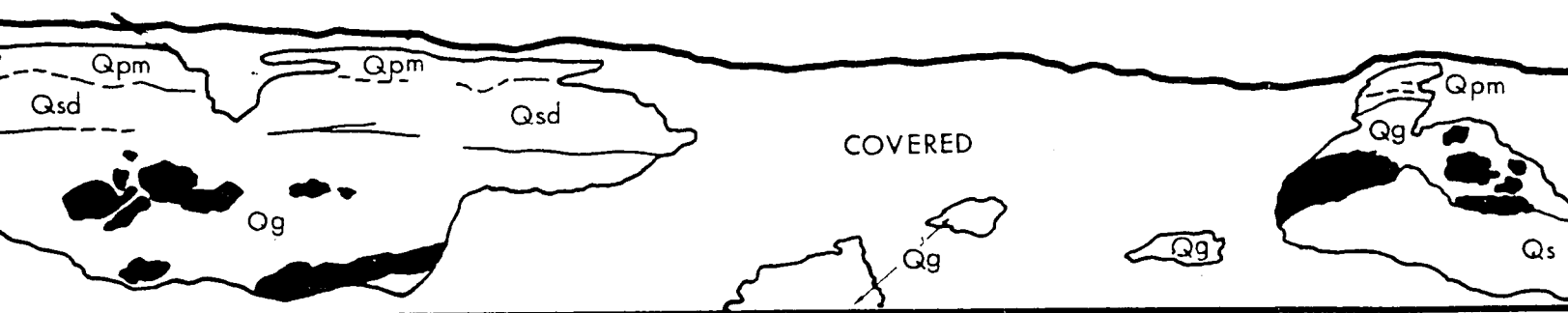
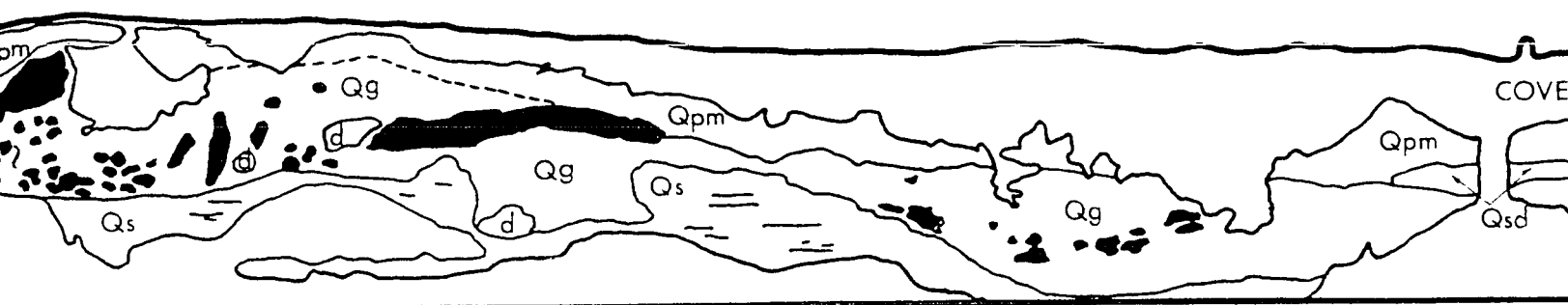
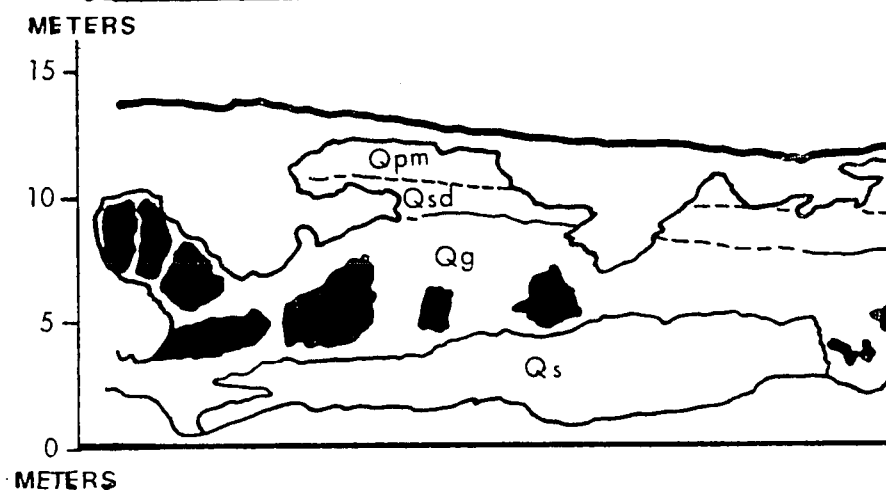
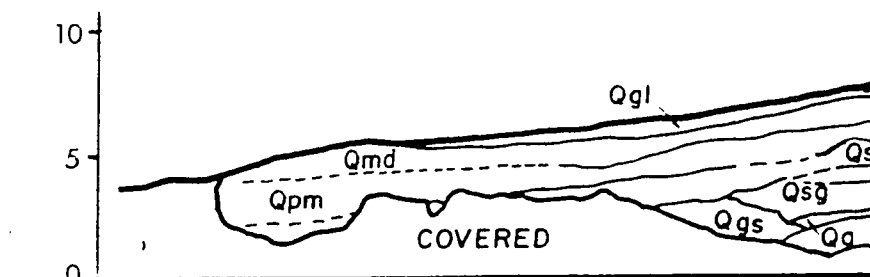
SAN DE FUCA, EAST

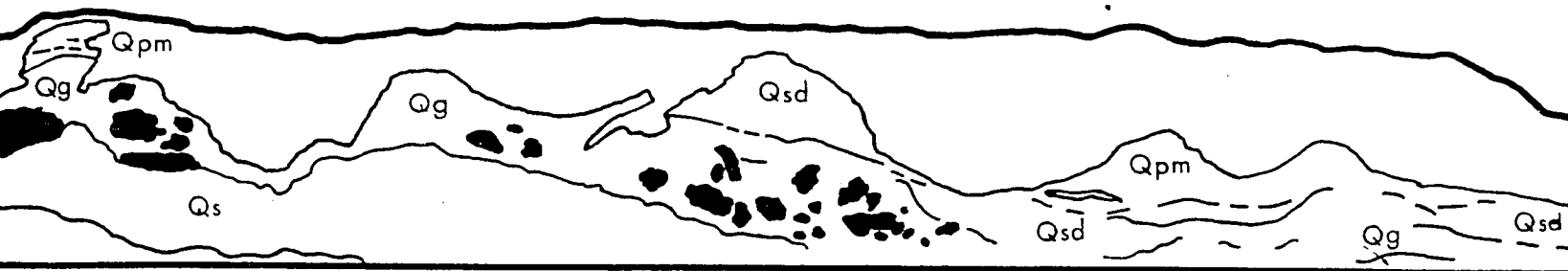
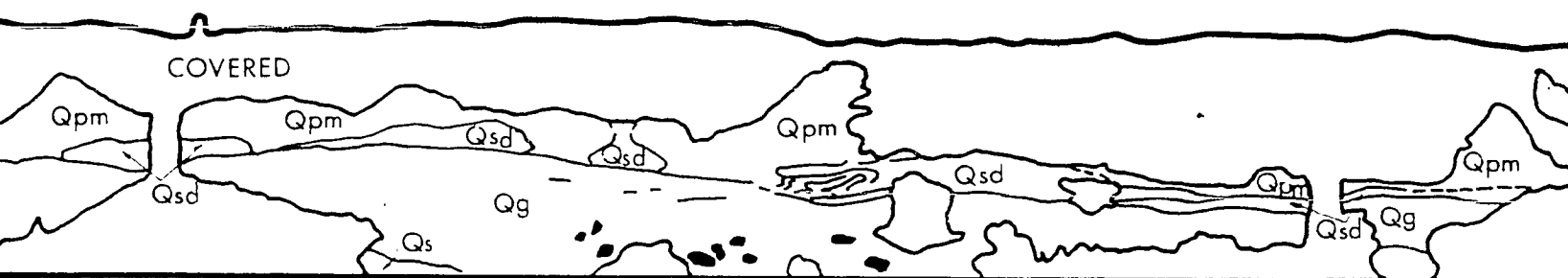
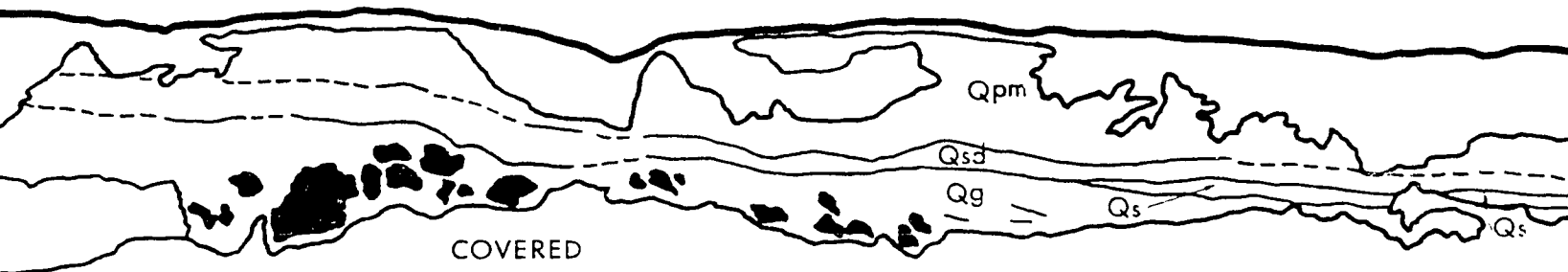
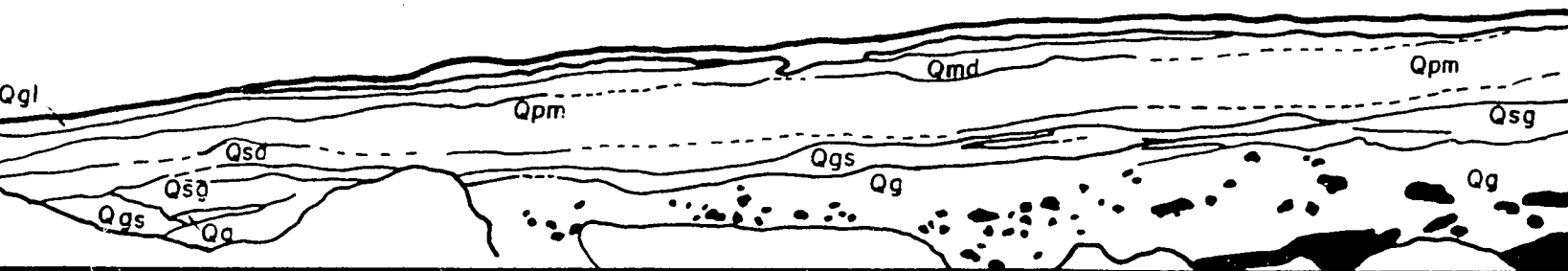
Qgl	gravelly sand, lag		E
Qmd	massive fossiliferous d		
Qpm	pebbly mud		
Qsd	stratified diamicton		I
Qs	stratified sand		
Qgs	gravelly sand		
Qsg	sandy gravel		
Qg	gravel		
	massive silt clast		
	diamicton clast		

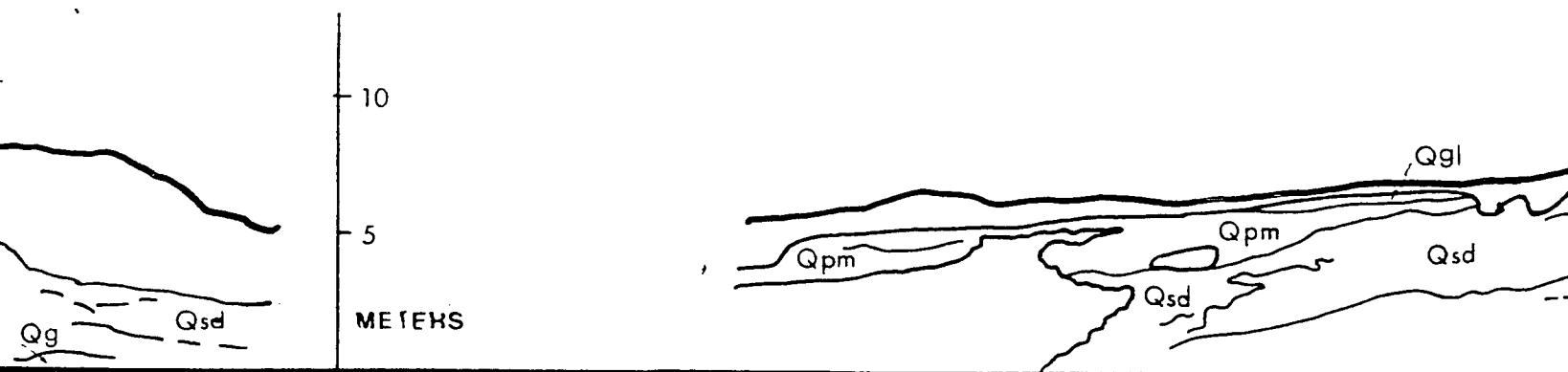
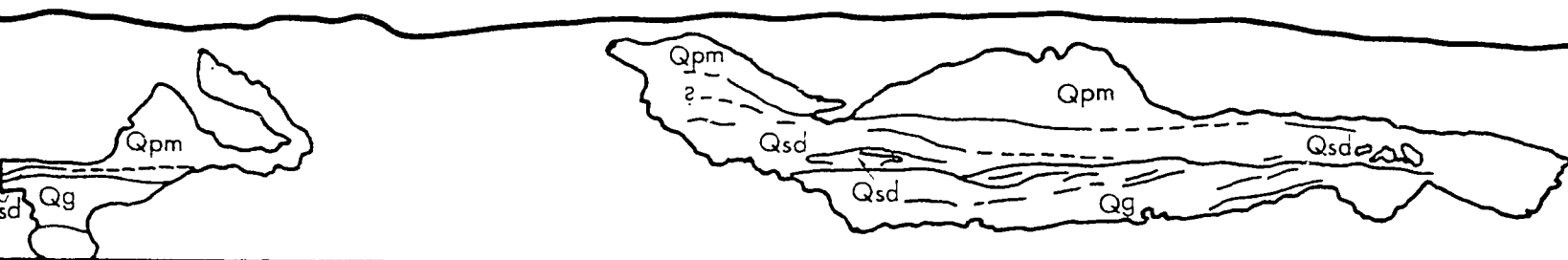
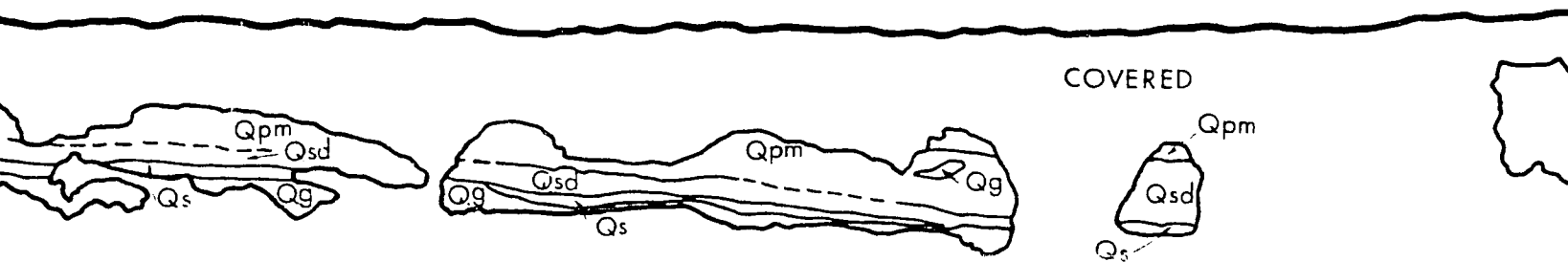
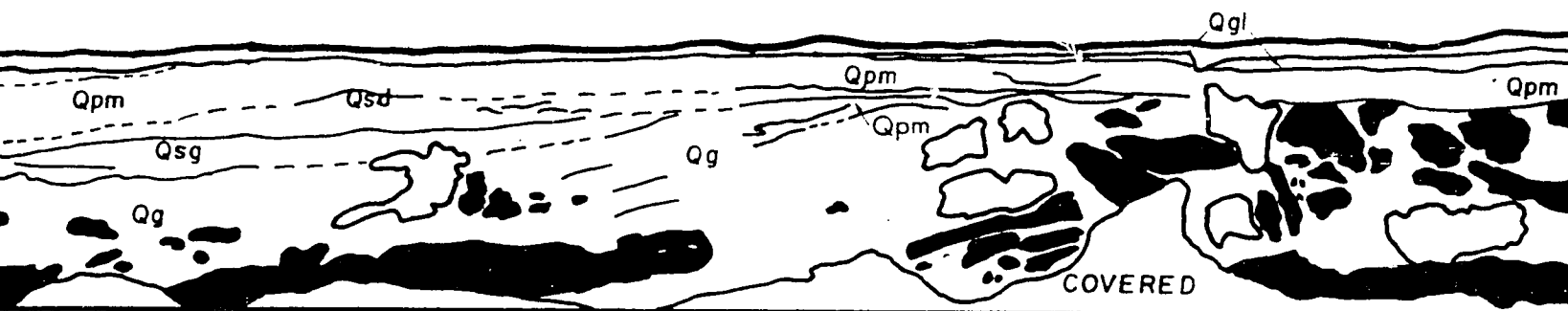


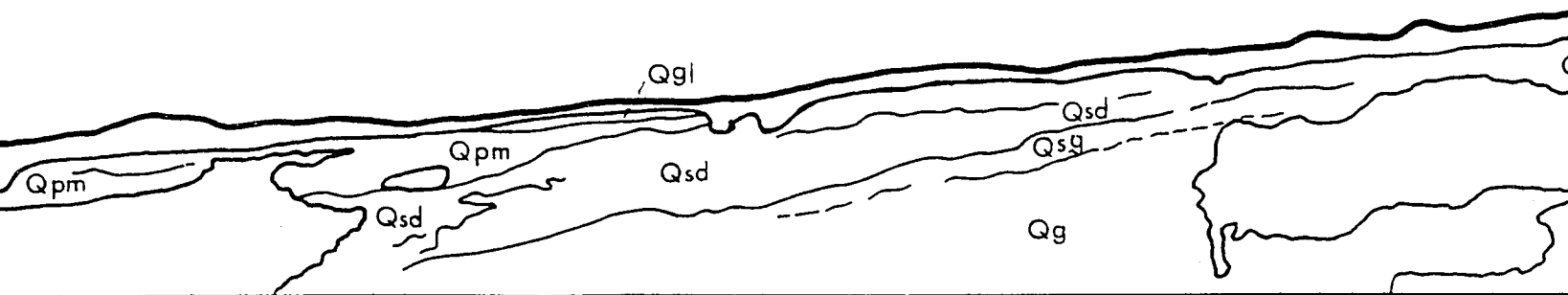
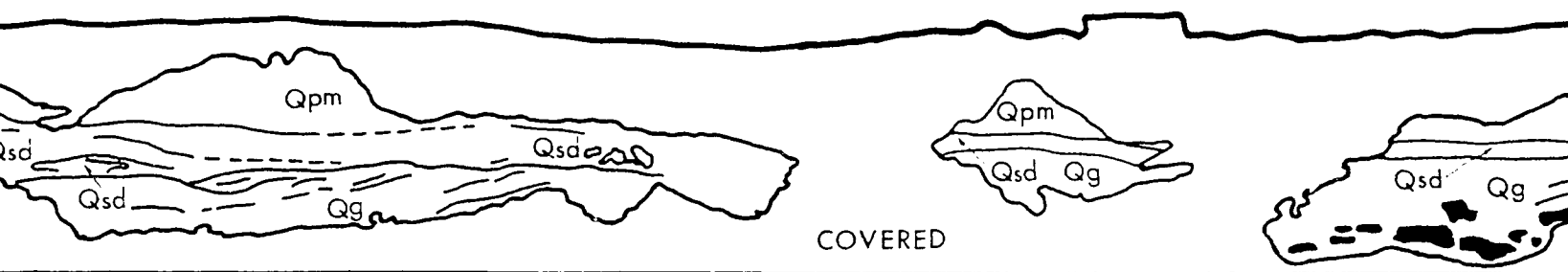
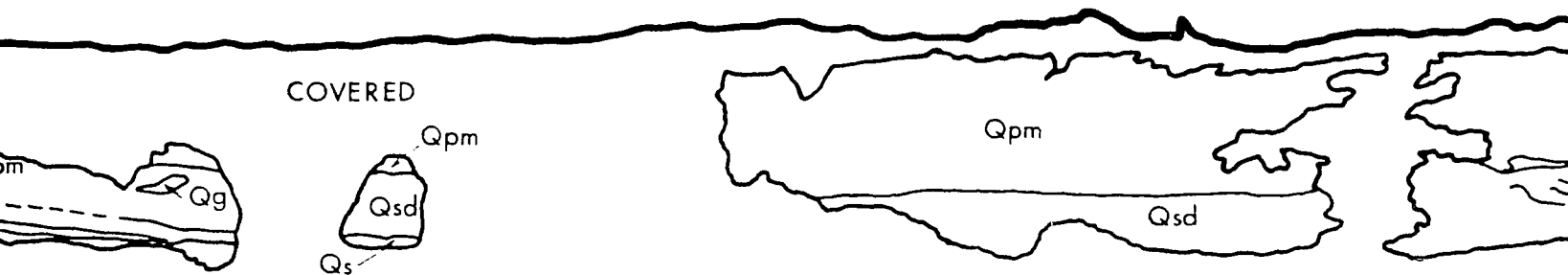
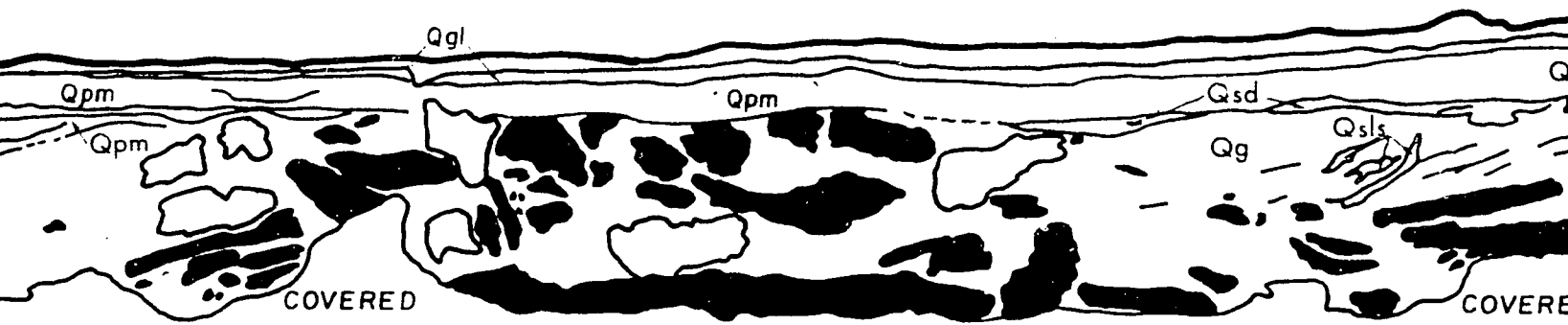
[] EMERGENCE DEPOSITS
 [] GLACIAL-
 [] MARINE
 [] ICE MARGINAL / MARINE

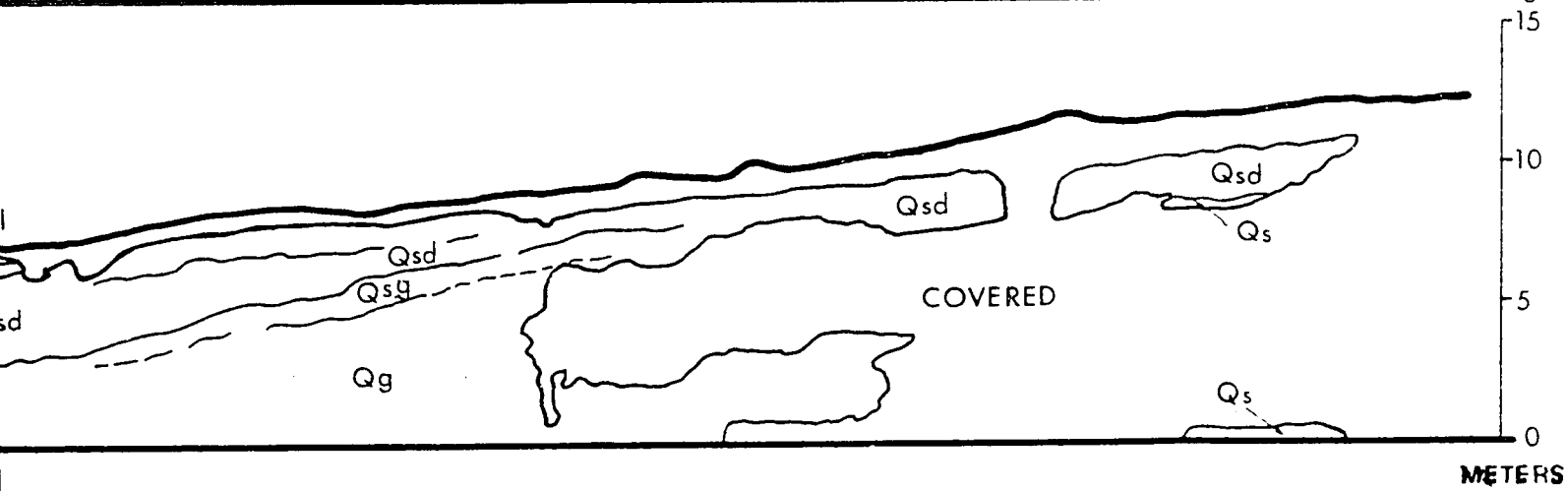
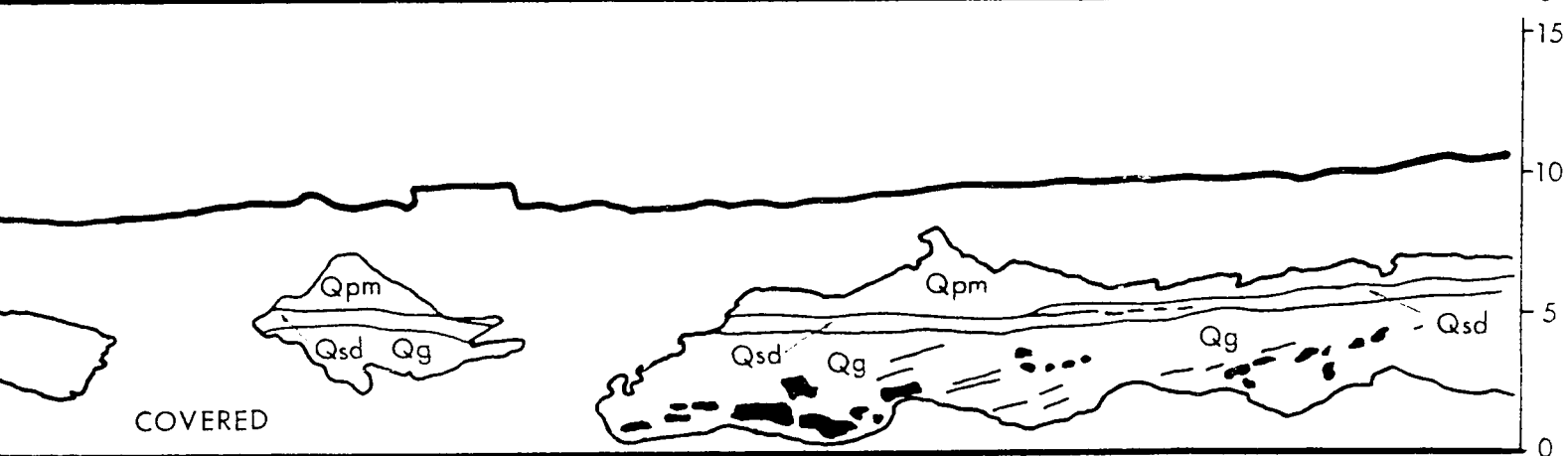
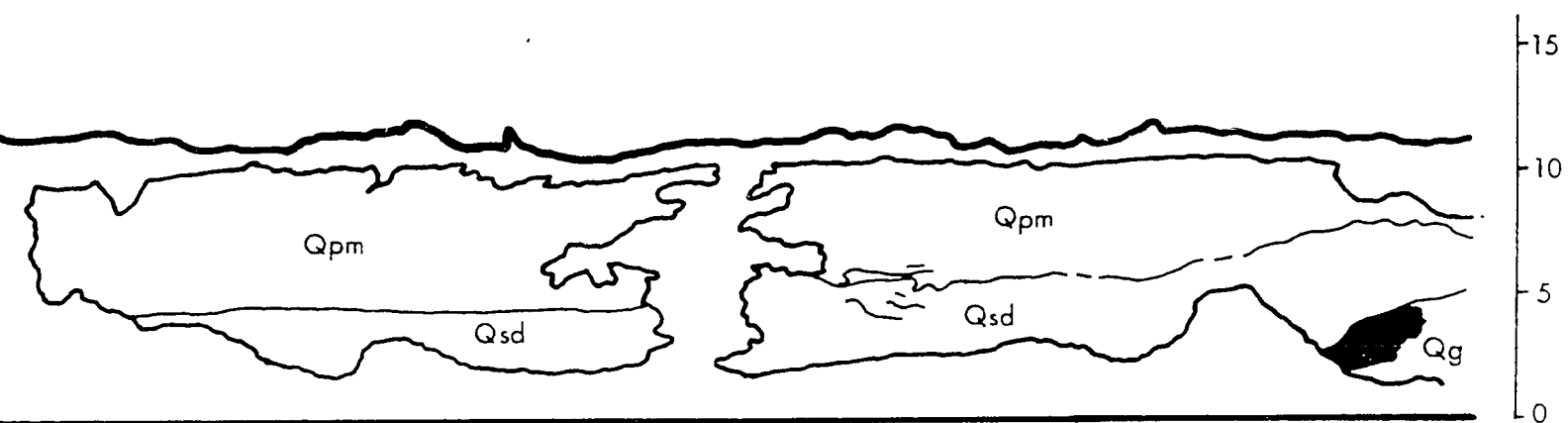
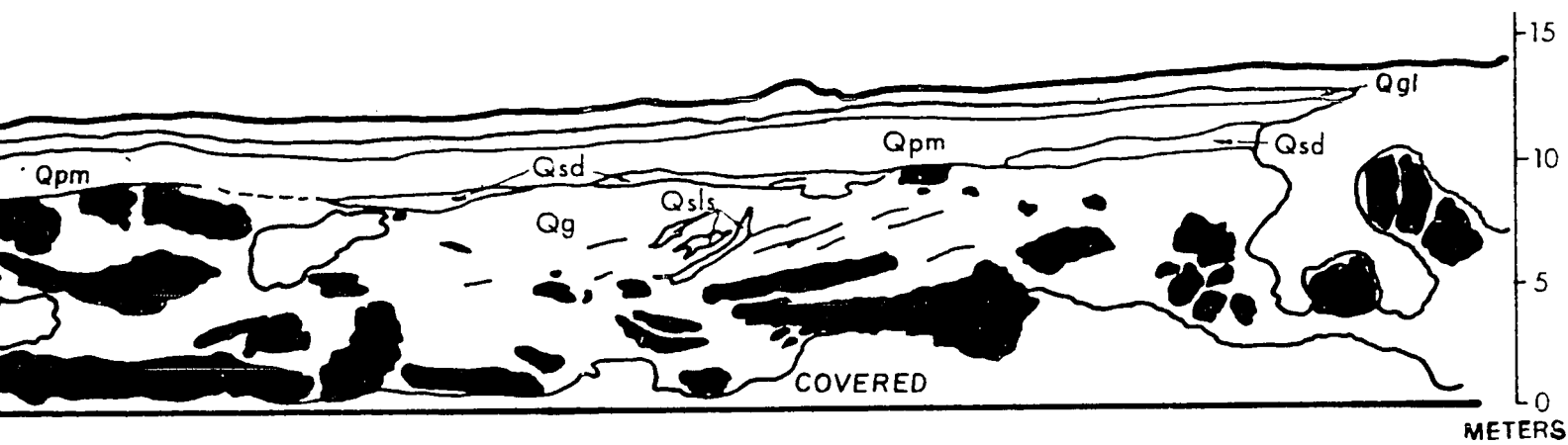
— contact
 — covered



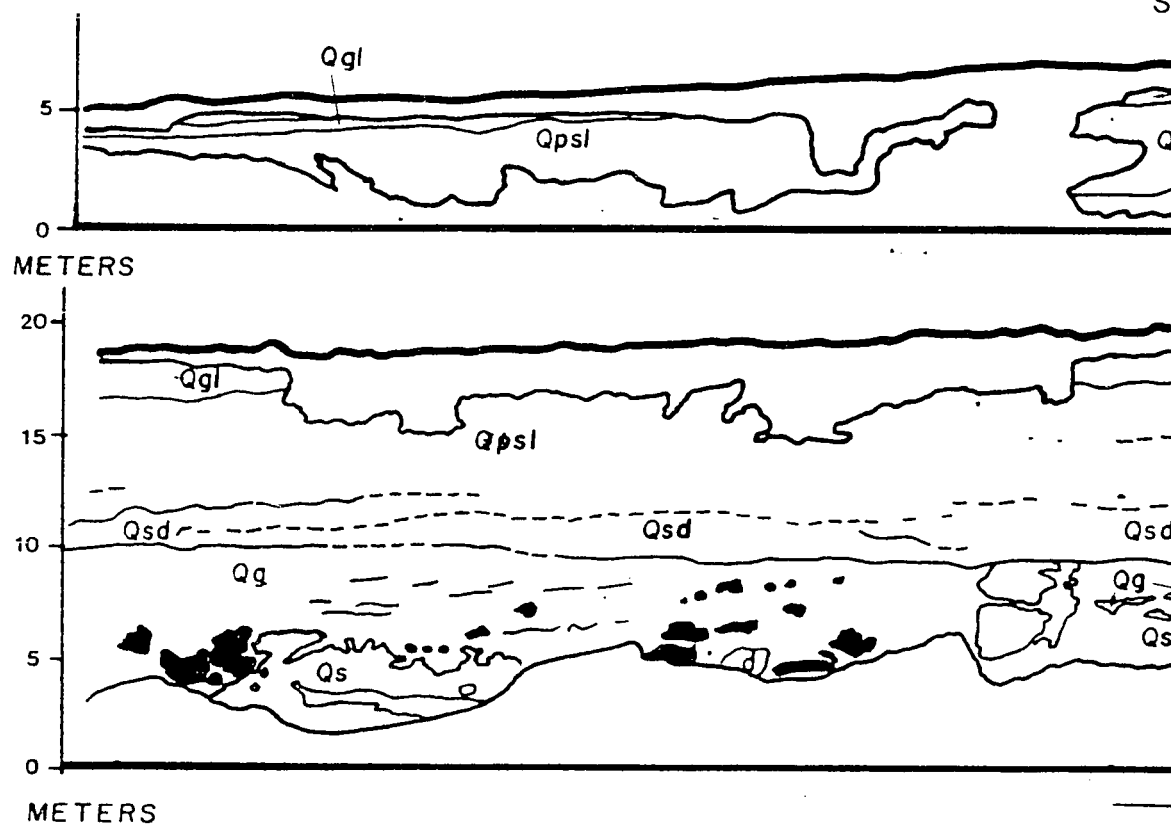








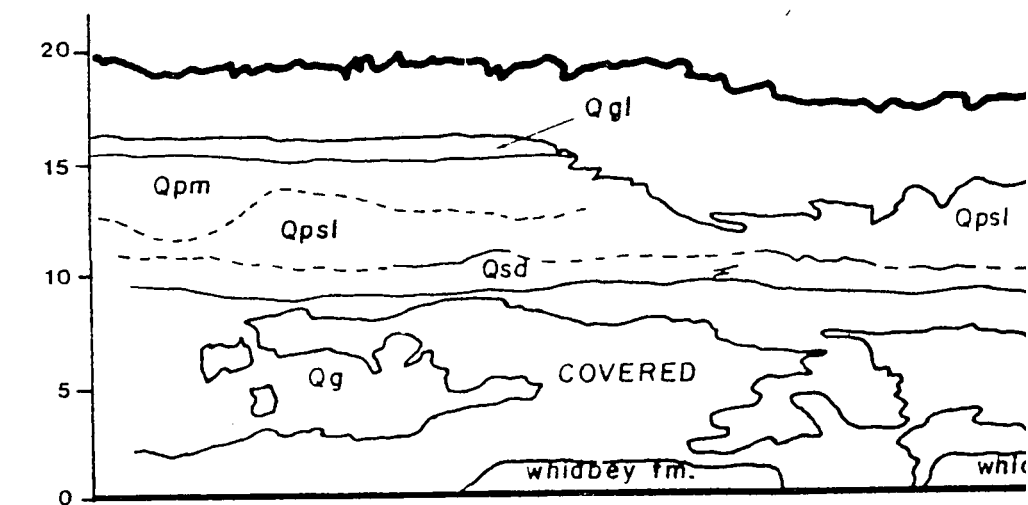
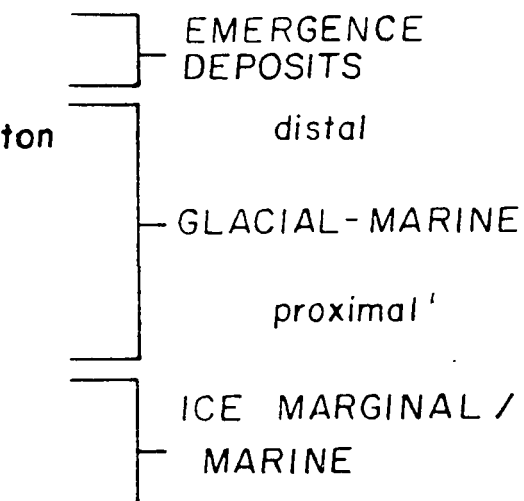
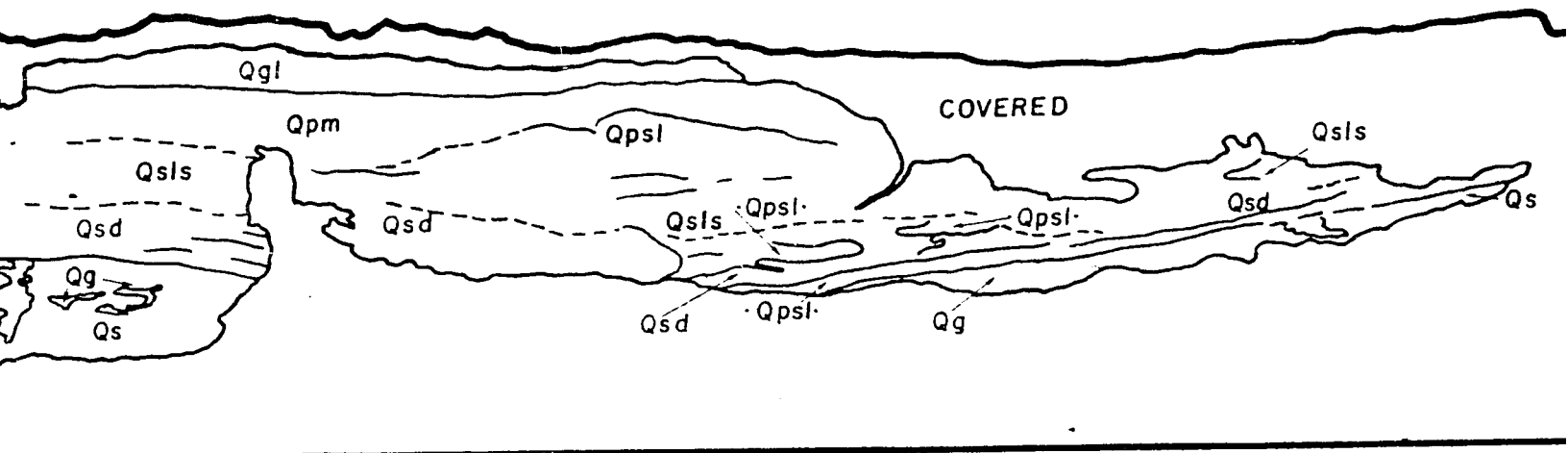
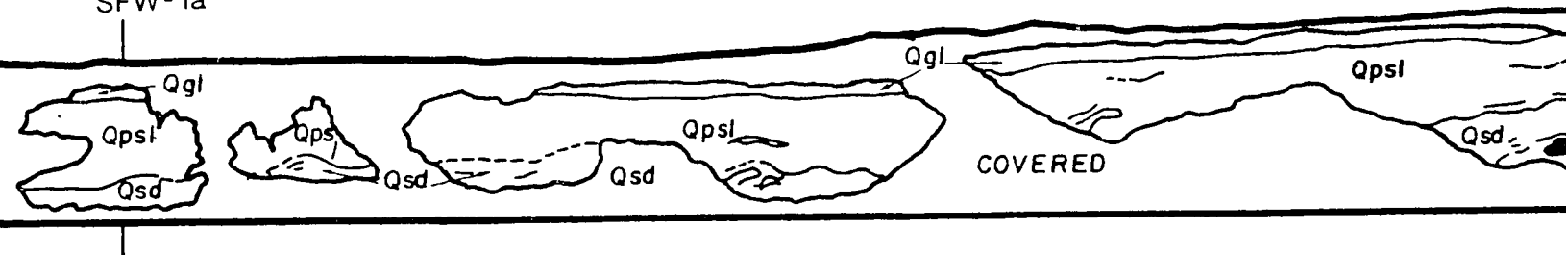
SAN DE FUCA, WE



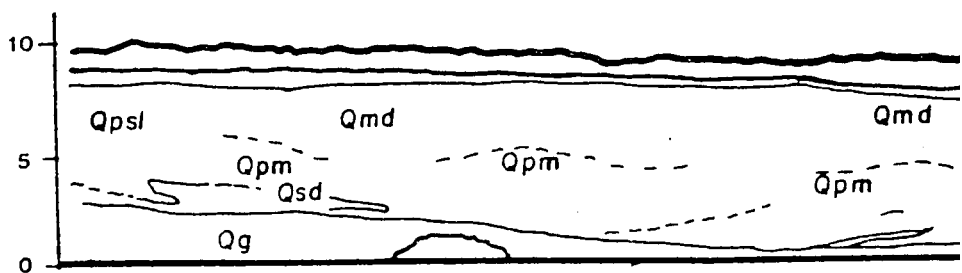
Qgl	gravelly sand, lag
Qmd	massive fossiliferous diamicton
Qpm	pebbly mud
Qpsl	pebbly silt
Qsls	sandy silt
Qsd	stratified diamicton
Qpsl	silty matrix
Qsg	sandy gravel
Qg	gravel
Qs	sand
Qsl	laminated silt

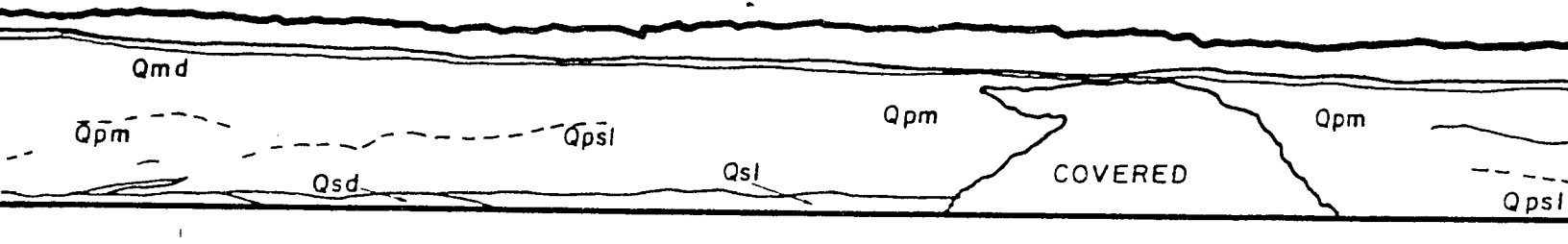
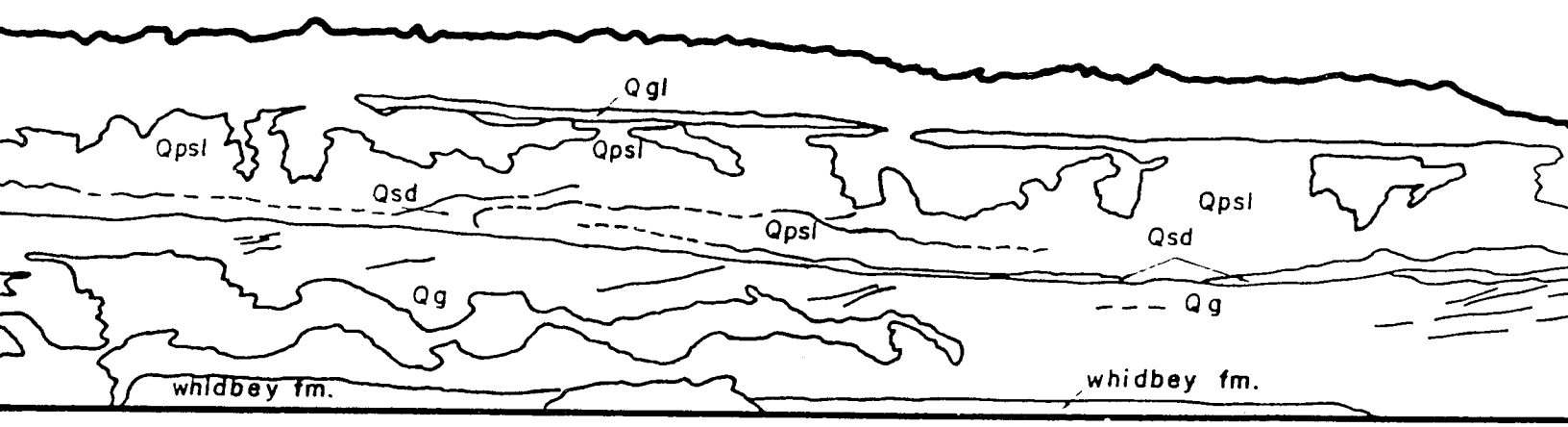
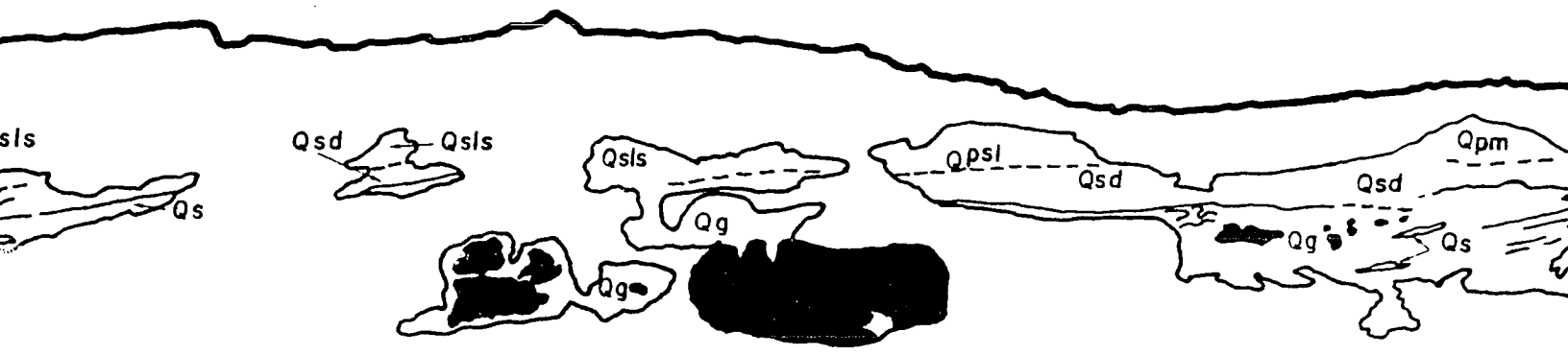
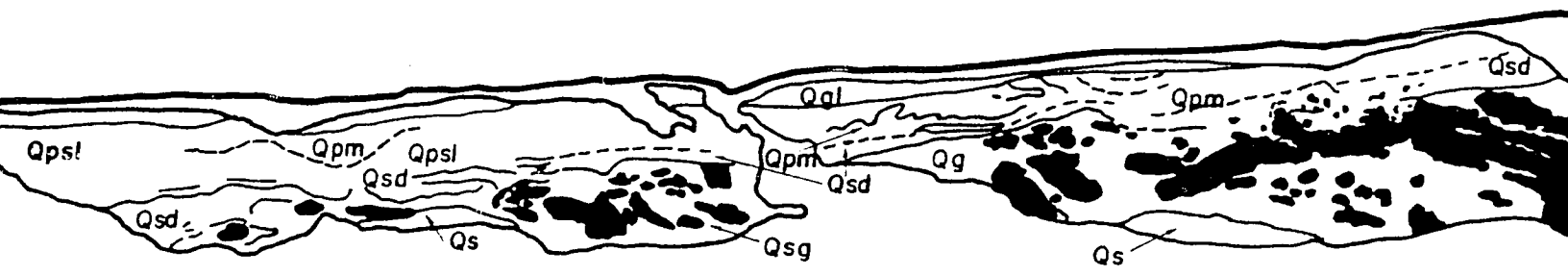
WEST

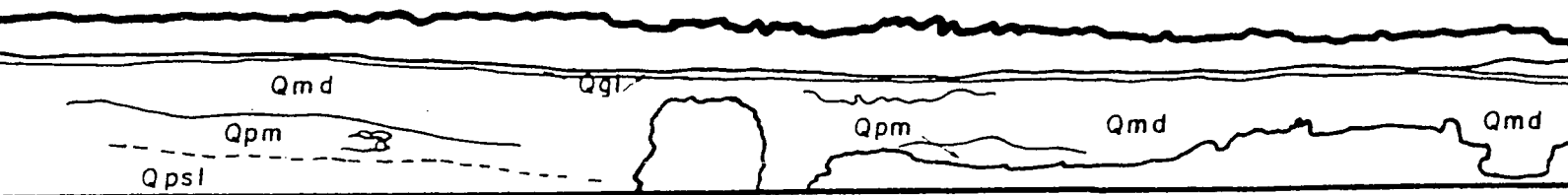
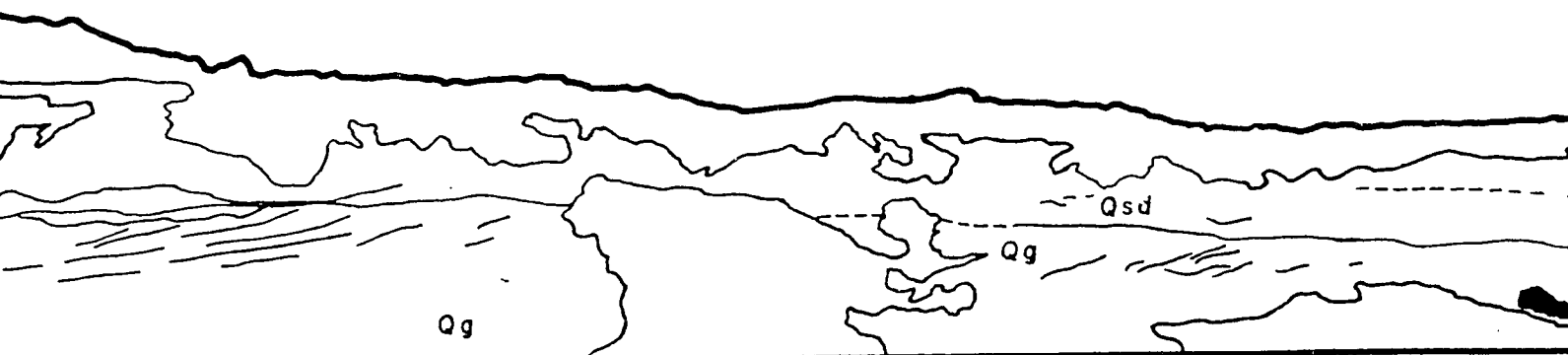
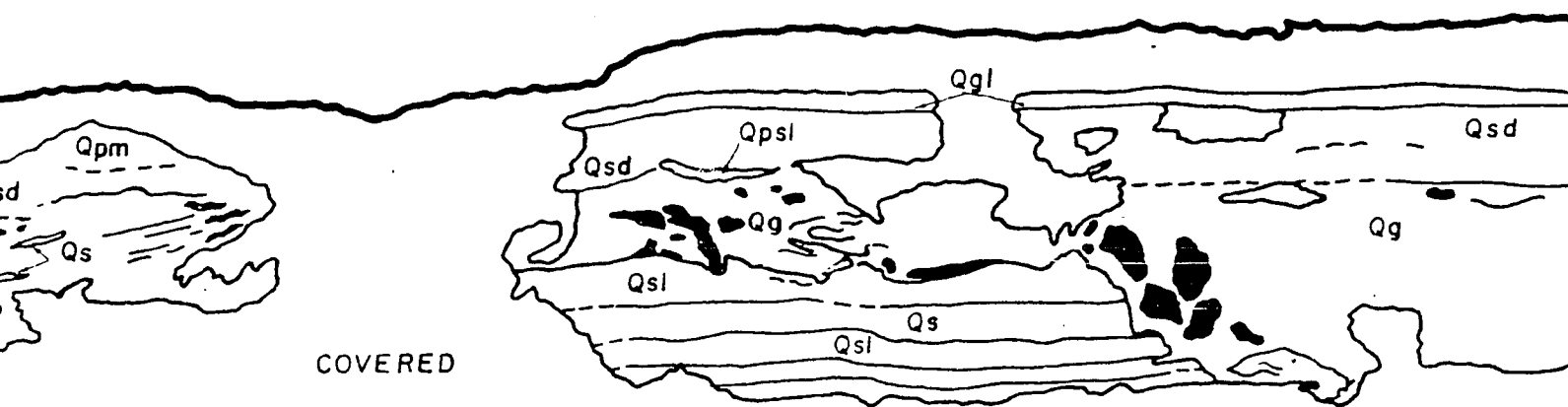
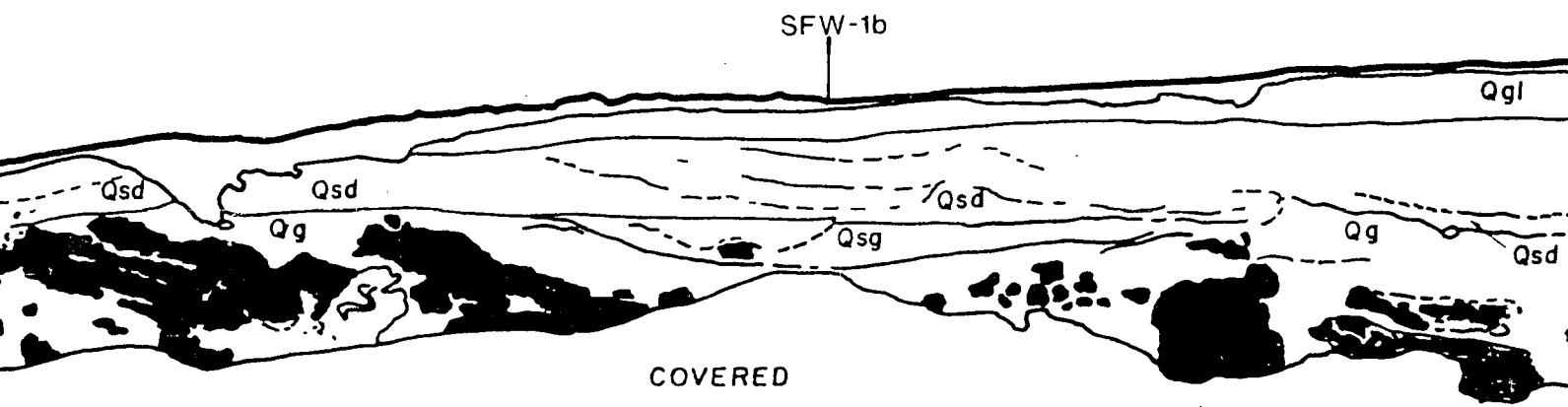
SFW-1a

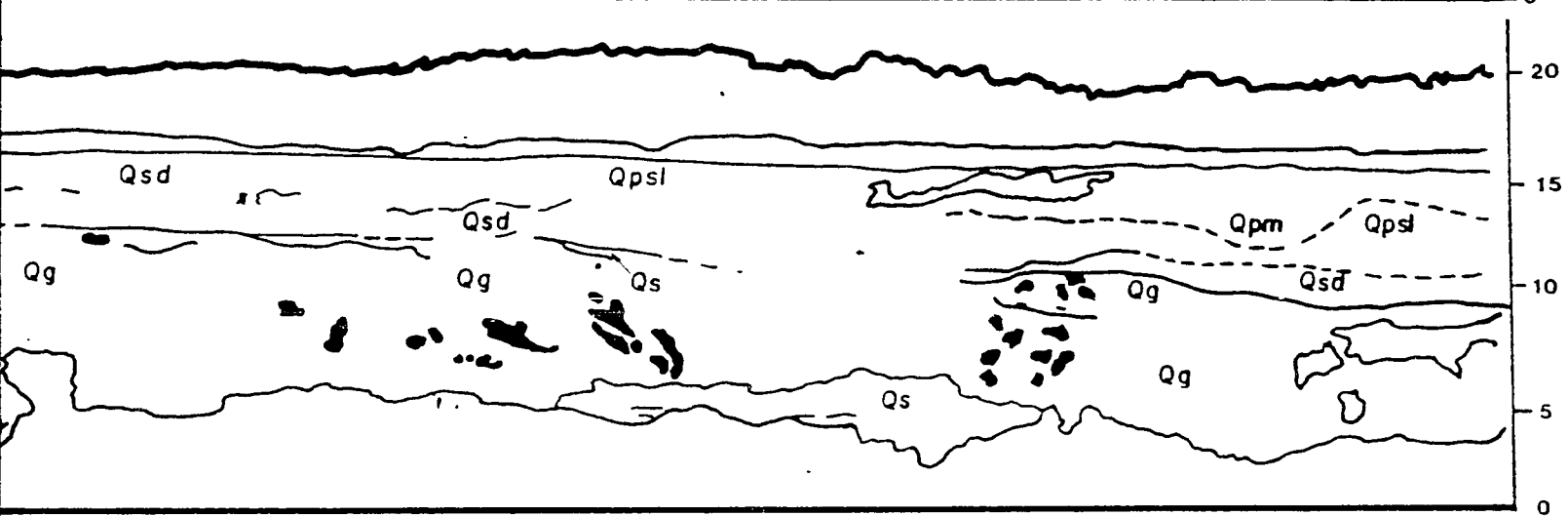
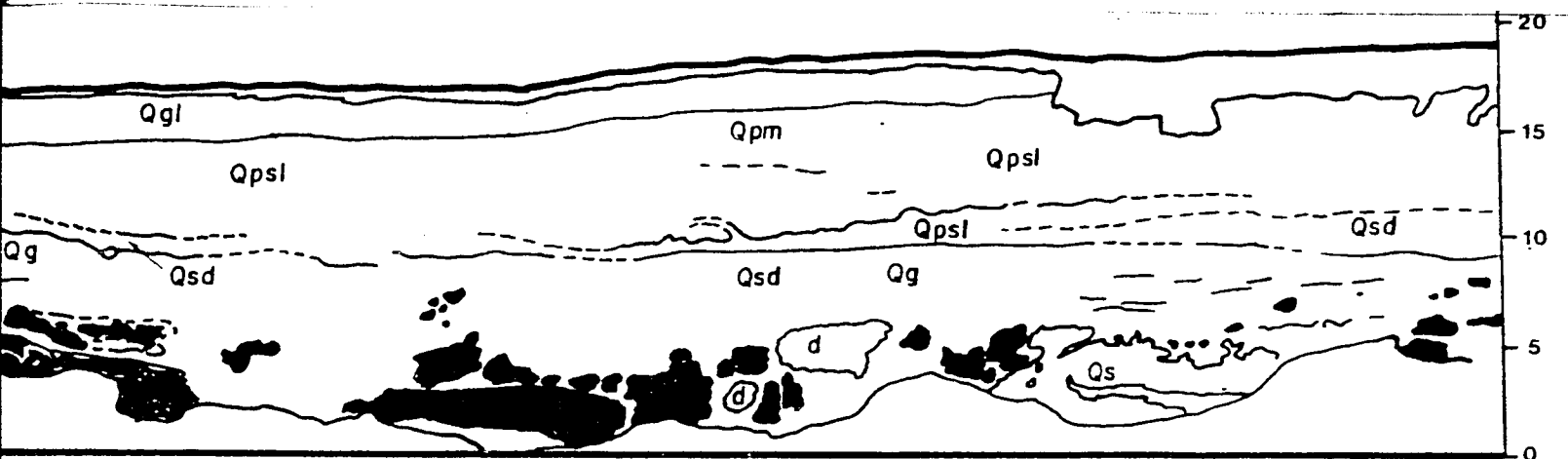


METERS

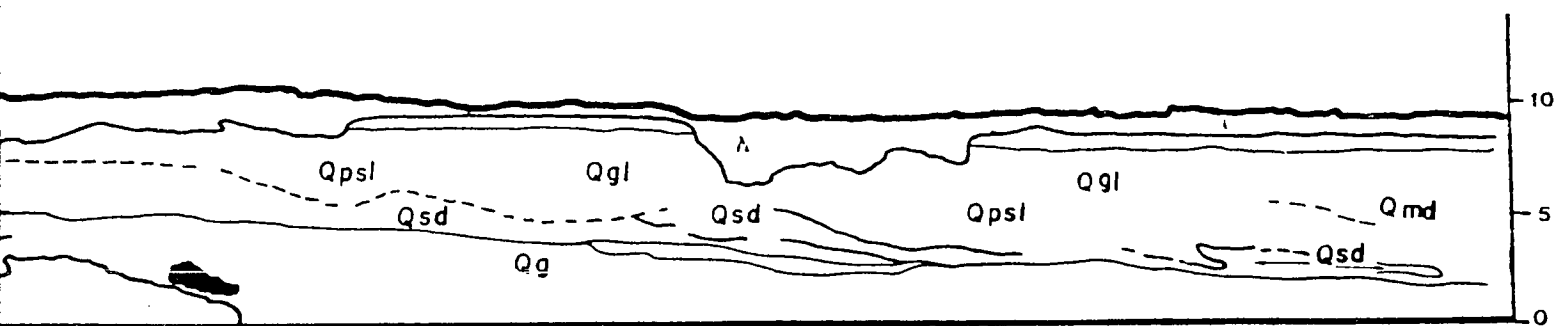




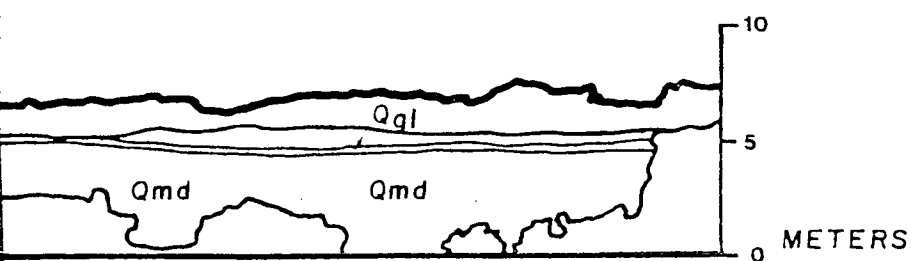




METERS

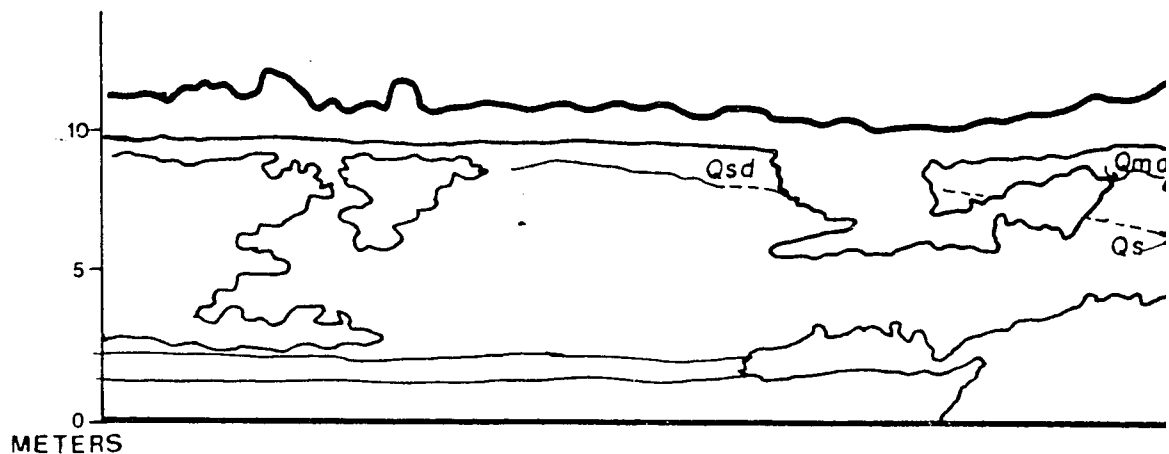


METERS

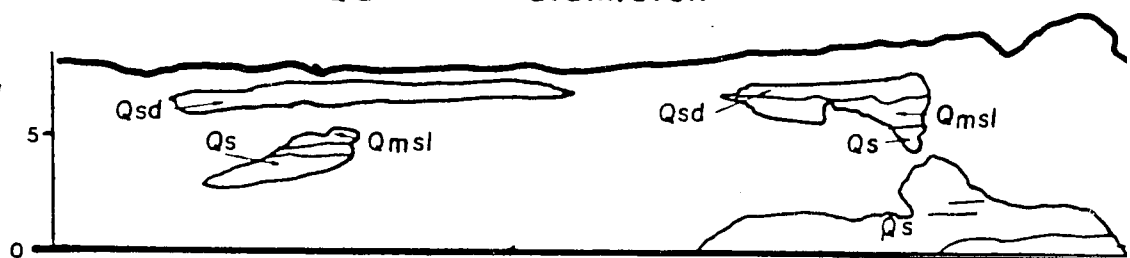


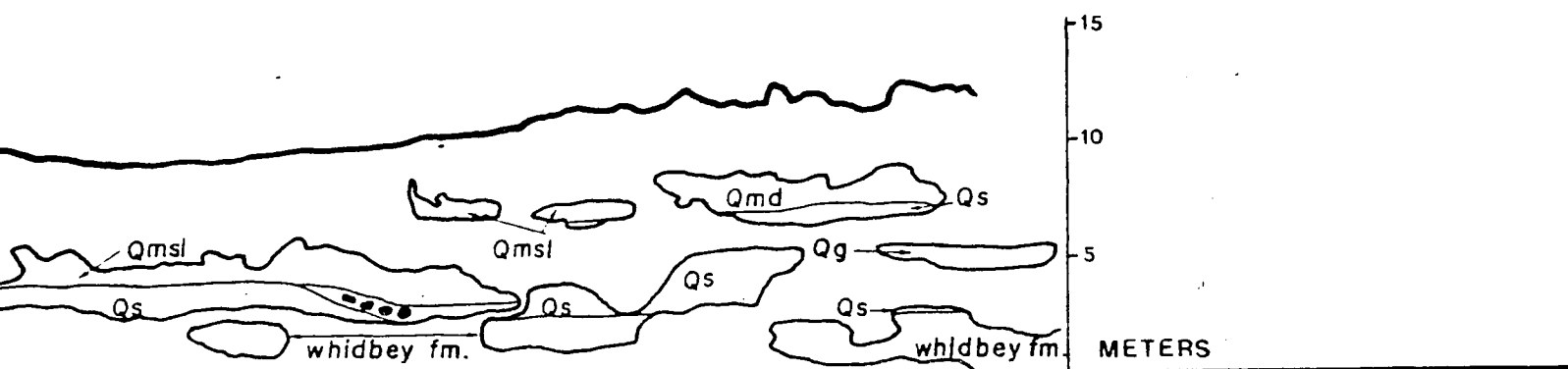
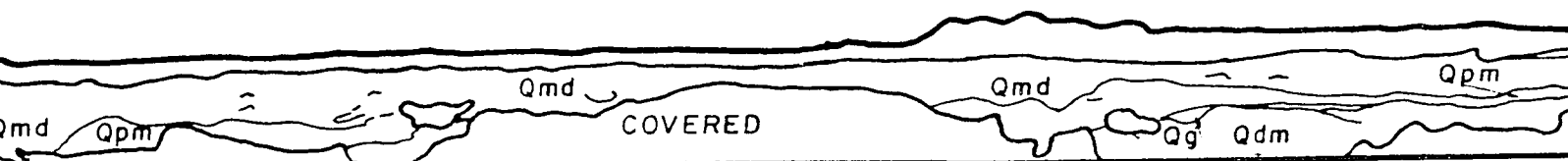
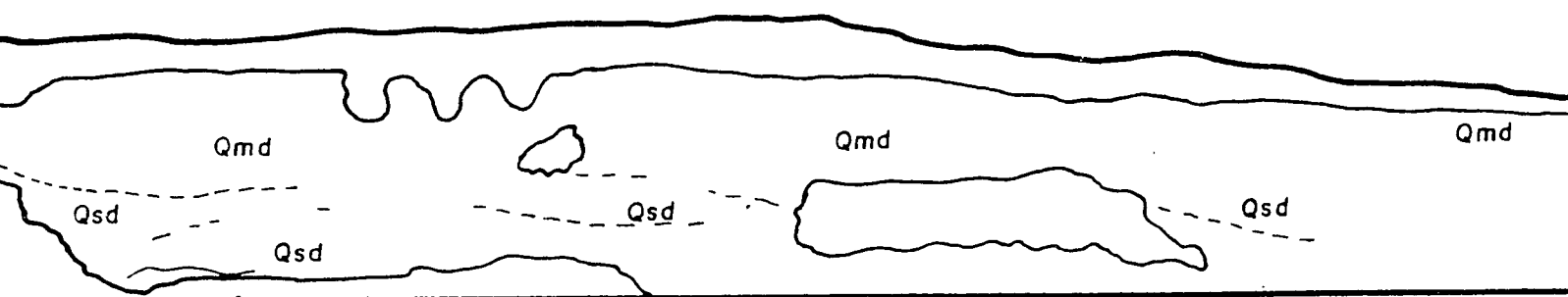
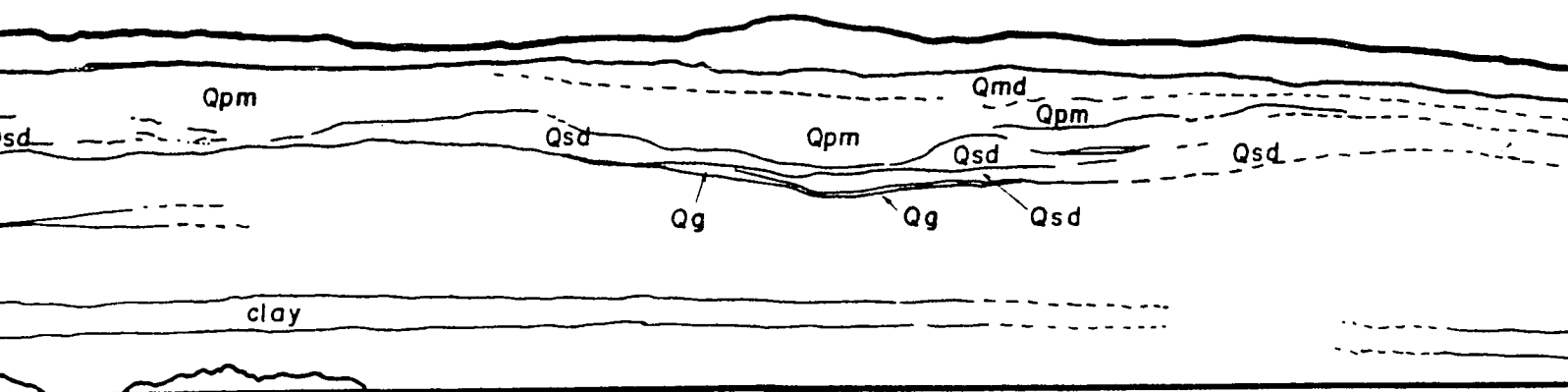
METERS

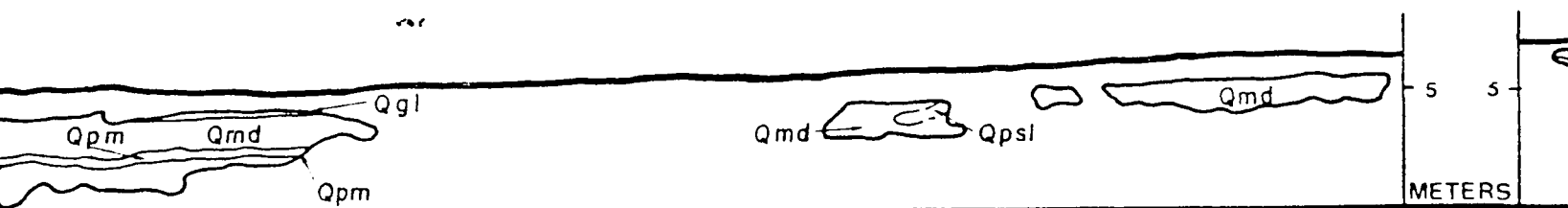
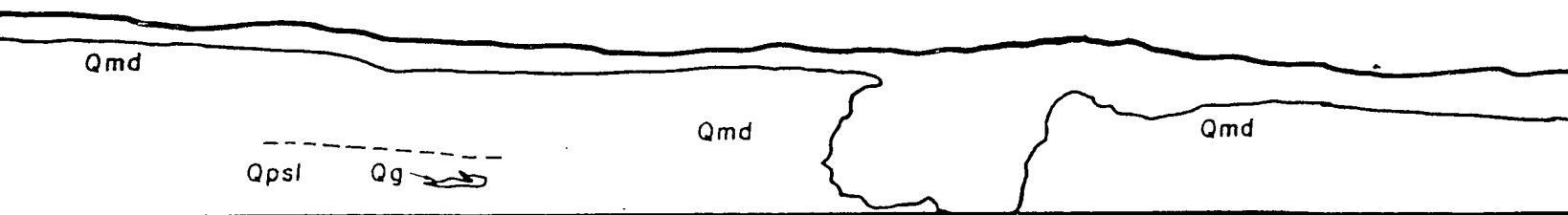
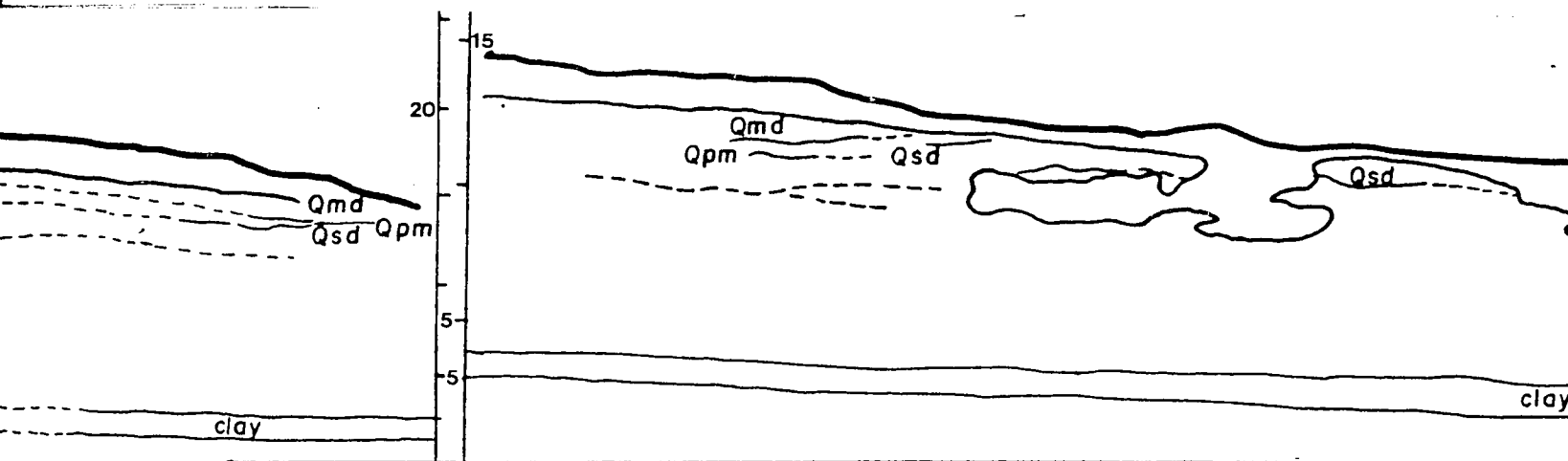
Qmd	massive fossiliferous diamicton
Qpm	pebbly mud
Qpsl	pebbly silt
Qsd	stratified diamicton
Qg	gravel
Qs	sand

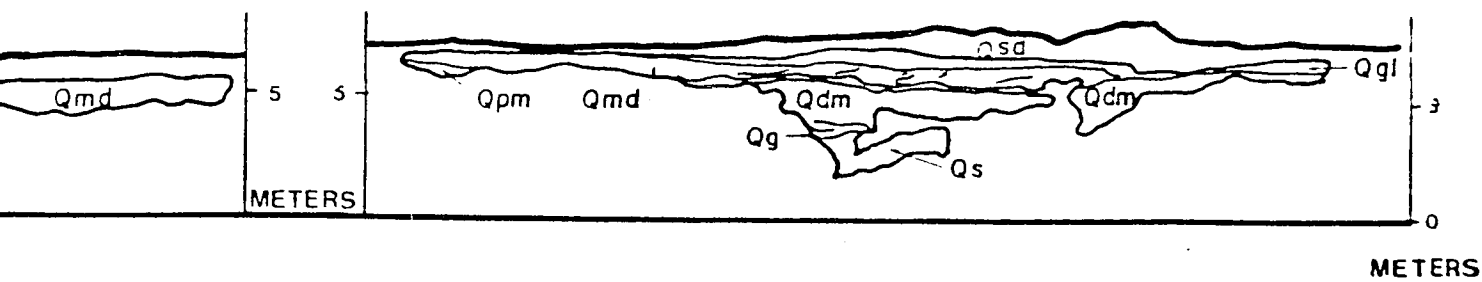
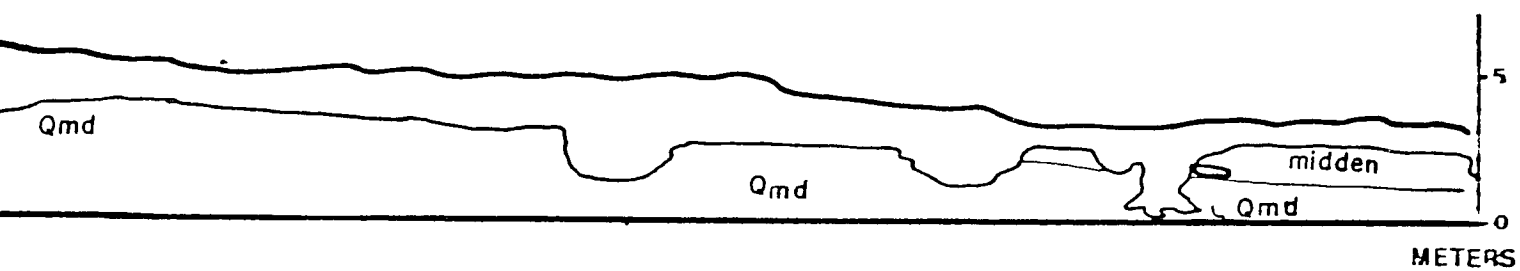
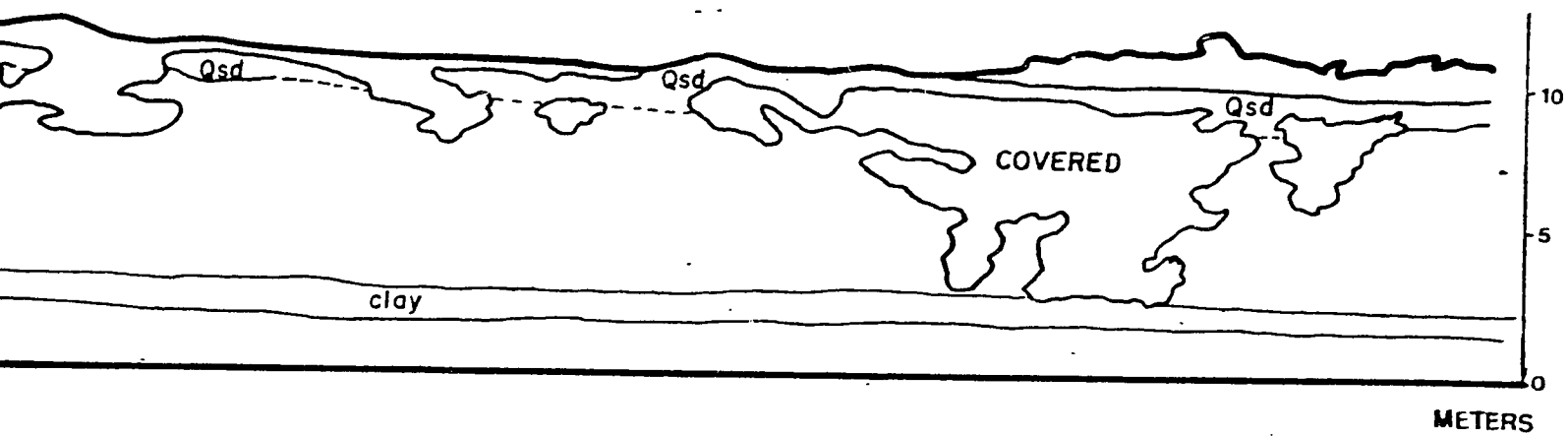


Qgl	gravel lag
Qmd	massive fossiliferous diamicton
Qpm	pebbly mud, lam. silt and clay
Qpsl	pebbly silt
Qsd	stratified diamicton
Qdm	massive diamicton
Qmsl	massive silt
Qs, Qg	sand, gravel
Qd	diamicton

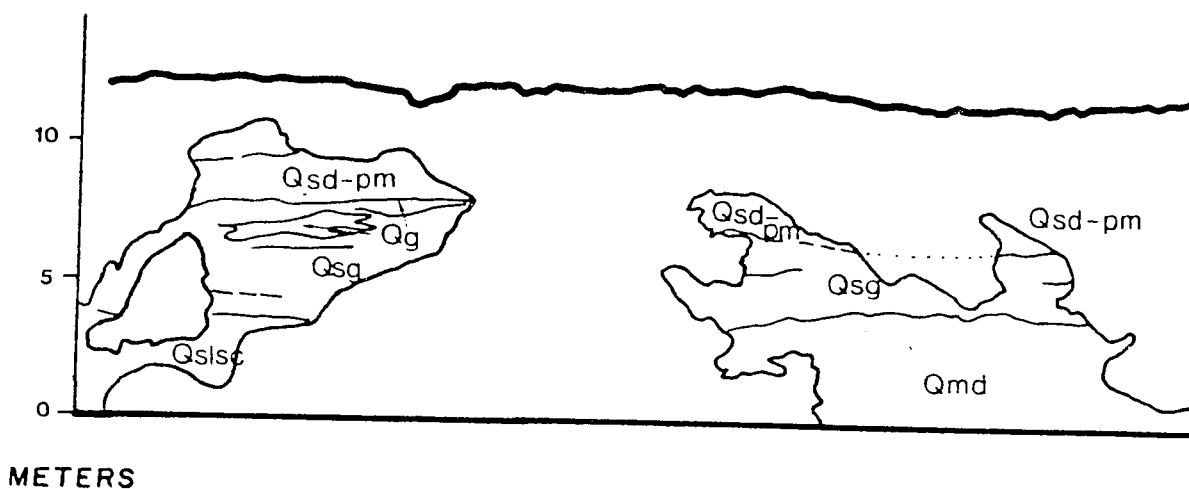




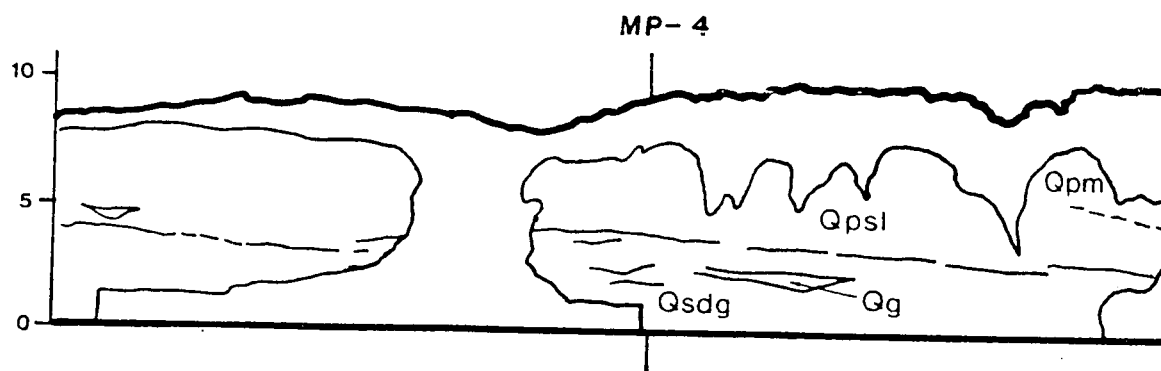




Qmd	massive diamicton	GLACI	disto
Qpm	pebbly mud		
Qpsl, Qps	pebbly silt, pebbly sand		
Qsls	stratified sandy silt, silty sand		
Qslc	silty clay	ICE M.	prox
Qc	clay		
Qsd	stratified diamicton		
Qg	gravel		
Qs	sand	GLA	
Qmd	massive diamicton		
Qsg	sandy gravel		
Qsds	silty stratified diamicton		
Qslsc	stratified sand, silt, clay		
Qsls	laminated silt and sand		



METERS



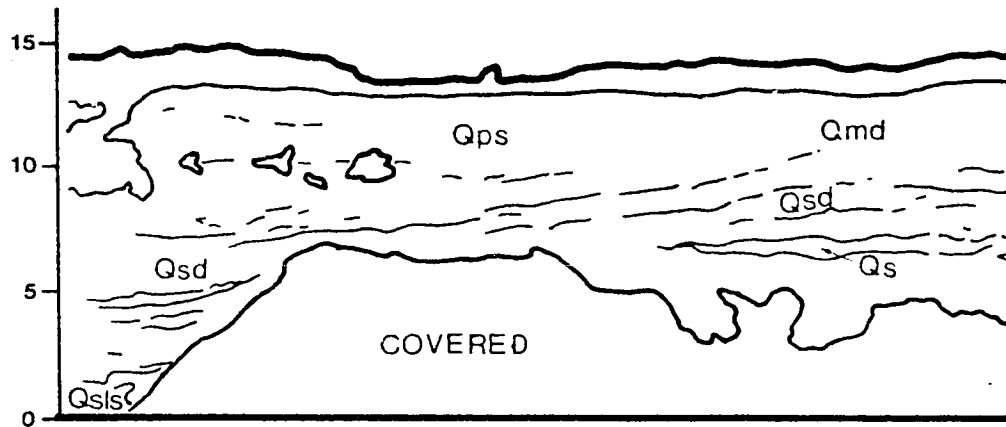
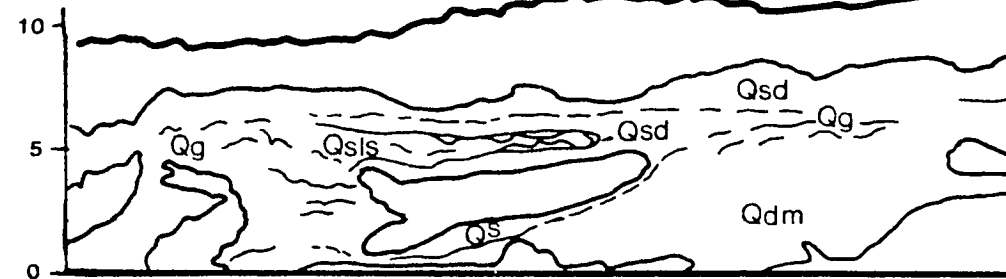
MAYLOR POINT

distal

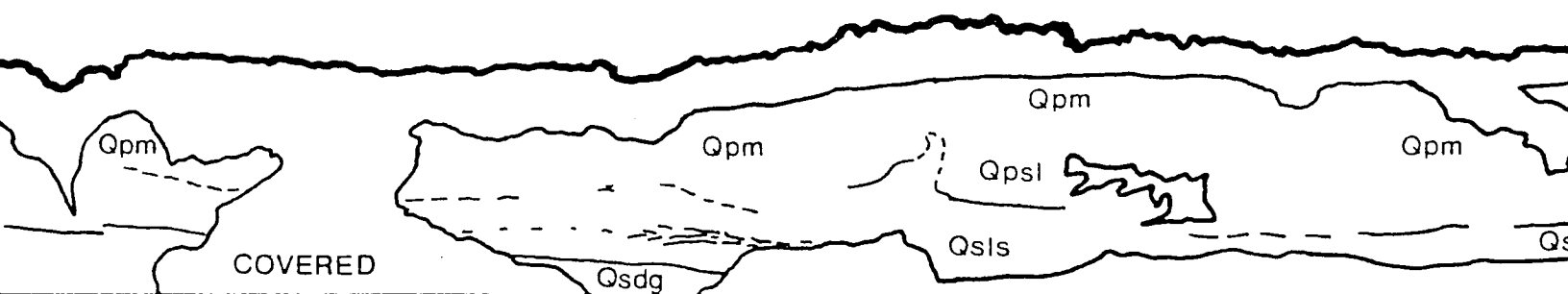
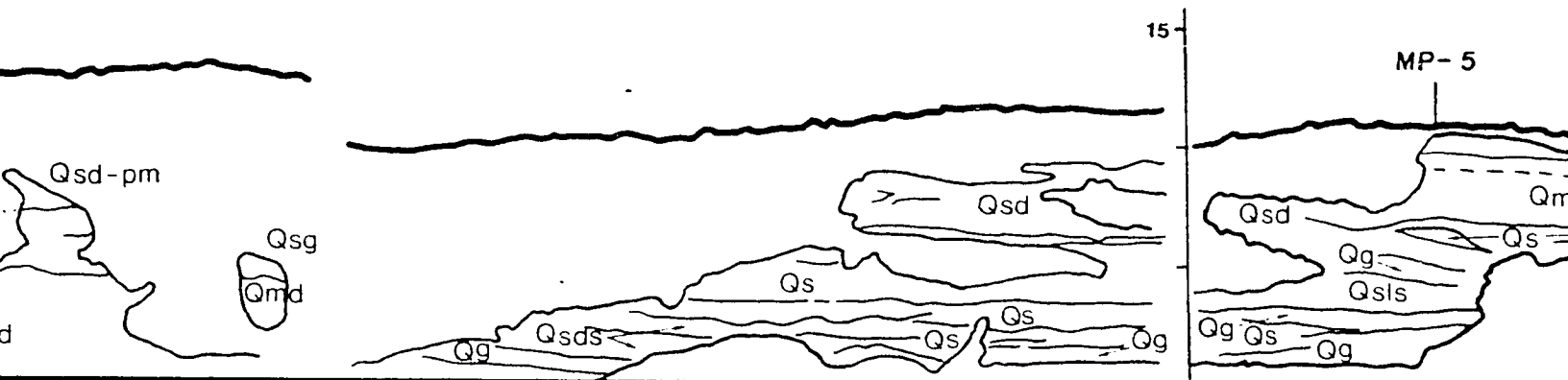
GLACIAL - MARINE

proximal

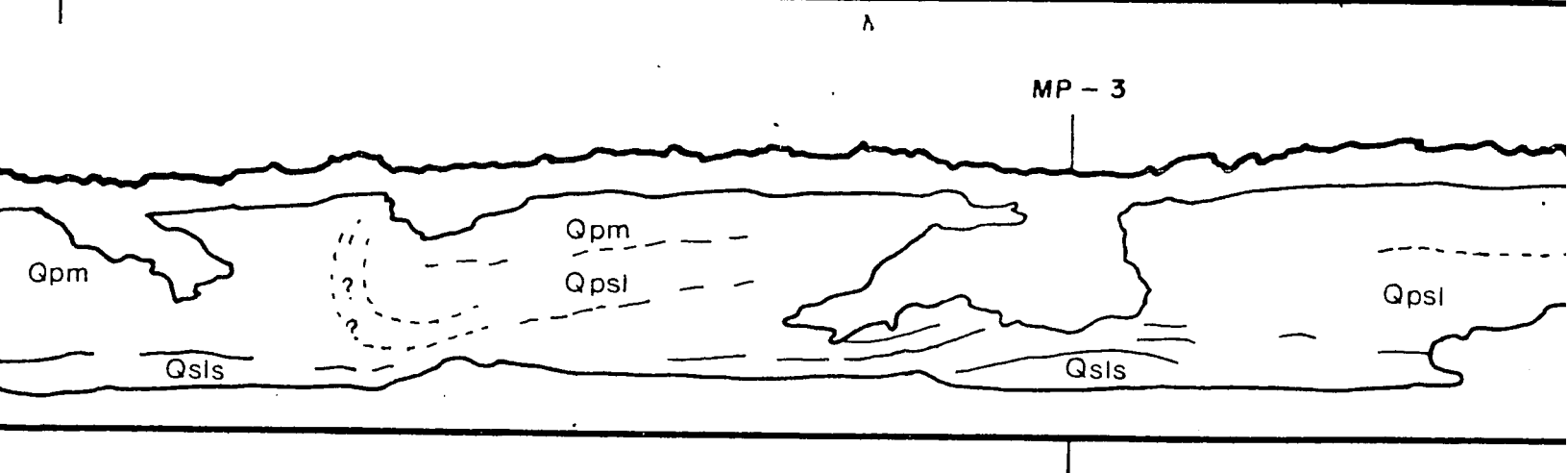
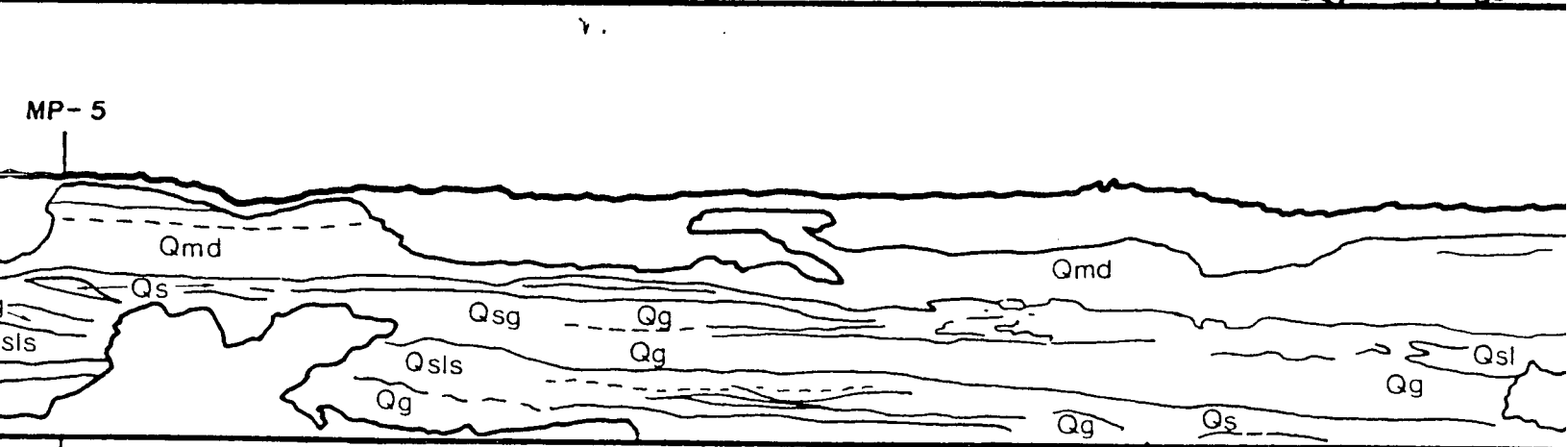
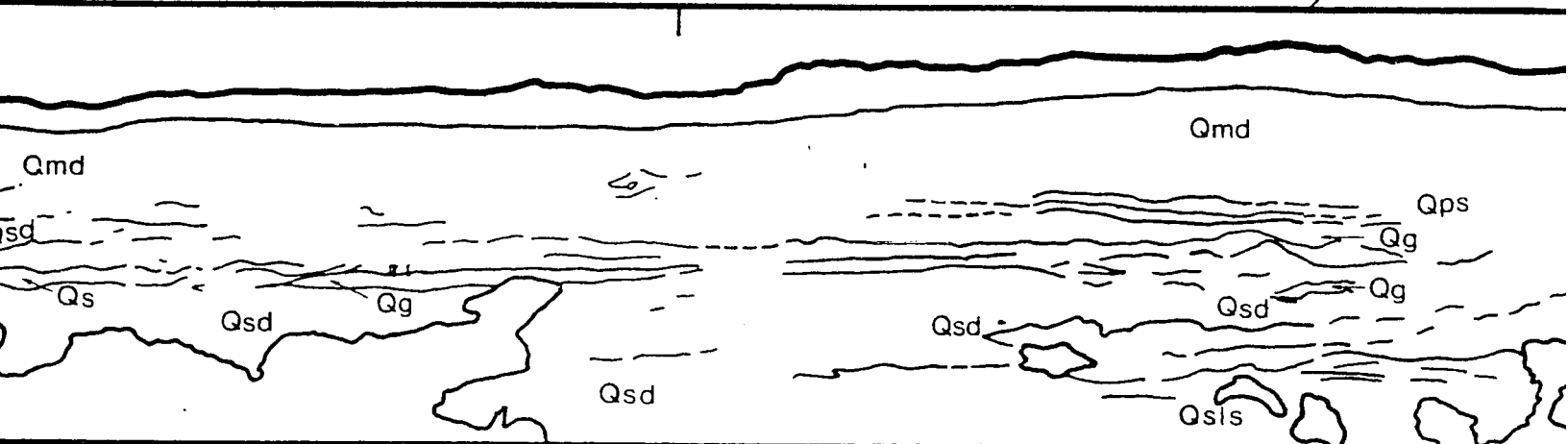
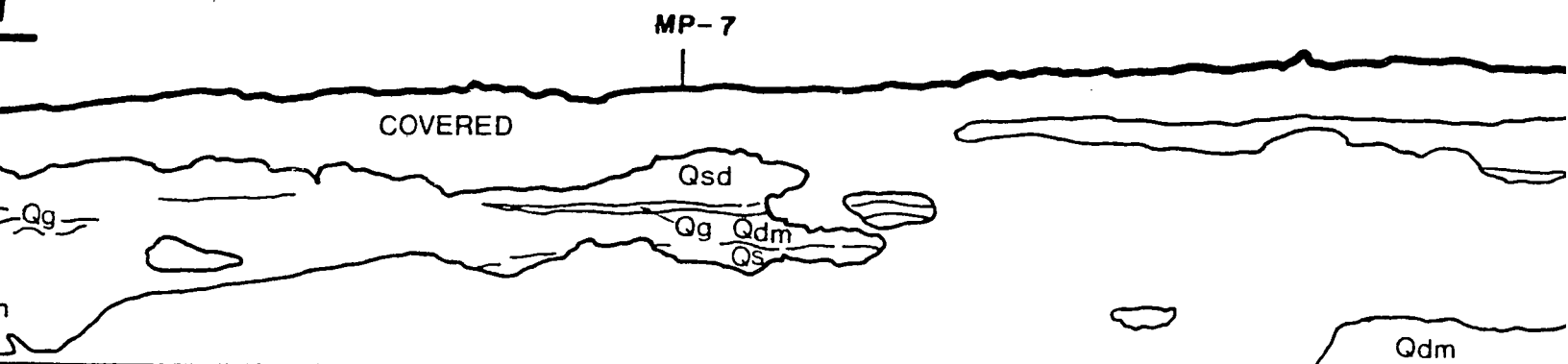
ICE MARGINAL / SUB -
GLACIAL ?

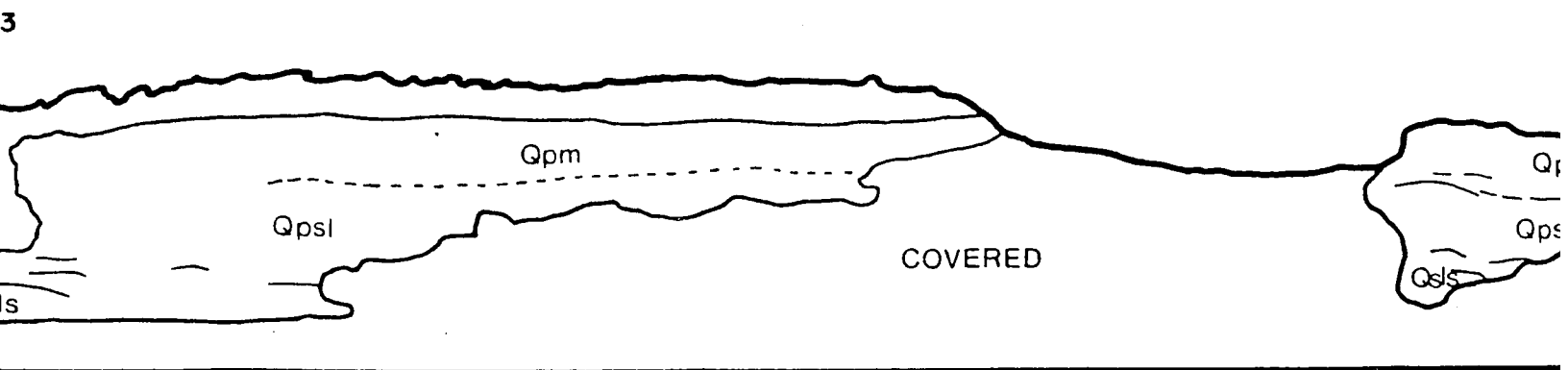
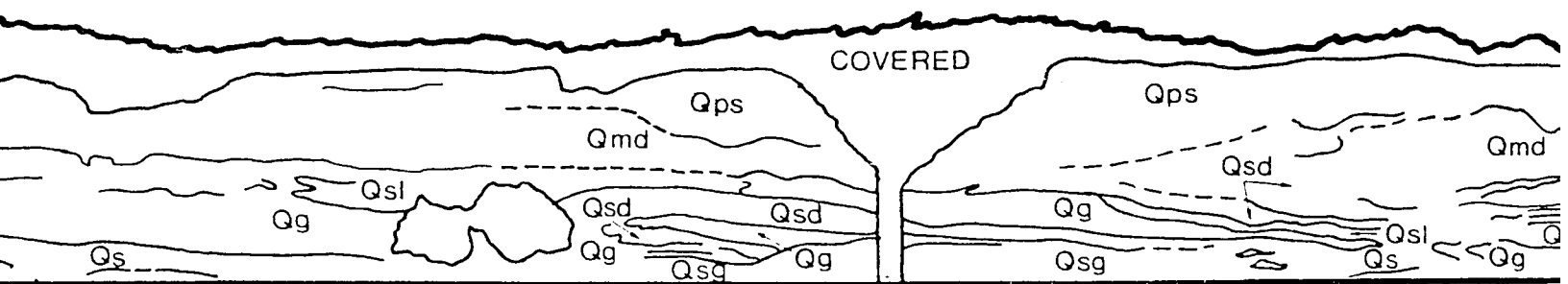
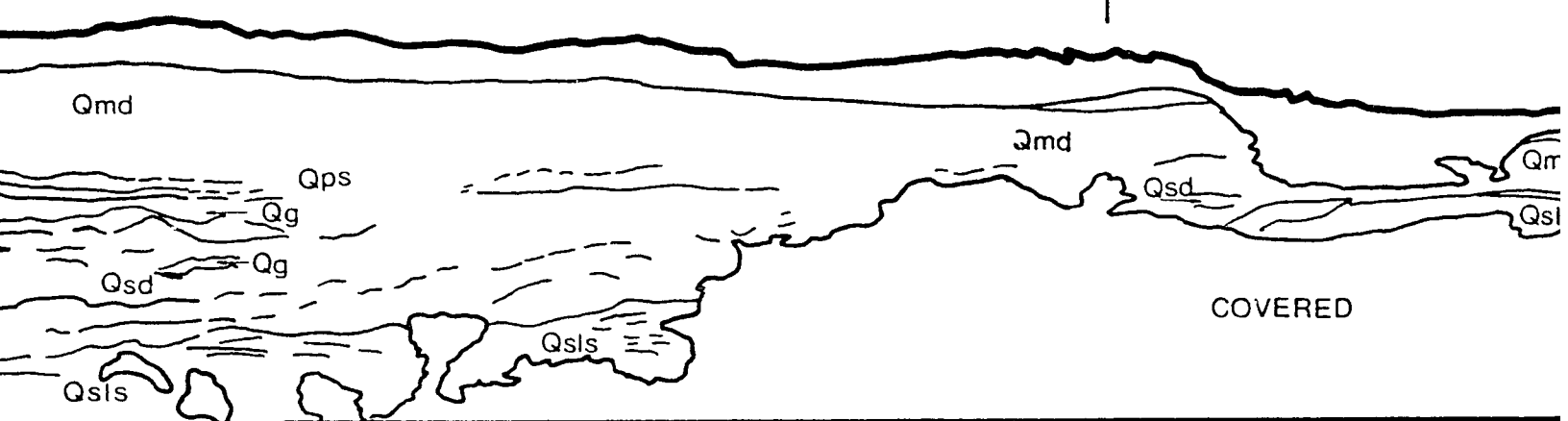
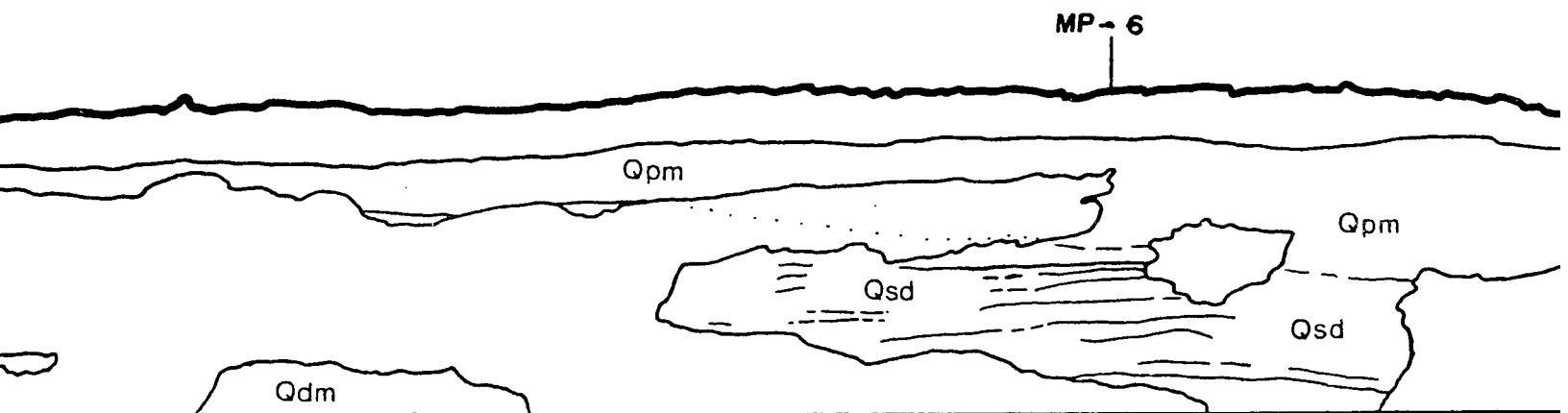


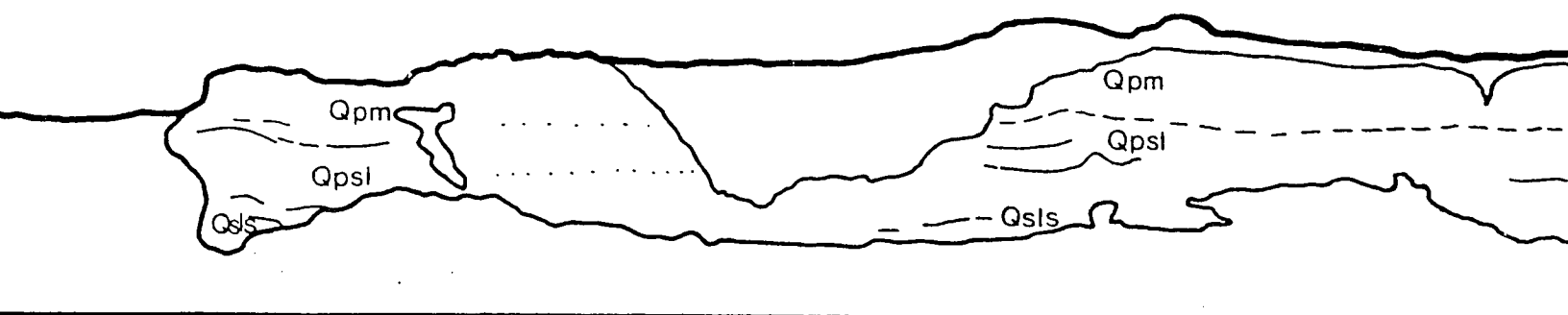
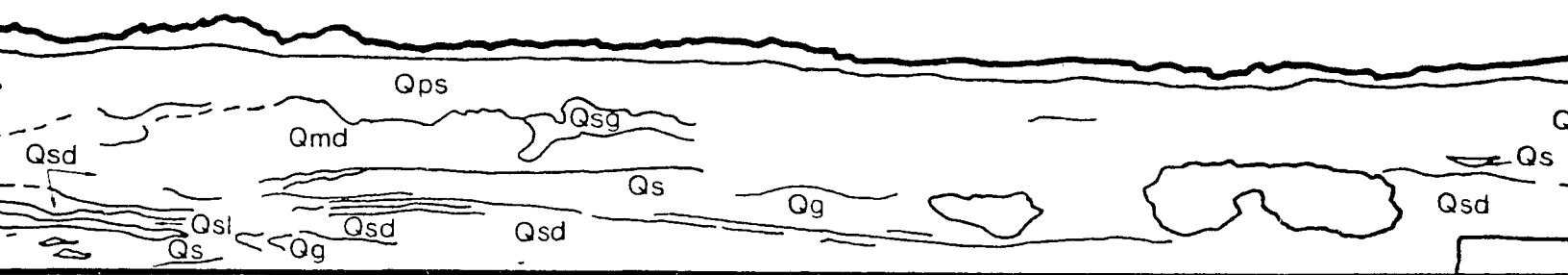
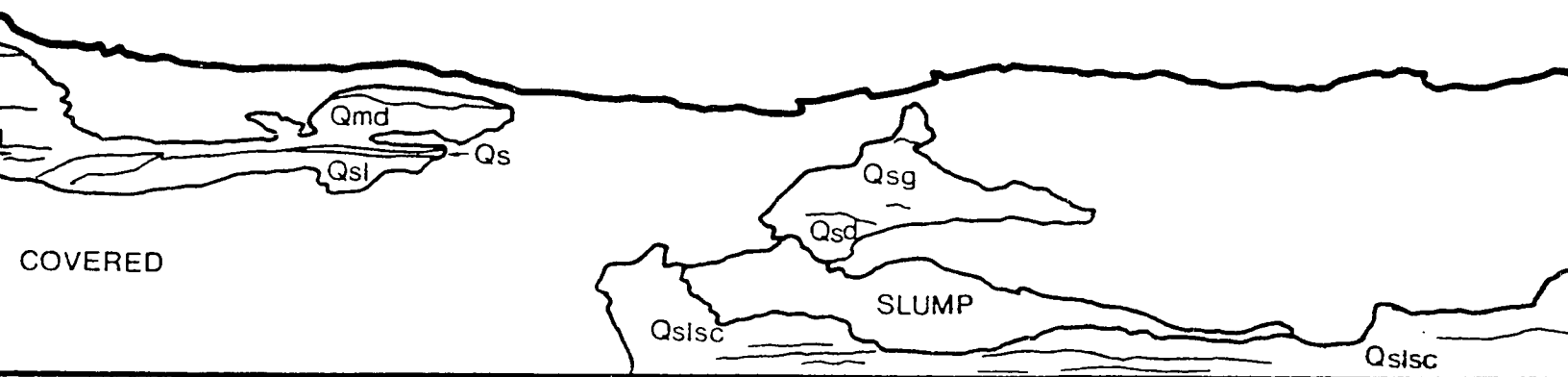
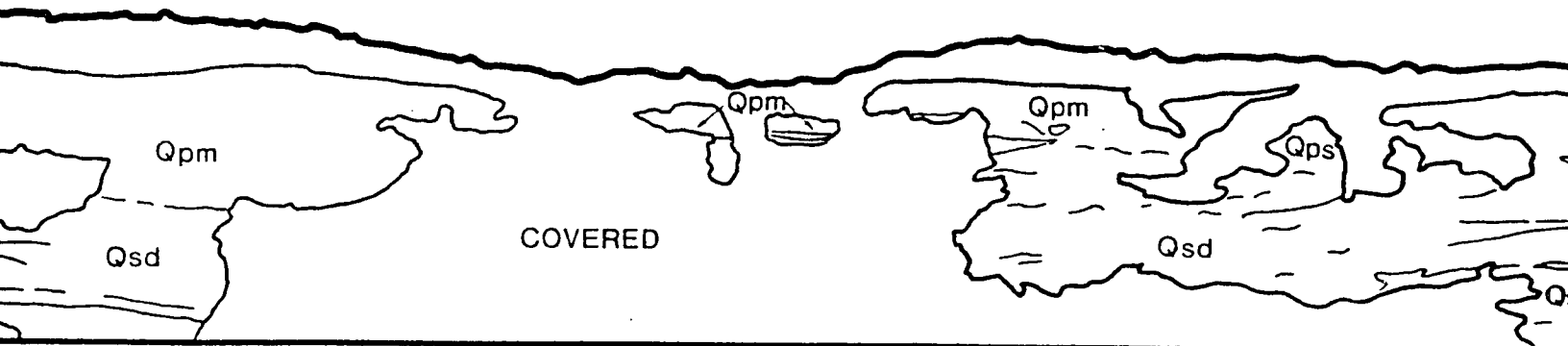
METERS

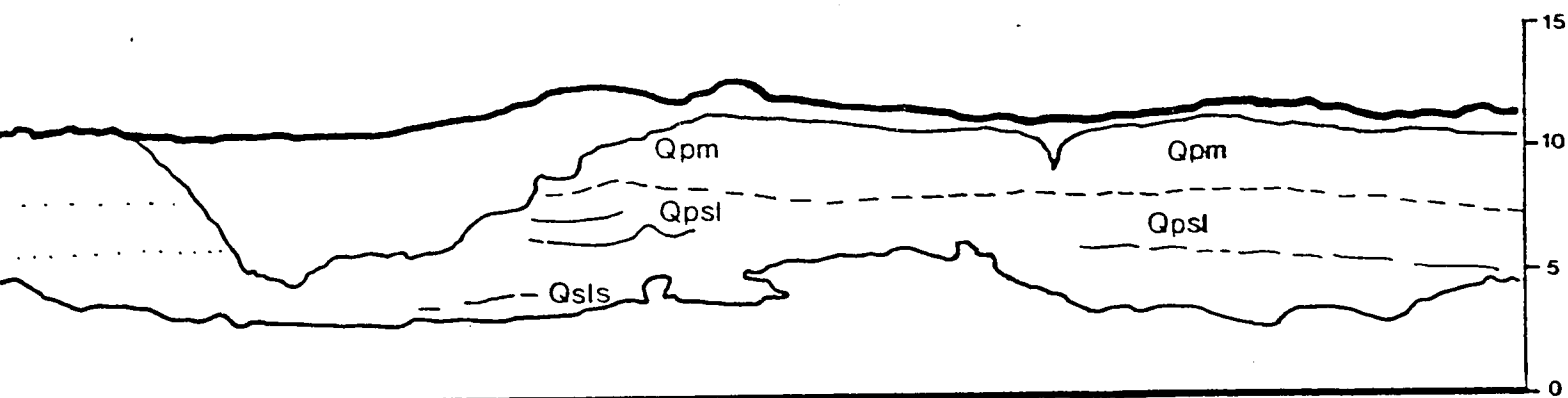
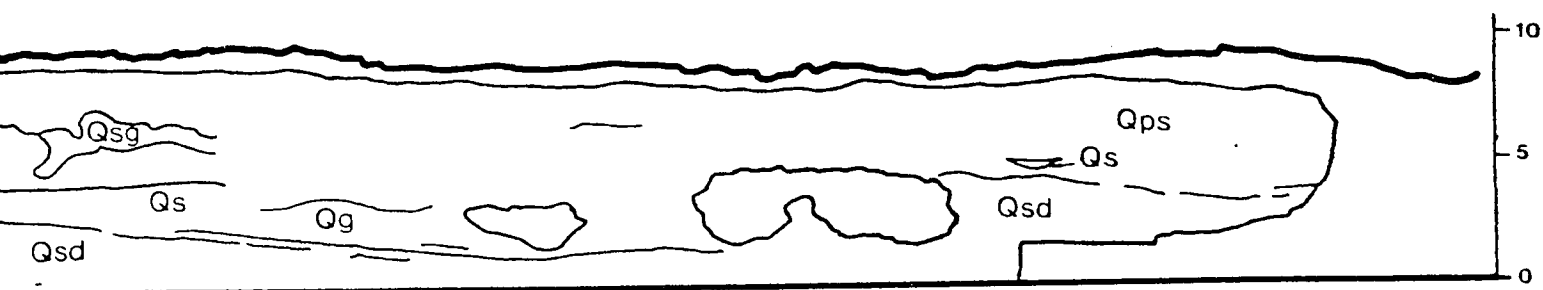
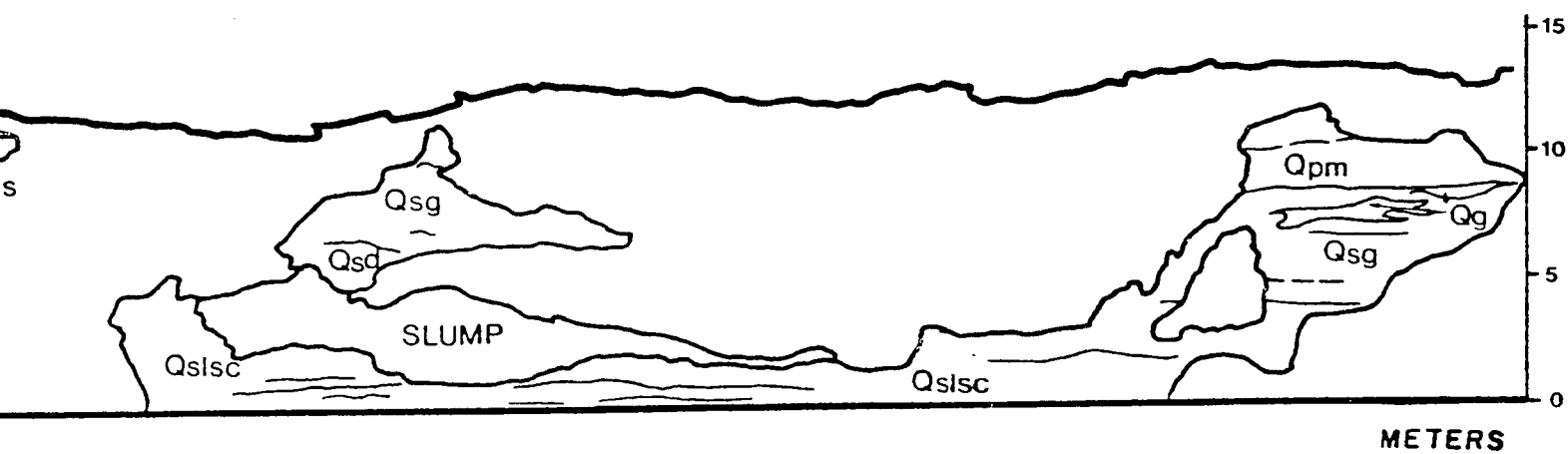
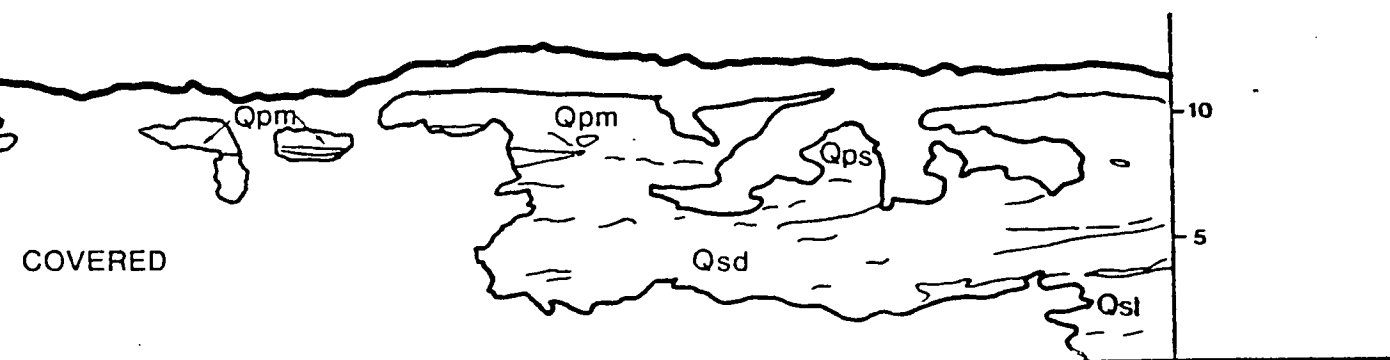


I

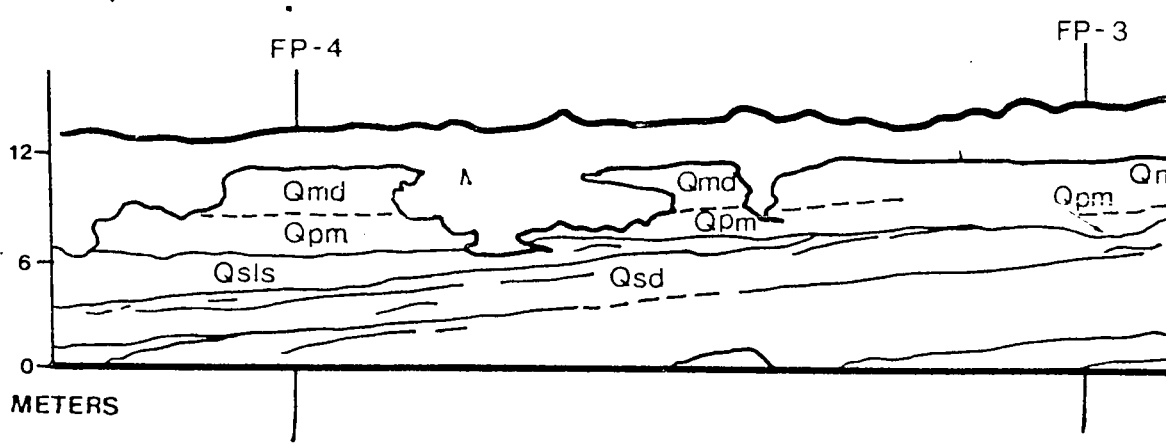




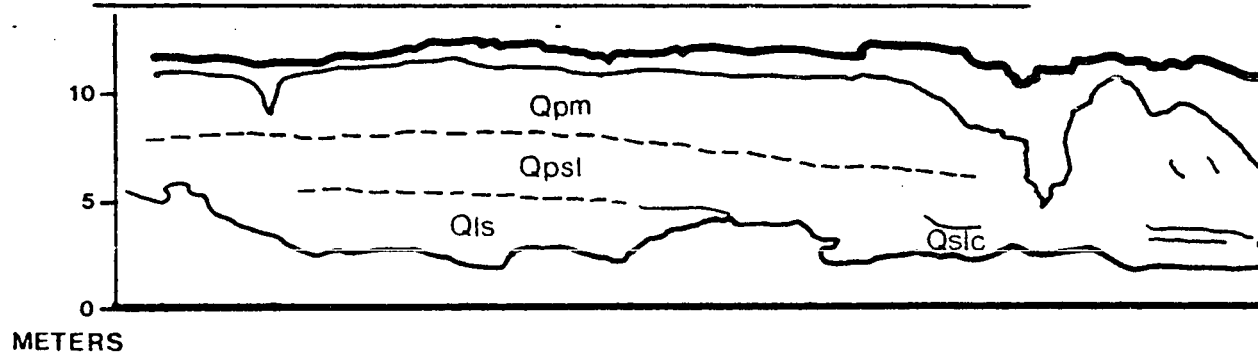




- Qmd massive fossiliferous diamicton
- Qpm pebbly mud
- Qsd stratified diamicton
- Qdm massive diamicton
- Qs sand
- Qsls stratified sand and silt
- Qpsl pebbly silty clay
- Qg gravel
- Qsg sandy gravel

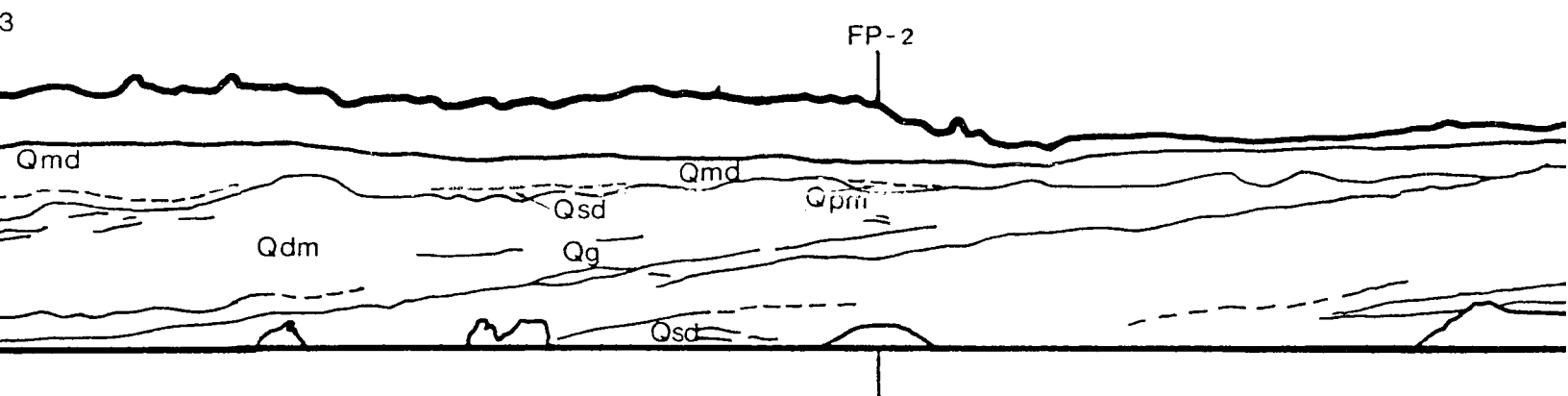
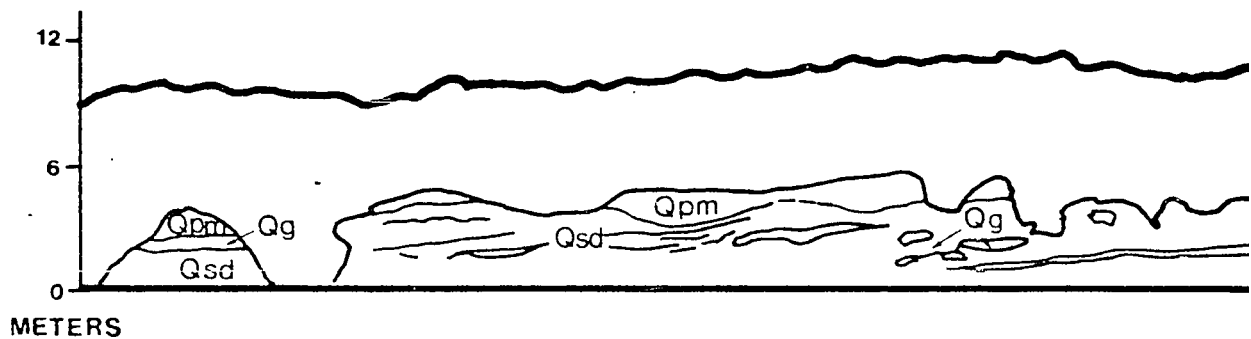


MAYLOR POINT (continued)

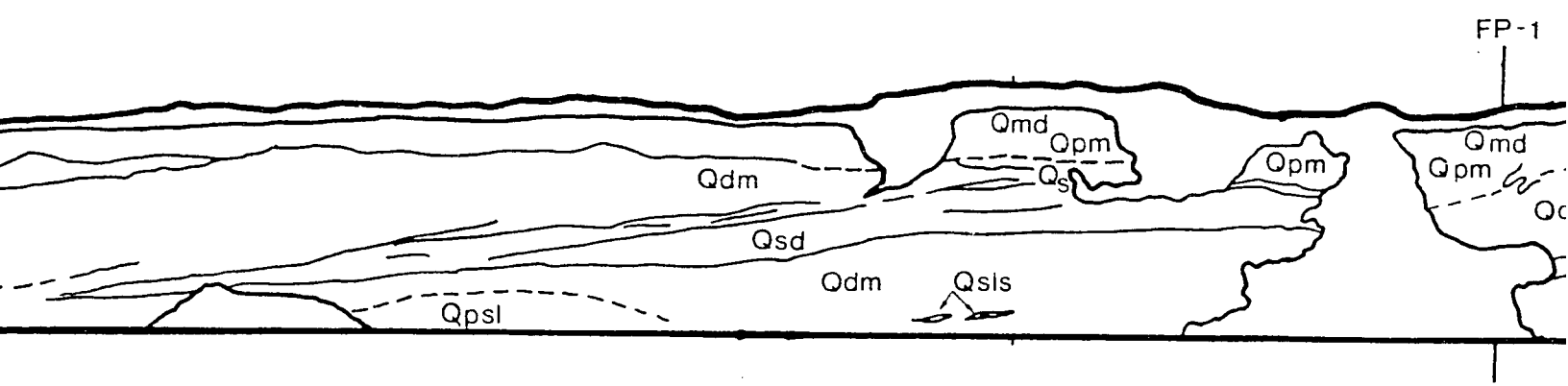
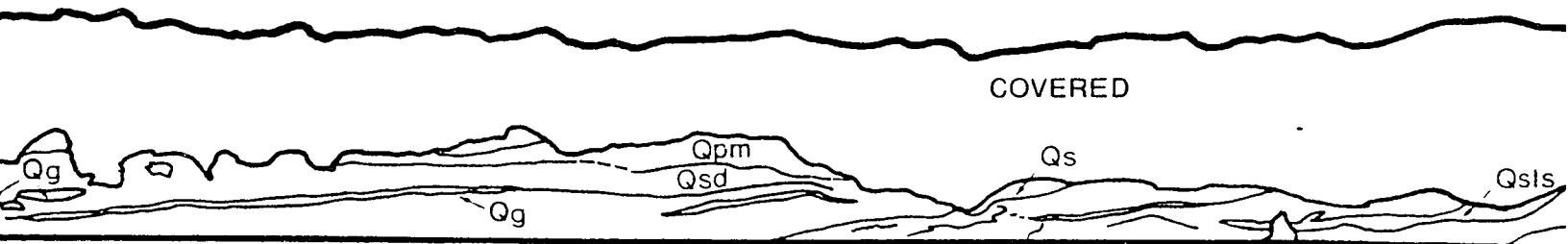
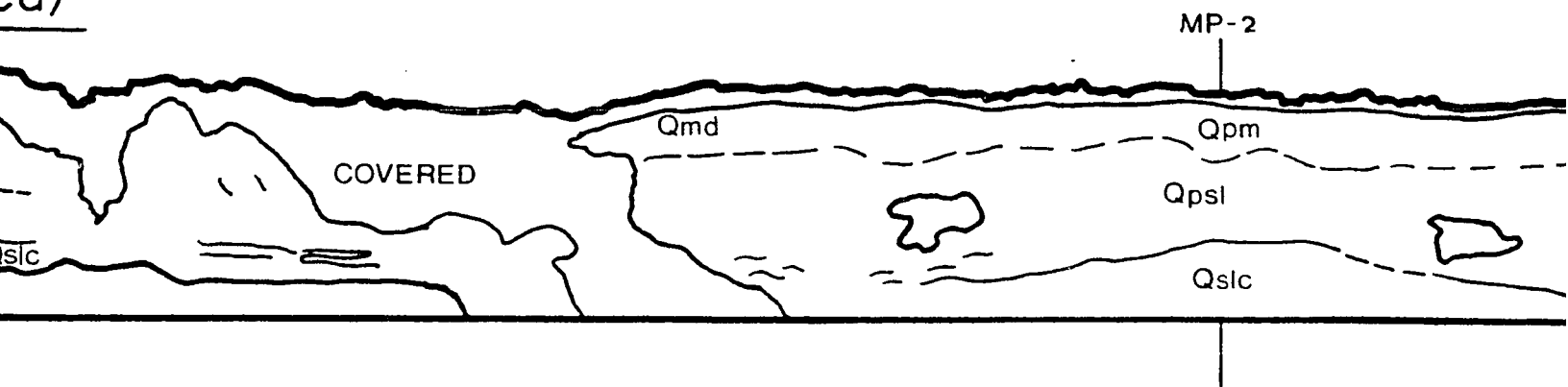


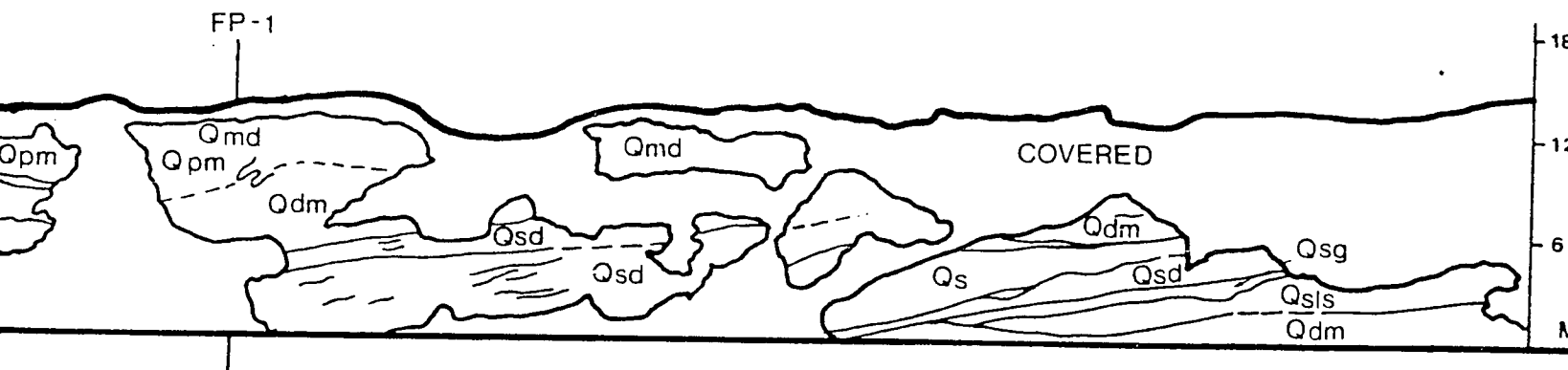
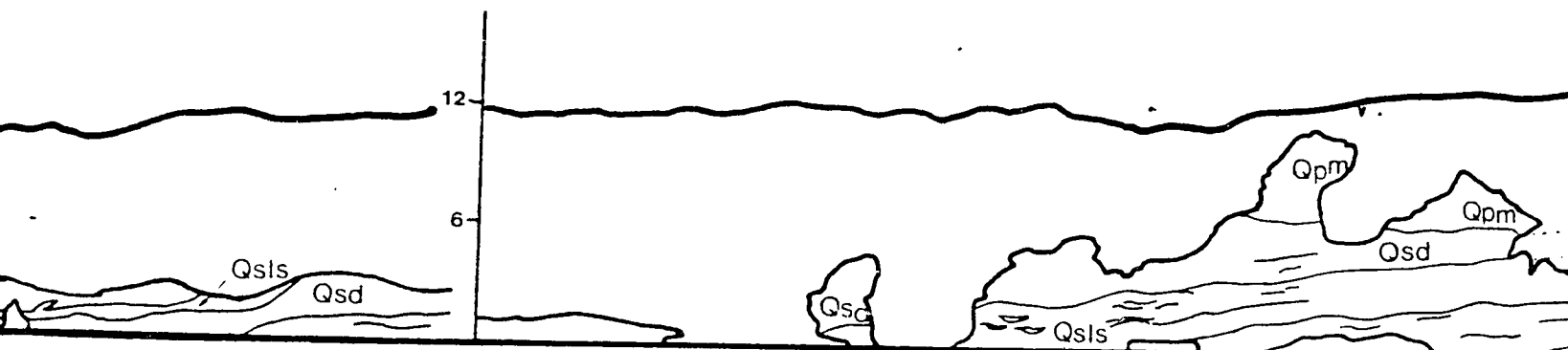
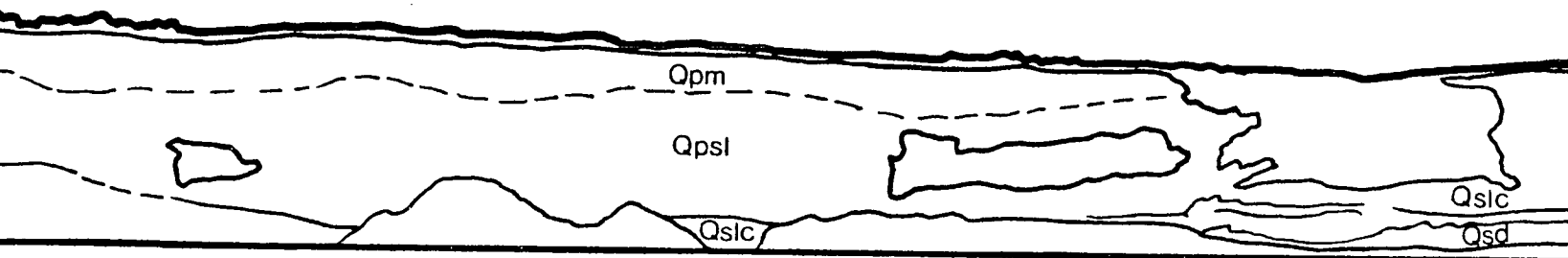
} distal
 } GLACIAL-MARINE
 }
 } ICE MARGINAL/
 } MARINE

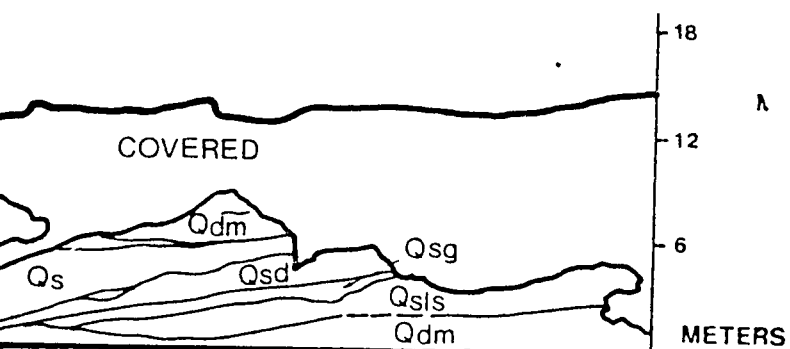
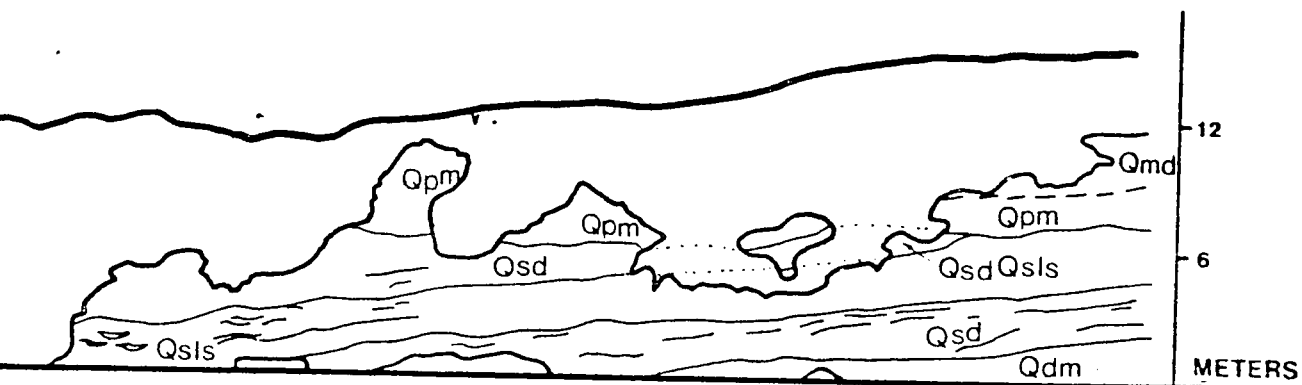
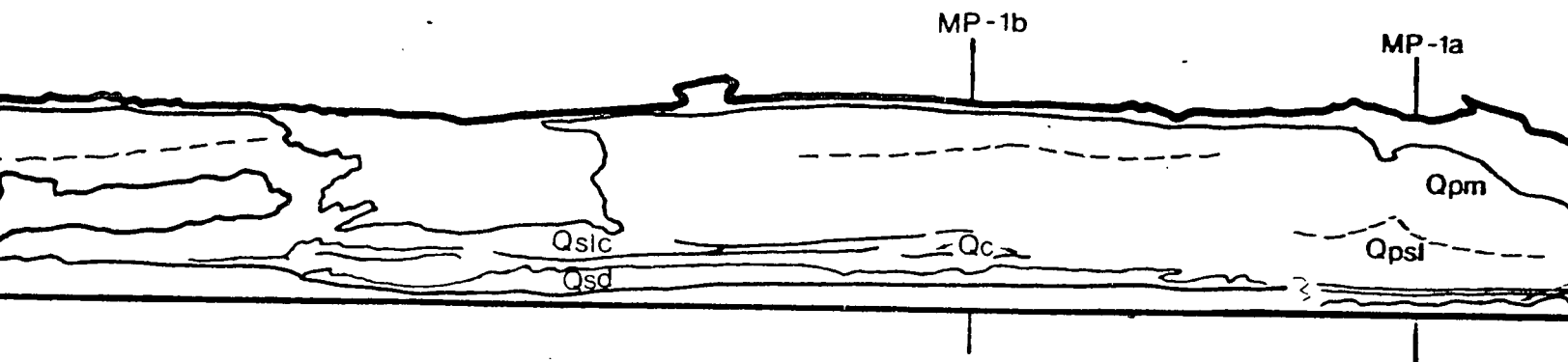
FORBES POINT

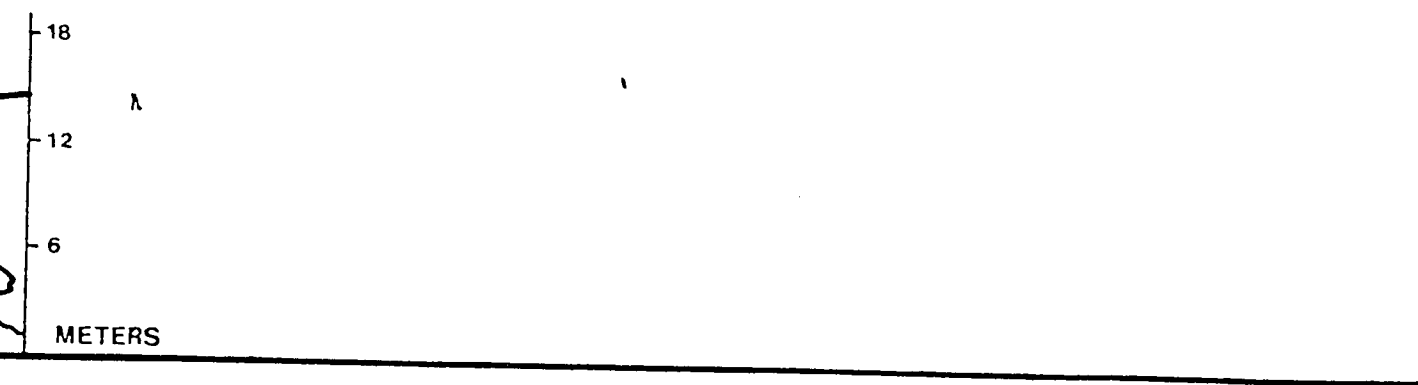
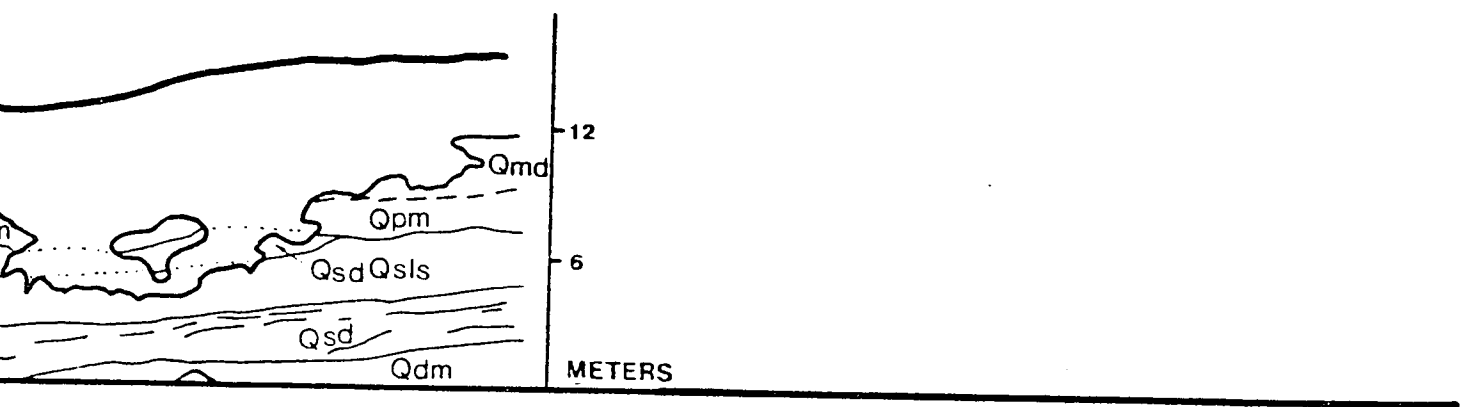
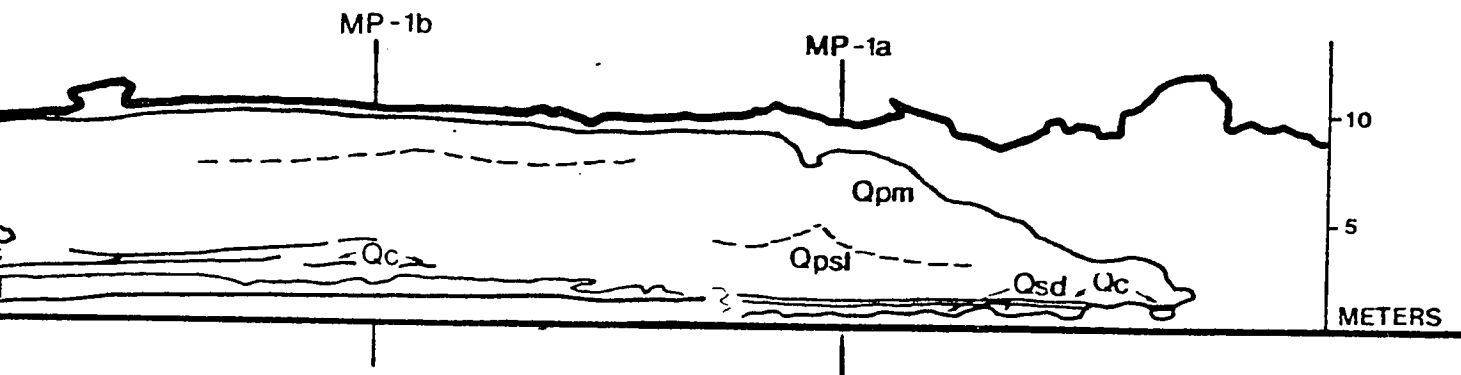


ed)









COUPEVILLE, LOVEJOY POINT

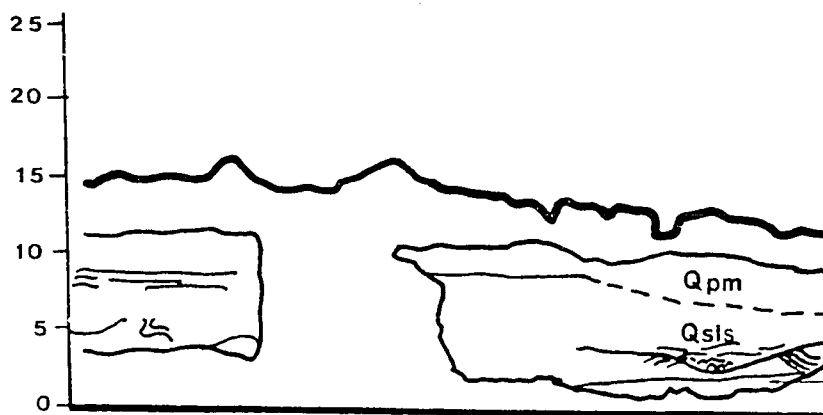
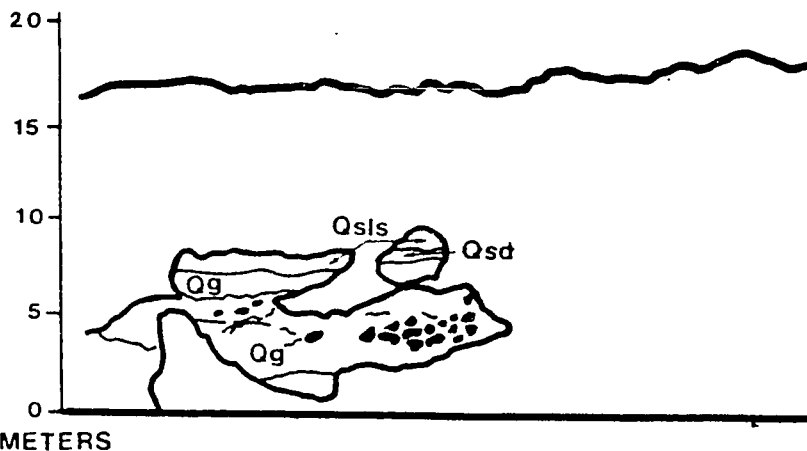
Qgl	sandy gravel, lag	EMERGE DEPOSIT
Qmd	massive fossiliferous diamicton	<div style="display: flex; align-items: center;"> <div style="width: 10px; height: 100px; border-left: 1px solid black; margin-right: 5px;"></div> <div> distal GLACIAL proximal </div> </div>
Qpm	pebbly mud	
Qpsi	pebbly silt	
Qsls	silty sand, sandy silt	
Qsd	stratified diamicton	ICE MAR
Qsl	well laminated sand and silt	
Qg	gravel	
Qsg	sandy gravel	
Qgs	gravelly sand	

SWANTOWN

Qgl	gravelly sand, lag	EMERGENCE
Qmd	massive diamicton	<div style="display: flex; align-items: center;"> <div style="width: 10px; height: 40px; border-left: 1px solid black; margin-right: 5px;"></div> <div> distal GLACIAL - M. </div> </div>
Qpm	pebbly mud	
Qsdc	convoluted, stratified diamicton	ICE MARGINAL
Qpml	laminated pebbly mud	<div style="display: flex; align-items: center;"> <div style="width: 10px; height: 100px; border-left: 1px solid black; margin-right: 5px;"></div> <div> GLACIAL - MA SUBGLACIAL proximal </div> </div>
Qsls	laminated silt and sand	
Qls	laminated, graded sand	
Qsl	thin. bedded, massive silt	
Qgs	massive, gravelly sand	GLACIAL - MA proximal
Qsd	stratified diamicton	ICE MARGINAL

POINT

- EMERGENCE DEPOSITS
- distal
- GLACIAL - MARINE
- proximal
- ICE MARGINAL / MARINE



EMERGENCE DEPOSITS

distal
GLACIAL - MARINE

ICE MARGINAL / MARINE

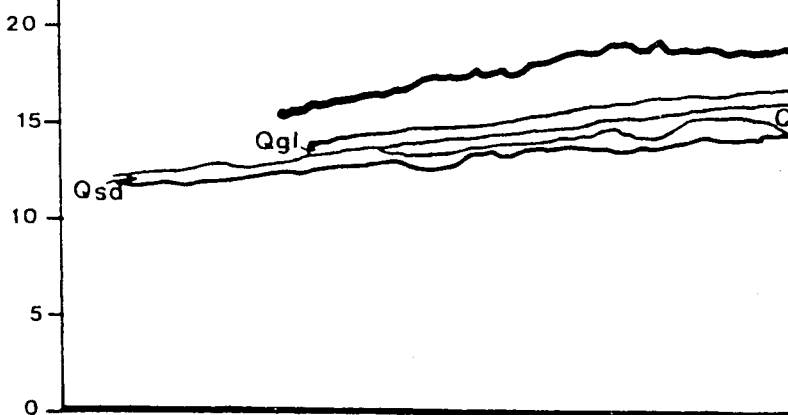
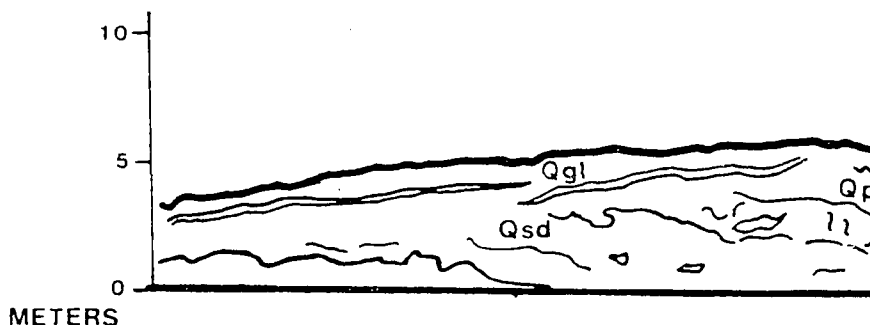
GLACIAL - MARINE

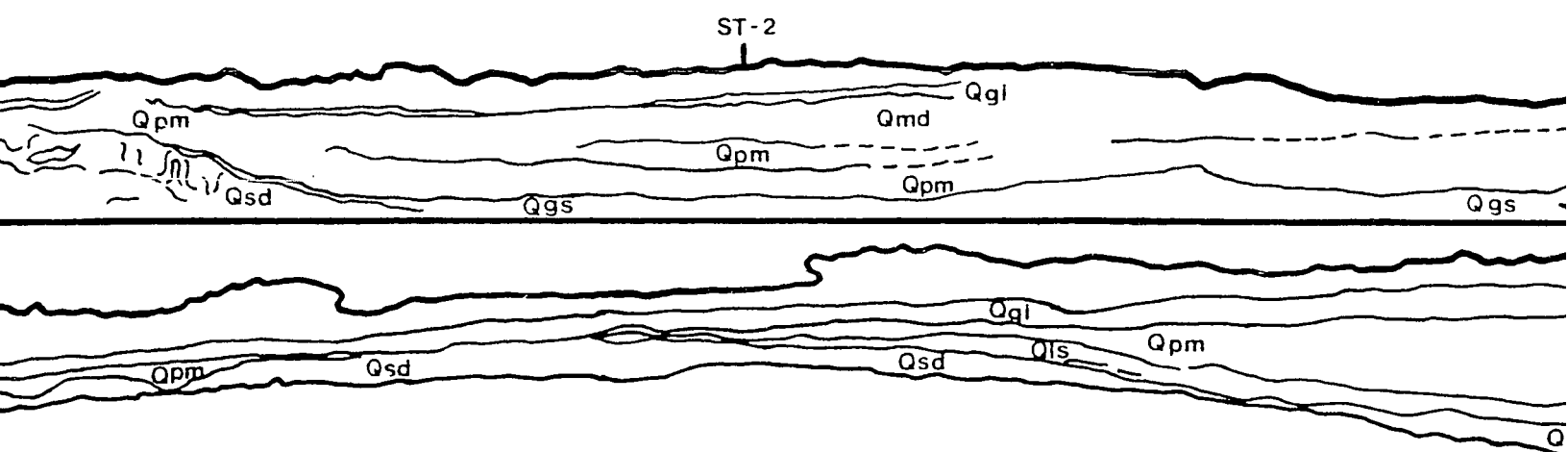
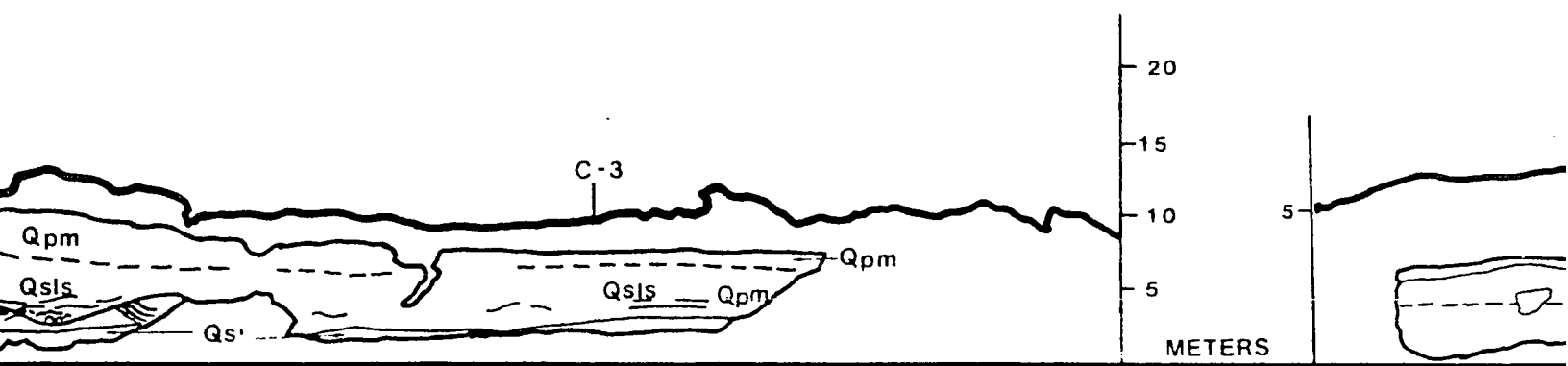
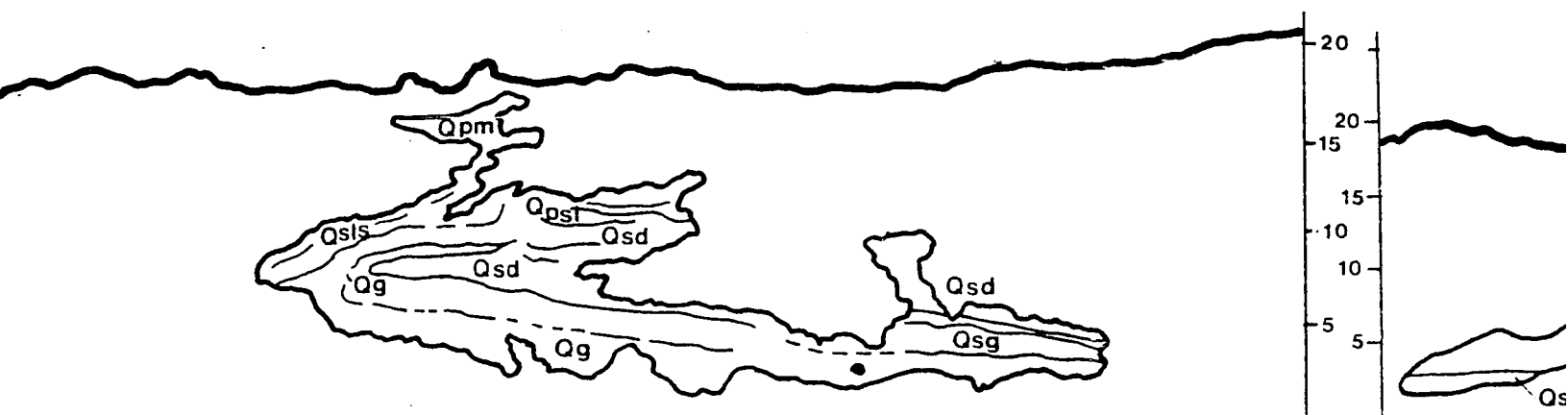
SUBGLACIAL / MARINE

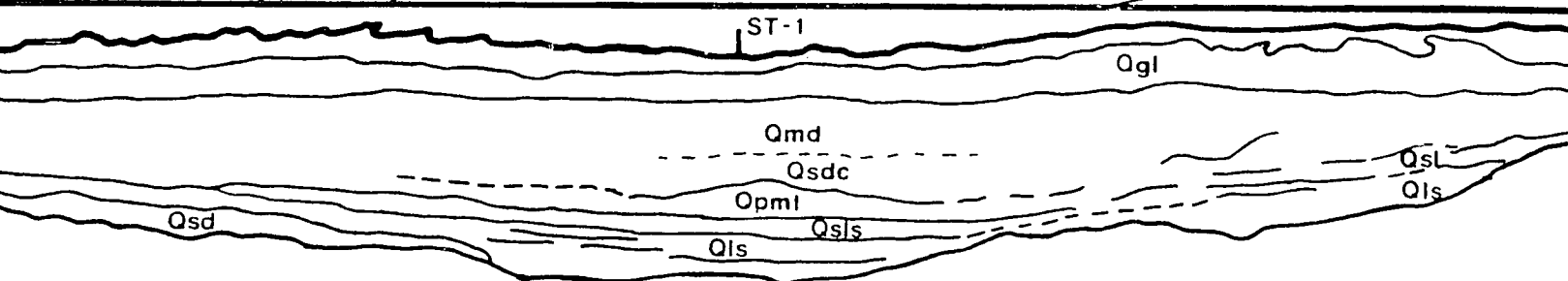
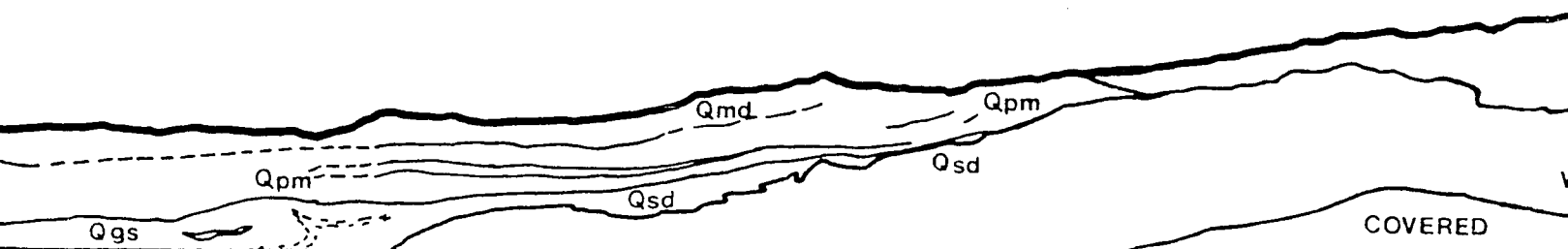
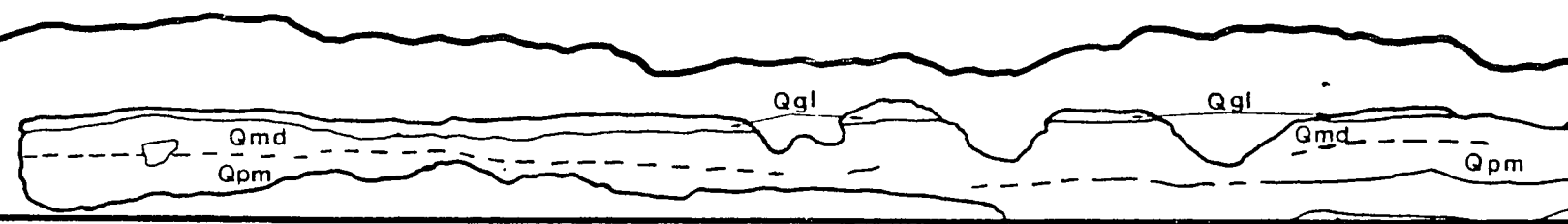
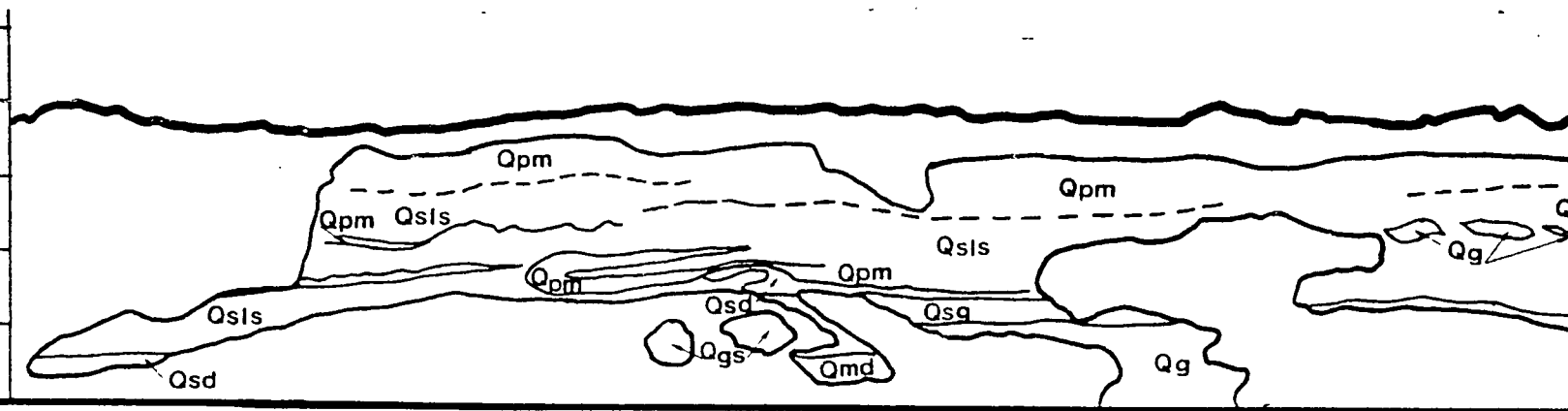
proximal

GLACIAL - MARINE
proximal

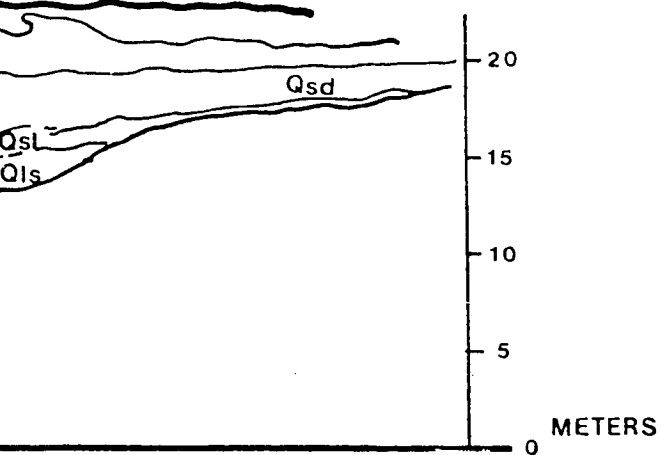
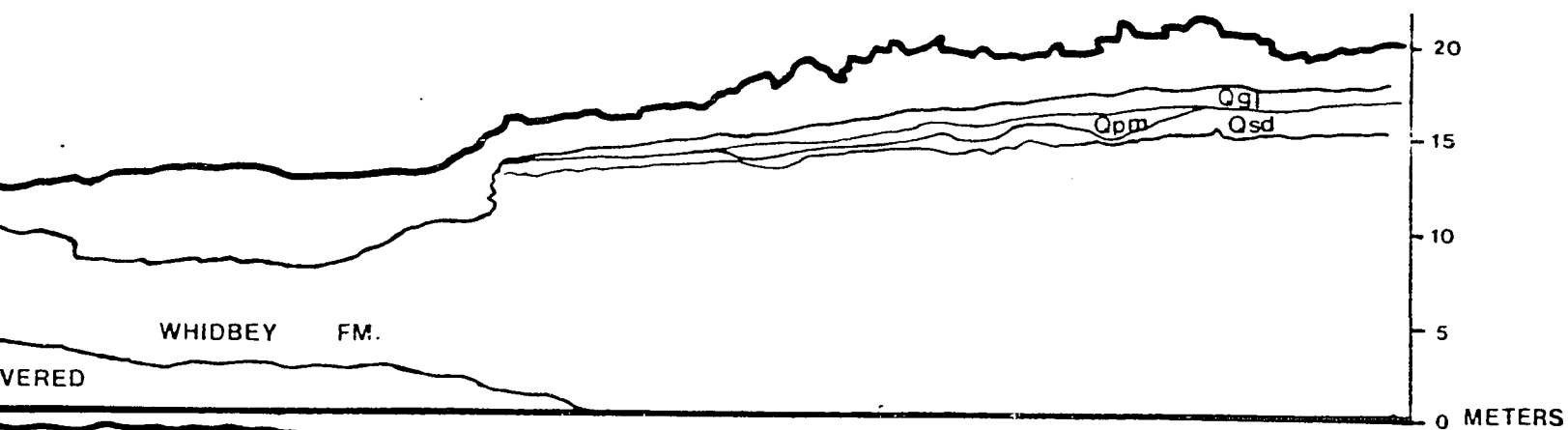
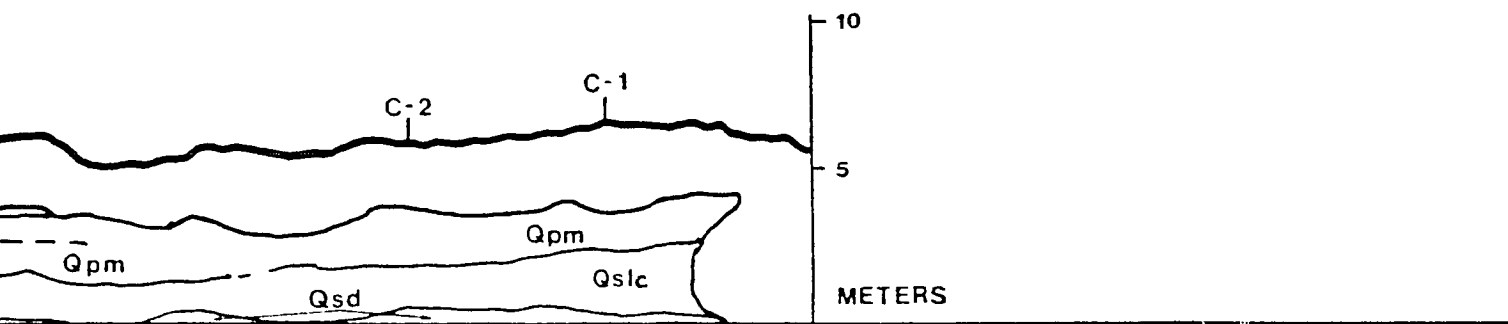
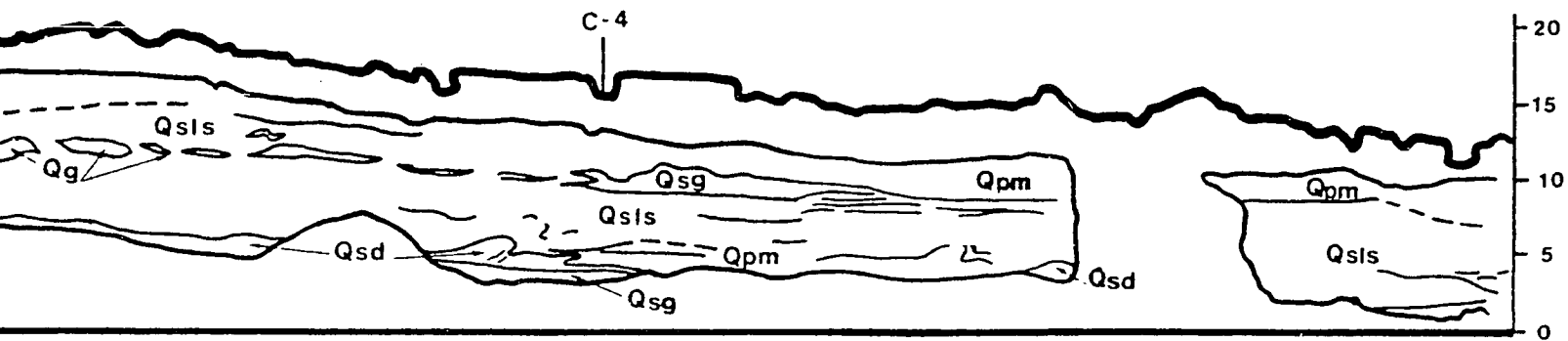
ICE MARGINAL





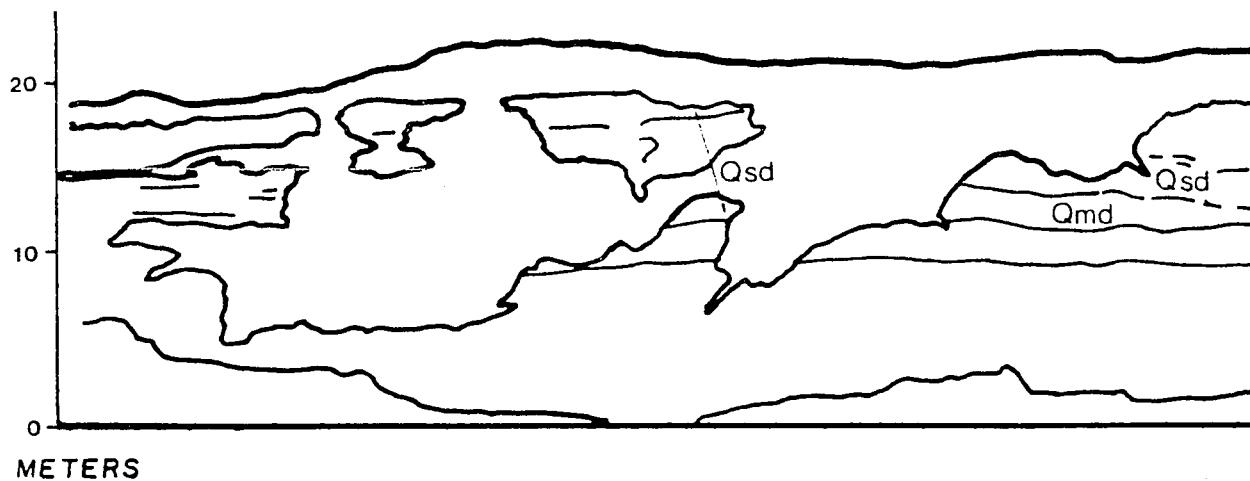


WHIDBEY FM.



Qpm	pebbly mud
Qpml	laminated pebbly mud
Qls	laminated sand
Qlss	laminated sand and silt
Qsg	sandy gravel
Qsd	stratified diamicton
Qmd	massive diamicton
Qg	gravel
Qs	sand

}	distal
	GLACIA
	proximc
	ICE MA



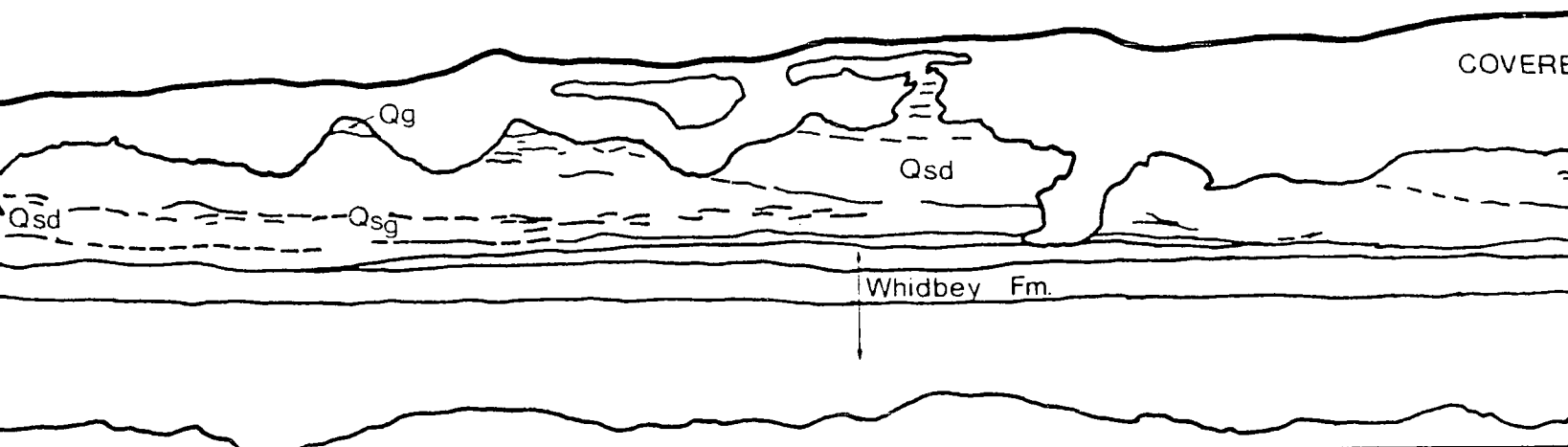
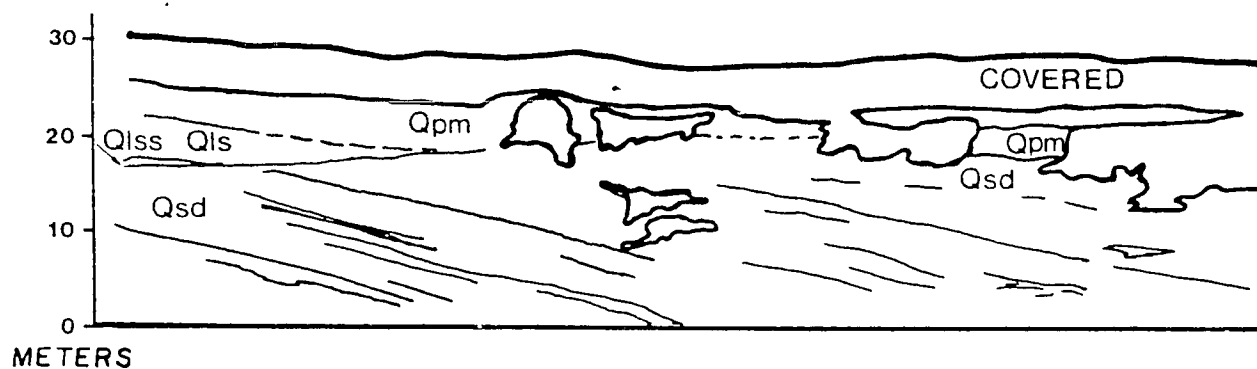
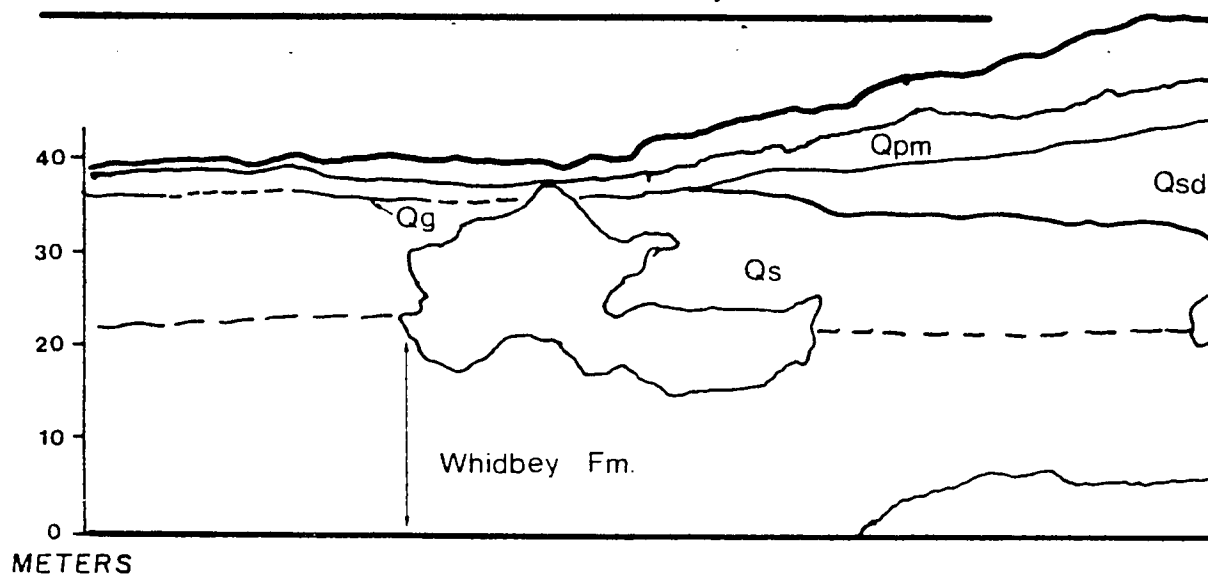
HASTIE LAKE ROAD, NORTH

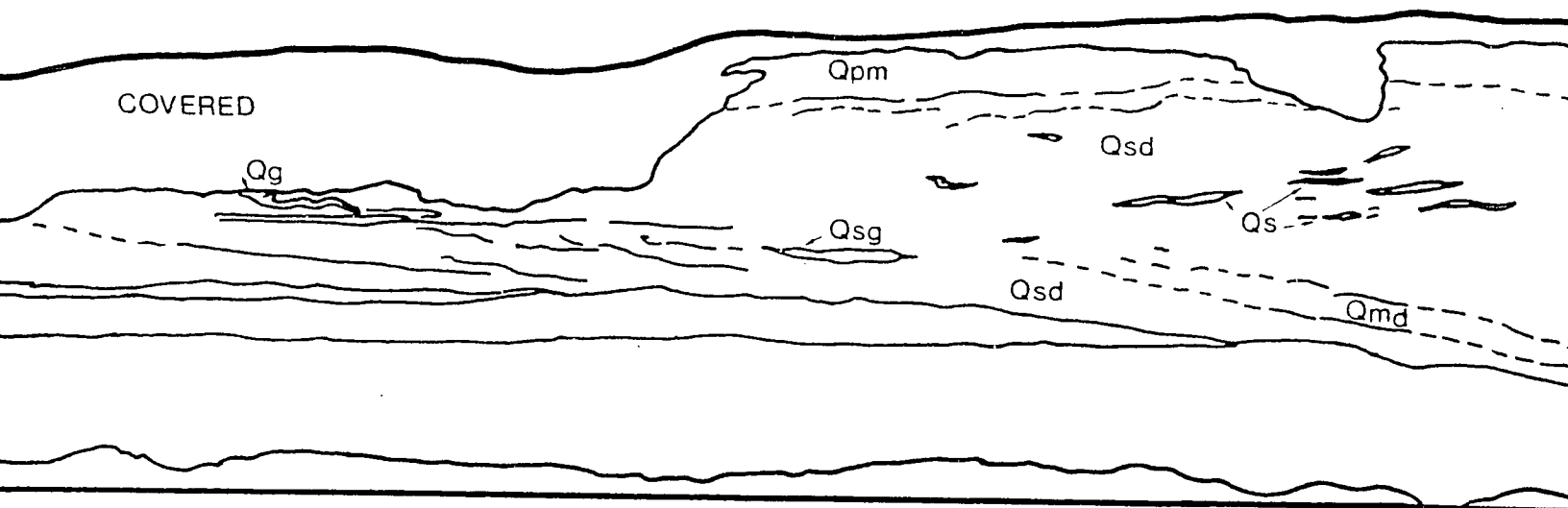
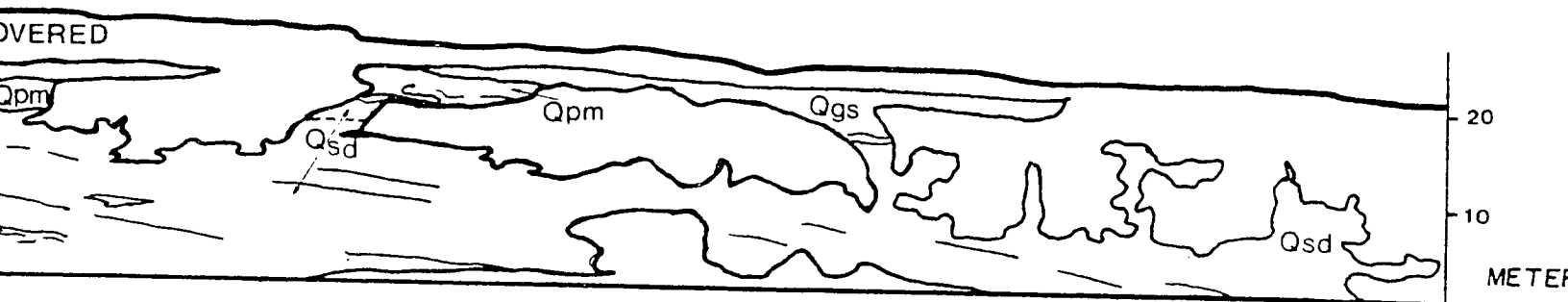
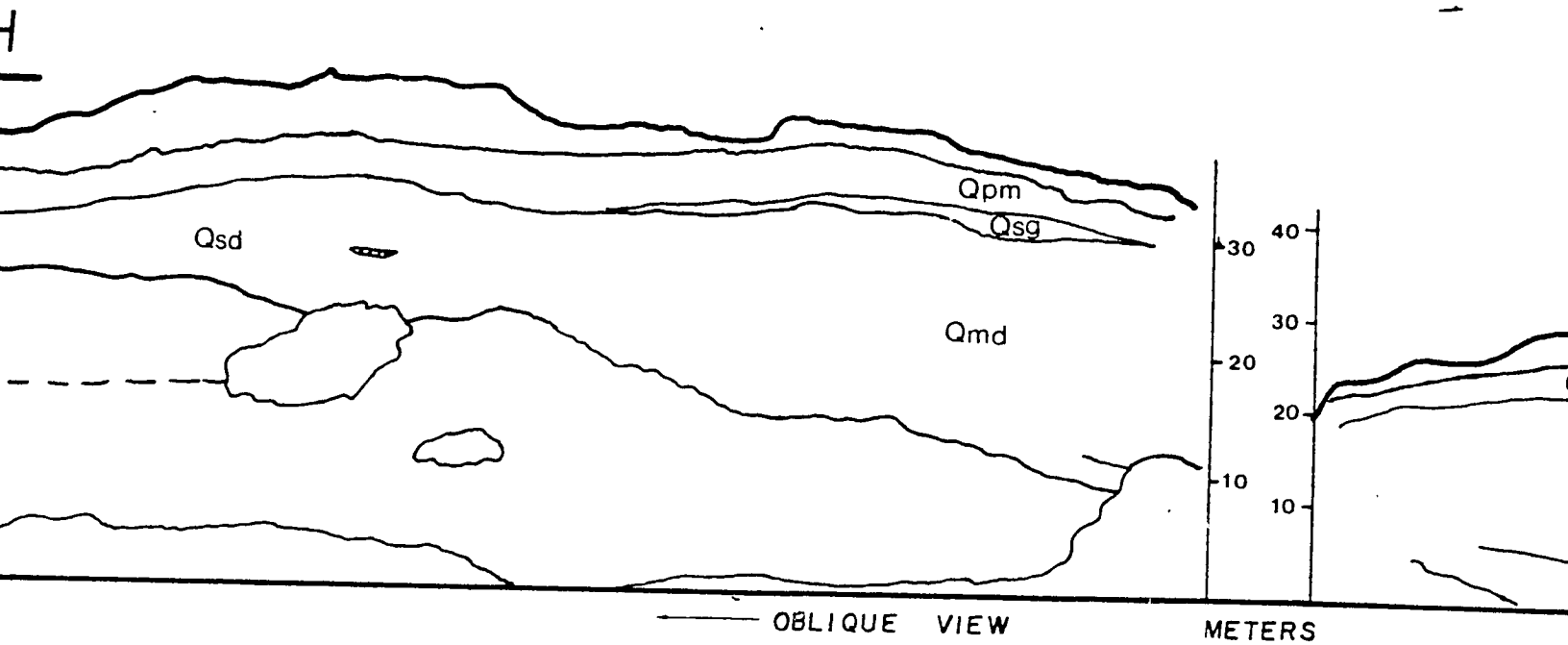
stal

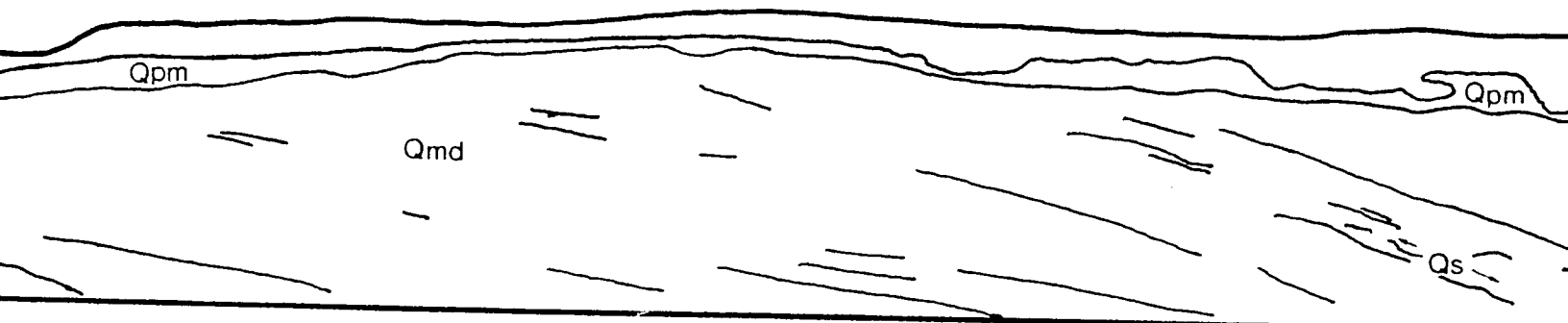
LACIAL - MARINE

roximal

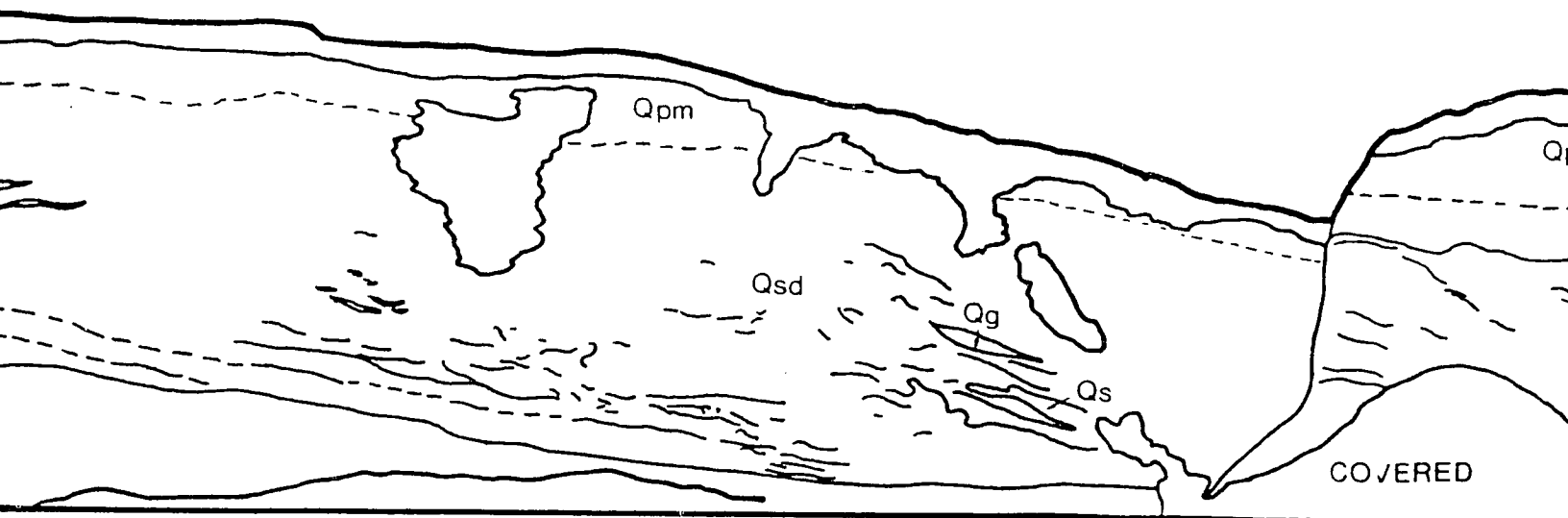
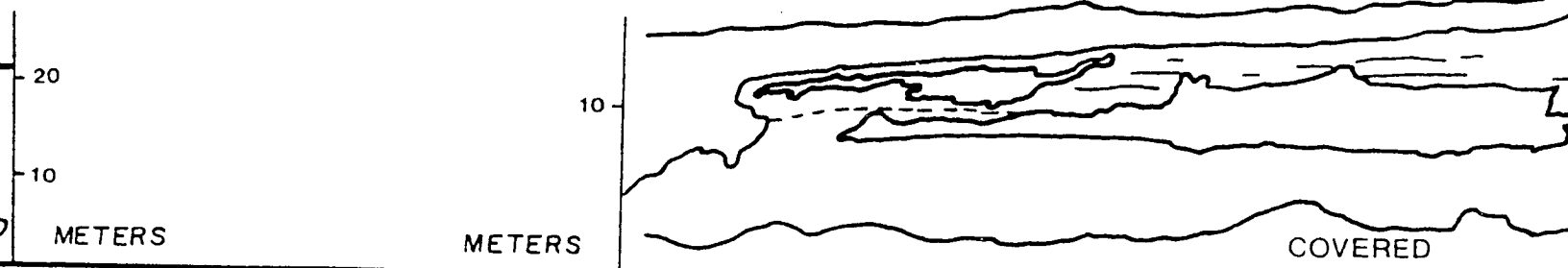
CE MARGINAL

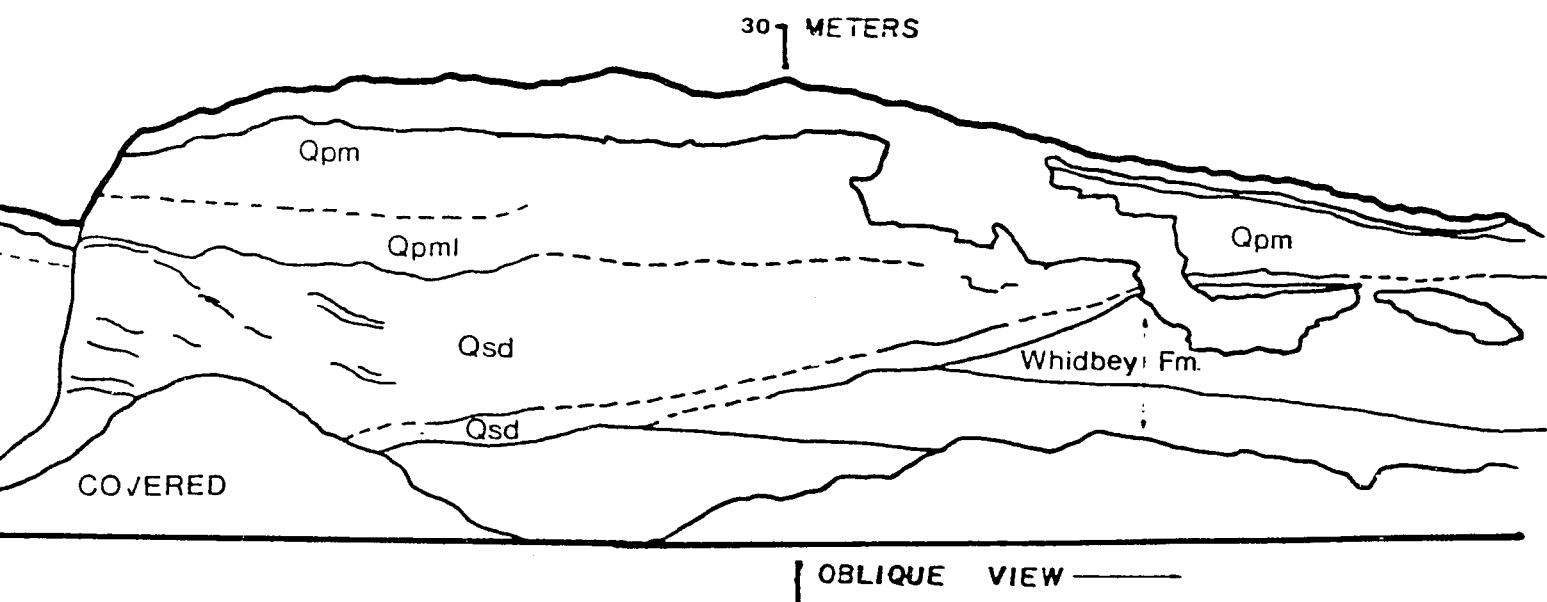
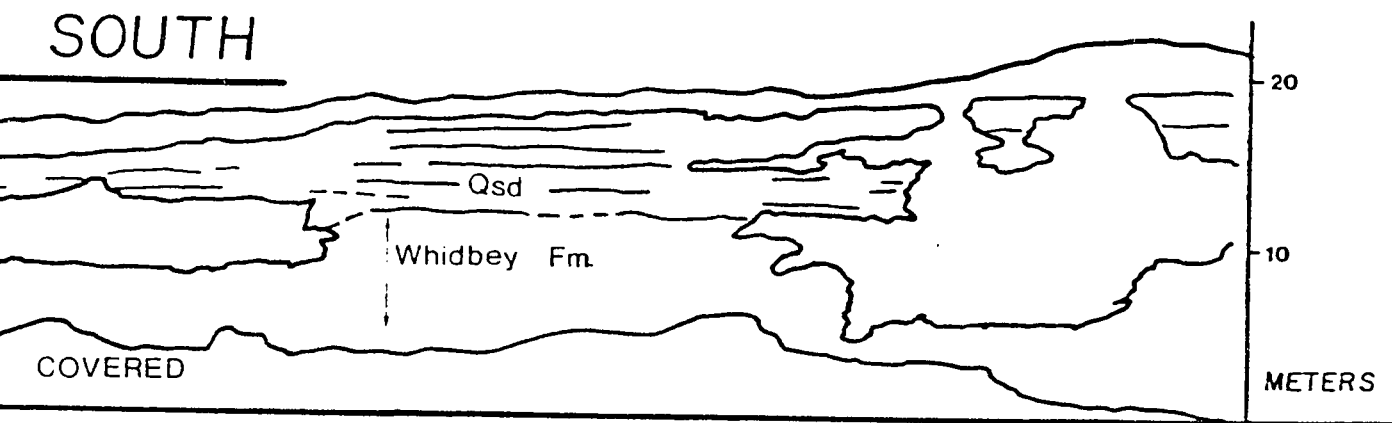
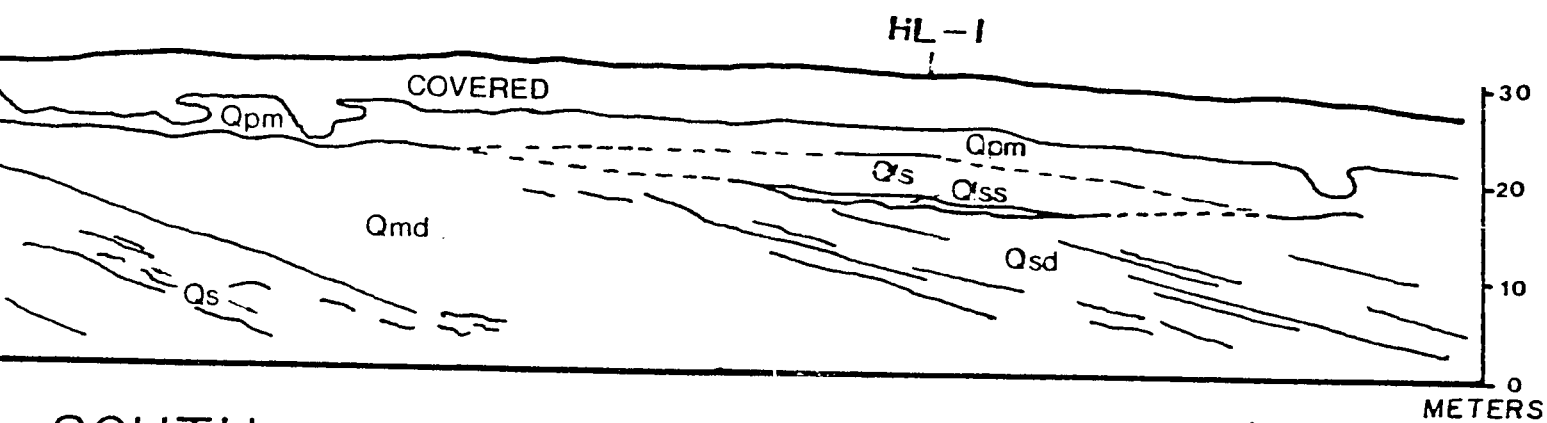




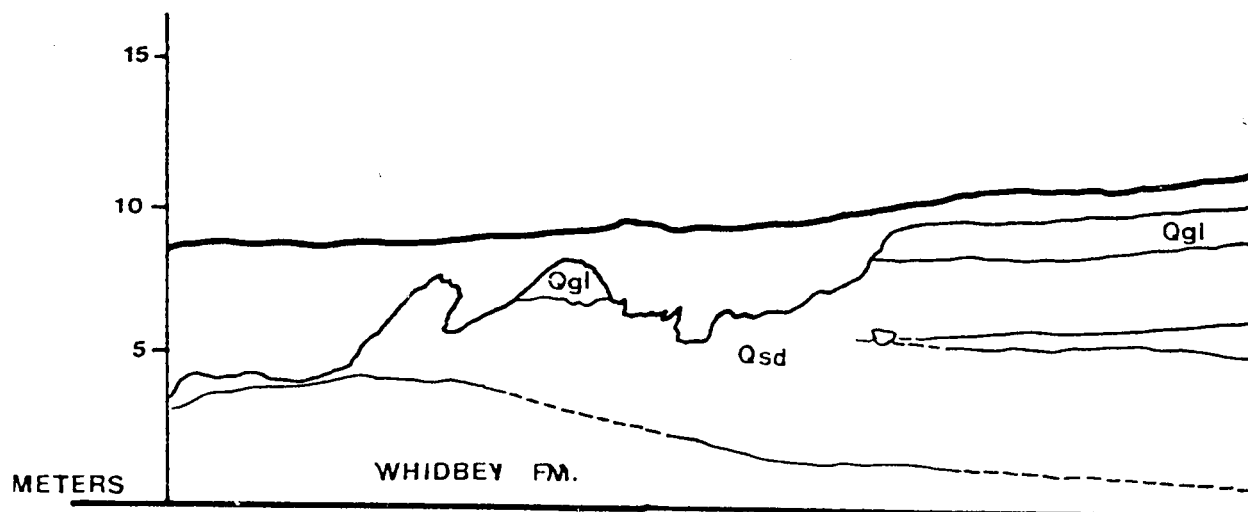


HASTIE LAKE ROAD, SOUTH





WEST BEACH, POINT PARTR



Qgl stratified gravel, silt

Qmd massive diamicton

Qpm pebbly mud

Qps pebbly sand

Qsdc convoluted, stratified diamicton

Qsd stratified diamicton

Qsls silty pebbly sand, convoluted

Qsl laminated silt and sand

Qs thin-med. bedded, laminated sand, silty sand

Qsdsi stratified silty diamicton

Qg gravel

Qsg sandy gravel, fossiliferous

EM

dis

GL

pro

ICE

A geological cross-section of the Whidbey Formation. The diagram shows several layers of sedimentary rock, with some areas labeled as "COVERED". The layers are labeled with geological codes: Qgl (Quaternary glacial), Qmd (Quaternary marine deposit), Qsd (Quaternary sand), Qg (Quaternary gravel), and Qs (Quaternary sand). The layers are shown in a sequence from top to bottom: Qgl, Qmd, Qsd, Qg, and Qs. The Whidbey Formation is labeled at the bottom right. The diagram illustrates the complex geological structure of the Whidbey Formation, including the presence of faults and the relationship between different sedimentary units.

distal

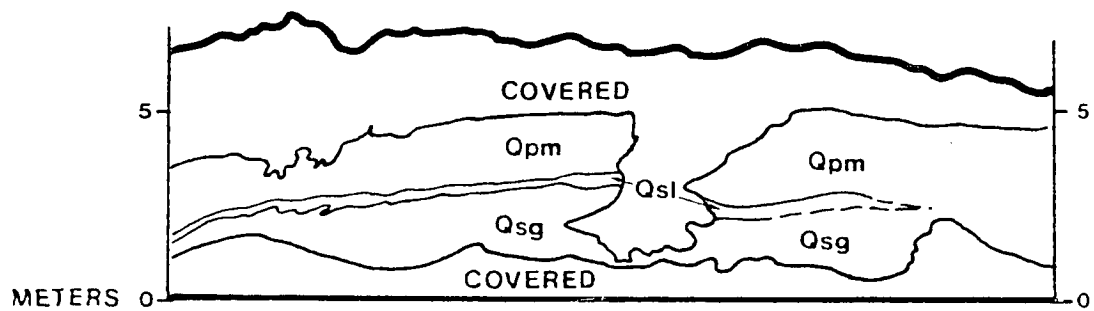
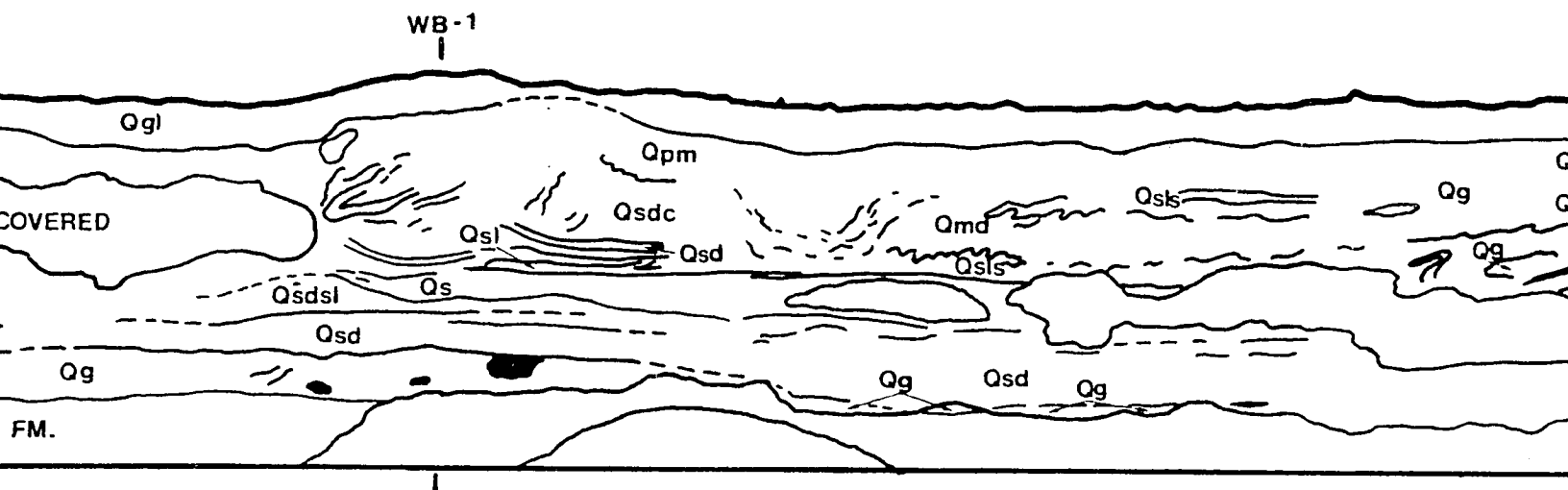
proximal

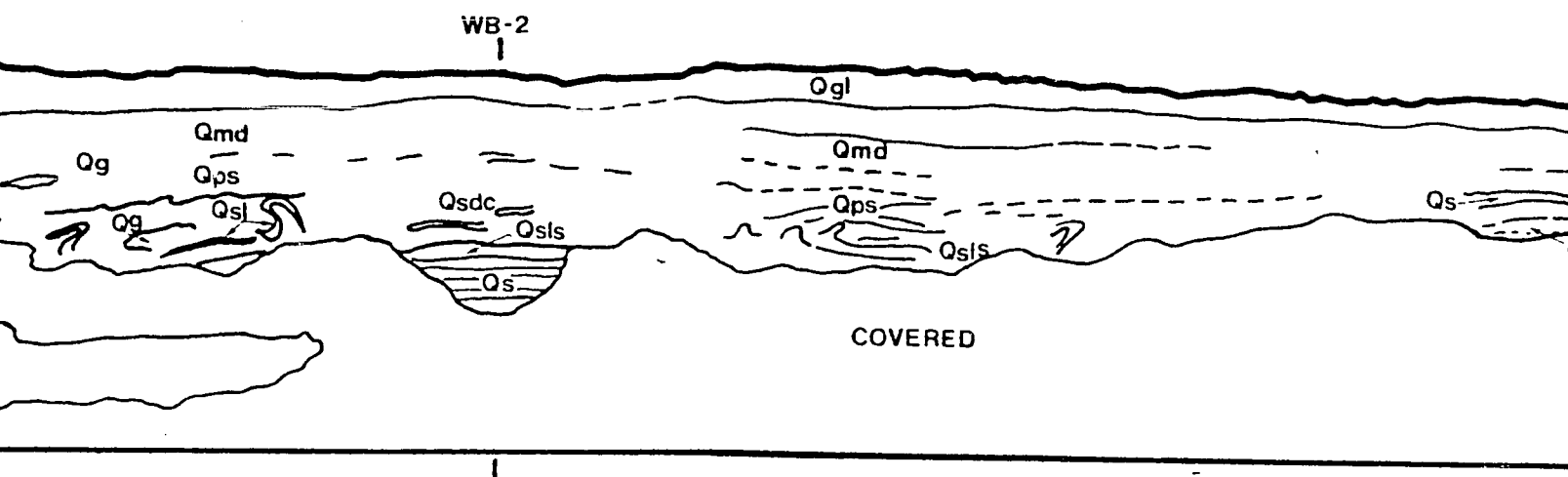
- ICE MARGINAL / MARINE

M1

```

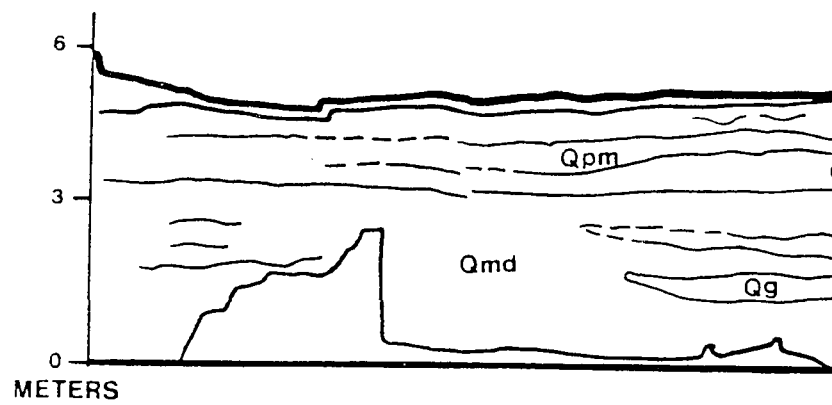
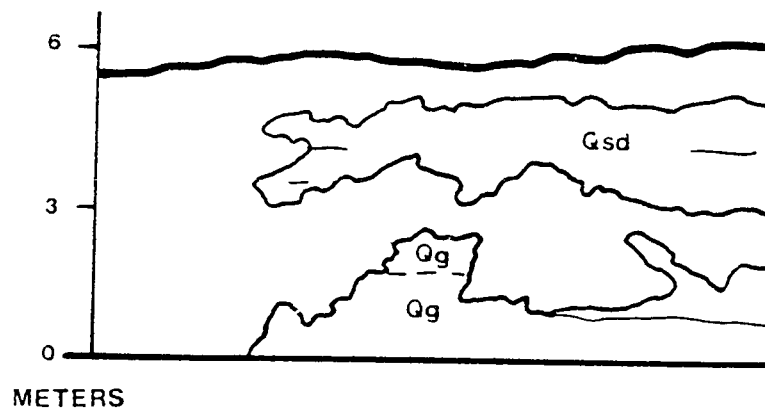
graph LR
    A[ty sand] --- B[ ]
    B --- C[proximal]
    B --- D[GLACIAL - MARINE]
    B --- E[ICE MARGINAL]
  
```



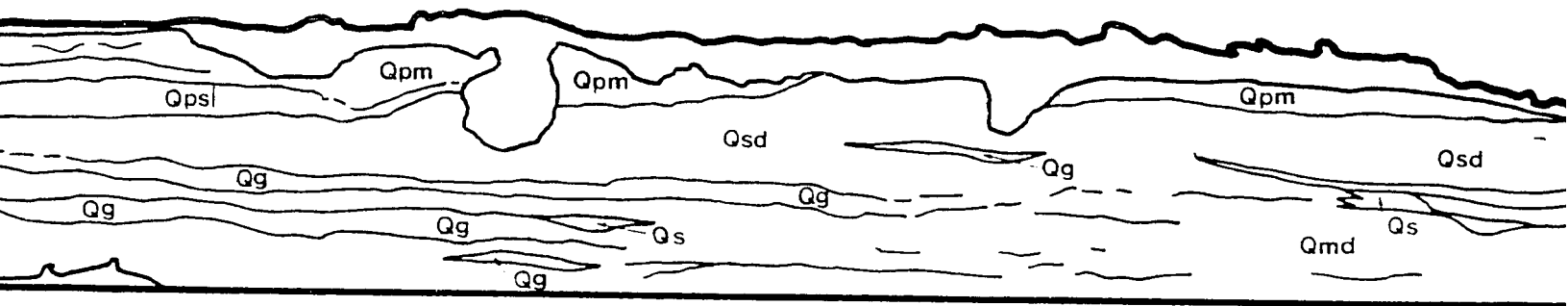
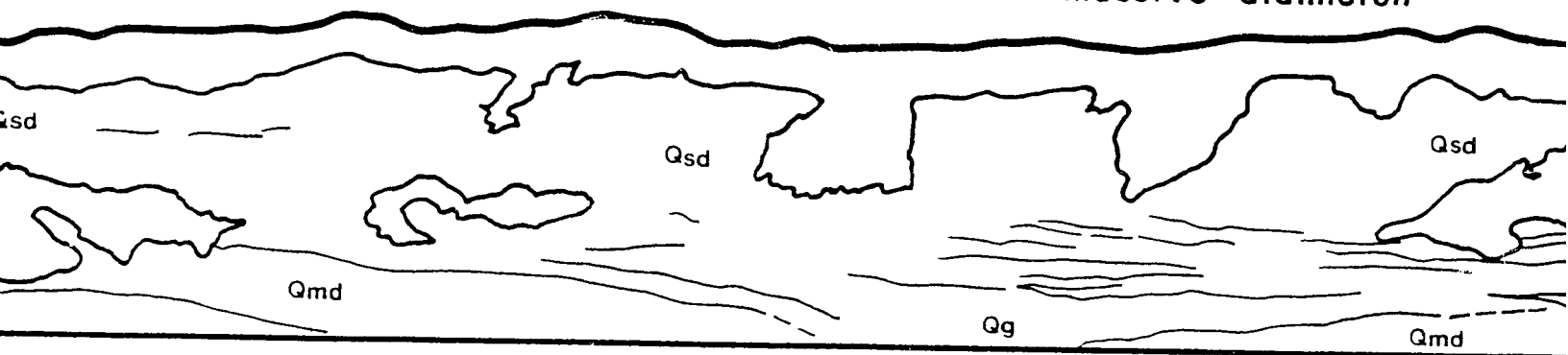


MUTINY B



NY BAY, EAST

Qpm	pebbly mud	
Qpsl	pebbly silt	
Qsd	stratified diamicton	
Qsl	silt	
Qs	stratified sand	
Qg	gravel	
Qmd	massive diamicton	



mud

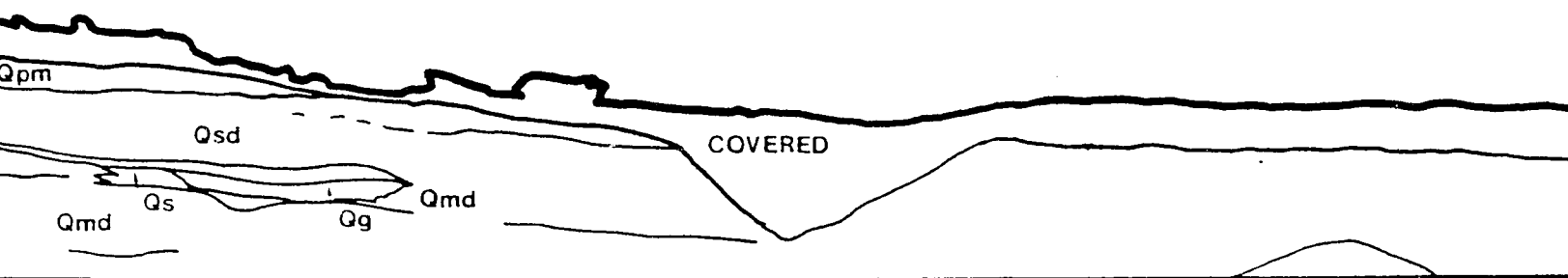
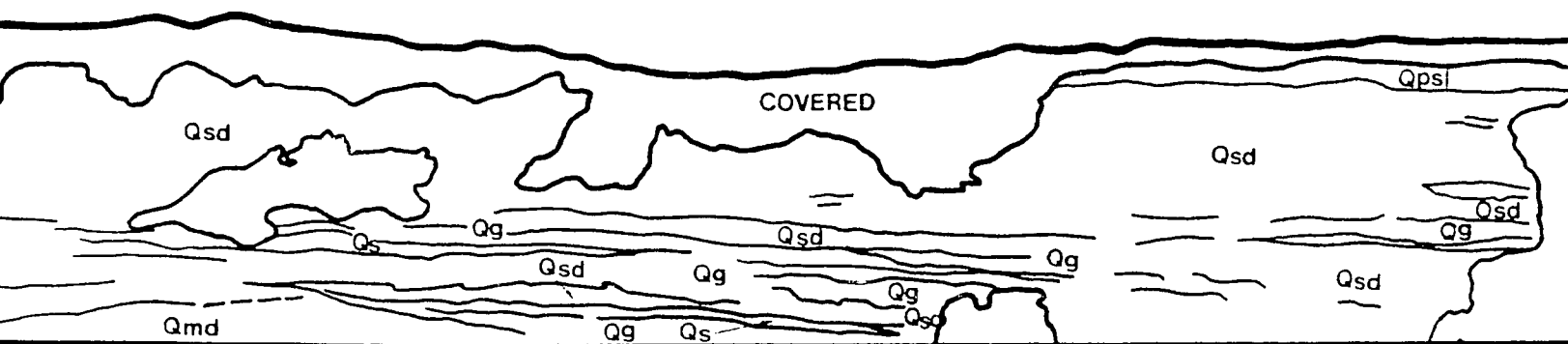


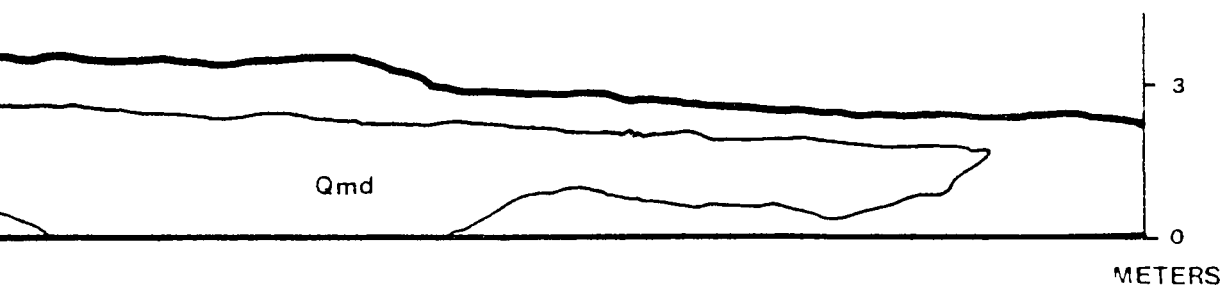
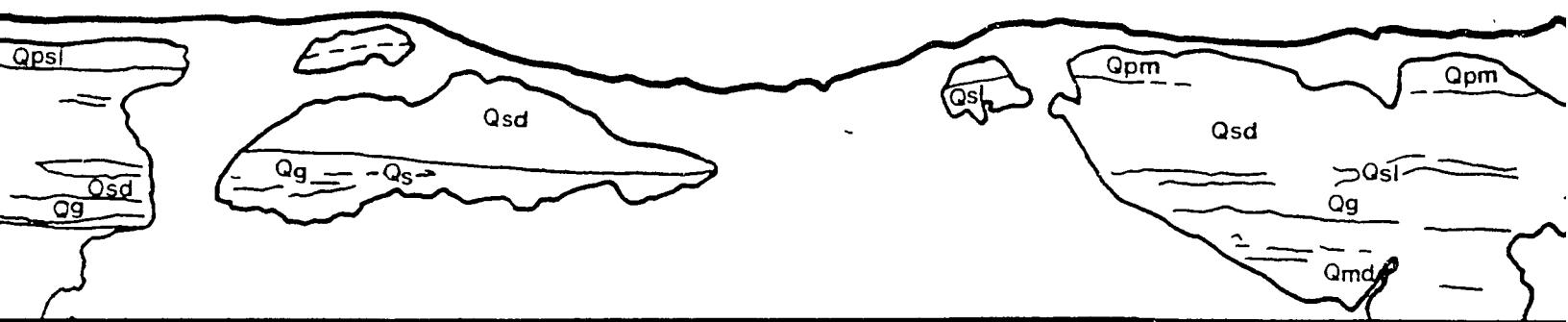
GLACIAL - MARINE (distal)

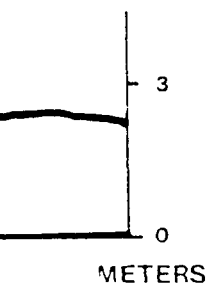
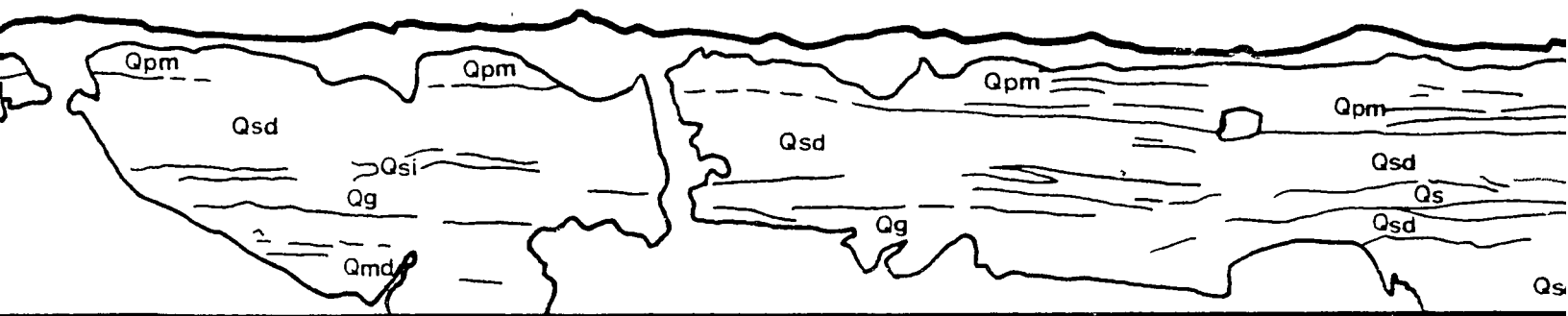
diamicton

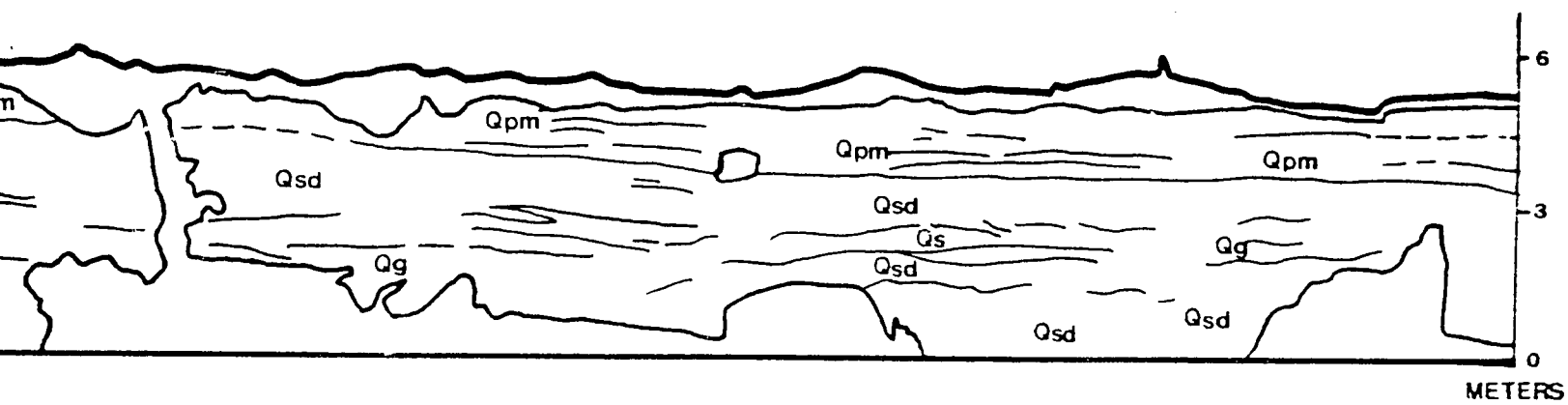
sand

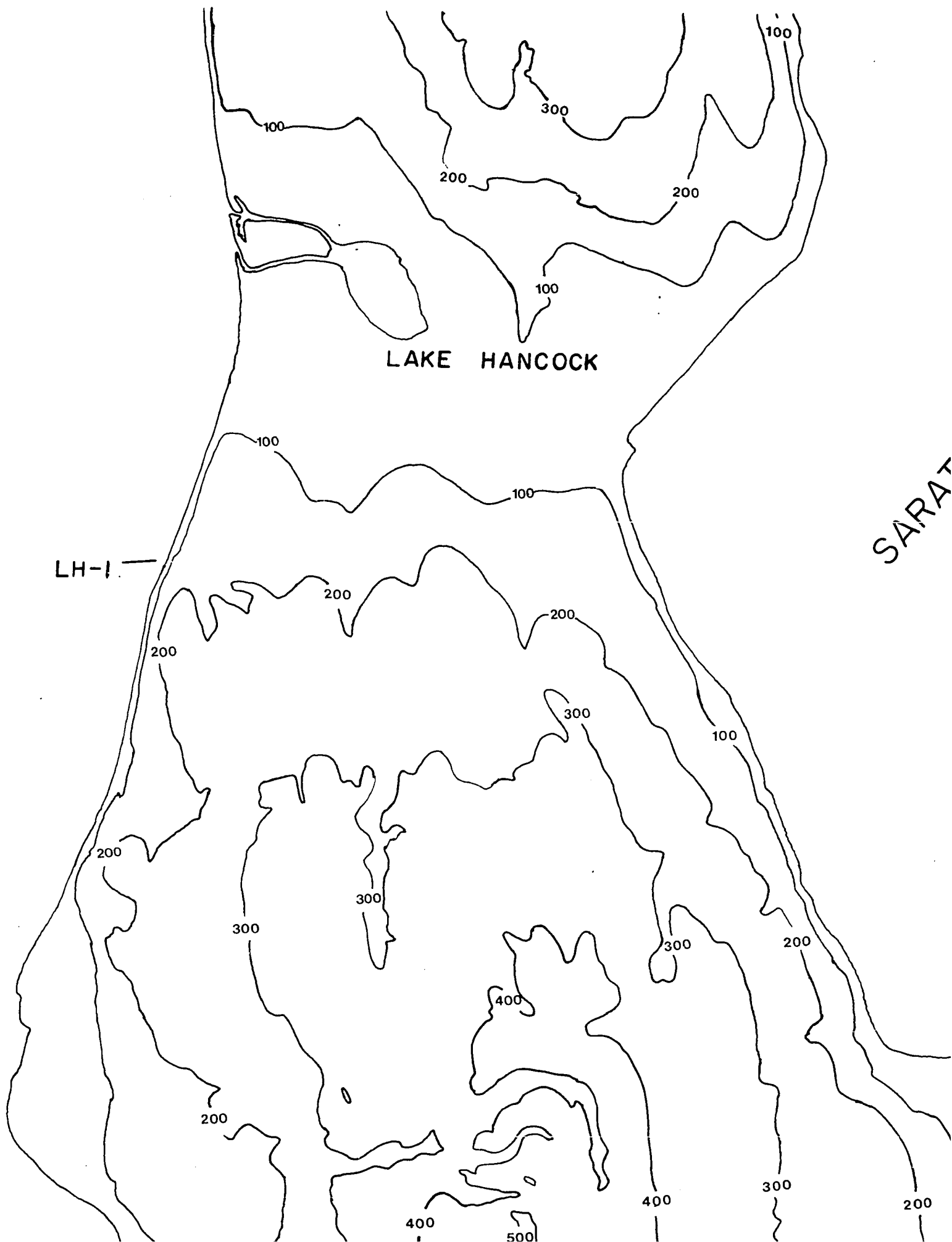
diamicton







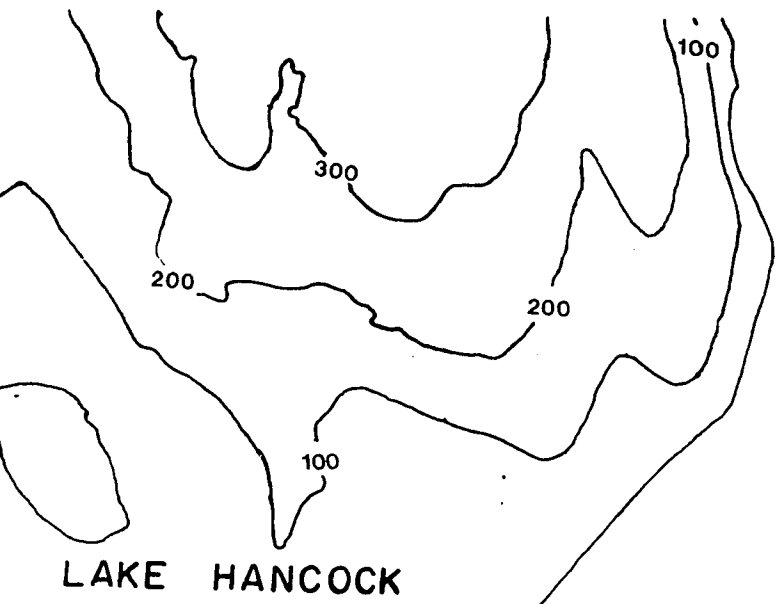




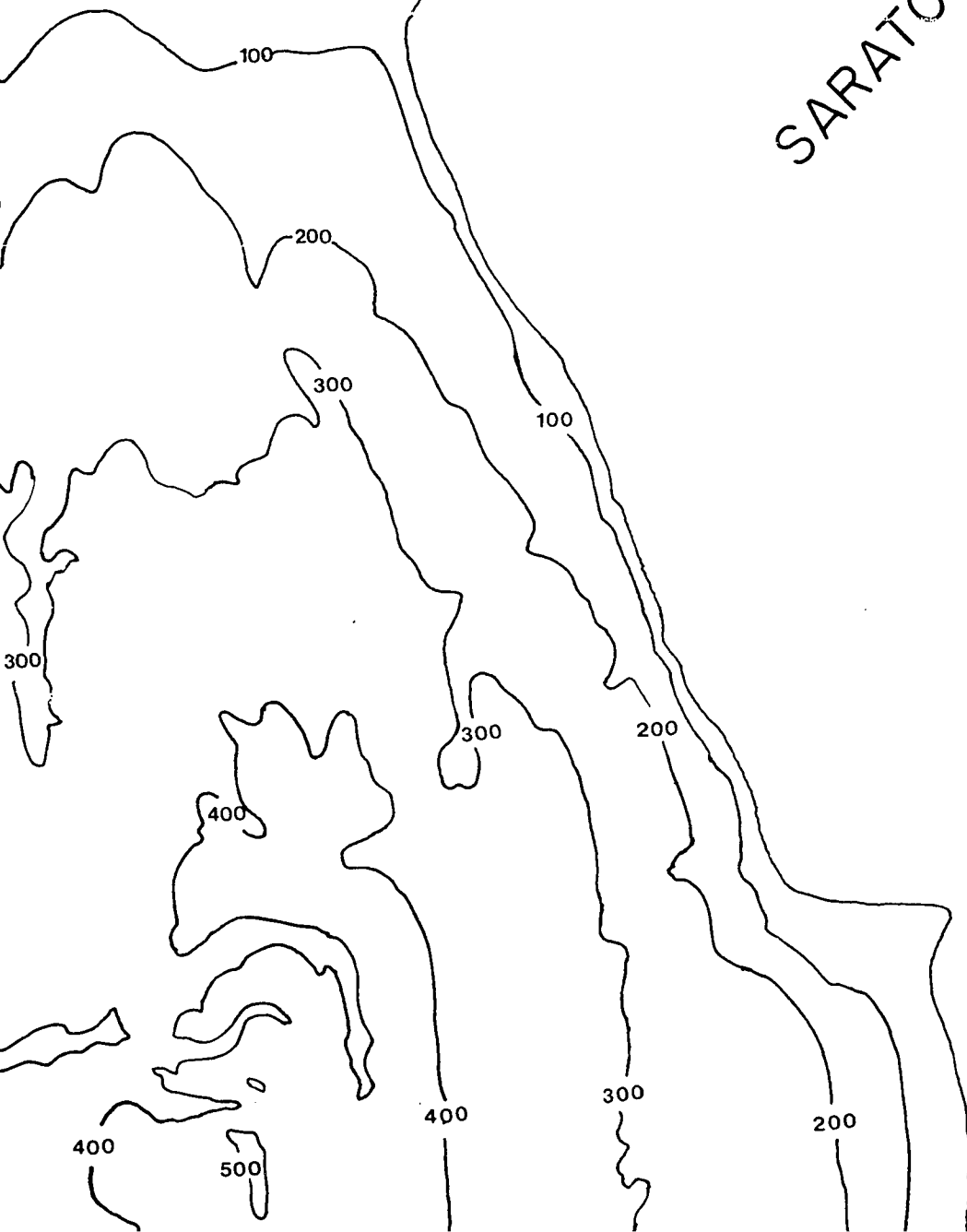
LAKE HANCOCK

LH-1

SARAT

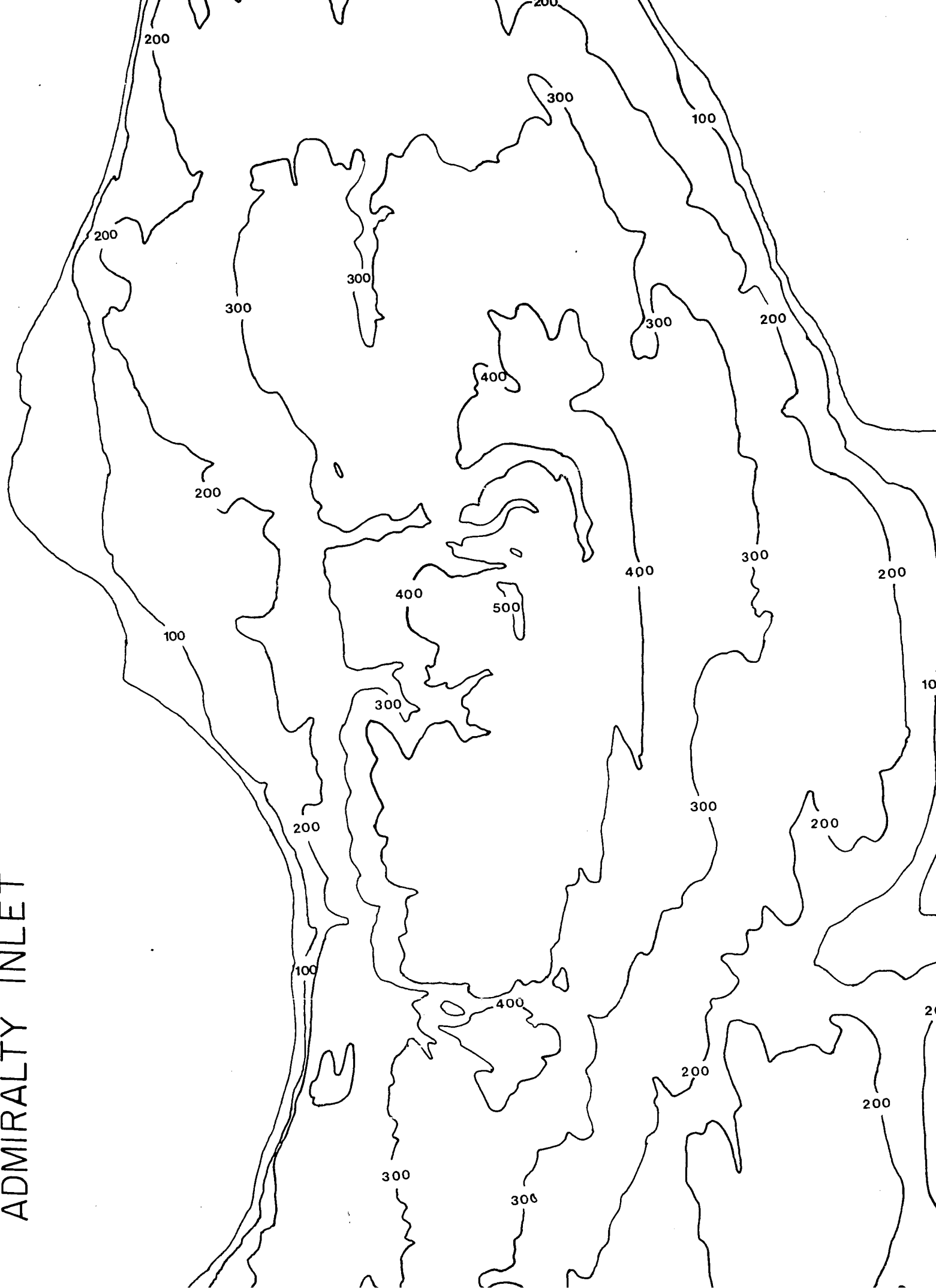


SARATOGA
PASSAGE



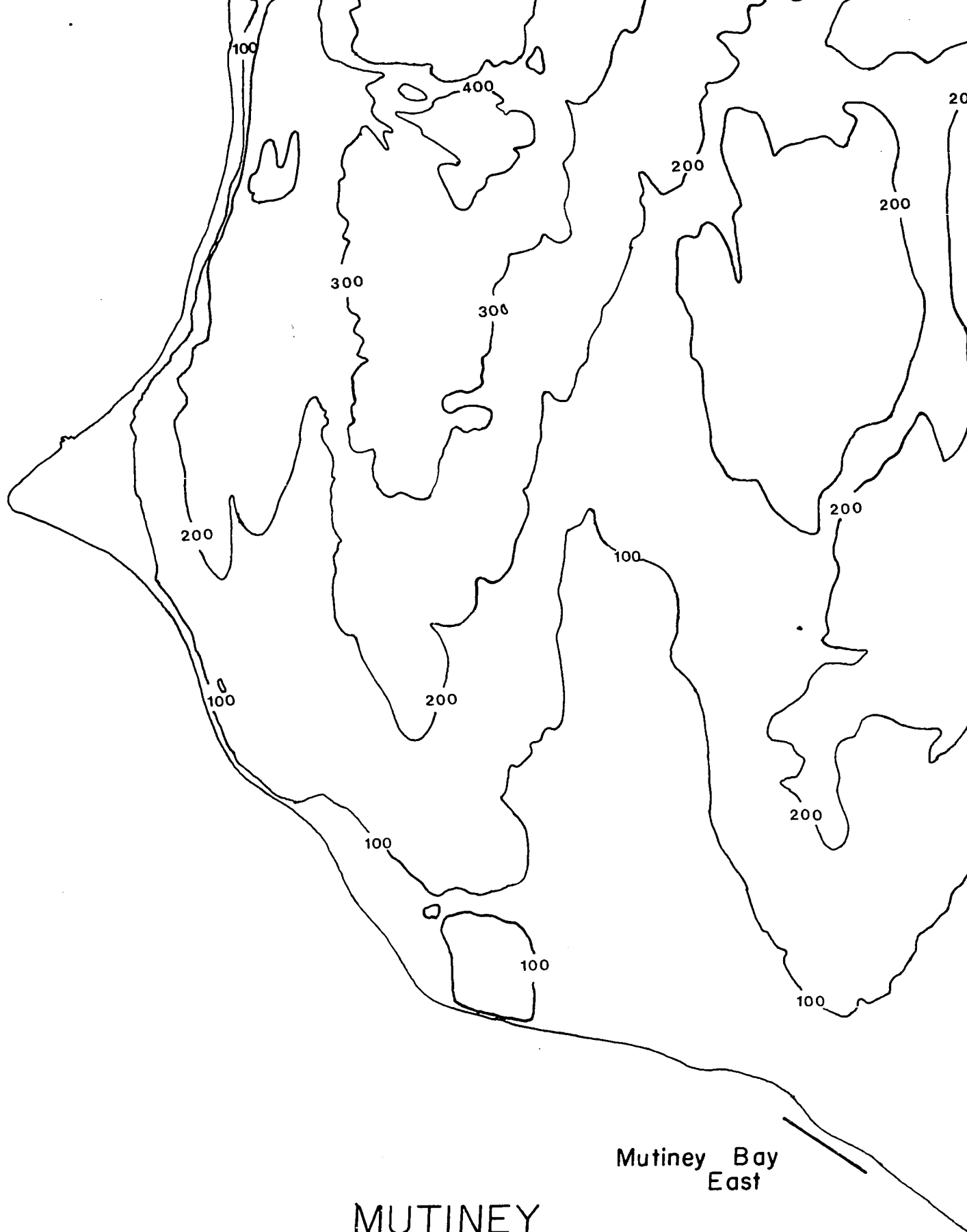
DR

ADMIRALTY INLET



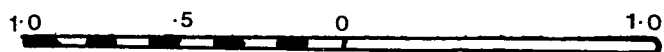


HOLMES HARBOR

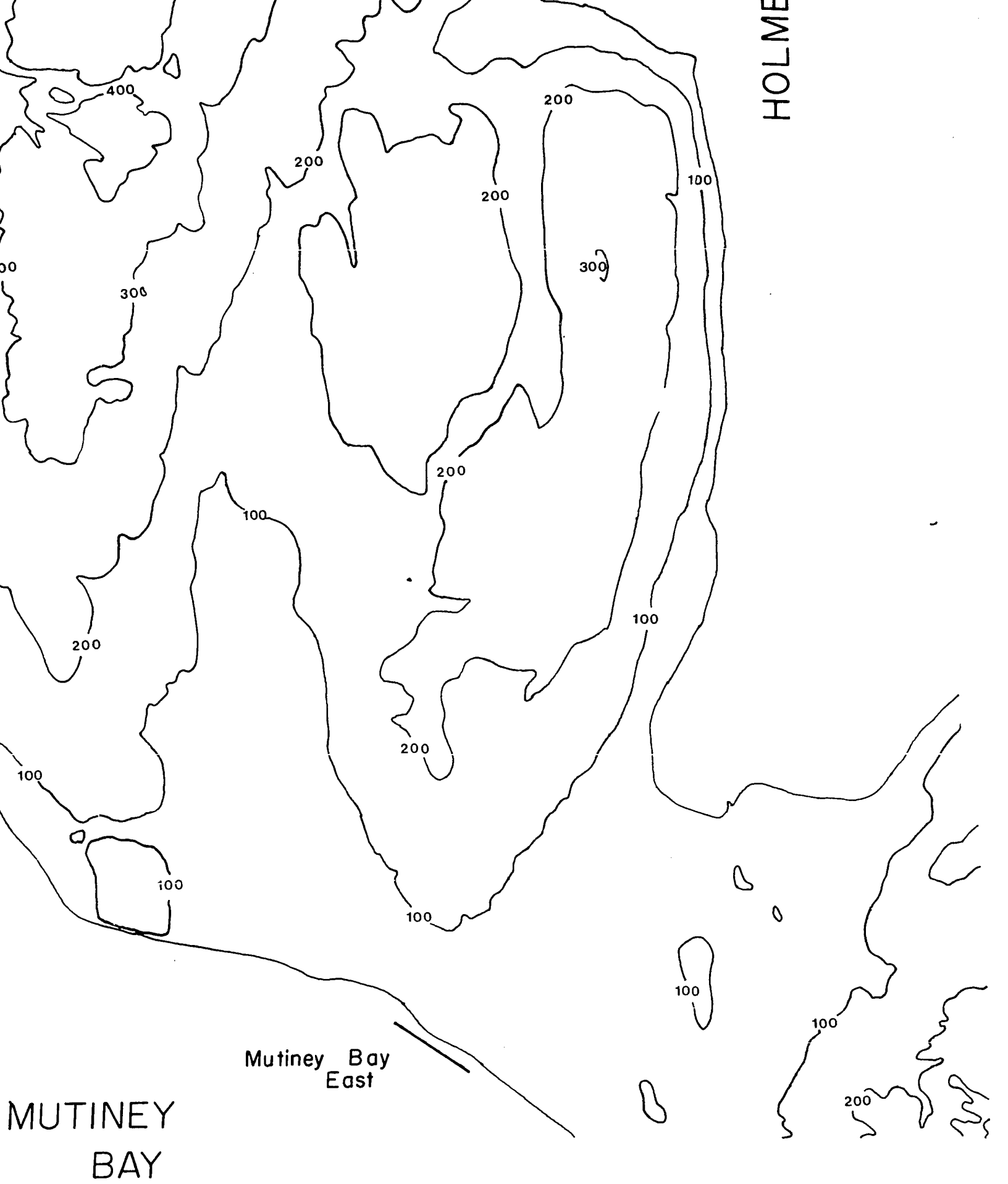


Mutiney Bay
East

MUTINEY
BAY



KILOMETERS

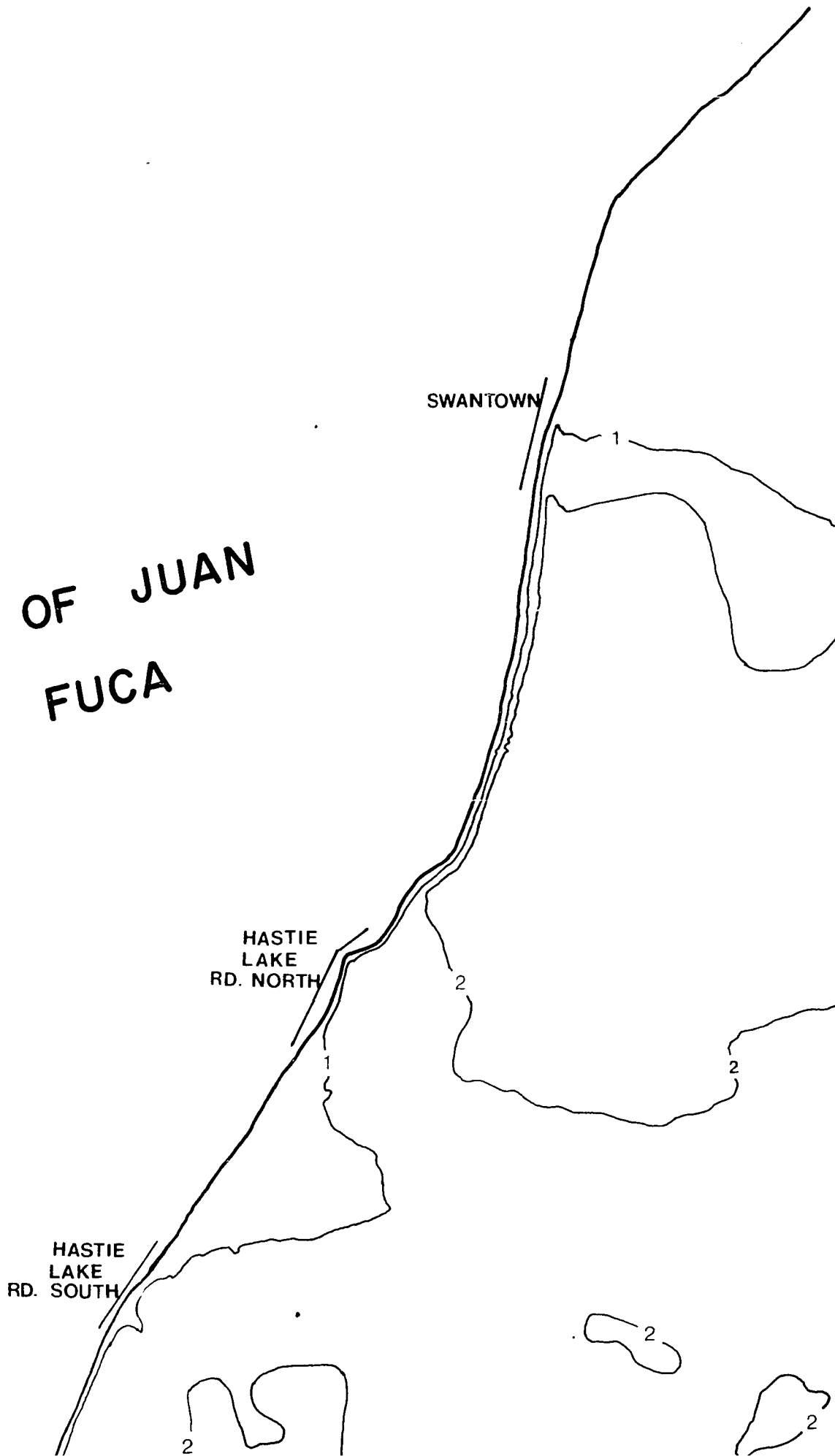


STRAIT OF JUAN DE FUCA

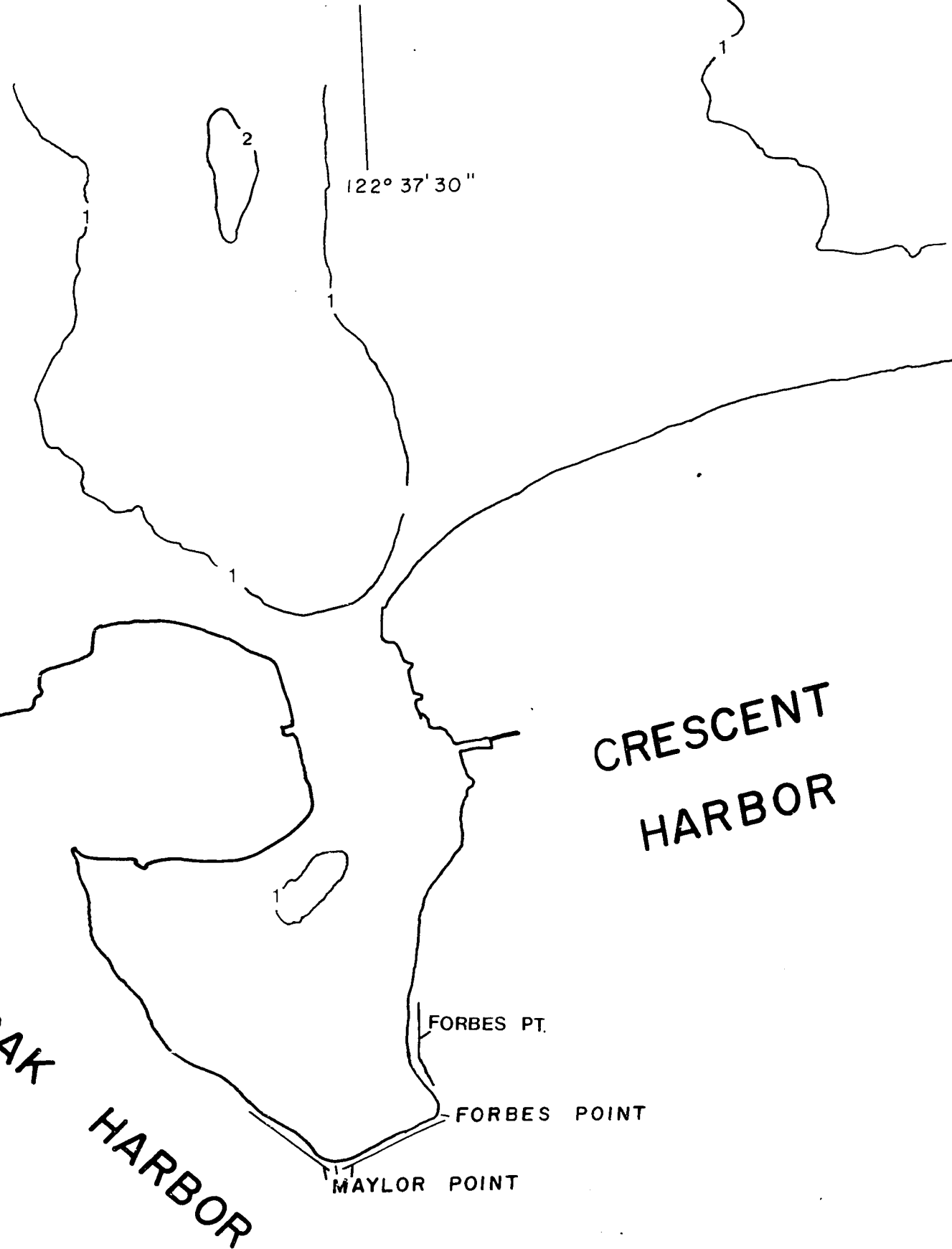
SWANTOWN

HASTIE
LAKE
RD. NORTH

HASTIE
LAKE
RD. SOUTH







HASTIE
LAKE
RD. SOUTH

48° 15'

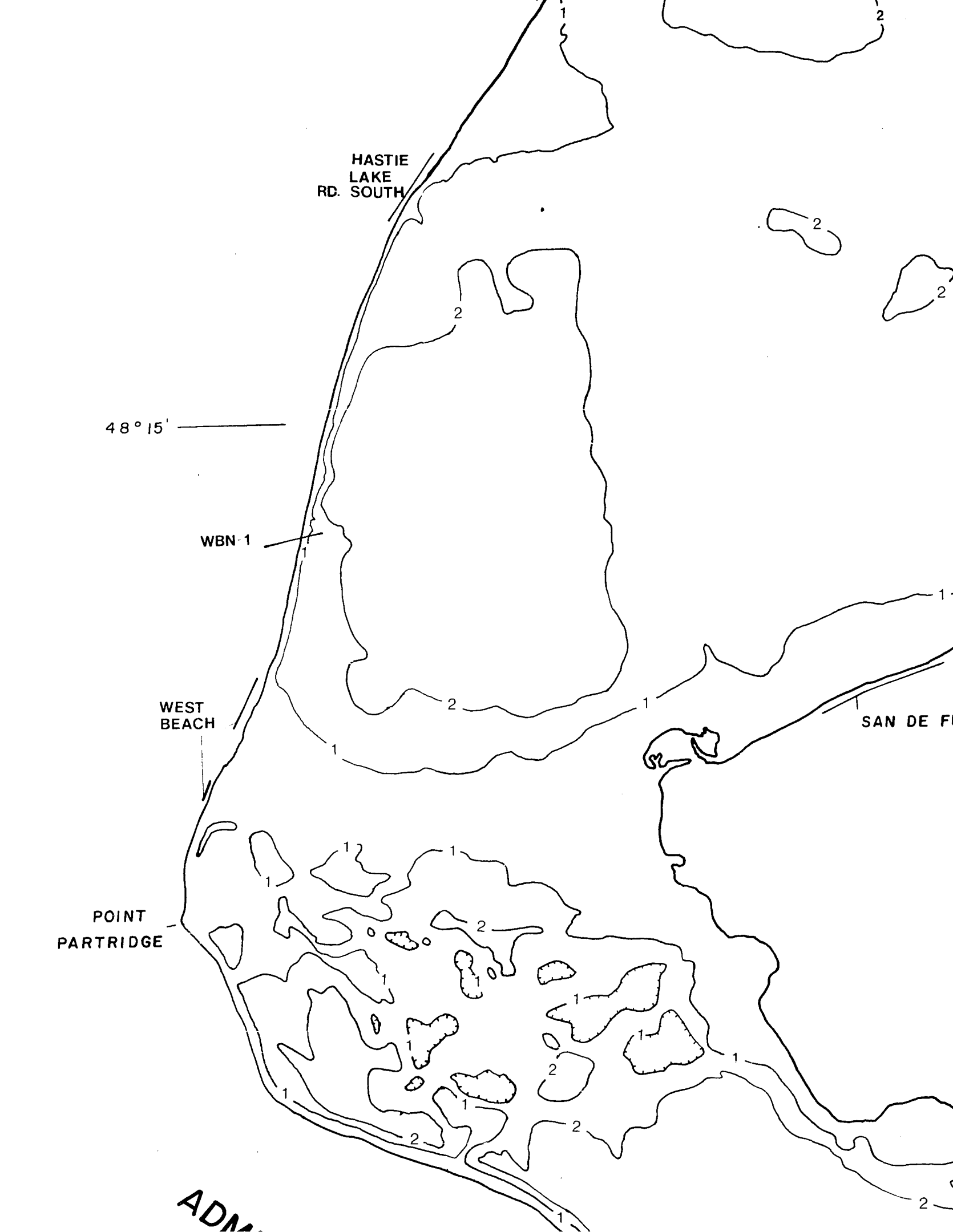
WBN-1

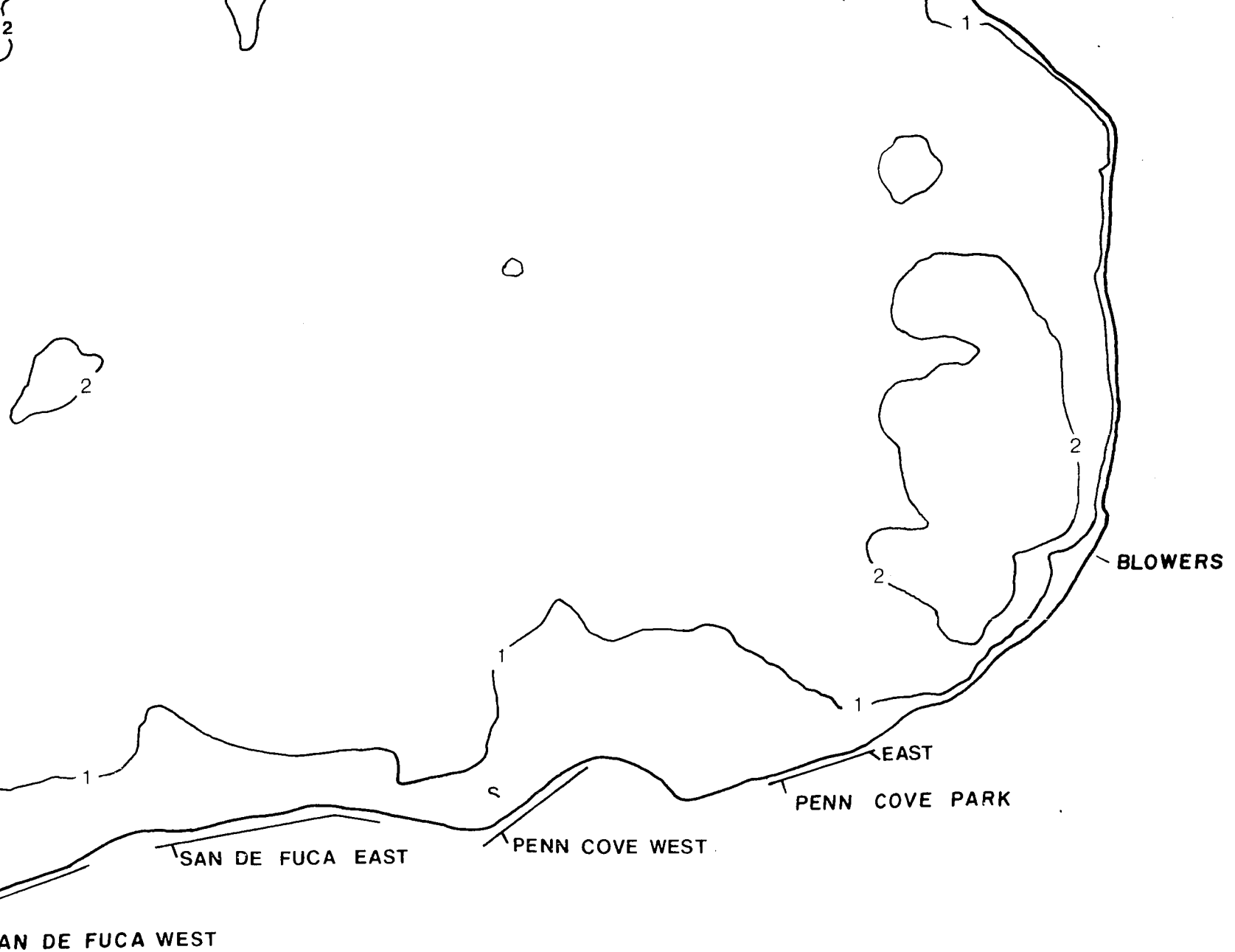
WEST
BEACH

POINT
PARTRIDGE

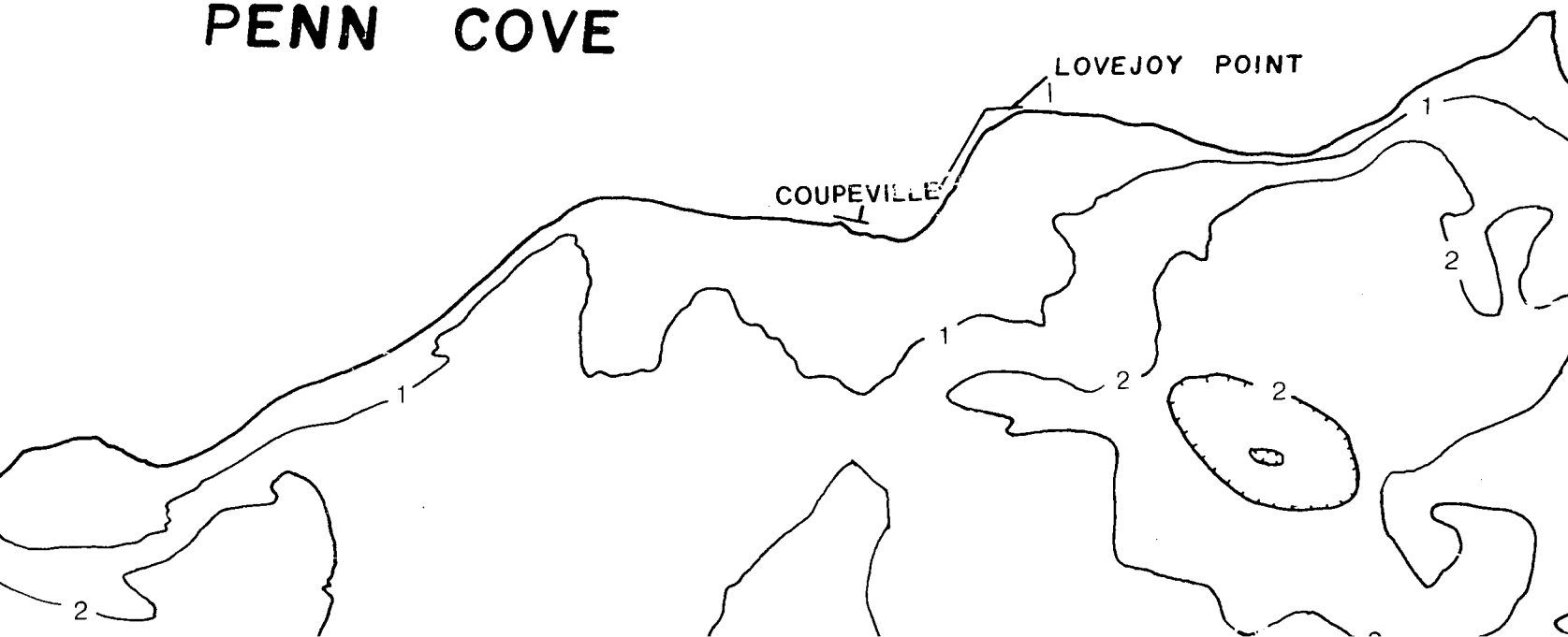
SAN DE F

ADM





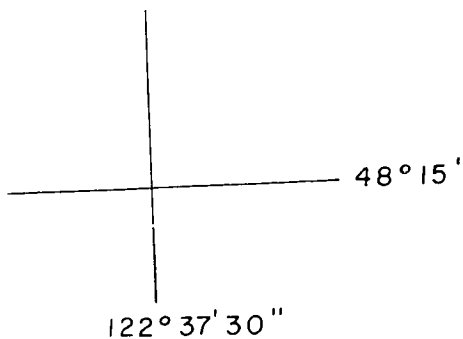
PENN COVE



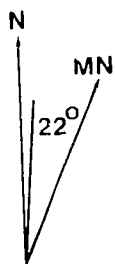
HARBOR

MAYLOR POINT

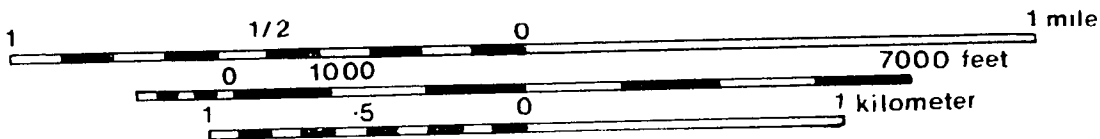
FORBES POINT



ERS BLUFF



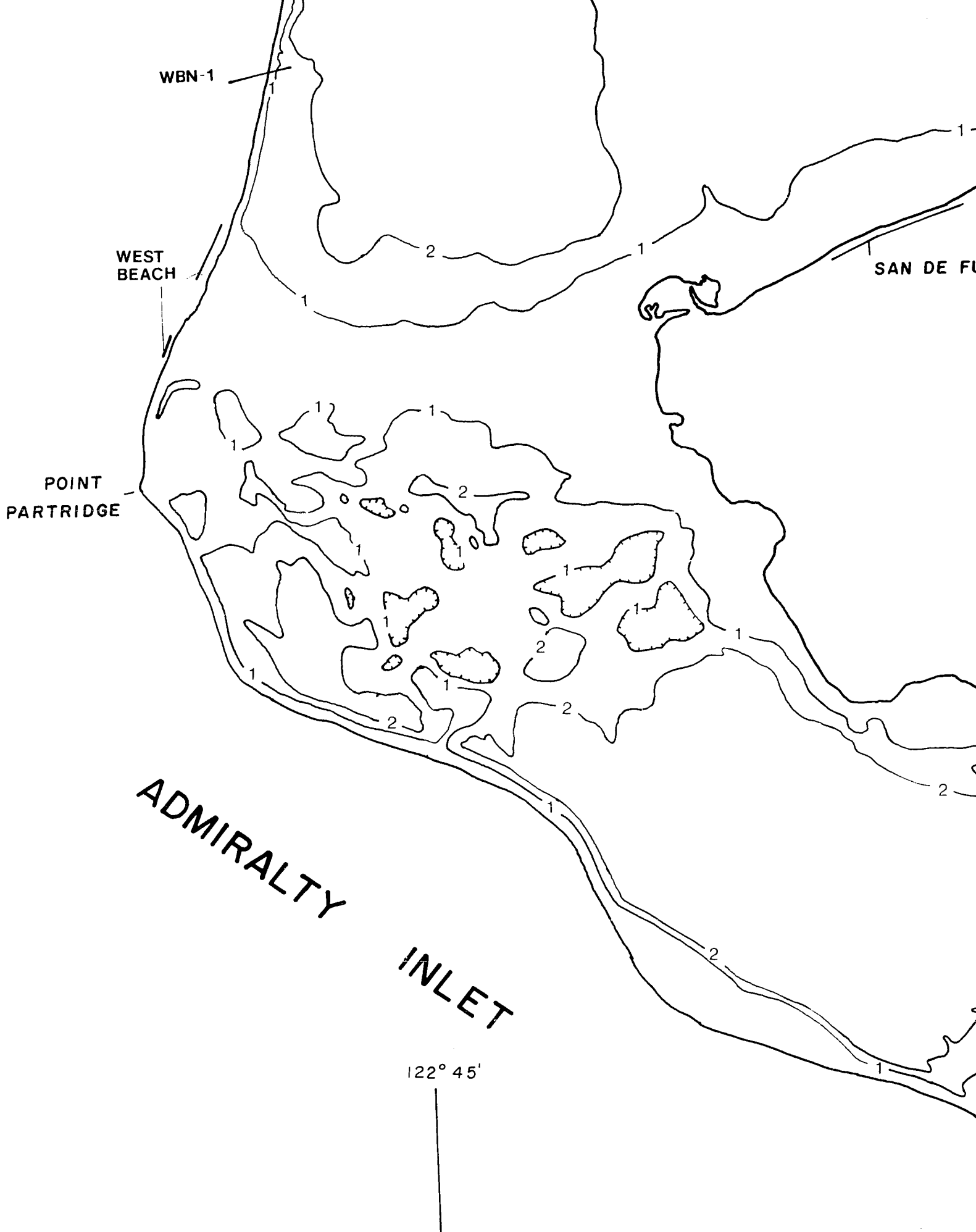
SCALE 1:24,000

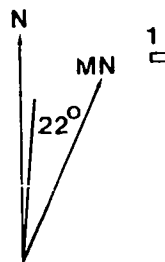
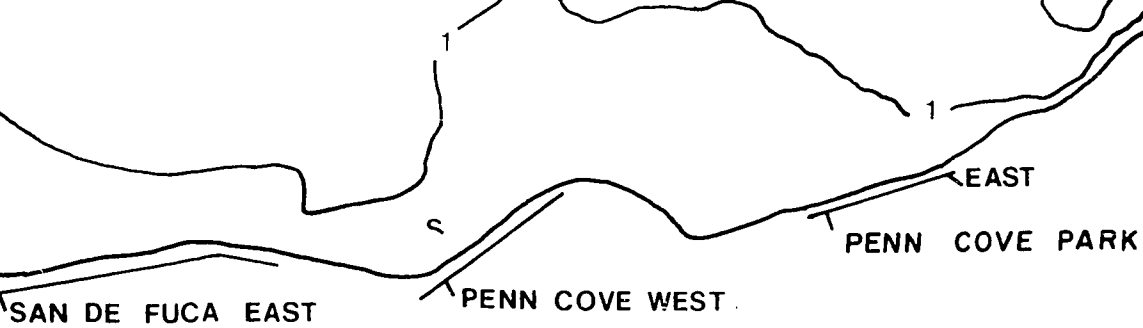


CONTOUR INTERVAL X 100 FEET

SARATOGA

PASSAGE





EST

PENN COVE

